Faculty of Science School of Geography, Archaeology and Environmental Studies

Remote Sensing Survey of Archaeological Sites in the Shashi- Limpopo Region

BY:

Olaotse Lokwalo Thabeng

Submitted to the Faculty of Science, University of the Witwatersrand, Johannesburg, in partial fulfilment of the requirements for the degree of Doctor of Philosophy (Geography and Environmental Science)

Supervisors: Dr Stefania Merlo
Dr Elhadi Adam

ABSTRACT

The African continent is rich with archaeological heritage, which needs to be preserved for the current and future generations. The majority of archaeological heritage sites in Africa are facing disappearance due to a number of challenges including looting, destruction from developments, expansion of agricultural land and natural hazards. Documentation and monitoring of archaeological heritage sites, therefore, is of paramount importance for effective site management and preservation. However, archaeological heritage sites in the continent are poorly documented and monitored due to a number of factors including lack of funds by heritage management institutions, lack of trained personnel and inaccessibility of some areas due to conflicts or land ownership rights. Traditionally, the documentation and monitoring of archaeological heritage sites in Africa have been done through fieldwork, which is costly, time-consuming and difficult to carry out over large areas. Remote sensing offers a relatively fast, cheap, systematic and reproducible method of surveying and monitoring archaeological sites over large and/or restricted areas. Remote sensing techniques are used to identify earth surface features based on their spectral signature, which is the variation of reflection or emittance of materials' electromagnetic energy. Spectral signatures for identifying archaeological sites are not universal, and an assessment of the applicability of remote sensing techniques in different archaeological landscapes is needed. The aim of this study, therefore, was to investigate the potential of using remote sensing techniques to document archaeological sites previously occupied by farming communities, which are traditionally associated with the Iron Age period in Southern Africa, using the Shashi-Limpopo case study.

The first part of this study gives a review of the use of remote sensing in the African archaeological context. Despite it being a fast, cost-effective and systematic method of survey, the results of this study have demonstrated that remote sensing is not widely used in archaeological applications in Africa. The aforementioned situation calls for studies investigating the potential of using remote sensing techniques to fast track archaeological site survey, documentation and monitoring in the continent.

The chemical composition of materials characterising different features have more or less subtle variations that, in turn influence the spectral behaviour of soil. This is an important principle that can be used for distinguishing archaeological soils from non-archaeological soils and can potentially help in discriminating different archaeological signatures. As such, the second part of this study investigated the possibility of using field spectrometer measurements

to discriminate middens, non-vitrified dung, vitrified dung and non-sites (natural soils) characterising archaeological landscapes previously occupied by farming communities. It then investigated the presence of differences in the chemical composition of elements between middens, non-sites, vitrified dung and non-vitrified dung. The findings indicated that there is a statistically significant difference in the concentration of soil elements between non-sites, middens, vitrified dung and non-vitrified dung byres. They also indicated that some bands in the visible and shortwave infrared regions of the electromagnetic spectrum important bands for predicting the aforementioned archaeological sites and non-archaeological sites.

In the third part of this study, the ability of multispectral sensors to discriminate archaeological and non-archaeological features in Shashi-Limpopo confluence area was investigated using field spectral data resampled to the spectral resolutions of common multispectral satellites namely GeoEye, Landsat 8 OLI, RapidEye, Sentinel-2, SPOT 5 and WorldView-2. This is because the spectral and spatial resolutions of various multispectral sensors determine the size and the type of archaeological data a sensor can detect. As such, another goal of this study was to identify multispectral sensors with the optimum spectral resolutions for detecting middens, non-vitrified dung, vitrified dung and non-sites. Additionally, the performance of advanced classification algorithms (random forest and support vector machines) in discriminating middens, non-vitrified dung, vitrified dung and non-sites was also investigated. The results proved the possibility of using multispectral satellites in mapping middens, non-sites, vitrified dung and non-vitrified dung sites. These results initiated the need to upscale the test to actual satellite images.

The fourth part of this study assessed the possibility of prospecting for archaeological sites previously occupied by farming communities in the Shashi-Limpopo Confluence Area, using a very high-resolution satellite WorldView-2 image. The findings have shown that WorldView-2 satellite images and advanced classification algorithms can be used in prospecting for archaeological sites previously occupied by farming communities in Shashi-Limpopo Confluence Area.

Finally, the ability of geographic object-based image analysis (GEOBIA) based on random forest and support vector machines, to discriminate archaeological and non-archaeological features on a very high-resolution satellite WorldView-2 image was investigated. The results of this study demonstrated the robust ability of the GEOBIA to integrate spatial attributes into

the classification model improves the chances of separating materials with limited spectral contrast.

Generally, this study has shown that remote sensing techniques can be used to map archaeological landscapes characterised by middens, non-vitrified dung, vitrified dung and non-sites. This will help archaeological heritage managers and researchers to document and monitor sites in archaeological landscapes characterised by the aforementioned features in a fast, systematic, reproducible and cost-effective manner.

DECLARATION

I declare that this work is my own original work and has not been previously submitted to obtain an academic qualification. Data and information obtained from published and unpublished work of others have been acknowledged in the text and a list of references is herein provided.

Signature:  ----------

Date: -18/04/2020----------

DECLARATION-PLAGIARISM

I, Olaotse Lokwalo Thabeng, declare that:

1. the research reported in this thesis, except where otherwise indicated, is my original research,
2. this thesis has not been submitted for any degree or examination at any other university,
3. this thesis does not contain other persons' data, pictures, graphs or other information, unless specifically acknowledged as being sourced from other persons,
4. this thesis does not contain other persons' writing, unless specifically acknowledged as being sourced from other researchers. Where other written sources have been quoted, then:
    a. their words have been re-written but the general information attributed to them has been referenced
    b. where their exact words have been used, then their writing has been placed in italics and inside quotation marks, and referenced
5. this thesis does not contain text, graphics or tables copied and pasted from the internet, unless specifically acknowledged, and the source being detailed in the thesis and in the references section.

Signed:  …….

DECLARATION- PUBLICATIONS AND MANUSCRIPTS

1. **Thabeng, O. L**., Merlo, S. and Adam, E., (In Preparation). "The use of remote sensing techniques in archaeological applications in Africa: a review."

2. **Thabeng, O. L**., Adam, E. and Merlo, S., 2019. "Spectral discrimination of archaeological sites previously occupied by farming communities using in situ hyperspectral data." Journal of Spectroscopy. Spectral Image Processing as a Tool for Analysis of Cultural Heritage: Special issue. 1-21.
   DOI: https://doi.org/10.1155/2019/5158465

3. **Thabeng, O. L**., Merlo, S. and Adam, E., 2020. "From the bottom up. Assessing the spectral ability of common multispectral sensors to detect surface archaeological deposits using field spectrometry and advanced classifiers in the Shashi-Limpopo confluence area." *African Archaeological Review* 37: 25–49

4. **Thabeng, O. L**., Merlo, S. and Adam, E., 2019. "High-Resolution Remote Sensing and Advanced Classification Techniques for the Prospection of Archaeological Sites' Markers: The Case of Dung Deposits in the Shashi-Limpopo Confluence Area (Southern Africa)." *Journal of Archaeological Science* 102:48–60.

5. **Thabeng, O. L**., Adam, E. and Merlo, S., (In Preparation). "Evaluating the performance of geographic object-based image analysis in mapping archaeological landscape previously occupied by farming communities: A case of Shashi-Limpopo Confluence Area."

Signed:……

ACKNOWLEDGEMENTS

I would like to express my heartfelt gratefulness to my supervisors, Dr Stefania Merlo and Dr Elhadi Adam for the incomparable academic supervision, support, and encouragements they gave during this study. Thanks also goes to the University of Botswana for the support in carrying out this research, SANParks for allowing access to Mapungubwe National Park and the DeBeers Group (through Duncan MacFadyen) for allowing access to the Venetia Nature Reserve and use their research facility. We are also thankful to the DigitalGlobe Foundation for making this research successful by providing WorldView-2 images for the study area. The foundation promotes the use of geospatial data by providing image grants, information and expertise to individuals at university-level academic institutions. I am also grateful to Prof. Thomas Huffman for making his data available and devoting his time by taking me through the study area, Lesego Madisha (former archaeologist at SANParks, Mapungubwe) for her kind assistance, South African National Parks Cultural Heritage Manager Crispen Chauke and the Venetia Nature Reserve staff for their help.

This work was funded by the University of Botswana, the University of the Witwatersrand and the DigitalGlobe Foundation.

TABLE OF CONTENTS

LIST OF FIGURES

LIST OF TABLES

LIST OF ABBREVIATIONS

CCP –Central Cattle Pattern

GEOBIA-Geographic Object-Based Image Analysis

GRRF-Guided Regularised Random Forest

IR –Irrigated Agriculture

MD –Midden

NS –Non-Sites

NVD –Non-Vitrified Dung

NDVI – Normalised Difference Vegetation Index

RF –Random Forest

SLCA –Shashi-Limpopo Confluence Area

SVM –Support Vector Machines

SWV –Savannah Woody Vegetation

VD –Vitrified Dung

CHAPTER ONE

1. General introduction

1.1 **Introduction**

This study is a contribution towards the development of methods for archaeological site survey and documentation using remote sensing techniques in archaeology, with a focus on Africa. This is an under-researched area, yet extremely important in particular in light of the increasing threats - infrastructure development, conflicts, looting, floods, earthquakes, and fires - that put known and unknown archaeological sites at risk in the continent and the world at large (Agapiou et al. 2015; Al-Houdalieh and Sauders 2009; Chirikure 2013; Contreras and Brodie 2010; Eloundou and Avango 2012; Hassani 2015; Holtorf 2001; Jones 1986; Kankpeyeng and DeCorse 2004; Lane 2011; Parcak 2007; Roosevelt and Luke 2006; Sever and Irwin 2003; Stone 2015). The thesis is, therefore, dedicated to investigating the potential of remote sensing techniques in mapping archaeological features.

The survey and documentation of archaeological sites are some of the major challenges faced by heritage managers and archaeological researchers, especially in the African continent, where there is lack of funding and trained personnel (Chirikure 2013; Connah 2008; Mcintosh 1993). Consequently, the national sites and monuments inventories of most heritage management institutions in the continent are incomplete, further complicating the management of archaeological heritage and understanding of the archaeological record. To improve heritage management and research in the continent, there is a need for cost-effective and less labour demanding methods, which can be used to systematically acquire accurate information and expand research to remote areas. Remote sensing applications have been identified as less labour intensive and cheaper methods than traditional surveys to acquire regional perspectives of archaeological landscapes, predict the location of sites, and archive and monitor their status through the use of repeated data collection offered by the different platforms (Corrie 2011; Parcak 2007; Sever and Irwin 2003). This is despite the popular opinion that remote sensing data is expensive and therefore not easy to be acquire with the limited budgets of most archaeological projects (Cracknell and Hayes 2007; Parcak 2009; Tang and Shao 2015). The thesis uses remote sensing data from the various sensors - field spectrometer and sensors aboard satellite platforms - to investigate the possibility of discriminating archaeological and non-archaeological features based on their spectral signatures. It also assesses the ability of random forest and support vector machines classification algorithms in classifying archaeological data, because of their ability to work with limited data, which is a common problem in archaeological research. In so doing the research will advance knowledge on the type of surface archaeological

features that can be detected using remote sensing, on the most appropriate satellites for the detection and suitable classification algorithms for the prediction. Ultimately the goal is to provide the wider archaeological community with methodological frameworks, aimed at widening the use of remote in archaeological research, in particular in Africa.

The study was conducted in an archaeologically well-documented landscape, the Shashi-Limpopo confluence, known for hosting one of the earliest complex societies in the continent (Huffman 2009a). This offered the opportunity to test the predictive ability of remote sensing models against a fairly well known archaeological record (in particular in South Africa). If the model yields positive results, it can then be deployed on less well-known parts of the confluence (such as Botswana and Zimbabwe) with confidence to detect more archaeological sites. This research mainly targeted sites previously occupied by farming communities because they are the most common archaeological sites in the study area. Moreover, some of the activities carried out by farming communities, such as animal penning, burning animal dung deposits in a pen/kraal and repetitive dumping of domestic refuge in one area, affected soil properties thus creating microenvironments (Denbow 1979; Huffman et al. 2013; Mothulatshipi 2008). The resulting microenvironments are characterised by spectral contrast with their surroundings which consequently makes it possible for remote sensing techniques to detect them (Parcak 2009).

1.2 Background on the use of remote sensing in African archaeological context and significance of the study

Since the early decades of the 20th century, remote sensing data in archaeology have afforded researchers and heritage managers with new perspectives for surveying, documenting, analysing and monitoring archaeological features (Elfadaly et al. 2018; Ginau et al. 2017; Masini et al. 2009; Masini and Lasaponara 2007; Parcak 2009; Parcak et al. 2016; Van Ess et al. 2006). This has led to increasing research on and with remote sensing techniques in archaeological studies and heritage management, especially in Europe and North America (Agapiou and Lysandrou 2015; Bewley 2003). For example, English Heritage developed a national mapping programme in 1992 to promote an extensive discovery and mapping of heritage sites in England using aerial photographs (Bewley 2003). Conversely, the potential of remote sensing techniques in African archaeological contexts has been less explored. The earliest large scale surveys in the continent made use of aerial photographs to detect and study the settlement layout patterns of archaeological sites based on on the visibility of stonewalls

on the images (Mason 1968; Seddon 1968b). Denbow (1979) conducted a pilot study using aerial photography to identify ecological indicators formed as a result of the effects of archaeological materials in the soil properties within the African archaeological context. However, the cost of acquiring aerial photographs and the bureaucracy made it difficult to carry out the research in most African countries (Connah 2008; Parcak 2007). Furthermore, the inability of film to capture data in regions beyond the visible spectrum limited its application in complex archaeological contexts.

The recent public availability of high-resolution multispectral satellite images provided heritage managers and researchers with a platform to regularly capture archaeological data using bands within visible, infrared and microwave regions of the electromagnetic spectrum at high temporal resolution. These include variations in vegetation health status and specific chemical composition of archaeological features, which are not detected by traditional aerial photography due to its low spectral resolution (Doneus et al. 2014; Lasaponara and Masini 2007). Additionally, the high spatial resolution of some multispectral sensors has enabled the detection of small archaeological features (Fowler 2002; Lasaponara and Masini 2005). The high temporal resolution of multispectral satellite sensors has enabled researchers and heritage managers to monitor archaeological heritage overtime (Parcak et al. 2016; Van Ess et al. 2006). Furthermore, the digital nature of multispectral satellite data allows for a deeper analysis of archaeological data by enabling the integration of datasets from different sources and the use of semi-automatic and automatic image classification algorithms for the mapping of archaeological features. Researchers and heritage managers across the African continent have used satellite data in a wide range of applications which include predicting site locations and studying the layout of various archaeological sites (Biagetti et al. 2017; Clark et al. 1998; Klehm et al. 2019; Morton 2013; Parcak et al. 2016; Reid 2016; Sadr and Rodier 2012; Segokgo 2012). The use of satellite data in archaeological applications has also enabled fast and cheap documentation and monitoring of archaeological sites in large and inaccessible areas (Biagetti et al. 2017; Elfadaly et al. 2018; Parcak 2007; Parcak et al. 2016).

Despite the potential of remote sensing data and techniques, challenges remain. Firstly, sensors are not constructed for the detection of archaeological data, as such, identifying sensors with spatial and spectral abilities to detect archaeological materials in the study area of interest is necessary (Agapiou et al. 2014a; Parcak 2009). Other than the aforementioned sensor challenges, one major limitation for the use of remote sensing in archaeological applications is the need to identify data processing techniques which can improve the results. To date, despite

the advances in remote sensing and the availability of multispectral and hyperspectral imagery, the reflectance of different archaeological materials in southern Africa (and in most of the world) has neither been studied nor catalogued. Thus this study assesses the possibility of discriminating natural soils (non-sites), ash middens, vitrified dung and non-vitrified dung using their spectral signatures. If successful, the study will help in expanding the techniques that can be used to survey and document archaeological sites. These will include the use of both pixel and object-based machine learning image processing algorithms such as random forest and support vector machines. This will also help archaeologists and other interested parties to harness the increasing available high-resolution remote sensing data in their research and the management of archaeological features.

1.3 Aims and Objectives

This project aims to investigate the potential of remote sensing techniques in mapping archaeological features characteristic of farming communities, which are traditionally associated with the Iron Age period in Southern Africa, using the case study of the Shashi-Limpopo Confluence Area.

The objectives of this research are as follows:

- To give a comprehensive overview of historic and current trends on the applications of remote sensing in African archaeology from a perspective of three themes which are research publication details, data capturing and processing, and the footprint of remote sensing applications across the continent.
- To discriminate a range of archaeological sites characteristics of farming communities in Southern Africa (ash middens, vitrified dung, non-vitrified dung) and natural soils (non-sites) using field spectra measurements and chemical characteristics.
- To identify the optimum spectral resolution for the identification of archaeological ash middens, non-vitrified dung and vitrified dung sites as opposed to non-sites using in situ hyperspectral data resampled to different spectral resolution remote sensing multispectral platforms
- To test the performance of pixel-based advanced machine learning classifiers (random forest and support vector machines) in archaeological applications and the feasibility of directly detecting archaeological sites characterised by vitrified dung and non-vitrified dung through the use of high spatial resolution satellite images.

- To further investigate the performance of other image classification techniques, namely geographic object-based image analysis based on advanced machine learning classifiers in mapping archaeological sites characterised by vitrified dung and non-vitrified dung through the use of high spatial resolution satellite images.

1.3.1 Research Questions

1. What are historic and current trends on the applications of remote sensing in the African archaeological context from a perspective of three themes which are research publication details, data capturing and processing, and the footprint of remote sensing applications across the continent?
2. Is it possible to discriminate archaeological ash middens, vitrified dung, non-vitrified dung and natural soils (non-sites) using their field spectra measurements and chemical characteristics?
3. Which bands are suitable for detecting ash middens, vitrified dung, non-vitrified dung and natural soils (non-sites)?
4. Which spaceborne sensor has the optimum spectral characteristics for detecting ash middens, vitrified dung, non-vitrified dung and natural soils (non-sites)?
5. Can machine learning algorithms successfully be used to classify ash middens, vitrified dung, non-vitrified dung and natural soils (non-sites) on remote sensing data captured by high spatial resolution spaceborne sensors?

1.4 Study area

This study was carried out in the Shashi-Limpopo Confluence Area (SLCA). The SLCA is where two rivers, the Shashi and the Limpopo, meet, forming the boundaries of three countries; Botswana to the west, South Africa to the south and Zimbabwe to the north as shown in Figure 1. 1 below.

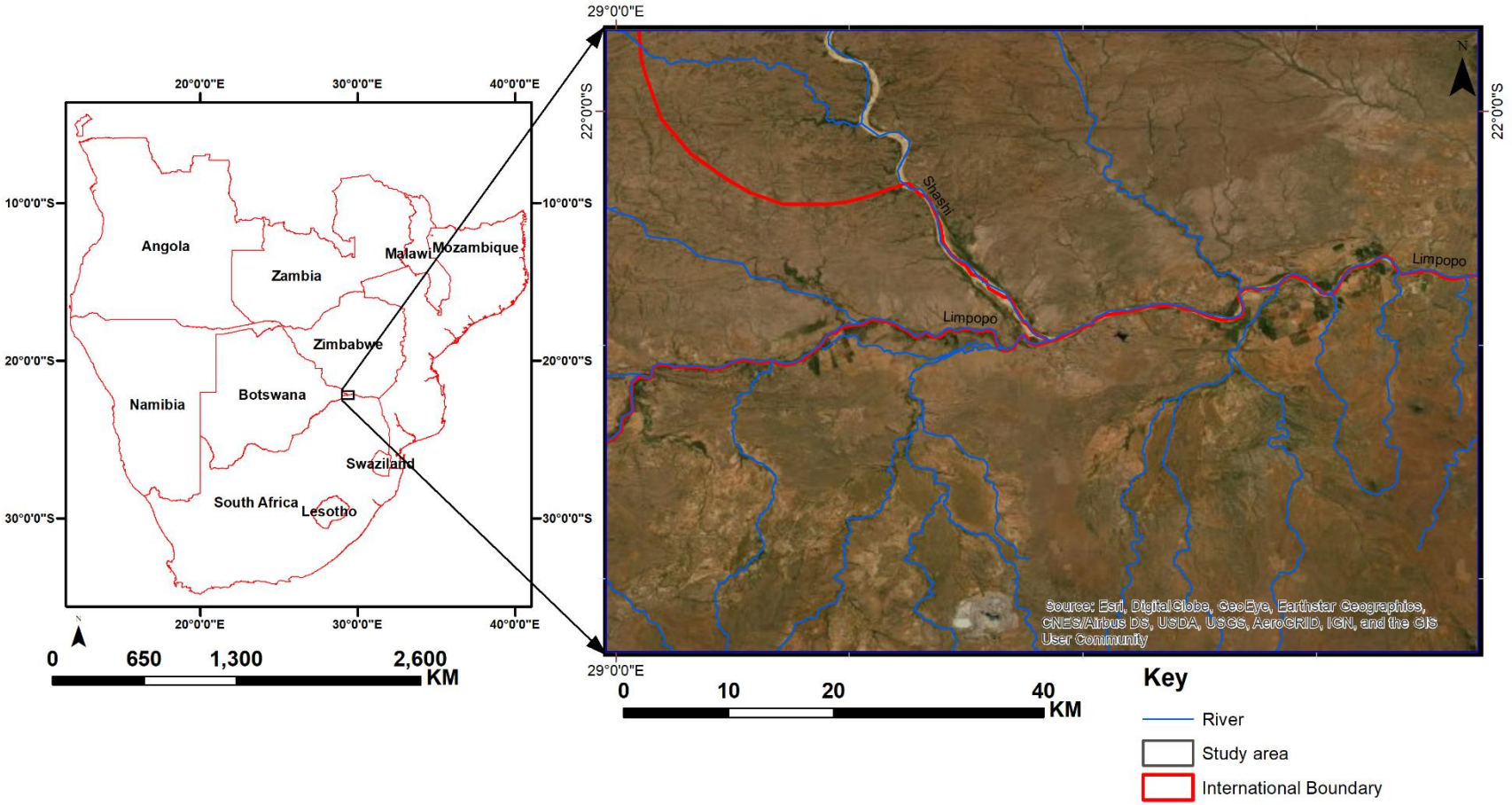

Figure 1. 1 Map situating the SLCA and study area within southern Africa.

1.4.1 Geology and geomorphology

The SLCA lies within the Limpopo Mobile Belt geological formation, which joins the Zimbabwe and Kaapvaal cratons (Chinoda et al. 2009a). This area is characterised by igneous and sedimentary rocks of the Karoo supergroup (Bordy and Catuneanu 2002). Erosion is rampant, in particular in areas closer to the river channels, forming sandstone ridges, and exposing dolerite dykes and outcrops which cover most parts of the SLCA with a sparse distribution of volcanic intrusions (Götze et al. 2008; Hanisch 1981a; Plug 2000). As a result, the topography of the SLCA is highly variable with undulating and rugged landscapes. The altitude varies from 300m to 1200m above sea level (Götze et al. 2003; Manyanga 2007). Generally, soils in the Limpopo mobile belt include clays and sands originating from the Karoo system (Götze et al. 2003).

1.4.2 Climate and Vegetation

The climate in the SLCA is semi-arid, characterised by cold and dry winters and hot and wet summers with unpredictable rainfall between October and March (Hanisch 1981b; Meyer 2000; Smith et al. 2007). The annual average rainfall in this area ranges between 140 and 500mm (Meyer 2000). Rivers and streams in this area are seasonal with some perennial water points along the main Limpopo river (Eastwood and Blundell 1999; Götze et al. 2008). Generally, temperatures range between 32ºC-18ºC in summer and between 22ºC-4ºC in winter (Hanisch 1981b; Voigt 1983). Vegetation in this region is highly variable with some areas dominated by mopane bushveld, arid sweet bushveld and riverine along the Limpopo River and its tributaries (Hanisch 1981b; Le Baron et al. 2010). There is a high diversity of plant species within this area (Götze et al. 2008). The mopane bushveld is dominated by mopane trees (*Colophospermum mopane*) with some occurrence of baobab (*Adansonia digitata*) and other plant species such as stink shepherd's tree (*Boscia foetida*) and mopane rhogozum (*Rhighozum zambesiacum baker*) (Voigt 1983). The riverine area is dominated by a number of vegetation communities generally classified into four main groups by Götze et al. (2003), based on their phytosociological characteristics: (1) *Croton megalobotys-Combretum microphyllum* community which is characterised by a variaty of species including sweet baffalo grass (*Panicum Schinzii*), love grass (*Setaria verticillata*), Guinea grass (*Panicum maximum*), flame creeper *(Combretum microphyllum),* fever tree (*Acacia xanthophloea*), feverberry *(Croton megalobotrys)*; (2) *Hyphaene petersiana-Acacia tortilis* including umbrella thorn *(Acacia tortilis),* narrow-leaved mustard tree (*Salvadora australis*), red spinach (*Trianthema triquetra*), palm (*Hyphaene petersiana*), white-leaved raisin (*Grewia bicolor*), love grass (*Setaria*

verticillata), white buffalo grass (*Urochloa mosambicensis*), sour grass (*Enneapogon cenchroides*); (3) *Salvadora australis-Cucumis zeyheri* community characterised by species inclunding the narrow-leaved mustard tree (*Salvadora australis*), *Ipomea sinensis subsp. Blepharosepala*, *Phyllanthus parvulus*, grey leaf heliotrope (*Heliotropium ovalifolium*), erect spiderling (*Boerhavia Erecta),* wild cucumber (*cucumis zeyheri)* and (4) *Diplachne fusca-Acacia xanthophloea* community consists of species such as *Corbichonia decumbens,* wild hibiscus (*Abutilon sonneratianum*), antelope grass (*Echinochloa pyramidalis*), Viper grass (*Dinebra retroflexa*), salt meadow grass (*Diplachne fusca*) and fever tree (*Acacia xanthophloea*).

1.4.3 Land tenure and land use

All three countries in the SLCA (Botswana, Zimbabwe and South Africa) are characterised by three mainland tenure systems, freehold, communal lands and state land which are used for a wide variety of activities (Forssman 2013; Huffman 2012; Manyanga 2007; Mothulatshipi 2008; Nyamushosho 2017; Selier 2007). Freehold land is used for a wide range of activities such as game ranching, commercial crop and animal farming (Selier 2007). Additionally, some of the freehold lands have been converted into game and nature reserves which include the Northern Tuli game reserve in Botswana and the Mapesu game reserve and Venetia nature reserve. South of the Venetia nature reserve there is the open-pit Venetia diamond mine. The state land, which is land set aside from communal and private use by the state to protect the biodiversity in the confluence area, includes Mapungubwe National Park in South Africa and the Tuli Safari Area in Zimbabwe. The communal lands are mostly used for animal and crop production by subsistence farmers. In summary, the Botswana side of the confluence is dominated by private game reserves, while in the South African side mining areas, national parks and private reserves cover the majority of the land. The Zimbabwe side of the confluence is dominated by communal lands which are currently utilised by agropastoral farmers. As a result, this study detected a lot of possible historical agropastoral features in the Zimbabwe side of the confluence.

1.5 Archaeology of the Shashi- Limpopo Confluence Area: a brief summary

The SLCA has been occupied by human societies from the early Stone Age to recent periods, leaving various traces of human occupation. Archaeological research in SLCA has focused more on the South African side of the confluence (Antonites 2016; Calabrese 2000; Du Piesanie 2009; Fagan 1964; Hall and Smith 2000; Hanisch 1980; Huffman 2007a, 2011, 2012;

Huffman et al. 2013; Kuman et al. 2005; Le Baron et al. 2010; Meyer 2000; Raath 2014; Schoeman 2006; Smith et al. 2007). Fewer archaeological studies have been conducted on the Zimbabwe side (Bandama et al. 2018; Chirikure et al. 2014; Garlake 1968; Manyanga 2007; Manyanga et al. 2000; Nyamushosho 2017) and Botswana side (Forssman 2013; Forssman and Pargeter 2014; Mosothwane 2011; Mothulatshipi 2008; van Waarden 1979; Walker 1994) of the confluence. Overall, the majority of the aforementioned archaeological researches in the SLCA has focused around the understanding of the development of early complex societies, linked to the establishment of the Mapungubwe culture, because of the rich archaeological record and the abundance of evidence for farming societies in the region (Calabrese 2000; Huffman 2007a, 2009a; Meyer 2000; Smith et al. 2007; Steyn 1997; Voigt 1983). Nonetheless, some research on the Stone Age periods of occupation has been conducted (Cooke 1960; van Doornum 2014; Eastwood and Blundell 1999; Forssman 2013; Pollarolo et al. 2010; Pollarolo and Kuman 2009; Thackeray 1992; Wilkins et al. 2010). For the purpose of the review here presented, Stone Age sites will be discussed together while sites occupied by farming communities will be divided into two periods being Early Farming Communities and Late Farming Communities.

1.5.1 Stone Age Sites

Early Stone Age (ESA) and Middle Stone Age (MSA) sites in the SLCA are characterised by very few surface scatters of stone tools such as flakes and cobbles, with a massive amount of material (lithics, bones and seeds) being covered by alluvial and aeolian deposits (Forssman 2013; Manyanga 2007; Pollarolo et al. 2010; Pollarolo and Kuman 2009). ESA sites in Southern Africa are difficult to date because the majority of them lack materials suitable for radiometric dating (Klein 2000; Phillipson 2005). However, most of the ESA sites in Southern Africa have been dated in association with sites from east Africa, with the earliest dates being about 2 million years (Klein 2000). Research has shown that sites such as Kudu Koppie have deep deposits of Stone Age material reaching up to 1.80m in-depth, with evidence of stratification between ESA and MSA assemblages and little vertical displacement of material (Pollarolo et al. 2010; Pollarolo and Kuman 2009; Wilkins et al. 2010). These sites are spread out in the confluence area and have different sizes, possibly linked to the purpose they served during their period of occupation. Some sites were industrial areas with much activity taking place around them while others were low activity areas which were used for specific purposes (Cooke 1960; Le Baron et al. 2010).

Late Stone Age (LSA) sites are mostly located in rock shelters formed along ridges caused by erosion. LSA technology began between 40 000 and 12000 years ago south of the Limpopo river (Wadley 1993). These sites are characterised by cultural materials such as rock art, and stone tools which are mostly found on the surface of rock shelters. The art includes rock engravings and paintings depicting some human beings and animals (Manyanga 2007) which might have existed in the area during that period. However, it has to be noted that not all rock art in this study area belongs to the LSA communities, as there are some rock art depictions done by the farming communities which might have used the shelters for ritual purposes (Hall and Smith 2000). These include "finger paintings of zoomorphic and geometric motifs" (Eastwood and Blundell 1999,p. 18). Material remains from some LSA sites in SLCA shows that the LSA and farming communities lived side by side with some possible trade ties (Forssman 2014; Hall and Smith 2000; Mothulatshipi 2008). However, this relations continued into the recent past with the two communities living side by side, especially in areas where resources and space were enough to support the hunting and gathering lifestyle without dependence on farmers (Barham and Mitchell 2008).

1.5.2 Early Farming Communities

Early Farming communities lived in small groups and simple chiefdoms characterised by large homesteads and villages. These societies occupied the SLCA in successive waves. The first group occupied the area during the early years of the first millennium, that is between 350 AD and 450 AD (Huffman 2009a), where they co-existed with the above-mentioned Stone Age foraging communities (Hall and Smith 2000; Van Doornum 2006). The origins of Early Farming Communities that occupied some parts of Southern Africa can be traced back to West-Central Africa (Huffman 1982, 1989a). This group of agro-pastoralists possibly came into SLCA through western Zimbabwe and eastern Botswana (Hanisch 1981a; Huffman 1982; Mitchell 2013; Smith 2005). The aforementioned Early Farming Communities kept domestic animals such as sheep, cattle and goats, cultivated plants, gathered wild fruits and hunted animals (Badenhorst 2010; Pikirayi 2007; Voigt 1986). Although there is no clear evidence as to which faunal remains dominated the assemblages due to poor bone preservation (Voigt 1986), archaeological faunal remains of this period are normally dominated by bones of sheep and/or goats (Badenhorst 2010). Archaeological sites previously occupied by the aforementioned communities are characterised by Happy Rest pottery, and are few or not easily identifiable in the Shashi-Limpopo region (Hanisch 1981b; Huffman 2002; Smith 2005). This

is probably due to the lack of surface material, which might be buried under alluvial deposits in the area (Huffman 2007a).

The second wave of early farming communities occupied the Shashi-Limpopo confluence towards the end of the first millennium AD. This group of agro-pastoralists came from south-west Zimbabwe in about 900AD and have been classified as Zhizo people (Huffman 2007a, 2009a). Sites occupied by Zhizo people in the SLCA include Schroda site (Hanisch 1981a). Excavations by Hanisch between 1975 and 1982 revealed the possible layout of homesteads at this site, and an enormous amount of cultural materials, which includes high concentrations of figurines (Hanisch 2002) described and classified by Hanisch and Maumela (2002). Decorative motifs of pottery remains found at these sites include some incisions and comb-stamping. In general, Zhizo period sites are characterised by large kraal deposits at the centre of the settlement, as such, indicating herding practices within the society. However, most of the Zhizo period sites are located in agriculturally poor soils, a characteristic that has fuelled the notion that Zhizo period people were more traders than agriculturalists (Huffman 2009a). This is also supported by substantial quantities of remains of exotic trade goods which indicate links with the East coast of Africa (Hanisch 1980; Huffman 2009a; Voigt 1983).

Some researchers (Huffman 2007a; Huffman and Kinahan 2003) posit that Zhizo people did not stay for long in the SLCA as they were replaced by Leopard Kopje people who drove them into eastern Botswana. However, research conducted by Calabrese (2000) at Leokwe hill has revealed evidence of coexistence between Zhizo and Leopard Kopje people. Leopard Kopje people went through an organisational transition while in Shashi-Limpopo. Their first capital, K2, was located at the base of Bambandyanalo hill (Figure 1. 2). Societies at K2 organised their settlement according to the central cattle pattern (CCP). The main features of this spatial organisation are: (1) a central cattle kraal with elite burials and storage pits for grains; (2) a men gathering area next to the kraal; (3) an outer residential zone characterised by huts which are arranged according to left/right seniority, with the one upslope behind the court being most senior; (4) the demarcation of space within the house into right for male and left for female (Fagan 1964; Huffman 2000, 2001, 2009a).

1.5.3 Late Farming communities

Late farming communities occupied SLCA during the early centuries of the second millennium AD (Schoeman 2013). This is a period when great social complexity occurred with the development of the first states, ruling elite and sacred leadership amongst the societies within

the SLCA (Huffman 2009a; Kim and Kusimba 2008) and in the broader region, ie Bosutswe (Klehm 2017). The aforementioned changes began when leaders were separated from the commoners during the occupation and establishment of Mapungubwe Hill as the capital of the first state by Leopard Kopje people from K2. Leaders occupied hilltops while commoners settled at the foot of the hill (Huffman 2009a). Stone walls were also built to seclude leaders from commoners and ritual areas from the public domain. Kraals were then moved from the centre of the village while people began to settle in front of the court. However, this settlement pattern change took place only at administration centres, as it is believed that societies which lived in smaller settlements surrounding administration centres continued to have features such as kraals and middens at the centre of their settlements (Meyer 2000). Artefact and ornamental remains at this sites generally comprise of a variety of locally produced and exotic goods such as ceramics, metallurgy and glass beads (Badenhorst et al. 2011; Calabrese 2000; Meyer 2000; Voigt 1983; Wood 2000). Exotic materials were mostly from the merchants in the African east coast who traded goods from China and India.

Research on Late Farming Communities in the SLCA has mostly focussed on Mapungubwe (Huffman 2001, 2007a) thus providing less account of other sites that existed at the same period or later (Calabrese 2000; Voigt 1983). For a long time, Mapungubwe has been regarded as a cradle of social complexity in southern Africa (Huffman 2000, 2009a). However, more recently there has been some research on other parts of the SLCA, especially in Zimbabwe, which has sparked debates concerning the evolution of the aforementioned social complexity. For example, Chirikure et al. (2014) posit that the evidence at Mapela, located about 85 km northwest of Mapungubwe, points to the development of sacred leadership and class distinction two centuries before it developed at Mapungubwe. With regard to the abovementioned arguments, it is evident that there is a need to intensify the archaeological research in other parts of the SLCA, especially in Botswana and Zimbabwe in order to get a balanced account of archaeological events in the area (Mothulatshipi 2008).

Even though there is no mention of Zimbabwe Period (1290-1450 AD) sites, which succeed the Mapungubwe period (1220-1290 AD), in the SLCA there are some reports of Khami sites (1450-1600 AD), which are the later developments of the Zimbabwe Culture and Icon sites associated with Sotho Tswana communities (Huffman 2000, 2007a; Huffman and Du Piesanie 2011). These sites have been associated with the ancestors of the modern-day Venda speaking people (Huffman 2012; Huffman and Du Piesanie 2011). The confluence area continued to be occupied into historic times by agro-pastoralists of Venda, Sotho-Tswana and European

origins, who arrived in the area at different periods of the late centuries of the second millennium AD (Huffman 2012; Huffman and Du Piesanie 2011; Manyanga 2007; Meyer 2000; Mothulatshipi 2008). As discussed in 1.3.3 Land tenure systems, the present land use is generally characterised by freehold, communal lands and state land which are mainly used for game ranching, crop and animal production. The archaeology located in ranching areas is generally better preserved than the one in crop-producing areas.

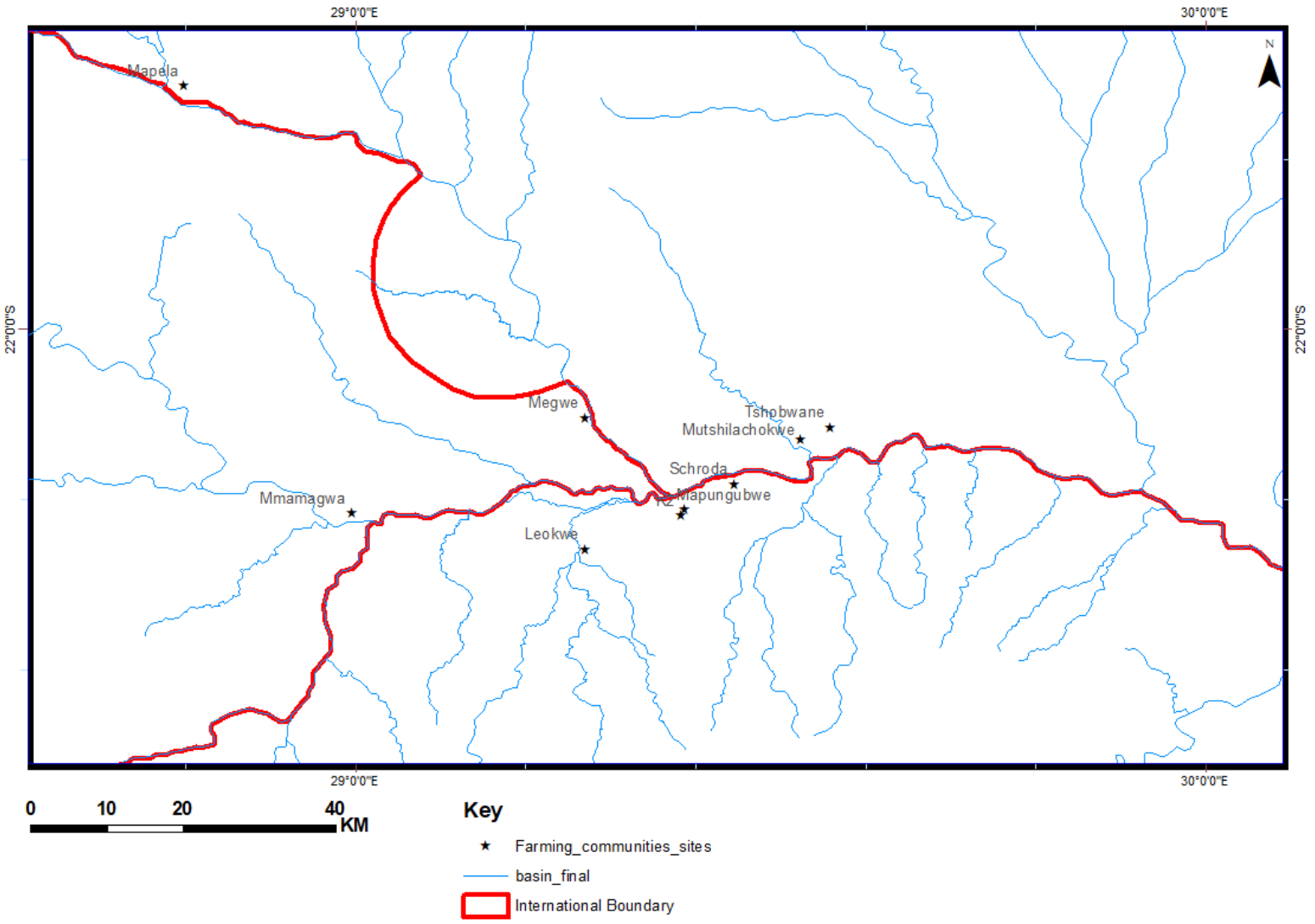

Figure 1. 2 Map showing the location of farming communities sites mentioned within the text

1.6 Structure of the thesis

This thesis is made out of a collection of seven chapters, five (2-6) of which have either been published as articles or are in preparation for publications in peer-reviewed journals. The five chapters which have been published or are in preparation for publication have been presented in standalone format, with each having its aims, results and discussion. The single chapters' conclusions collectively address the main aim of the study. Very few changes if any were done to the content of the published papers. Consequently, the aforementioned approach creates some recurrences of method description and illustrations, unavoidable under various chapters. However, this downside is reasoned to be insignificant when taking into account the fact each chapter is peer-reviewed as a standalone paper which can be independently read without losing the meaning. Overall, the thesis has seven chapters including (this) introductory chapter, which gives the background, justification and general aim of the study. **Chapter 2** explores relevant literature on the use of remote sensing in African archaeology. It identifies the most common remote sensing techniques used in archaeological applications within the African continent. It also assesses the patterns of the use of remote sensing techniques in archaeological research in Africa. **Chapter 3** investigates the possibility of discriminating natural soils (non-sites), ash middens, vitrified dung and non-vitrified dung from each other using in situ spectral measurements. This chapter also provides some analysis of the chemical components of non-sites, ash middens, vitrified dung and non-vitrified dung. **Chapter 4** resamples the hyperspectral data to spectral resolutions of different satellite and test their ability to discriminate natural soils (non-sites), ash middens, vitrified dung and non-vitrified dung. **Chapter 5** assesses the feasibility of detecting archaeological sites characterised by surface features through the use of high-resolution satellite imagery and advanced classification algorithms. **Chapter 6** assesses the possibility of predicting the locations of archaeological sites characterised by surface features using very high-resolution satellite image and object-

based classification algorithms. Lastly, **Chapter 7** provides a synthesis of the study and the summary of the outcomes. It concludes by underlining the major findings of the study and their implications on archaeological research. It highlights the limitations of the current study and outlines recommendations for future studies. A single reference list is given at the end of the thesis. This study contributes towards developing fast, cheap and systematic methods of surveying, documentation and monitoring archaeological sites, which will help to improve site inventories and management of archaeological heritage in southern Africa and the world.

CHAPTER TWO

2. The use of remote sensing techniques in archaeological applications in Africa: a review

This chapter is based on:

Thabeng, O. L., Merlo, S. and Adam, E., (In Preparation). "The use of remote sensing techniques in archaeological applications in Africa: a review."

2.1 Introduction

Archaeologists and heritage managers world over have been involved in surveying, documenting and monitoring archaeological heritage sites for effective management, preservation and research (Cleere 1989; Salman et al. 2010; Van Ess et al. 2006). Traditionally, surveying, documenting and monitoring archaeological heritage sites by archaeologists and heritage managers has been done through intensive fieldwork which is time-consuming, costly and difficult to carry out over some areas, especially conflict zones (Biagetti et al. 2017; Connah 2008; Van Ess et al. 2006). The use of remote sensing has made it possible for archaeologists to document and analyse buried archaeology without any excavations (McCauley et al. 1982), study inaccessible war zones (Biagetti et al. 2017; Schmid et al. 2008; Thomas et al. 2008) and cover large areas within a short period (Clark et al. 1998; Corrie 2011). In some cases, high temporal accuracy and the archival nature of remote sensing data proved to be essential for archaeological site monitoring (Blasco et al. 2017; Parcak 2007; Rayne et al. 2017). As a result, a number of papers and textbooks on the use of remote sensing in archaeology have been published, and some reviews have been done on the ability of different remote sensing sensors from different platforms, application of different image processing methods in prospection and monitoring of archaeological sites. These include reviews by scholars such as Challis and Howard (2006) who reviewed the use of remote sensing at different scales of analysis in alluvial geoarchaeology. Myers (2010) gives a review of the benefits and challenges incurred in the use of satellite images loaded on Google Earth program in both archaeological research and heritage management. Leisz (2013) gives an overview of the history of remote sensing in archaeology by giving a historical account of different platforms and sensors which have been used for archaeological survey in the twentieth century. Lasaponara and Masini (2013) provided an overview of limitations, challenges and their solutions on the use of remote sensing in archaeological surveys and monitoring. A regional overview on the use of remote sensing in archaeological research was given by Corrie (2011) with a specific focus on the use of satellite images in Egyptian archaeology and the Middle East. Despite the wide use of remote sensing applications in archaeology, there is no review on the trends of remote sensing applications in African archaeology, at least known to this research at present. This review, therefore, focuses on the use of remote sensing techniques in the context of African archaeology.

2.2 African biomes and application of remote sensing

The African continent is characterised by a number of ecological regions ranging from deserts, shrubland, grasslands, forest, woodland, bushland and thickets (Figure 2.1). Different human societies occupied and interacted with these biomes through time (Barich 2014, 2016; Denbow 2012; Hassan 2002; Liverani 2000; McBrearty and Brooks 2000; Mercader 2002; Mitchell 1997; Oslisly et al. 2013; White and Oates 1999). The aforementioned biomes varied significantly in nature and latitudinal location throughout the long period of human habitation in the continent which resulted in the differential distribution and preservation of archaeological sites across the continent ie.archaeological remains characteristic of wet periods being now detected in desert areas like the Sahara or the Kalahari desert (deMenocal 1995; Hassan 2002; Huffman 2008; Jahns 1996; Kröpelin et al. 2008; Salzmann and Hoelzmann 2005; Tierney et al. 2017) Moreover, each biome has its unique context including land cover, seasonality and weather which have different effects not only on the preservation of archaeological materials but their level of visibility and the survey. For example, dense vegetation in rainforests obscure archaeological materials and presents difficulties in accessing the forest during the survey (Denbow 2012). Furthermore, the general acidic nature of the soils in rainforest leads to poor preservation of bones (Meister 2008; Mercader 2002). On the other hand, desert environments present a well preserved archaeological record with some of the materials being clearly visible on the surface (Churcher et al. 1999). Surveying and documenting the traces of ancient anthropogenic activities within present-day biomes need to take into consideration the effects of each biome on the visibility and accessibility of archaeological material. Notwithstanding these considerations, the benefits of remote sensing in surveying and documenting surface and sub-surface archaeological features in various biomes has been recognised by archaeologists (Bennett et al. 2013; Biagetti et al. 2017; Denbow and Wilmsen 1986; Doneus et al. 2008; Evans et al. 2013; Mason 1968; Parcak 2007). These benefits include the ability to use proxy archaeological indicators such as vegetation and soil marks to identify buried archaeological features (Agapiou et al. 2012a; Bennett et al. 2012; Lasaponara and Masini 2007; Reid 2016). Ecological regions with similar preservation and visibility prospects for remote sensing applications in archaeology have been grouped in the discussion below in three broader areas: 1. Deserts, 2. shrubland and grassland and 3. forest, woodland, bushland and thicket and the potentials and limitations of remote sensing application in them have been highlighted.

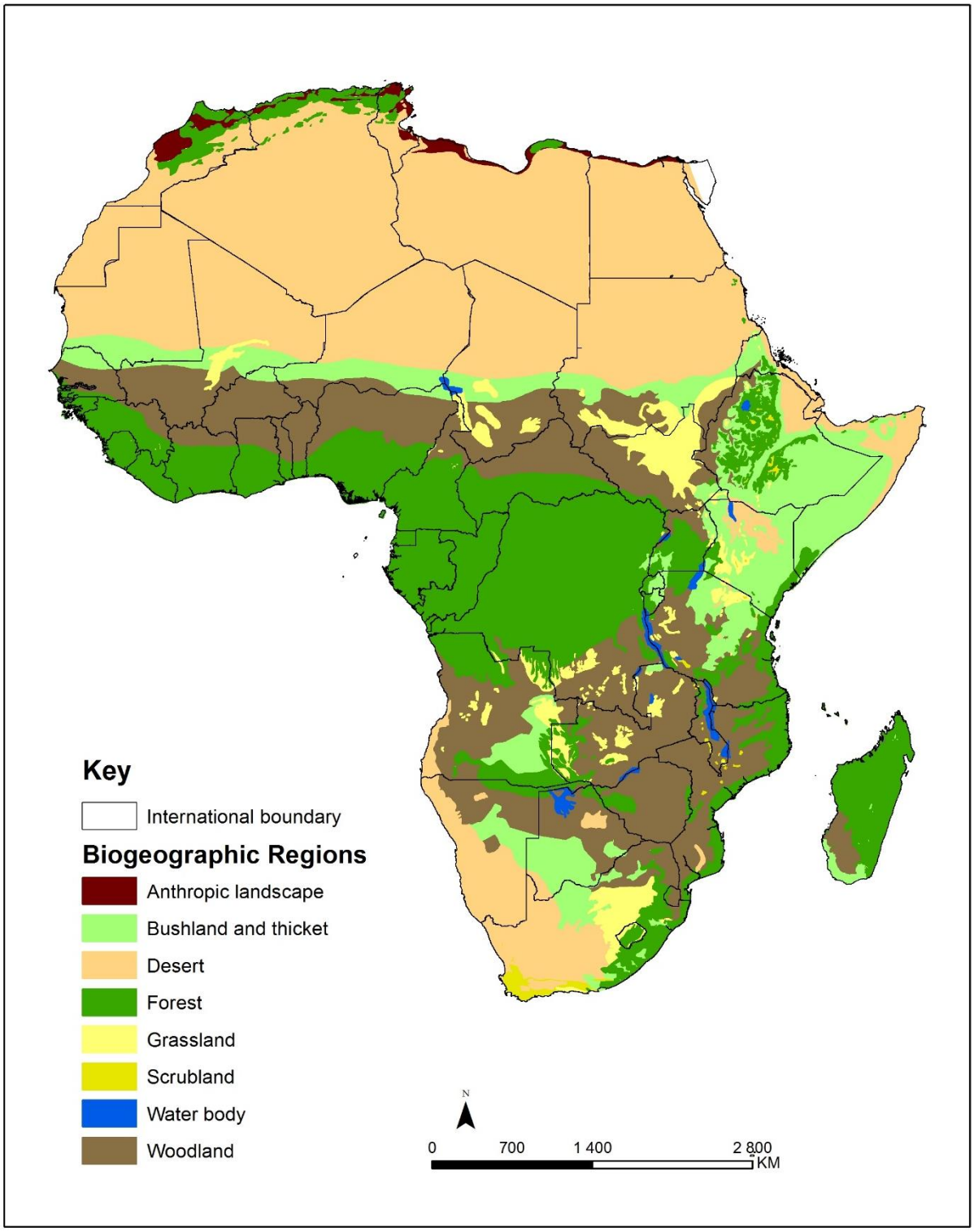

Figure 2. 1 The generic distribution of biomes across the African continent. The biogeographic region map has been modified from White (1983) and Burgess et al. (2004).

2.2.1 Desert

African deserts consist of barren seas of sands, gravels and rocky peaks (Lovegrove 1993; Ward 2009). Vegetation grows mostly on areas with the ability to temporarily or permanently host some moisture such as riverbeds (wadis), depressions and areas where there is surface water seeping from underground aquifers (Lovegrove 1993; Malika et al. 2015; Van Zinderen Bakker 1975). Vegetation in African deserts comprises of a wide variety of species which varies depending on local conditions (El-Amier et al. 2015; Foissner et al. 2002; Jürgens 1991; Lakhdari and Dehliz 2016; Lovegrove 1993; Schulz et al. 2009; Treichel et al. 1984; White 1983).

Researchers have used a wide variety of remote sensing techniques to document and survey for archaeological sites in desert areas, most of which were densely occupied by humans during wet periods prior to their early Holocene desertification (Biagetti et al. 2017; El-Baz et al. 2007; Gaber et al. 2013; Parcak et al. 2016; Sterry et al. 2011). The use of remote sensing for the detection of sites in desert environments has been largely focused on archaeological materials which are noticeable on the landscape through visual inspection (Altaweel 2005; Biagetti et al. 2017). The visibility of archaeological material on the desert landscape is facilitated by its lower ratio of vegetation to the soil. Nevertheless, depending on the spatial resolution of the sensor that is used to capture data, small features may be invisible on satellite images and thus be missed during the survey. Most of the archaeological features in the desert were also constructed using materials from their surroundings; as such it is problematic to map them using semi-automatic and automatic image classification approaches. Hence the need to visually inspect the images for archaeological features, a process which is laborious and time-consuming especially when the study area is big. Furthermore, the majority of archaeological materials in the deserts have either been deflated by wind or buried deep under sand deposits (Nsanziyera et al. 2018). This presents a challenge when using remote sensing techniques to map archaeological features in the desert environment, especially features which are buried under sand deposits because optical sensors cannot penetrate the soil surface. In studies where paleo-environments were considered, features such as paleo-hydrologic networks which are buried under sand have been mapped using radar sensors because of their ability to capture data below the earth surface (Blom et al. 2009; Farr and Paillou 2012; McCauley et al. 1982, 1986). However, the complex nature of radar data processing and interpretation tools makes its use unpopular in archaeological applications (Nsanziyera et al. 2018). More recently, studies employing geographic information systems and remote sensing techniques have also used a

combination of vegetation and paleo-hydrological network as proxy indicators of archaeological sites in a desert environment (Biagetti et al. 2017; Bubenzer and Riemer 2007; Nsanziyera et al. 2018).

2.2.2 Shrubland and grasslands

Shrubland and grassland regions consist of short vegetation generally being 2m of height or less, perennial and annual grasses (Cilliers et al. 2004; Djoudi et al. 2013; Hassan 2011; Snyman et al. 2013; White 1983). The vegetation cover in these biomes is highly diversified with thousands of species spread across the landscape depending on the rainfall patterns, anthropogenic activities, soils water retention ability, soil types and altitude, because of its influence on the micro-climate (Ajbilou et al. 2006; Diarra 1988; Le Houérou 2001; Milton and Dean 2000; White 1983). The environmental conditions in shrublands and grasslands have proven to be conducive for using remote sensing techniques to identify archaeological features in the landscape due to their prominence, resulting from shorter vegetation cover, which makes a number of prominent features (graves, mudbrick and stone walling structures, ditches, field systems) highly visible (Fowler 1996; Sadr and Rodier 2012). As such, a number of studies have investigated the potential of identifying archaeological features in shrubland and grasslands regions using groundborne, airborne and spaceborne sensors (Lasaponara et al. 2011; Mumford and Parcak 2002; Sadr and Rodier 2012). The most common proxy indicator used to identify areas of archaeological activity within the shrub and grassland are vegetation marks, which appear as variation in vegetation growth patterns or health status (Agapiou and Hadjimitsis 2011; Bennett et al. 2013). Additionally, evidence of short and long-term impacts of human settlement patterns on ecology (such as the variation of the chemistry of soil) can be used as evidence of prior human occupation in these biomes (Bennett et al. 2012; Marshall et al. 2018; Masini et al. 2009).

The major limitation of using remote sensing in a landscape characterised by grasses and shrubs is that majority of both surface and subsurface features get hidden by vegetation during the wet season (Bennett et al. 2013; Sadr 2019). Furthermore, proxy indicators are more effective in arable areas than non-arable areas and therefore cannot be applied to wider archaeological environments where spectral differences are insignificant (Bennett et al. 2013). This is further elaborated, with examples, in section 2.4.3

2.2.3 Forest, woodland, bushland and thicket

Forest, woodland, bushland and thicket biomes are characterised by deciduous and non-deciduous vegetation with a height of 2 m and above (Cumming et al. 1997; Geldenhuys and Golding 2008; White 1983). Vegetation varies in richness and composition within and across the aforementioned biomes depending on the rainfall gradient, soil types and altitude with some areas being characterised by more than 8500 plant species of higher plants (Chirwa et al. 2008; Fayolle et al. 2014; Gole et al. 2008; Hart 1995; Myers 1988; Otto et al. 2013; White 1983). Vegetation in the forest, woodland, bushland and thicket biomes forms a canopy covering at least 40% of the area in woodlands to 100% in forest areas (White 1983).

Researchers have used passive and active remote sensing datasets for a number of archaeological applications in the forest, woodland, bushland and thicket biomes based on variations in the vegetation patterns resulting from anthropogenic disturbances of soil chemical and physical properties (Clark et al. 1998; Devereux et al. 2005; Evans and Fletcher 2015; Garrison et al. 2008; Saturno et al. 2007). These include variations in species composition (Denbow 1979; Reid 2016; Sever and Irwin 2003) and vegetation growth (Clark et al. 1998). In a study aimed at identifying grave mounds in the Altai Mountains forest, Caspari et al. (2014) used images from IKONOS-2. They identified grave mounds which stood out from the surrounding landscape as circular vegetated features. However, investigations on the use of remote sensing techniques in archaeological applications have revealed that an increase in vegetation cover leads to difficulties in detecting subsurface and surface archaeological features, especially when using datasets from passive sensors (Doneus et al. 2008; Sittler 2004). In order to curb the aforementioned limitation of passive sensors, researchers have used active sensors to map archaeological sites underneath vegetation because of their ability to penetrate vegetation cover (Crow et al. 2007; Devereux et al. 2005; Doneus et al. 2008). For example, airborne light detection and ranging (LIDAR) has been used to map sites under woodlands in Britain (Crow et al. 2007), the settlement of Caracol covered by forest in Belize (Chase et al. 2011), medieval capitals of the Khemer empire beneath forests in Angkor (Evans et al. 2013). In the African continent, Sadr (2019) successfully used LIDAR data to map the stonewalls of a precolonial Tswana capital, now known as Kweneng, which are hidden beneath vegetation about 35 km south of central Johannesburg on the foothills of the Suikerbosrand massif. The cost of LIDAR data and the technical challenges, more especially during the planning and collecting data in remote areas of the forest using LIDAR, prohibits its wide use in archaeological applications (Fernandez-Diaz et al. 2014). Most of archaeological material in

densely vegetated areas remain undetected and hidden under vegetation thus leading to the incomplete presentation of archaeological records and imbalanced interpretation of the archaeology of the affected areas (Crow et al. 2007; Sadr 2019).

2.3 Archaeological traces in the African continent: a broad review

African archaeology is highly diverse, nevertheless the past societies which occupied the continent can generally be grouped into hunter-gathers, pastoralists, early farming and complex societies based on the lifestyles (Connah 2004; Phillipson 2005). Due to variations on how humans utilised and affected their environment throughout their stages of development, a brief description of sites previously occupied by past human societies and a discussion of their possible visibility on the landscape are provided below. This is fundamental in understanding the types of archaeological traces in the continent and the possibilities of detecting them using different remote sensing approaches.

2.3.1 Hunter Gatherers

Hunting and gathering lifestyle began during the Pleistocene period in Africa (Kusimba 2005). Hunter-gatherers colonised and occupied a wide variety of areas, with enough resources for their subsistence (Cornelissen 2013; Phillipson 2005). There is notable lack of evidence of hunter gatherer occupation in forested areas probably due to lack of edible plants in them, more especially during dry periods (Bailey et al. 1989; Hart and Hart 1986; McBrearty and Brooks 2000). However, improvements in technologies such as fishing are believed to have reduced the size of space needed to sustain one person and enabled hunter gatherers to spread to previously inhabitable areas (McBrearty and Brooks 2000). It is difficult to ascertain when the hunter-gathering lifestyle began in many parts of the continent (Kusimba 2005). However, research into the development of modern culture within the hunter-gatherer societies has shown that it evolved from about 100,000years ago in sub-Saharan Africa (Brown et al. 2009; Henshilwood et al. 2001, 2009; Lombard 2013). Generally, modern culture is characterised by the development of cognitive complexity and differences in cultural adaptations which facilitated human expansion into a wide variety of challenging environments (Henshilwood et al. 2001; McBrearty and Brooks 2000). The aforementioned behaviour spread out of Africa about 60,000 years ago with anatomically modern human beings (Fagan 2012; Henn et al. 2011). Hunter-gatherer societies occupied open air spaces, rock shelters and caves close to permanent water sources (Basell 2008; Shea and Hildebrand 2010) and raw materials for artefacts (Barich 2016; Pollarolo et al. 2010). The majority of the aforementioned sites are

characterised by surface scatters of lithic artefacts, which in most cases are the sole indicator of the sites (Cornelissen 2013; McDonald 2009b; Pollarolo et al. 2010), with often (but not always) poor stratigraphic context. Poor and shallow stratigraphic deposits which characterise most hunter gatherer sites are mostly associated with low population densities and their nomadic lifestyles (Barich 2016; Kusimba 1999; McBrearty and Brooks 2000; Plug 1998). Thin deposits resulting from high mobility and low population densities also led to poor preservation of organic materials in most open air sites (Barich 2016). However, there are a number sites, most of which are rock shelter/cave sites such as Ghar Cahal in Morrocco (Bouzouggar et al. 2008), Kintampo rock shelters in Ghana (Stahl 1994), Mumba in Tanzania (Gliganic et al. 2012), White Paintings rock shelter in Botswana (Robbins et al. 2000) belonging to hunter gatherer societies, with deeply stratified deposits indicating frequent re-occupation. As a result, this has led to over-representation of caves and shelter sites in the studies of hunter gatherer societies (Coulson et al. 2011; McIntosh and McIntosh 1988; Shea and Hildebrand 2010). Other material culture indicative of later hunter-gatherer sites which is also mostly found in rock shelters/caves and includes bone tools, rock art, ornaments and hearths (Ambrose 1998; Kusimba 1999; Villa et al. 2012; Warfe 2003). In addition to the aforementioned indicators, North African sites previously occupied by late hunter-gatherers during the Holocene period are also characterised by pottery and remains of semi-permanent housing structures indicating some form of sedentism within the societies (Barich 2016; Garcea 2004; Haaland 1997).

Sites previously occupied by semi-sedentary hunter gatherers do have potential for the application of remote sensing in their surveying and mapping. However, hunter gatherer societies which occupied most parts of the African continent were nomadic and lived in low population densities which resulted in them having insignificant impact on the landscape. As such, it is difficult to visually detect these sites on the landscape through walking surveys or use remote sensing to detect them. At present, there are no known cases where remote sensing applications were successfully used to detect archaeological sites previously occupied by hunter-gatherers, besides a study in the Sahara (Biagetti et al. 2017).

2.3.2 Pastoral societies

Pastoralism in Africa occurred before the domestication of plants (Ambrose 1998; Henshilwood 1996; Marshall and Hildebrand 2002; Von Den Driesch and Deacon 1985). Pastoralism began in the Sahara between 10000 and 8500 BP (di Lernia 2013; Marshall and

Hildebrand 2002) with the domestication of cattle in Bir Kiseiba and Nabta Playa regions as a response towards the increasing aridity and unreliable rainfall by hunter gatherer societies. It later spread to other Saharan regions (Smith 1992). Sheep and goats were introduced at a later period from the Levant (Garcea 2004). The earliest evidence of domesticated animals south of the Sahara coincides with climate change, end of humid African phase, during the fifth millennium BP in Central Eastern Africa (Ambrose 1998; Marshall et al. 1984). In other areas south of Sahara such as West African woodland savannah pastoralism began around 3000 BP (Breunig et al. 1996; Stahl 1986; Watson 2010) and about 2000 BP in the southern tip of Africa (Klein 1986). Dissimilar to West and North Africa, earliest pastoralists in East and Southern Africa kept ovicaprines before cattle (Ambrose 1998; Henshilwood 1996; Von Den Driesch and Deacon 1985).

Generally, pastoral societies gathered wild plants and were seasonally mobile in search of resources (Marshall and Hildebrand 2002). Their movement was influenced by social events and other factors which affected their subsistence such as vegetation, rainfall and diseases. These societies mostly occupied rock shelters, caves and open-air sites next to rivers and lakes (Barich 2016; Breunig et al. 1996; Carter and Flight 1972; Causey 2010; Cremaschi and Di Lernia 2001; Lane 2013; Mercuri 2008). In some cases, domestic animals were kept in caves and rock shelters (Cremaschi and Di Lernia 1999). However, in southern Africa, there has been a lack of evidence linking Pastoral Neolithic societies to open-air sites, a phenomenon which Arthur (2008) linked to research methods employed in identifying them. This might be due to the fact that the arrival of ovicaprines in southern Africa did not significantly affect the settlement and subsistence patterns, foraging and hunting animals, of indigenous communities (Sadr 2008).

Archaeological sites previously occupied by pastoral Neolithic societies are generally difficult to identify on the landscape when using both traditional field walking surveys (Arthur 2008; Gifford-Gonzalez 2005) and remote sensing techniques. This aspect has been attributed the low population densities and mobile nature of pastoralists over extensive areas, in search of pasture for animals, which does not allow significant accumulation of materials on the surface (di Lernia and Gallinaro 2010; Garcea 2004; Hildebrand and Grillo 2012). Furthermore, the occupation of specific biomes by pastoral societies is highly dependent on factors such as seasonality, which influence their aggregation and dispersal patterns (Hildebrand et al. 2011; Malville et al. 2008). However, in some cases, pastoral societies intensify the use of their environmental resources by seasonally reoccupying the sites or practising semi-sedentism, as

a result, leaving traces of anthropogenic activity and materials such as grinding stones, hearths and potsherds (Cremaschi and Di Lernia 1999; Cremaschi and di Lernia 1998; Malville et al. 2008; Marshall and Hildebrand 2002). Important regional instances of monumental architecture, such as funerary structures for cattle and human beings, characterise pastoral societies of the Sahara in its entirety (di Lernia 2006, 2013; Wendorf and Schild 1994; Wengrow et al. 2014). Multi-purpose megalithic structures consisting of large stone platforms are also documented in east-central Africa (Hildebrand et al. 2018; Hildebrand and Grillo 2012). The occurrence of the abovementioned archaeological materials provides a possibility for the use of remote sensing techniques in surveying, documenting and monitoring archaeological sites previously occupied by pastoral societies.

2.3.3 Early Farming Communities

Farming communities in Africa first settled in northern Africa from the eastern Mediterranean about 7000 BP (Haaland and Haaland 2013; Kuper and Kröpelin 2006). These societies/culture reached North Africa at different points through the northwestern and northeastern regions (Haaland and Haaland 2013; Morales et al. 2016). They brought in domestic plants such as wheat, barley and pulses (Barich 2016; Marshall and Hildebrand 2002; Morales et al. 2016; Wenke et al. 1988). In west Africa, farming began in the about 4500 BP with the indigenous domestication of pearl millet at Lower Tilemsi Valley (Manning et al. 2011) before being practiced at other sites such as Dhar Tichitt belonging to Tichitt Tradition and Birimi belonging to Kintampo Complex (D'Andrea et al. 2001; D'Andrea and Casey 2002). In central-eastern Africa and southern Africa, farming was introduced by Bantu communities originating from west Africa in areas around Cameroon and the Nigeria borders (Mitchell 2002). Bantu societies have been divided into two groups being the Eastern stream and the western stream (Huffman 2007b). The Eastern stream comprised of communities that moved along the northern fringes of the rainforest towards the Great Lakes, where their secondary relocation down south along the Indian ocean coast occurred (Huffman 2007b). The eastern Bantu of Urewe tradition introduced farming in central-eastern Africa during the third Millenium BP (Schoenbrun 1993). The western stream which comprises the societies that migrated down south along the Atlantic coast and Angolan Highlands (Antonites and Ashley 2016). In southern Africa, farming was introduced during the early centuries of the second millennium BP by Western Bantu of Kalundu tradition and Eastern Bantu of Urewe tradition (Denbow 1986; Huffman 1989a; Klapwijk 1974; Maggs 1984).

The various crops indigenously domesticated in different parts of the continent include African rice, sambar groundnut, baobab and oil palm in West Africa (D'Andrea et al. 2001; D'Andrea and Casey 2002; Fuller and Hildebrand 2013; Manning et al. 2011), sorghum in Sudan (Haaland 1995) and Tef in east Africa (D'Andrea 2008). Although the material remains across archaeological sites previously occupied by early farming communities varies from region to region, they are generally characterised by ceramics, faunal and lithic materials, metal implements and features such as middens, animal byres, and house floors (Badenhorst 2010; Clist 1987; Denbow 1981; Holdaway et al. 2016; Huffman 2007a; Klapwijk and Huffman 1996; Phillipson 2005; Pwiti 1996; Shaw et al. 1993). The monumental architecture includes megalithic funerary structures in north and central Africa (Phillipson 2005). The presence of large features in archaeological sites previously occupied by early farming communities provides the potential for the use of remote sensing applications to record and monitor sites. However, detecting sites belonging to Early Farming Communities in most parts of the continent will be a challenging task because they were generally semi-sedentary, and had low population densities which resulted in them producing archaeologically invisible stratigraphies and insignificant impact on the environment (Huffman 1982; Mitchell 2002). Additionally, their material may be buried under soil deposits where it cannot easily be identified or was not preserved (Huffman 2007a; Phillipson 2005; Shaw et al. 1993).

2.3.4 Complex societies

Social complexity developed at different periods across the African continent within food-producing societies (Fuller and Hildebrand 2013). Researchers have attributed these changes to various factors such as trade links, foreign influence, ecological changes and regional economic growth which variably led to complexity and, at times, social stratification (Bard 1994; Brooks 2006; Hassan 1988; LaViolette and Fleisher 2005; McIntosh and McIntosh 1988; Spear 2000; Wynne-Jones 2007). The development of social complexity among farming communities in the Nile Valley is dated to about 6000 years BP (Bard 1994; Hassan 1988), whilst in other parts of the continent, it is attested at slightly later periods, (Brooks 2005, 2006; Chirikure et al. 2014; Dueppen 2016; Horton 1979; LaViolette 2008; MacDonald 2013; Mattingly et al. 2003; Mattingly and Sterry 2013; Mitchell 2002; Nikita et al. 2011; Ogundiran 2013; Phillipson 2013). For example, the Butana and Gash societies which occupied the Horn of Africa developed social complexity about 5000 years BP (Fattovich 2010) and in Southern Africa, the Leopard Kopje societies which occupied the SLCA in southern Africa developed social complexity in the thirteenth century AD (Huffman 2009a).

The traces of sites previously occupied by complex societies are spread across the continent with the majority of them being characterised by monumental architecture and/or large monumental cemeteries (Bard 1994; Hassan 1997; Huffman 2009a; Munson 1980). These include the stone walls of Tichitt tradition societies (MacDonald et al. 2003; Munson 1980), stonewalled sites in southern Africa (Chirikure et al. 2014; Huffman 2009a), earthworks in the west African rainforest (Connah 2004; Ogundiran 2013), walled Swahili towns, "*D'MT*" polity temples and pillars (Fattovich 2010; Japp et al. 2011; Wynne-Jones and Fleisher 2016). The monumental cemeteries include pyramids in Egypt and Sudan (Andreu-Lanoe 1997), pyramid tombs of the Garamantes (Belmonte et al. 2002; Mattingly 2011) and Islamic cemeteries in the Swahili coast (Baumanova 2018; Wynne-Jones and Fleisher 2016). Remote sensing has been used to identify some of these monumental features, such as the pyramids of at Gebel Barkal (Patruno et al. 2020). However, not all of the sites associated with complex societies are visible on the ground due to a number of factors including poor preservation conditions, materials used for construction, the lifestyle of society occupying the site and researchers survey strategies (Bard 1994; Clist et al. 2015; Connah 2008). For example, the capitals of states in east-central Africa were constructed using non-durable materials and not permanently occupied, as such leaving thin stratigraphic deposits which are invisible in the archaeological record (Reid 2013). This, therefore, means that it might be impossible to detect them using remote sensing techniques due to the limited impact of the societies which occupied them on the landscape. As a consequence, this will lead to an imbalance knowledge of archaeological record of complex societies in the continent as research will be skewed towards the ones who have left more prominent traces.

2.4 Mapping archaeological landscapes using remote sensing techniques

The use of remote sensing techniques in archaeology became common after the First World War, with airborne true colour, panchromatic and infrared film sensors (cameras) as the major source of data. This was triggered by the improvement of camera devices that were used to take photographs, for example by Crawford in the 1920s at Stonehenge (Reeves 1936). Archaeological sites were identified on photographs based on form, variations on the soil colour or vegetation characteristics which are visible in the photograph. Since then, archaeologists around the world have used digital multispectral (wide spectral bands) and hyperspectral (narrow spectral bands) remote sensing data acquired from groundborne, airborne and spaceborne sensors, to study settlement patterns, subsurface features, surface features, and monitor archaeological heritage sites (Agapiou et al. 2012a; Altaweel 2005; Buck

et al. 2003; Cavalli et al. 2007; Deroin et al. 2012; Parcak 2007; Siart et al. 2008; Wilkinson et al. 2006). The use of multispectral and hyperspectral sensors for the detection of surface, buried and semi-buried archaeological features, is based on their added ability to produce an electrical signal that relates with differences in the energy reflected and emitted from materials on the surface of the earth (Agapiou et al. 2014a; b). This information (called spectral signature) varies to different degrees for different materials and is therefore used to identify and differentiate them. In archaeology, the spectral contrast between areas of archaeological interest and their surroundings and the different spectral signatures of different archaeological features can, therefore, be exploited for detection (Corrie 2011; Parcak 2009).

The presence of archaeological features in the soil alters its biological, chemical and physical properties, thus making it different from the surrounding soils (Oonk et al. 2009; Wilson et al. 2008). For example, the presence of walls buried in the soil makes it more compact and less moisture-retentive, whilst buried ditches increase moisture retention (Gojda and Hejcman 2012); areas where animal byres were previously located, have higher phosphorous than the surrounding landscapes (Wilson et al. 2008). These alterations lead to the formation of microenvironments which have different properties compared to the surrounding natural landscape, therefore making them react differently to electromagnetic spectrum waves (Rowlands and Sarris 2007). These microenvironments are referred to as either surface features or proxy site indicators in a case where they appear as soil marks or vegetation marks (Agapiou et al. 2014a; Aqdus et al. 2008; Lasaponara and Masini 2007), can be easily detected at a minimum vertical distance above the ground. Recently, with improvements in both spectral and spatial resolution of remote sensing devices (Fowler 2002) and availability of remote sensing images to a wider community (Osicki and Sjogren 2000), these marks (soil and crop) are captured as anomalies in spectral reflectance both within and beyond the visible spectrum. The various types of archaeological indicators, such as surface features, soil marks and vegetation marks which can be detected through visual inspection and digital processing of remotely sensed data are described below.

2.4.1 Surface features

Surface features are major indicators of archaeological sites (Renfrew and Bahn 2012). The composition of surface features characterising a site varies, depending on the the societies that occupied it (Haaland 1997; Klein 1986; Renfrew and Bahn 2012). These ranges from artefact scatters characterizing Early Stone Age sites to monumental structures on sites previously

occupied by complex societies (Ambrose 1998; Connah 2004; Haaland 1997; Huffman 2009a; Mitchell 2002; Phillipson 2005, 2013; Reid 2013). Traditionally, surface features were detected through the use of aerial photographs based on their shape (Mason 1968; Seddon 1968b). Recently, with the availability of multispectral and hyperspectral data surface archaeological features have been mapped using their spectral properties, in addition to form (De Laet et al. 2015; Rayne et al. 2017; Subias et al. 2013b). However, the size and the type of archaeological materials to be detected by different sensors depends on the spatial and spectral resolutions of the sensor being used (De Laet et al. 2007; Lasaponara and Masini 2011; Luo et al. 2014; Parcak 2007).

2.4.2 Soil marks

Soil properties such as soil moisture content, tone, geometric pattern and texture have been vital in identifying traces of anthropological activities on the surface as soil marks. Differences in soil colour (soil marks) help in the identification of archaeological features (Fowler 2002). These marks may appear as a result of differences in soil texture. Archaeological sites with soils which are coarser than those of the surrounding landscape may absorb more radiation, therefore appearing as a dark patch in an image. This is mostly caused by large pore spaces between the particles which allow more radiation absorbance (Custer et al. 1986). Soil marks can appear in ploughed fields (Lasaponara and Masini 2006) or during a dry period (Beck et al. 2007) as a result of differences in moisture content within the soil. Lightfoot (2008) used aerial photographs to identify outlines of walls dividing space at the old oasis city of Sijilmassa basing to the differences in soil properties such as tone, texture and geometric patterns.

Soil moisture plays a significant role in the identification of archaeological remains in satellite images too (Altaweel 2005; Parcak 2007). Wet soil has a lower reflectance rate of electromagnetic radiation than dry soil, a difference mainly caused by the reduction in light scattering processes and increase in light-absorbing processes (Weidong et al. 2002). As such, moist soil appears darker in remote sensing images while dry soil appears brighter, therefore, any sensor capturing data can pick this up. However, optimum conditions are needed for one to pick the areas of archaeological interest based on moisture variations between the archaeological features and their surroundings. Parcak (2007) used a combination of Landsat 7 images, SPOT 4 and CORONA images to identify tell sites in Egypt. Benefitting from the high temporal resolution of the satellite sensors, she identified a period when the tell sites had a higher moisture content than their surroundings, which as a result, made them have a unique

spectral signature different from the surroundings. Furthemore, Link et al. (2014) used synthetic aperture radio detection and ranging (SAR) to map subsurface archaeological features in the Roman fortress located about 12km west of Deir az-Zor in Syria. Their study demonstrated that SAR has the ability to penetrate dry soil and detect archaeological anomalies in soil composition beneath the surface.

2.4.3 Vegetation

Archaeologists have used several vegetation characteristics as indicators of archaeological sites. This is because the impacts of anthropogenic activities in the soil properties lead to the formation of vegetation microenvironments, which have different properties compared to their surroundings, therefore making them react differently to electromagnetic spectrum waves (Rowlands and Sarris 2007). Generally, these include crop (vegetation) marks indicated by differences in the growth of crops as a result of past human activity in the area, which affected soil physical and chemical properties (Wilson 1975). These affect vegetation such as cereal crops and grasslands (Aqdus et al. 2008; Evans and Jones 1977; Gojda and Hejcman 2012; Riley 1987; Wilson 1975). In the African archaeological context, common ecological indicators appear as differences in vegetation species or growth (Clark et al. 1998; Reid 2016). Denbow (1979) prospected for archaeological sites previously occupied by farming communities in central-eastern Botswana based on microenvironments formed by the differences in vegetation species within archaeological landscapes. The vegetation covering middens from these farming communities' sites formed microenvironments conducive for the growth of *cenchrus ciliaris* grass, within *colophosperm mopane*, acacia and *terminalia* species dominated woodlands. The *cenchrus ciliaris* dominated microenvironments appeared as bright bald spots within the woodlands when viewed from black and white aerial images.

In recent times the use of satellite images in surveying for archaeological sites has led to the use of vegetation indices which capture information about the vegetation beyond the visible spectrum. The most commonly used vegetation index, the Normalised Difference Vegetation Index (NDVI) (Agapiou et al. 2014a; Lasaponara and Masini 2006; Parcak 2009), helps in analyzing the types of vegetation present, the health status of vegetation and understanding the conditions affecting it (Cihlar et al. 1991; Govaerts and Verhulst 2010; Tucker 1979). However, the performance of various vegetation indices differs across archaeological contexts therefore there is always a need to test the accuracies of various vegetation indices in detecting the archaeological features of interest (Agapiou et al. 2012a; Agapiou and Hadjimitsis 2011).

Bennett et al. (2012) has demonstrated that vegetation indices such as Modified Red Edge Normalized Difference Vegetation Index the outperformed the widely used NDVI when mapping archaeological features on the calcareous grassland of the Salisbury Plain, Wiltshire.

2.4.4 Challenges in mapping archaeological sites using remote sensing

Mapping archaeological resources using remote sensing encompasses using a wide range of groundborne, airborne and spaceborne sensors, all of which have external and internal limitations when used in archaeological applications. These limitations may either be a result of environmental conditions or the sensors' spectral and spatial resolutions (Ebert 1984; Fowler 2002; Parcak 2009).

The spatial resolution of remote sensing devices used in archaeological applications determines what can or cannot be detected on the ground (Parcak 2007; Siart et al. 2008). This means that archaeological sites which are smaller than the smallest spatial unit which can be detected by the remote sensing device, will not be detected (Keay et al. 2014; Lasaponara and Masini 2007; Wilkinson et al. 2006). This is because archaeological sites differ in size depending on their material composition (Renfrew and Bahn 2012). Their size ranges from a small distribution of artefacts which can be about 10m² or less in size, up to the distribution of features covering stretches of a few square kilometres (Buck et al. 2003; Denbow 1979; Phillipson 2005; Renfrew and Bahn 2012; Sadr 2003). In using aerial photographs to detect archaeological sites in Botswana, Denbow (1979) was not able to identify middens which were less than 50m in diameter, because they were not visible in the photograph. Earlier satellites produced low-resolution images both in spatial and spectral terms (Challis and Howard 2006; Ebert 1984). Even though the spatial resolution of satellite sensors has improved, there are still some archaeological features which are small enough not to be detected thus leading to a bias towards the discovery of larger archaeological sites, which then results in misrepresentation and interpretation of the archaeological record.

The composition of archaeological material also has an effect on the use of remote sensing in archaeology (Beck 2007; Parcak 2007). In most cases some of the materials making the archaeological features were harvested from the surrounding environment or modern structures being constructed using similar material; for example, modern towns being constructed from the same soil that was used to construct ancient tells (Corrie 2011; Parcak 2007). The aforementioned processes, as a consequence, result in the archaeological resources and their background environment having subtle spectral differences which makes it difficult for remote

sensing to be applied, depending on the spectral and spatial abilities of the sensor, in archaeological researches (De Laet et al. 2007). This is because some sensors, especially hyperspectral sensors, may have spectral bands which are better positioned to detect the subtle spectral difference existing between the archaeological features and their environment.

Environmental factors such as the vegetation and atmospheric conditions can prohibit the detection of archaeological features through remote sensing. This is because the detection of archaeological material using aerial photographs largely depends on archaeological marks that can be seen from the air (Riley 1987) while distinct spectral signatures play a major role when using satellite images (Buck et al. 2003). Vegetation may cover the archaeological features thus obscuring their visibility on photographs and satellite images or obscuring their spectral reflectance (Denbow 1979; Mason 1968; Parcak 2009). Mason (1968) identified most of the stone walls through the ground survey. Atmospheric conditions such as cloud cover may prevent visibility of archaeological features on the images (Parcak 2007). Other factors affecting the use of remote sensing in archaeology include environmental conditions such as vegetation cover (Devereux et al. 2005; Doneus et al. 2008; Pryce and Abrams 2010). Studies have also shown that the visibility of archaeological signatures is affected by seasonality (Bennett et al. 2012; Corrie 2011; Gojda and Hejcman 2012). For example, Parcak (2007) found out that the wet season is the best for detecting tell sites in Egypt because of their high moisture content than their surroundings.

The computing concept of *garbage in garbage out* is critical in collecting, processing and interpreting the remote sensing data because its value is not intrinsic, but rather requires a transformation to become information (Jensen 2015). This is because the methods used, experience and the ability to plan, map features, read and interpret images by the personnel engaged in collecting, processing and analysing remotely sensed archaeological data also play a critical role in influencing the outcome of a remote sensing based study (Cerra et al. 2018; Parcak 2009; Sadr 2016a; Tapete and Cigna 2018). For example, Sadr (2016b) found high variability in the way analysts digitised and classified stone-walled structures of archaeological sites previously occupied by pre-colonial societies in the southern part of Gauteng Province, South Africa.

Research has been done on the application of remote sensing techniques in archaeology by scholars and heritage managers in the African continent. However, limited research concerning the trends on the use of remote sensing, which has been regarded as the cost-effective

systematic way of data collection and monitoring in archaeology, has been carried out (Corrie 2011; Lasaponara and Masini 2011; Tapete 2018). A recent review for the African continent was published by Davis and Douglass (2020), which nevertheless is limited in that it specifically focussed on the use of data from aerial and spaceborne sensors in African archaeology. Furthermore the review highlights some of the data processing methods used by researchers in the continent with without providing a deeper analysis the intensity of their use across the continent. Therefore there is a need for an extensive review that will give a clear representation about the trends on the use of remote sensing techniques in the archaeological applications by researchers who are doing their work in the continent. These include the statistical presentation of data processing and analysis methods used by researchers, locations of the funding institutions and lead authors.

Based on the above challenges and the recent improvements in spectral and spatial resolutions of the remote sensing sensors, it is imperative to review the use of remote sensing in African archaeology and give a reflection of how archaeologists have adopted this technique across the continent. This paper offers a critical overview of the literature on the use of remote sensing in African archaeology. It seeks to establish: i) the remote sensing methods that have been used in archaeological applications across the continent ii), the distribution of remote sensing in archaeology across the African continent and, iii) the location of institutions that the lead authors are affiliated to and the locations of funding institutions.

2.5 Material and methods

2.5.1 Literature search

The search for literature in this review was limited to articles exploring remote sensing applications in African archaeology from 1940 to the first semester of 2019. The search was principally carried out on Web of Science was chosen because it gives access to a number of multidisciplinary databases, comprising 180 000 conference proceedings, more than 80 000 books, and 18000 journals which give a representative account of the wider trend on the use of remote sensing in archaeology. The search was done by using different combinations of search words which are likely to be used in the title, abstract and author keywords of an article on the use of remote sensing in African archaeology. The search words used in this review include; ‘remote sensing’, ‘LIDAR’, ‘aerial photo’, ‘radar’, ‘airborne’, ‘satellite’, ‘archaeology’, ‘archaeometry’, ‘geophysics’, ‘Africa’ and the names of individual African countries. In the instances where country names were not used, the search was refined using countries/regions

from the Web of Science menu, in order to confine the search results to articles published about research in African countries. Furthermore, only two search operators, 'AND' and 'OR' were used to combine the keywords. Topic field tag was chosen in all the searches because it looks for the used search words in the title, abstract, and author keywords of an article of interest. Moreover, the Topic field tag uses Keywords Plus® to search for additional keywords which are relevant to the search and may have been overlooked by the author of an article. The results were manually verified by reading the articles appearing after conducting the search in order to make sure that only papers addressing the use of remote sensing in African archaeology are selected and avoid data redundancy. The literature search focussed on all research papers and conference proceedings where different methods of remote sensing such as geophysics, aerial photography, multispectral satellite and hyperspectral airborne remote sensing were employed for data collection. In addition to the aforementioned searches, further searches were conducted on ScienceDirect databases using search words similar to those used in the web of science as discussed above. ScienceDirect databases offer subscription-based access to 34,000 e-books and 3,500 journals featuring scientific and medical research. ScienceDirect was chosen to supplement the Web of Science searches because of its strength on technology-based research (Samadzadeh et al. 2013). However, ScienceDirect has limited features and does not have the ability to provide information on indexes such as funding information which are available on the Web of Science. As such, the supplementary papers identified in ScienceDirect were then manually added to the Web of Science list prior to analysis. Furthermore, an additional search was carried out on the reference lists of papers which were picked by the aforementioned database searches. The identified papers were added to those from the main searches carried out on the databases, for them to be included in the statistical analysis. However, the search on the reference lists of the chosen articles did not reveal many additional papers, which means only a few papers were not picked by the main searches.

2.5.2 Thematic grouping of literature

Group categories were developed to analyse the content of the research papers which meet the set criteria for the use of remote sensing in the African archaeology. The sections underneath elucidate the various steps of the content analysis.

2.5.2.1 Geographical region

The data was classified based on the African biogeographic regions such as desert, grasslands, woodland, forest, shrubland, bushland and thickets. These biogeographic regions are spread

across the African continent and are not confined to a single geographical region. Biogeographic regions play a significant role in the application of remote sensing in archaeological research as they have the ability to obscure or enhance the contrast of archaeological feature to its surroundings.

2.5.2.2 Publication details

The information on the affiliation of the lead authors, type of publication and year of publication were assessed. Publications were also divided according to the journals on which they were published.

2.5.2.3 Funding bodies

The data on the funding agencies which supports the use of remote sensing in African archaeology was also assessed. This was done in order to investigate the base location of agencies which fund research in the African continent. Data indexed by Web of Science on the funders of research papers was used in this analysis.

2.5.2.4 Remote sensing systems

The articles were grouped into systems, which were used for data collection in order to find out the preferred system. Retrieved literature was then divided according to the methods used when collecting data for each publication. The chosen methods were grouped into geophysical surveys, satellite remote sensing, aerial photography, multispectral and hyperspectral airborne remote sensing. In cases where more than one method was used for data collection, the paper was put into a general remote sensing category.

2.5.2.5 Data processing

The retrieved articles were grouped into methods, which were used for data analysis in order to find out which one is preferred by the researchers. The chosen methods were grouped into visual inspection, image enhancement, supervised and unsupervised classification.

2.6 Results

2.6.1 Publication details

An in-depth literature search for the use of remote sensing methods in archaeological research in Africa revealed 80 journal articles. The first articles identified were published in 1968 and since then there was a single publication every 8 to 11 years until 1996 (Figure 2. 2). The

frequency of publications between years increased from 1996 with at least one publication in every three years or less. Beginning 2007, there were regular publications using remote sensing applications in archaeological research in Africa with at least three or more papers being published each year. Most publications were done in the year 2016, which had a total of 16 articles.

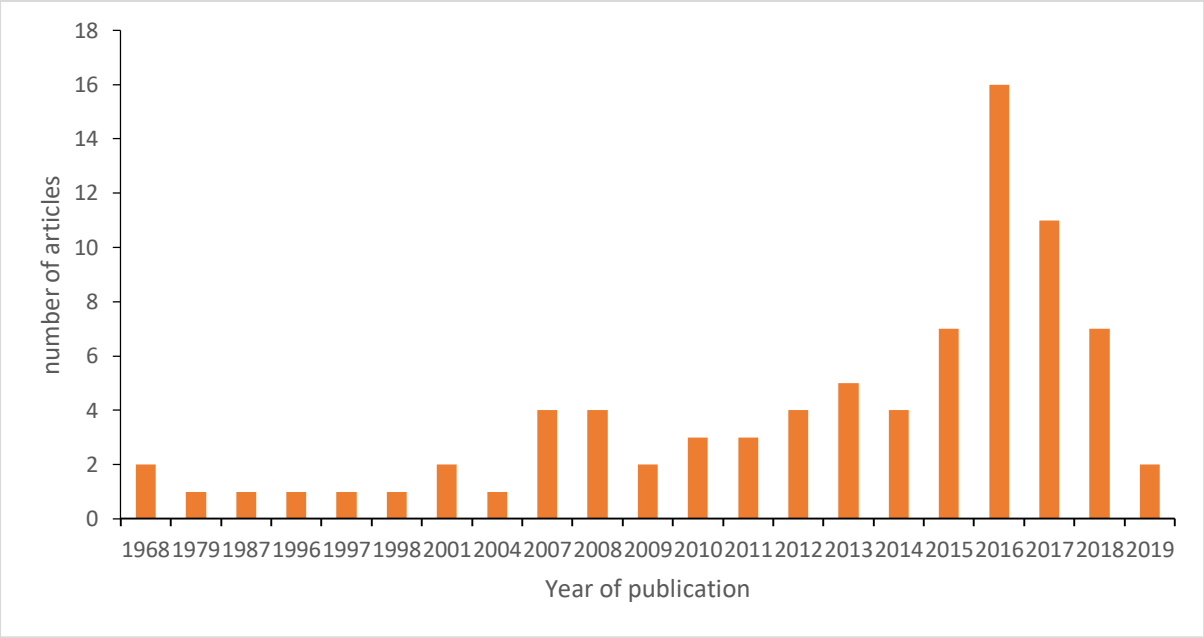

Figure 2. 2 Annual number of published articles, which used remote sensing methods in archaeological research in the African continent

The articles were published in 40 different journals. The majority of the papers were published in international scientific journals, as shown in Figure 2. 3. The Journal of archaeological science was the most preferred journal carrying 10 articles which are 12.19% of the overall publications. Less than half of the articles were published in local and regional journals such as African studies and South African Archaeological Bulletin.

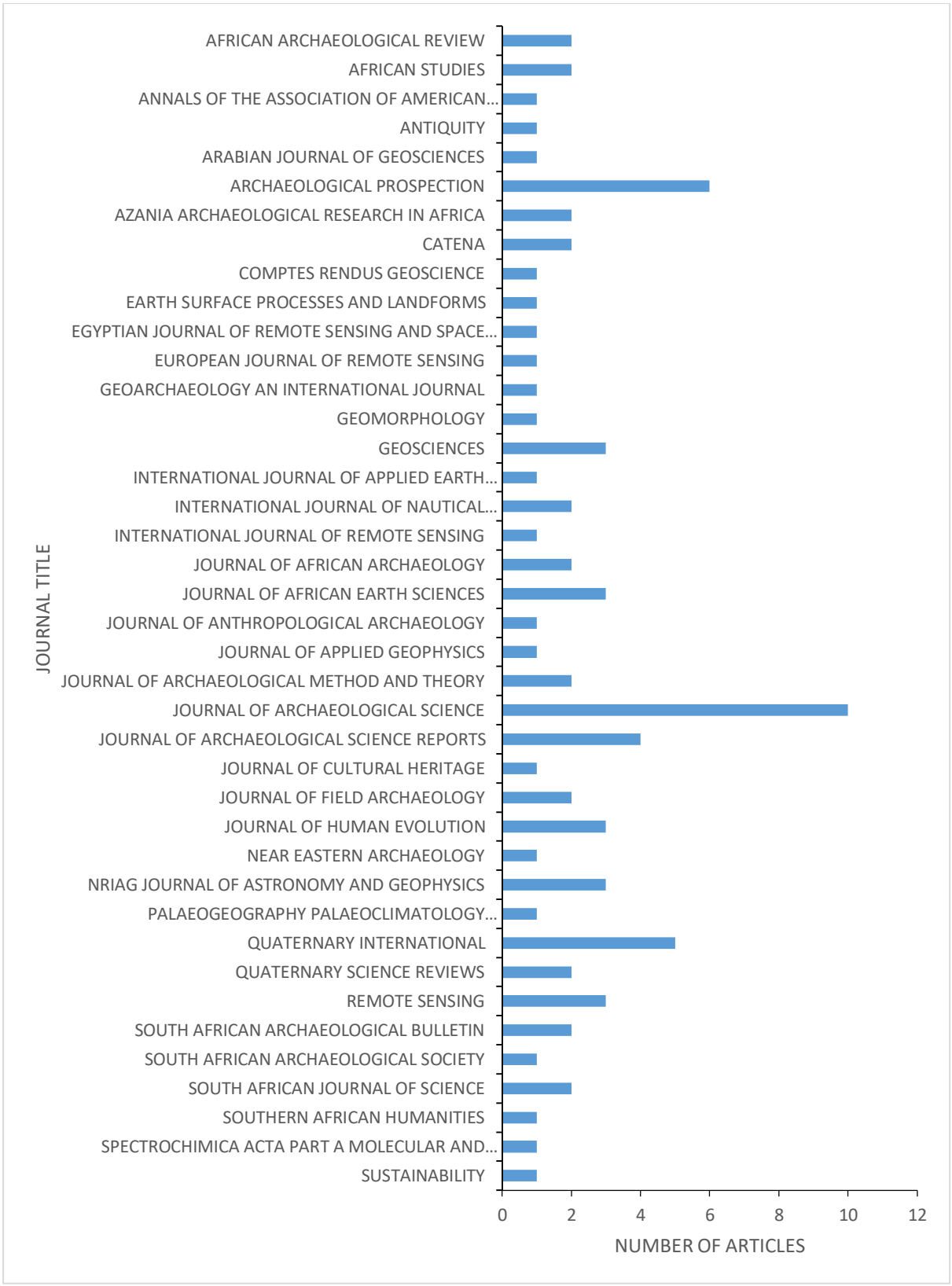

Figure 2. 3 Number of published articles per journal where remote sensing has been used in archaeological applications in Africa.

Researchers who are interested in the use of remote sensing applications in archaeological research in the African continent are based in fifteen different countries across the world (Figure 2. 4). A large number of these researchers are affiliated to foreign institutions. The USA has 19 authors affiliated to its institutions, thus making it the country with most lead authors. UK and Italy are also non-African countries with high numbers of lead authors being affiliated with their institutions. On the other hand, Egypt (10) and South Africa (8) are the only African countries with a relatively high number of authors who are affiliated with their institutions.

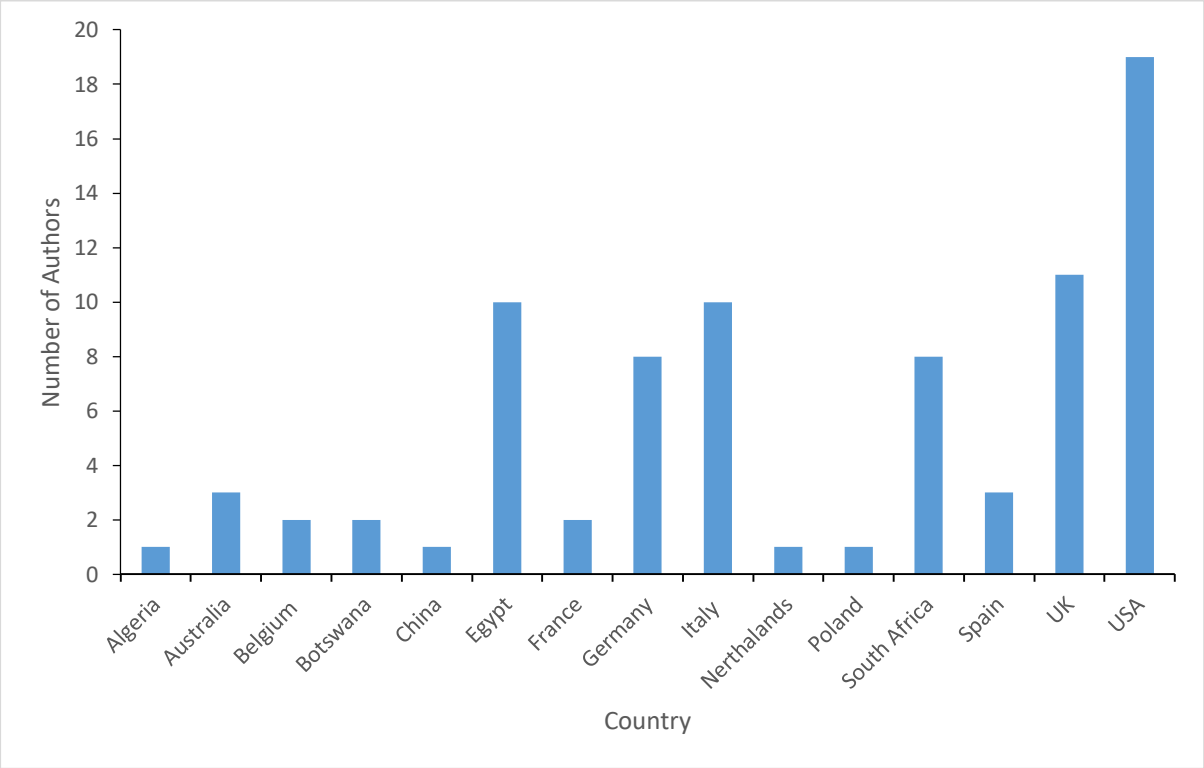

Figure 2. 4 National affiliation of the lead author for remote sensing literature in African archaeological contexts.

Research funding in Africa largely comes from foreign-based institutions. European based institutions contribute 58% of research funds to the African continent (Figure 2. 5). African based institutions contribute only 15% of the funds. Asian based institutions were the least contributing institutions at 1%.

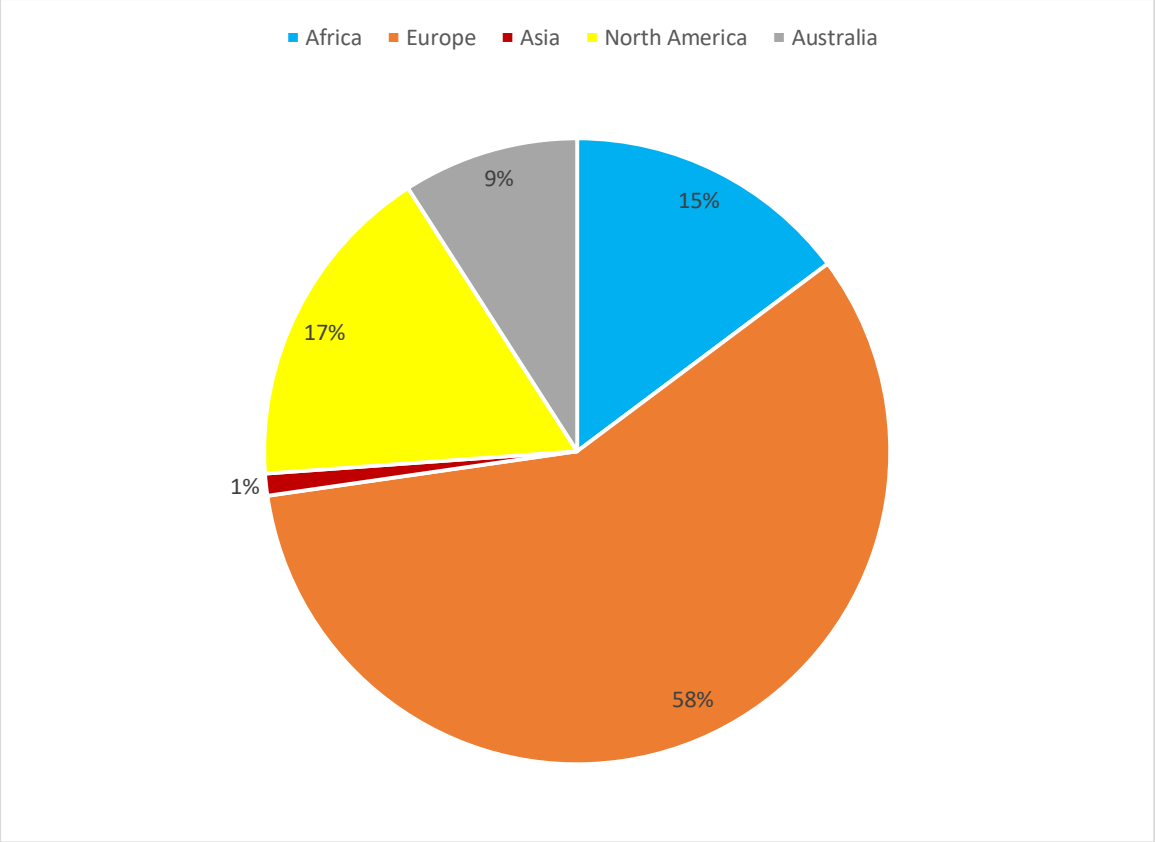

Figure 2. 5 The continental distribution of institutions funding research that adopted remote sensing applications in African archaeological contexts.

2.6.2 Remote sensing systems

The results from this study show that remote sensing data from various groundborne, airborne and spaceborne sensors have been widely used in African archaeology. These include the use of multispectral data from optical and radar sensors aboard satellite platforms. The majority of researchers studying African archaeology used data collected from satellite sensors (Figure 2. 6). Geophysical survey techniques are the second most common method of data collection in African archaeology, with 26% of the studies using it alone and 6% of the studies using geophysical methods in combination with other methods of data collection (i.e. aerial photography and satellite imaging). Only 1% of the studies collected data using a laser scanner.

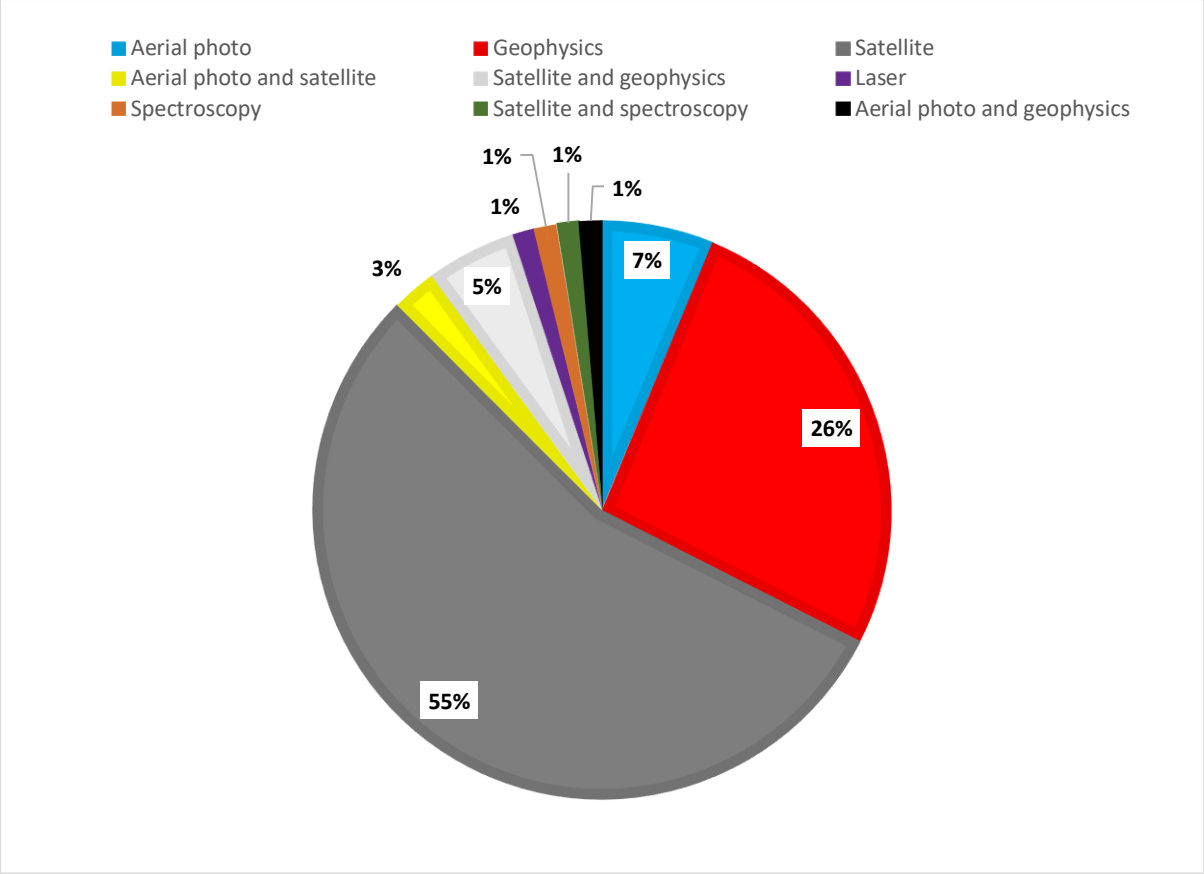

Figure 2. 6 Remote sensing systems used to capture archaeological data in Africa

2.6.3 Data processing

The results of this study demonstrate that researchers who are using remote sensing data for archaeological applications in the African continent prefer image enhancement methods (33). Visual inspection is the second most popular method, with 29 publications, of image analysis amongst Africanist archaeologists using remote sensing data for archaeological applications. Combining two or more data processing methods is uncommon amongst archaeologist doing research in African continent. There were only three publications per each combination of image enhancement & visual inspection (De Laet et al. 2015; Rayne et al. 2017; Subias et al. 2013a), classification & visual inspection (Biagetti et al. 2017; Reid 2016; Salvi et al. 2011) and classification and image enhancement (Blasco et al. 2017; Gaber et al. 2013; Parcak 2007).

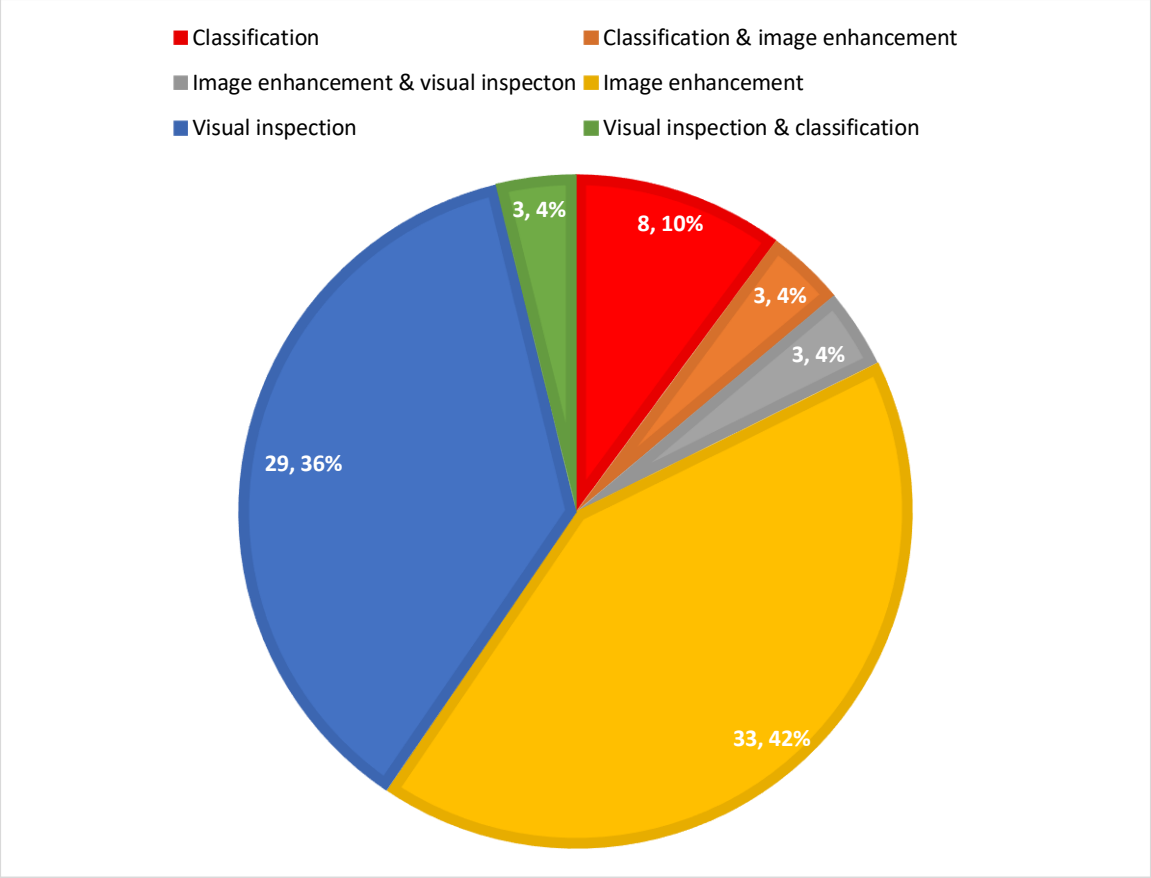

Figure 2. 7 Data processing techniques used for image analysis

2.6.4 Distribution of remote sensing applications in African archaeology

The use of remote sensing applications in archaeological research in Africa is unevenly distributed, as it covers only fourteen countries out of 54 (Figure 2. 8). A large number of researches were carried out in the Sahara desert and grassland environments of Eastern and Southern Africa. Very few researches were conducted in the forest, woodlands and bushland and thickets environments. At the national level, Egypt has 35 publications where remote sensing methods where remote sensing techniques were used in archaeological applications. This made it a country with the highest number of publications where remote sensing techniques were applied in archaeological researches, followed by South Africa with 12 publications. There is a notable lack of research using remote sensing in central African countries, which include Gabon, Democratic Republic of Congo, Congo, Central African Republic, Burundi, Rwanda and Uganda, no publication was recorded.

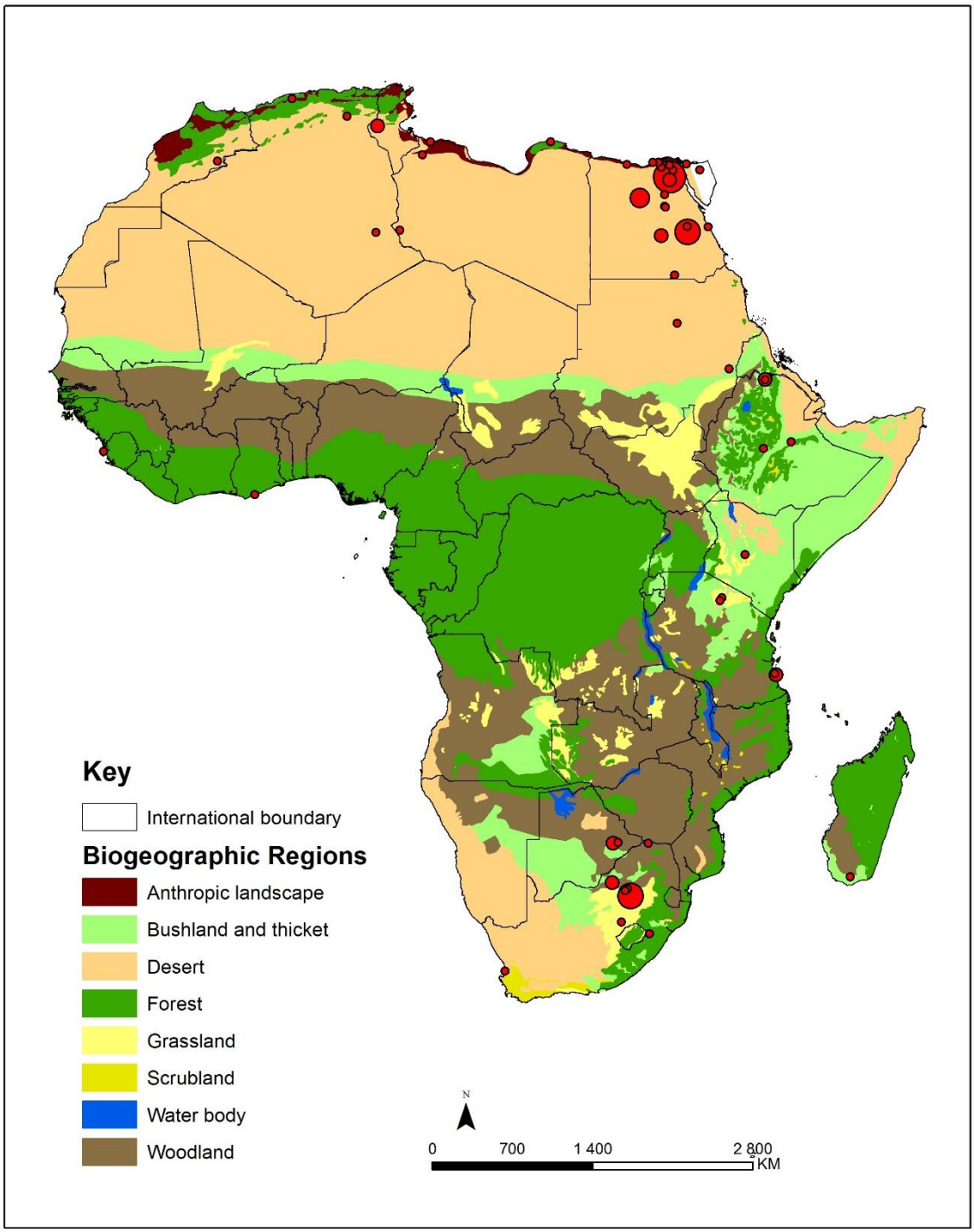

Figure 2. 8 Distribution of research publications in relation to biogeographic regions. The biogeographic region map has been modified from White (1983) and Burgess et al. (2004)

2.7 Discussion

This paper aims to provide a comprehensive review of publications on African archaeology, which used remote sensing applications. This was achieved by a search using Web of Science supplemented by ScienceDirect and reference lists of known articles for studies on the applications of remote sensing techniques in African archaeology. The findings of this study have revealed that remote sensing techniques have not widely been adopted for use in African archaeology. However, this search was not exhaustive because it was only based on English written publications from the two above-mentioned databases and their reference lists. The review shows that very few studies were conducted during the late 20th century. This might be due to the expensive nature of aerial photographs which were widely used during the aforementioned period and the bureaucratic limitations resulting from legislative measures that regulated ways in which aerial images can be captured (Connah 2008; Parcak 2007).

This study shows that most of the lead researchers' in studies where remote sensing techniques were used in archaeological applications and the funds used in those studies are from institutions based outside the continent. This is in line with findings of Schmidt (2006) who posited that funding of archaeological research in the African continent is dependent on foreign researchers and institutions. This might be due to lack funding for African based researchers as governments in Africa prioritise poverty alleviation programmes than archaeological research which is deemed to be of less importance (Chirikure 2013; Pikirayi 2015), less research time and high teaching loads for researchers in institutions of higher learning (Ucko 1993). Hence the need to encourage African countries to channel funds towards heritage researches as an effort to support local researcher's interpretation of archaeology by natives. Furthermore, channelling funds towards intensifying research on local heritage will help improve communities self-esteem, create employment and build national identity (Chirikure 2013). Additionally, the development and use of cost-effective systematic site surveying, documentation and monitoring techniques will encourage local researchers and heritage managers to take a more active part in research and fieldwork.

This review has shown that the researchers who are doing their work in the continent published it in both local and international journals. The most targeted journals were peer-reviewed international scientific journals with high impact factors, which therefore highlights the quality of the researches done in the continent (Garfield 1999; Tahmtan et al. 2016). Furthermore, international journals expose the articles to a wider international audience, such as scholars and heritage managers, therefore increasing their chances of being globally influential in remote

sensing applications in archaeology and cited. However, publishing the data in specialised journals which are published on subscription-based databases might be hampering the spread of knowledge of techniques to other scholars, heritage managers and the interested public, especially in African countries where funding is an issue.

The review has revealed that early archaeological researches based remote sensing techniques employed aerial photographs to map surface archaeological features based on the visibility of their form (Mason 1968; Seddon 1968b) and ecological indicators (Denbow 1979). Despite the success achieved by the previous researches that mapped archaeological sites using aerial photographs, studies surveying for archaeological sites using aerial photography are limited by the fact that it only captures data within the visible spectrum. As a consequence, archaeological sites with characteristics beyond the visible spectrum are missed during the survey. Hence, the need for further research using sensors which can cheaply capture data beyond the visible spectrum.

In recent years with public availability and the improvement of spatial, spectral and temporal capabilities, the ability of various optical and radar satellite sensors in a wide range of archaeological applications in Africa has been investigated. This is in line with the worldwide use of remote sensing techniques in archaeological applications which increased during the late 1990s and early new millennium (Agapiou and Lysandrou 2015). Some of the commonly used data in African contexts include images from optical sensors aboard satellite platforms such as Quickbird-2, WorldView-2, Landsat, CORONA, IKONOS and those loaded on software platforms such as Google Earth (De Laet et al. 2007; Elfadaly et al. 2018; Mondino et al. 2012; Parcak et al. 2016; Subias et al. 2013b). These include a study by Parcak (2007) data from a wide range of satellite sensors such as Landsat 7, SPOT 4, Corona, and Quickbird was used to detect tell sites over large and inaccessible areas in Egypt. The study demonstrated the utility of multispectral satellite images in detecting archaeological sites using spectral signatures beyond the visible spectrum, especially in the contexts where they possess similar visual characteristics with their surroundings. However, the importance of spatial resolution in detecting archaeological features was highlighted in the study by Parcak, as known features that did not meet the required smallest spatial unit that can be detected by SPOT sensor missed during the survey. The archival nature and high temporal resolution of satellite images have also enabled archaeologist to monitor the status of archaeological sites over time and identify hazards that threaten their preservation (Blasco et al. 2017; El-Behaedi and Ghoneim 2018; Salman et al. 2010). In some cases, spectral difference of archaeological data captured by

multispectral sensors has been referenced using field spectroscopy data, due to its high spectral resolution (Salvi et al. 2011; Schmid et al. 2008).

The layout of subsurface archaeological features within an archaeological landscape have been primarily investigated using data from radar satellites (Blasco et al. 2017; Chen et al. 2015; Gaber et al. 2013; Stewart et al. 2013) and geophysical survey methods (Creasman et al. 2010; Fleisher et al. 2012; Klehm and Ernenwein 2016; Parcak et al. 2017). The aforementioned studies proved the worth of remote sensing techniques in improving the knowledge of both surface and subsurface archaeological record in the continent without using destructive methods like excavation.

Researchers across the continent used a wide variety of image processing techniques. The image enhancement techniques were mostly used to improve the visibility of archaeological features and/or proxy indicators in the images (Ginau et al. 2017; Rayne et al. 2017). Mondino et al. (2012) assessed the ability of several image enhancement methods including filtering, density slicing and histogram stretching to reveal invisible archaeological traces of old Egyptian cities at Jebel Barkal. Their findings indicated that image enhancement methods have different abilities to enhance the visibility of archaeological traces captured using bands beyond the visible spectrum. Visual inspection was primarily used to identify archaeological traces which are prominent in the landscape when analysing data captured using airborne and spaceborne sensors (Biagetti et al. 2017; Parcak et al. 2016, 2017; Rayne et al. 2017; Reid 2016; Sadr 2015). Image classification methods were used to discriminate different archaeological features using bands within the visible spectrum (Clark et al. 1998; Reid 2016). Parcak (2007) successfully used unsupervised and supervised classification methods to detect tell sites in Egypt based on the variations on their moisture content. She established that there are moisture content variations between tell sites and their surroundings which are captured by red, green and blue bands of multispectral sensors.

The application of remote sensing techniques in African archaeology is concentrated in areas characterised by open environments such as deserts, shrubland and grasslands (Biagetti et al. 2017; Parcak 2007; Sadr and Rodier 2012). This might be influenced by the ability of sensors to capture data at the surface level with less interference from vegetation in those areas. This review identified only two publications on the use of remote sensing in archaeology, which were carried out within the forests of West Africa. The limited research using remote sensing applications in archaeology within the forests and woodlands of Central and West Africa might

be due to the interference from the vegetation. This is also in line with findings from Pryce and Abrams (2010) who posits that archaeological materials covered by vegetation canopy are not being picked by remote sensing instruments especially multispectral sensors because of their inability to pierce through tree cover. Even though active sensors with the ability to penetrate vegetation cover can be used to curb the aforementioned limitation, their price tag is a huge hindrance to their use in archaeology. Furthermore, Devereux et al (2005) found out that the other limitation to using them is their inability to work well in wet seasons when the vegetation has not lost its leaves. However, some studies in vegetated areas have used vegetation health or type as a proxy indicator of archaeological features covered by vegetation (Clark et al. 1998; Corrie 2011; Denbow 1979; Reid 2016). The other limitations leading to less representation in the above-mentioned African regions might be due to political instabilities hampering research and the language barrier since this search was for English written articles. The publications for researches carried out within Central and West African countries are likely to be published in French because the majority of countries in those regions are French-speaking.

2.8 Future research

Even though there has been some progress on the use of remote sensing in the archaeological applications, research using remote sensing in Africa is sporadic and limited to a few features. As a result, there is a need to assess the possibility of using remote sensing systems with varying spatial, spectral and temporal abilities under different sites, surface conditions and environmental setting in African archaeology. This is because factors affecting the reaction of archaeological features towards electromagnetic radiation are local in nature, therefore each area needs its own spectral signature library as similar materials may react differently under different conditions (Altaweel 2005).

The context of African archaeology is highly variable as discussed above and most of the sites are undocumented due to restricted access, lack of funding and in some cases trained personnel (Chirikure 2013; Connah 2008; Corrie 2011; Mcintosh 1993). Furthermore, a number of both natural and anthropogenic factors threatens the preservation of archaeological heritage in the continent (Blasco et al. 2017; Chyla 2017; El-Behaedi and Ghoneim 2018; Parcak 2007; Parcak et al. 2016; Salman et al. 2010). Hence, the need to develop cheaper, fast and systematic ways of surveying, documenting and monitoring archaeological sites in the continent (Biagetti et al. 2017; Connah 2008; Mcintosh 1993; Parcak 2007). Remote sensing offers the aforementioned capabilities, however, the ability of remote sensing systems to detect most of the surface and

sub-surface archaeological features in the African archaeological context has not been tested. These include the use of remote sensing in mapping archaeological features characterising some landscapes previously occupied by Hunter Gatherers, Pastoral Societies, Early Farming Communities and Complex Societies. Furthermore, in order to exploit properties of archaeological materials which are beyond the visible spectrum, the ability of advanced classification algorithms to work with limited data calls for the assessment of their capability in archaeological applications due to limited nature of archaeological data. Above all, in order to increase the output of remote sensing-based archaeological researches in the continent, there is a need to improve access to remote sensing data and software (Klehm and Gokee 2020). Additionally, where possible, the development of academic courses on remote sensing applications in archaeology in African institutions should be encouraged or encourage archaeologists to take remote sensing courses offered in other disciplines. Since this study revealed that visual inspection of images is the most prefer methods of image analysis, the use of semi-automatic classification methods is also encouraged amongst Africanist archaeologists in order to enable fast, unbiased systematic surveys over large areas (Davis and Douglass 2020).

2.9 Conclusion

The main conclusions of this study are:

1. The use of remote sensing in African archaeology begun during the last decades of the 20th century with the use of aerial photographs. Satellite data is the most widely used remote sensing system in the African archaeology followed by geophysical methods.
2. The use of remote sensing in African archaeology is skewed to open environments such as deserts, grasslands while highly vegetated areas such as forests and woodlands receive less attention.
3. The studies in African archaeology is led by foreign-based researchers and the majority of research funding comes from foreign institutions.

The use of remote sensing techniques provided archaeological data beyond the visible spectrum and facilitated large-scale archaeological site documentation and monitoring, especially in restricted areas. Overall, this study has shown that the application of remote sensing in African archaeology has increased since 2007. However, the research is largely dependent on international researchers and funds. With the recent increase on the availability of open-source high-resolution satellite data, there is a need to train the local researchers on the use of remote

sensing methods and expand remote sensing applications to other archaeological contexts in the continent.

CHAPTER THREE

3. Spectral discrimination of archaeological sites previously occupied by farming communities using in situ hyperspectral data

This chapter is based on:

Thabeng, O. L., Adam, E. and Merlo, S., 2019. "Spectral discrimination of archaeological sites previously occupied by farming communities using in situ hyperspectral data." Journal of Spectroscopy. Spectral Image Processing as a Tool for Analysis of Cultural Heritage: Special issue, 1-21.DOI: https://doi.org/10.1155/2019/5158465

Abstract

The use of remote sensing in archaeological applications is still at its infant stage. Therefore, information on the spectral properties of archaeological features is needed to guide the future developments of multispectral and hyperspectral satellite sensors with bands suitable for archaeological applications. Hence, this study investigates the ability of field spectra measurement to discriminate amongst non-sites ('natural' soils) and archaeological soils from middens (rubbish-dumping areas) together with vitrified and non-vitrified dung from animal byres of farming communities, using soil properties as indicators. First, we used traditional geoarchaeological lab analysis methods (in general expensive and laborious) to identify chemical compositions of different activity areas and tested for variations in the concentration of elements between different soil types using analysis of variance. Feature selection methods, random forest (RF) and forward variable selection (FVS), were used to select important soil elements for the classification of the archaeological sites. FVS is a stepwise regression method which repetitively adds one variable to the model that gives the best prediction per each step forward while RF is a machine learning classification model inherent ability to test prediction accuracy. Iteratively In the second approach, we evaluated the ability of new cheaper and less labour intensive techniques, field spectroscopy reflectance measurements, to discriminate among non-sites, middens, vitrified dung and non-vitrified dung byres. A feature selection method, guided regularised random forest (GRRF), was used to identify important wavelengths for the discrimination of abovementioned archaeological and non-archaeological soils. Thereafter, the selected soil elements and wavelengths were used as input variables in RF classification algorithm to classify the non-sites, middens, vitrified and non-vitrified dung. The findings reveal that there is a significant difference in the composition of chemical elements and spectral signatures of non-sites, middens, vitrified and non-vitrified dung. In summary, high classification accuracies achieved when using field spectroscopy data proves that remote sensing techniques can be used to exploit the spectral differences among the above-mentioned soil types in mapping archaeological features characteristic of farming communities' settlements.

Keywords: archaeology; remote sensing; guided regularised random forest; midden; non-vitrified dung; vitrified dung

3.1 Introduction

This study tests the feasibility of using remote sensing techniques to detect contrast which might exist between archaeological features characterising archaeological sites previously occupied by Farming Communities in the Shashi-Limpopo Confluence area. The presence of archaeological material in the soil has a localised impact on the composition of physical and chemical properties thus making different from surroundings (Oonk et al. 2009; Wilson et al. 2008). Anthropological activities such as animal penning and rubbish damping change soil structure and colour. For example, refuse middens containing ash are normally characterised by loose fine greyish particles (Walker 1983), whilst animal penning areas appear grey because of the deposition of high organic animal secretions (Huffman 2009b). Chemically, human activities have an impact on soil organic content, affecting the amount of phosphates (Luzzadder-Beach et al. 2011) and potassium (Huffman et al. 2013). Middleton and Price (1996) found out that there is a high concentration of K, P and Mg in the hearth area. Huffman (2013) studied the formation and difference in the chemical composition of non-vitrified dung and vitrified dung deposits in archaeological sites. This alteration of soil physical and chemical properties occur through weathering and incorporation by depositing matter into an area and tipping the balance in the pedogenesis process (Hejcman et al. 2011; Oonk et al. 2009; Schmidt et al. 2014). Approaches for identifying different past human activity areas through geochemical analysis are routinely used at intrasite level (Middleton 2004; Oonk et al. 2009; Parnell et al. 2002; Wilson et al. 2008). Material remains and changes in soil physical properties such as texture and colour are also of interest at a landscape level for the purpose of the archaeological survey and site identification (Huffman 2009b; Jacobson et al. 2003). Fieldwalking survey is the main method for identifying archaeological features visible on the earth's surface (Huffman 2009b; Huffman et al. 2013; Renfrew and Bahn 2012). However, in areas where archaeological features are not clearly visible or structural information about the use of space within a site is inconclusive, geochemical analysis methods have been employed to identify archaeological sites (Oonk and Spijker 2015) or different activity areas within the site (Parnell et al. 2002). The aforementioned traditional archaeological survey methods, geochemical analysis and field walking, are time-consuming and expensive to carry out. On the other hand, remote sensing techniques provide a cost-effective, reproducible and timely approach to systematically surveying and monitoring large archaeological areas. Therefore, they have been recently investigated as a potential preferred replacement for the costly and laborious traditional archaeological surveying methods.

The advent of very high-resolution multispectral sensors in the late 1990s did not only offer the possibility of exploiting higher spectral resolutions with new bands but also offered an opportunity for effective data processing methods in archaeological prospection (Rowlands and Sarris 2007; Traviglia and Cottica 2011; Van Ess et al. 2006). The effective data processing approaches include the use of digital processing methods which allowed for the integration of data from various sources and the use of statistical methods in image analysis (Lasaponara and Masini 2007, 2012; Leucci et al. 2002). The new bands in high-resolution multispectral sensors are better positioned to analyse soil types and their properties. Furthermore, they are also good for detecting plant stress, as such, most published remote sensing based researches in archaeology has tested the use of vegetation indices calculated from multispectral remote sensing data to identify archaeological anomalies (Agapiou et al. 2013; Agapiou and Hadjimitsis 2011; Bennett et al. 2012; Lasaponara and Masini 2006). However, the complex nature and small size of most archaeological features limit the wide use of multispectral sensors, which are prone information loss and confusion due to low spatial and spectral resolution (Mulder et al. 2011; Siart et al. 2008). The low spatial resolution here means fewer pixels while lower spectral resolution means broad wavelength interval size. The consequent spectral confusion can lead to a poor distinction between archaeological features in a landscape with multiple features within a pixel or adjacent pixel energy transfer. Moreover, some archaeological features may have subtle chemical and physical differences with their environment, which might be masked by multispectral sensors.

Spectroscopy data, which are commonly captured using airborne, handheld and spaceborne sensors offer hundreds of narrow spectral wavebands in the visible and infrared spectral regions. These narrow wavebands allow for an exhaustive exploration of detailed archaeological data that is otherwise missed by the generic wavebands captured by multispectral sensors (Aminzadeh and Samani 2006; Fowler 2002). These include the detection of subtle variations of attributes such as vegetation health status (Doneus et al. 2014). However, using spaceborne and airborne data comes with challenges related to the spectral mixture of features, radiometric and wavelength calibration uncertainties which as a result affects the quality of captured data (Casa et al. 2013; Gomez et al. 2008; Lagacherie et al. 2008; Mulder et al. 2011). Radiometric uncertainties are generally caused by the effects of solar illumination and atmospheric conditions on the signal (Aqdus et al. 2008; Lillesand et al. 2008). Spaceborne and airborne sensors also lack high spatial and spectral resolution similar to that of the handheld spectrometer (Adam et al. 2012; Analytical Spectral Devices, Inc. 2018; Casa et al. 2013;

Gomez et al. 2008; Kokaly 2016; Kruse et al. 2003; Lagacherie et al. 2008; Mulder et al. 2011; Rani et al. 2017). In consequence, the aforementioned challenges have resulted in the limited use of both airborne and spaceborne hyperspectral data in soil analysis (Mulder et al. 2011).

In recent years, laboratory visible-near infrared (VISNIR)/ short-wave infrared (SWIR) spectroscopy data has been viewed as a potential cost-effective option to the field-based survey and traditional laboratory approach for soil analysis (Ben-Dor et al. 1997; Gandariasbeitia et al. 2017; Lagacherie et al. 2008; Rossel and Behrens 2010; Shepherd and Walsh 2002; Vohland et al. 2014). This has led to the development of spectral libraries documenting the spectral signatures of different soils and their properties. Researchers have used field spectroscopy data to assess soil properties such as organic content, minerals, texture and moisture (Kopačková and Koucká 2017; Nawar et al. 2016; Ogen et al. 2017, 2018; Shepherd and Walsh 2002; Xu et al. 2016). Therefore, field/handheld spectroscopy data might be useful for documenting the spectral signatures of archaeological sites with subtle variations in the aforementioned soil properties. These include sites characterised by archaeological features including middens, vitrified dung and non-vitrified dung deposits because of their variations in physical properties such as texture, colour and material composition. Middens are characterised by fine ashy deposits which are highly moisture retentive and as a result may increase its spectral absorption. The vitrified dung is composed of pebbles of highly reflective, less moisture retentive glassy like material while non-vitrified dung is characterised by fine deposits of greyish dung.

The documentation of the reference data for the spectral reflectance of different archaeological features in a library is lacking. In the recent past, only a few researches have used field spectroscopy/hyperspectral data to document the spectral signatures of vegetation overlaying archaeological material and investigate the potential of detecting and mapping the vegetation health as a proxy indicator of buried archaeological materials (Agapiou et al. 2010, 2012a; b; Sarris et al. 2013). Additionally, hyperspectral data has also been used to detect geological areas which were possibly sourced for raw materials, chloritite and obsidian, by past societies (Dumitru and Harrower 2018; Sivitskis et al. 2018). Consequently, the role of field spectroscopy in archaeological applications is still poorly explored. For instance, and to the best of our knowledge, there is no study to date examining the use of field spectroscopy in discriminating archaeological surface features using soil characteristics as indicators.

One of the most notable challenges in the use of field spectroscopy is the large data redundancy due to high spectral resolution leading to a strong correlation between the spectral features

(Feng et al. 2016). This high dimensionality requires sufficient training sample and computational process which might be time-consuming and prohibitive in cost (Burger and Gowen 2011; Farrell and Mersereau 2005). Dimensionality in this study means the number of spectral attributes our dataset have. In most archaeology studies, the size of the training samples is restricted by a number of factors such as the magnitude of archaeological sites, heterogeneity of potential samples or issues of accessibility. This may result in some problems such as the Hughes phenomenon or "curse of dimensionality", whereby the accuracy of classification algorithms decreases when working with a limited number of training samples (Fukunaga and Hayes 1989; Taşkın et al. 2017). This is because the training sample has to be large enough to capture the variability between the features (Fukunaga and Hayes 1989; Ham et al. 2005; Jain and Waller 1978). As a result, there is a need for the reduction of dimensionality when processing field spectroscopy data in order to avoid the aforementioned challenges. Dimensionality reduction methods improve the discriminative ability of the dataset by decreasing the number of spectral bands without dropping vital information (Cai et al. 2014; Jia and Richards 1999; Wei et al. 2016). Numerous variable selection methods have been used to decrease the high dimensionality in hyperspectral data by selecting the most important bands for data classification. The most commonly used feature selection methods are genetic algorithms (Li et al. 2011; Ma et al. 2003; Zhuo et al. 2008) and random forest (RF) (Abdel-Rahman et al. 2013; Adam et al. 2012). Genetic algorithms (GA) are based on the process of natural selection, influenced by the principle of survival of the fittest. GA is usually embedded in classifiers such as SVM as a band selection algorithm (Bazi and Melgani 2006; Li et al. 2011; Zhuo et al. 2008), in order to improve classification accuracy. However, genetic algorithms are vulnerable to random correlations of the features (Jouan-Rimbaud et al. 1996) and have high computational demands (Li et al. 2011; Zhang et al. 2009).

RF classifier, which has been described as the best machine learning algorithm for handling high dimensional data (Gislason et al. 2006), measures the importance of each variable in classification. However, it is prone to producing redundant features because of its biases towards the correlated predictors (Nicodemus et al. 2010; Uddin and Uddiny 2015). In RF samples for bagging are most commonly dominated by less important features, therefore, degrading the classification accuracy (Nguyen et al. 2015). RF also ranks features without selecting a subset of optimal features (Adam et al. 2012).

Recently, Deng and Runger (2013) developed a guided regularized random forest (GRRF) algorithm aimed at curbing the limitations of the traditional RF algorithm. GRRF eliminates

feature redundancy by not selecting features carrying similar information with the already selected ones in a subset at each node (Deng and Runger 2013). GRRF algorithm guides feature selection process in the regularised RF using importance scores from the normal RF (Deng and Runger 2013). To date, only two studies that have used GRRF for the reduction of high dimensionality in hyperspectral data for vegetation studies (Adam et al. 2017; Mureriwa et al. 2016).

This study investigated whether field spectra measurement can discriminate archaeological sites using soil properties as indicators. More precisely, the objectives of the study were to (i) investigate if there is any significant difference in concentration of soil elements across different archaeological sites, namely middens, vitrified and non-vitrified dung byres (ii) use in situ hyperspectral measurements to discriminate among non-sites (natural soils), middens, vitrified and non-vitrified dung (iii) identify important wavelengths for discriminating among the aforementioned features using the guided regularized random forest algorithm.

3.2 Materials and Methods

3.2.1 Study area

The study was conducted in the Mapungubwe cultural landscape, located at the confluence of the Shashi and Limpopo rivers, in the province of Limpopo, South Africa, shown in Figure 3. **1**. The Shashi-Limpopo Confluence Area (SLCA) forms the boundary of three countries; Botswana towards west, South Africa towards south and Zimbabwe towards the north. Geologically, the SLCA lies within Limpopo Mobile Belt which joins the Zimbabwe and Kaapvaal cratons (Chinoda et al. 2009b). This area is characterised by igneous and sedimentary rocks of the Karoo super group (Bordy and Catuneanu 2002). Erosion is rampant, in particular in areas closer to the river channels, therefore, forming sandstone ridges and outcrops which cover most parts of the SLCA with a sparse distribution of volcanic intrusions (Götze et al. 2008; Hanisch 1981a). Generally, soils in the Limpopo mobile belt include clays and sands originating from the Karoo system (Götze et al. 2003).

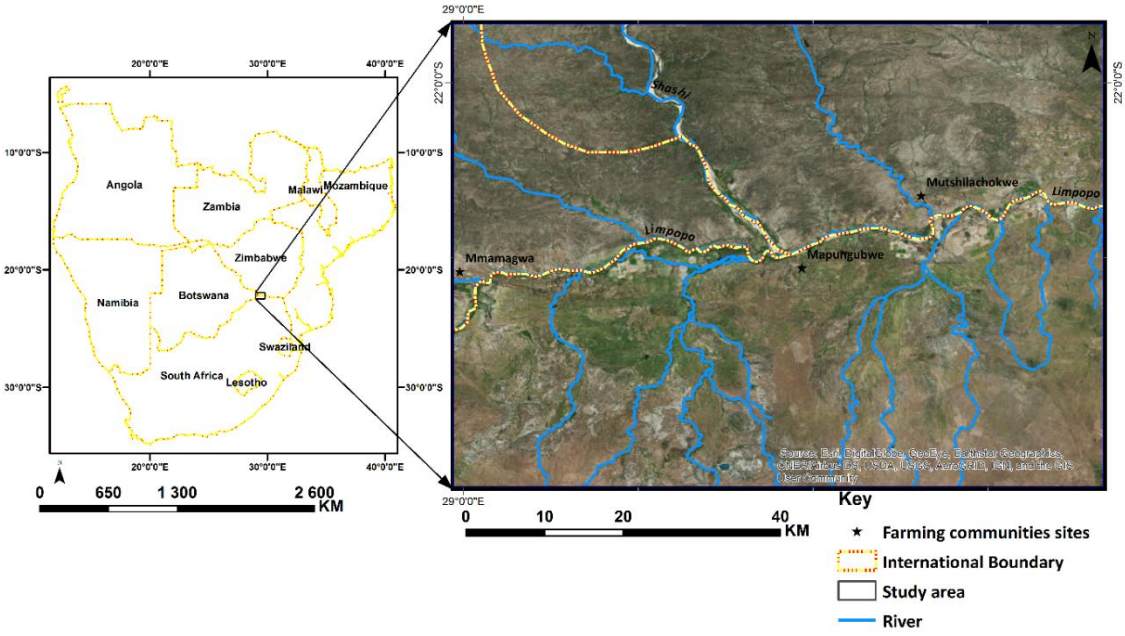

Figure 3. 1 Location of the SLCA in southern Africa with some of the major farming communities sites mentioned in the text.

Archaeologically, the study area has been continuously occupied by different groups of farming communities since 900 AD (Calabrese 2000; Eloff and Meyer 1981; Huffman 2000; Vogel and Calabrese 2000). These societies practised the central cattle pattern (CCP) settlement system (Hanisch 2002). This is a settlement system whereby animal byres are located at the centre of the settlement, close to the male gathering area (Huffman 2009a) (Figure 3. 2). Social changes in the SLCA occurred during the twelfth century AD, with the occupation of Mapungubwe hill, when leaders and commoners became physically separated (Huffman 2000; Meyer 2000). Animals were only kept at commoner settlements where the CCP continued to be practised, whilst rulers would reside in stone walled elevated areas, secluded from the commoners (Huffman 2000). The archaeological features characterising these sites are vitrified and non-vitrified dung byres, middens, grain bins and pottery scatters. The great majority of archaeological sites occupied by late farming communities in the SLCA appear as open spaces within woodland vegetation especially those characterised by vitrified and non-vitrified dung. The aforementioned differences in vegetation cover might possibly be influenced by the chemical composition of vitrified and non-vitrified dung sites which was found to be different from that of their surroundings (Denbow 1979; Huffman et al. 2013).

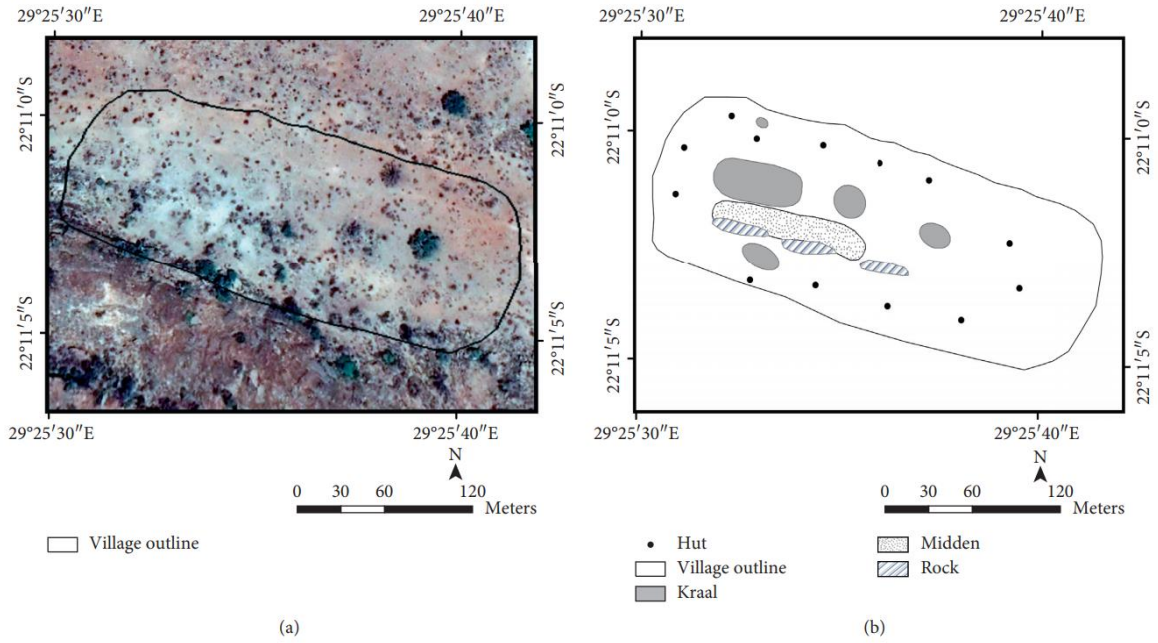

Figure 3. 2 Scketch of Schroda village 1 (a) RGB Google Earth imagery; (b) a sketch detailing the outline of the early farming community as interpreted by Hanisch from excavation (adapted from Hanisch 1980, p. 224)

Middens are areas where the general waste of a household, including remains of unused materials such as broken potsherds, animal bones, beads and other utensils and ashes from fireplaces were discarded (Chirikure et al. 2014; Huffman 2012). Middens differ in size depending on the duration and density of site occupation (Eloff and Meyer 1981). Some of the middens in areas classified as capitals, such as K2, reached a diameter of 182.88 metres and a depth of 6 meters (Fagan 1964; Huffman 2009a; Voigt 1983) while others are just few centimetres wide and very shallow. Vitrified dung and non-vitrified dung are two types of dung deposits in the study area, which indicates areas where animals were kept in the settlement. Vitrified dung is formed by the burning of dung deposits which at least more than a meter in thickness, at very high temperatures (in the region of 1100 ^{o}C) (Peter 2001; Thy et al. 1995). Vitrified dung contains high quantities of nitrates and phosphates which makes it impossible for some grasses to grow on them (Peter 2001). Non-vitrified dung is dung deposits, which maintained their original form. The byres for both livestock and cattle have an average diameter of 3 meters and 18 meters, respectively (Huffman pers comm. 2018)

3.2.2 Soil samples collection and analysis

Soil samples for three archaeological features (middens, vitrified and non-vitrified dung areas) and bare soil (non-archaeological site) from the surrounding natural landscape were collected for lab spectral measurement and chemical analysis. A purposive sampling technique was used

during the fieldwork data collection by visiting sites which appear in the literature and are affirmed to have dung deposits and middens (Huffman 2009b, 2011). In order to avoid contamination with the archaeological features due to wind and water erosion, bare soil samples were collected from areas far away from the archaeological sites. A representative sample of a feature was attained by collecting at least three per feature identified. The samples were collected at the centre, mid-way between the centre and the edge and towards the edge of the feature. This was done in order to overcome the potential heterogeneity of a single feature and establish a range of value that accounts for variations within the same feature. A total of 356 samples were collected at 0-20 cm depths which corresponded to the surface horizon at each sampling site and a GPS point was taken as a spatial reference. All the collected soil samples were packaged in zip-lock plastic bags for field spectral measurements and chemical analysis in the laboratory.

3.2.3 Laboratory spectral data acquisition

Soils collected in the field were air dried and sieved to 2mm (Ogen et al. 2017) before being flattened on a black plastic plate to create a smooth surface. Spectral reflectance measurements were carried out in a controlled environment using the Analytical Spectral Devices (ASD) FieldSpec® 4 optical sensor with a sampling interval of 1.4nm between 350-1000nm and 2nm between 1001-2500nm (Analytical Spectral Devices, Inc. 2018; Danner et al. 2015). The Analytical Spectral Devices (ASD) FieldSpec® 4 optical sensor has a 350-2500nm spectral range and spectral resolutions ranging from 3nm in the visible-near infrared region (350-1000nm) to 10nm in short wave infrared region (1001-2500nm) (Analytical Spectral Devices, Inc. 2018). The spectral measurements were taken from the surface of each soil sample at nadir position with 10mm field of view using Hi-Brite contact probe fitted with 100W halogen reflector lamp. The spectrometer was calibrated using a white spectrolon reference panel after every 10 to 15 measurements. Soil samples from each bag were randomly divided into three samples. Three spectral measurements were taken per each sample by randomly moving the probe over the soil surface. The nine (n = 9) spectral measurement were then averaged to represent the whole soil sample (Figure 3. 3). Between 60 and 117 samples were collected from non-sites, middens, vitrified dung and non-vitrified dung sites in the field. All 2151 bands were included in the analysis because the data was collected within a controlled environment so there was no need to remove spectral bands to improve the signal-to-noise ratio. The reference data was arbitrarily separated into training (70%) and test (30%) datasets.

Classes	Number of samples	Reflectance curve
Midden (MD) 	86	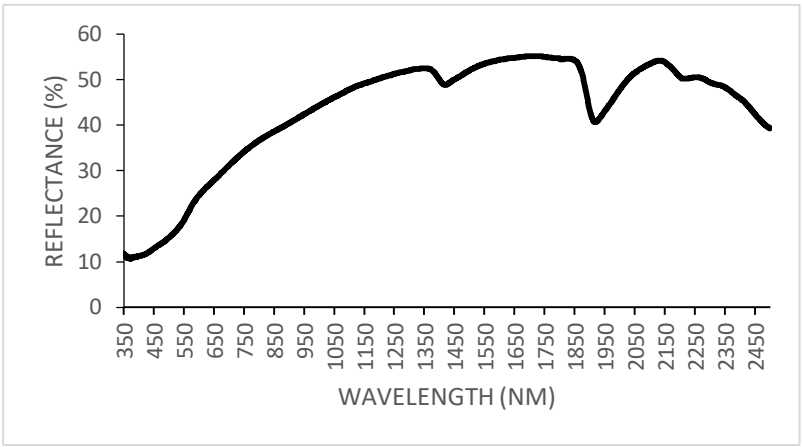
Vitrified-dung (VD) 	60	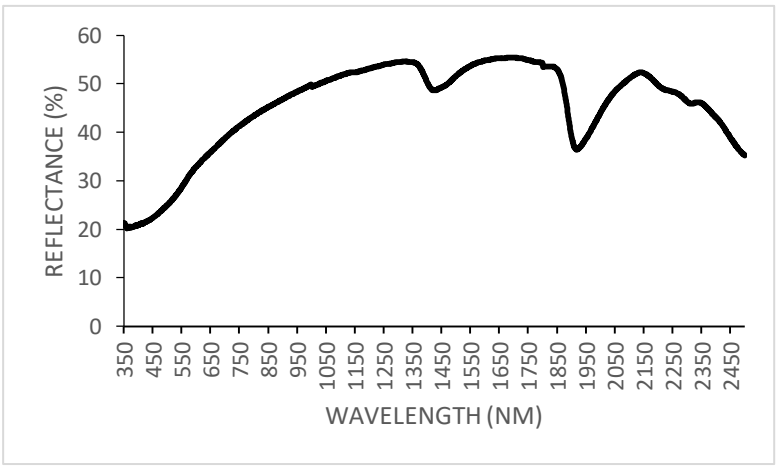
Non-vitrified dung (NVD) 	117	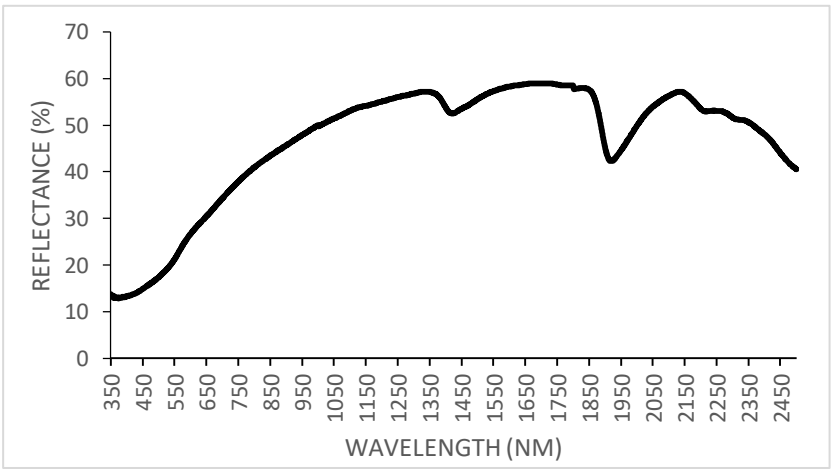

Non-sites (NS) 	93	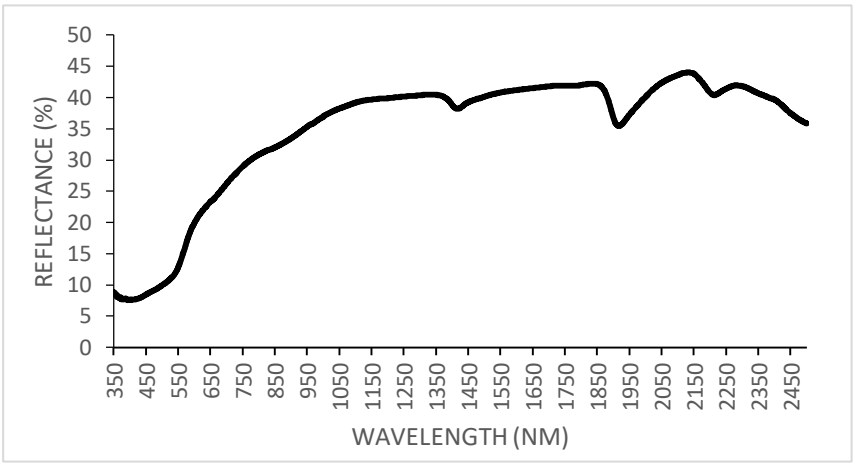
Average reflectance spectra for Non-sites (NS), Midden (MD), Non-vitrified dung (NVD) and Vitrified dung (VD) sites		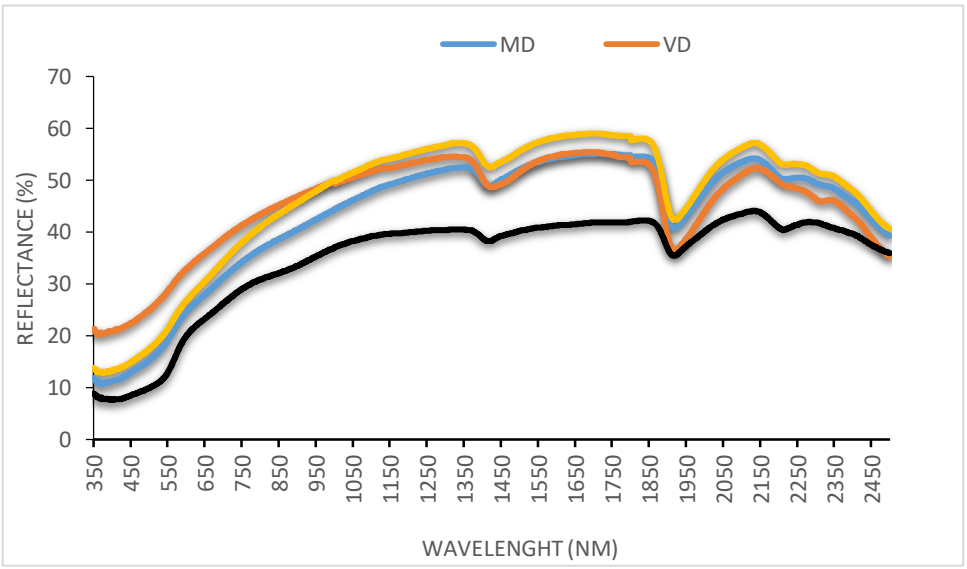

Figure 3. 3 Images and mean spectra for non-sites (NS), Midden (MD), Non-vitrified dung (NVD) and Vitrified dung (VD) sites. The mean reflectance curves were constructed using spectral data collected under laboratory conditions.

3.2.4 Soil analysis

The samples were analysed for the composition of 33 elements by ALS in Johannesburg. The samples were air-dried and dry-sieved using a 180-micron screen (Tyler 80 mesh). Thereafter, 0.25 grams of a readied sample was then digested with perchloric, nitric, hydrofluoric and hydrochloric acids. Thereafter, a dilute hydrochloric acid was mixed with the residue and the resulting solution was analysed using inductively coupled plasma-atomic emission spectrometry (ALS 2018).

3.2.5 Statistical methods for soil analysis

Various statistical methods were used to test for variation and homogeneity of elements within and between samples. Descriptive statistics were performed for the individual soil classes to get the typical values, mean, median, standard deviation of the concentration of elements within each class. The variation of the concentration of elements between and within classes was measured using the coefficient of variation (CV) and interquartile range. The two aforementioned measures of variation were chosen because of their ability to get rid of the challenges associated with outliers (Fletcher and Lock 2005; Shennan 1997). The coefficient of variation also has the ability to standardise data for comparing the variability of two or more distributions from different or the same data with different means (Bedeian and Mossholder 2000; Fletcher and Lock 2005). The Levene's test of homogeneity was used to test for homogeneity of variances and Welch's analysis of variance (ANOVA) was used whenever homogeneity was violated. ANOVA was used to test if there are statistically significant differences on the average composition of chemical elements between non-sites and each archaeological features - middens, non-vitrified and vitrified dung (Bewick et al. 2004; McDonald 2009a). The Games-Howell post hoc test was performed to find out which elements are significantly different across the classes since variances were heterogeneous and sample sizes were unequal. The level at which differences between the means were considered significant was set at $p \leq 0.05$. However, the major limitation of ANOVA is that it is not linked to any machine learning classifier therefore, it does not measure the importance of each element in the prediction model (Ismail and Mutanga 2011).

To curb the aforementioned limitation, RF was combined with forward variable selection (FVS) procedure in an attempt to locate the ideal subset of elements with the least classification error (Adam et al. 2013). RF was used for ranking the variables based on the importance score of the mean in decrease accuracy determined using out-of-bag (OOB) data and evaluating the classification accuracy. Then a stepwise procedure was employed for FVS, whereby elements were added into the model according to their importance beginning with the most important one (Mansour et al. 2012). The method continued by repetitively constructing new RF models while adding a single element in each iteration and recording the OOB error. The parameters for the number of trees to be grown (*Ntree*) and the number of variables needed to split each node (*Mtry*) were optimised using grid search at each iteration. This procedure was reiterated until all elements were utilised; then the smallest subgroup of elements with the least OOB

error was identified. The optimal elements chosen were then used as input variables to construct two different classification models in RF classifier. In the first model, the subset of optimal elements was used to classify non-sites, middens, vitrified dung and non-vitrified dung sites. In the second model, the subset of optimal elements was combined with the optimal bands chosen by GRRF and classification of non-sites, middens, vitrified dung and non-vitrified dung sites was done. This was done in order to check if they would be an improvement in the classification accuracy of the general model when optimum bands and soil elements are combined.

3.2.6 Using guided regularized random forest for variable selection

GRRF is a feature selection algorithm which applies some form of regularisation to different types of decision trees models, performing a selection of feature subsets (Deng and Runger 2012, 2013). The regularisation is guided by scores of feature importance measured by the traditional RF using the Gini index. Gini importance assesses the level of impurity of each variable in relation to the importance it gained over others, in the sampled set of variables, and select the optimal split at each node (Archer and Kimes 2008; Touw et al. 2012). The Gini index at a node *y*, can be defined as follows:

$$Gini(y) = \sum_{k=1}^{k} p_k^y \left(1 - p_k^y\right) \qquad \text{Equation 3.1}$$

whereby p_k^y denotes the proportions of observations for class k at node y. The Gini information gain (h_i,v) is then calculated as the difference between the Gini index at node y and the weighted mean of Gini indexes at each child node of y. Gain information of feature h_i based on impurity at node y can be defined as follows:

$$\text{Gain}\ (h_i,y)=\text{Gain}(y)-w_L\text{Gini}(y_L)- w_R\text{Gini}(y_R) \qquad \text{Equation 3.2}$$

here, Gini(y_L) and Gini(y_R) represents the impurities while w_L and w_R are the weights for the left and right child nodes.

In GRRF regularisation is added to the Gain information from the traditional RF and each individual feature is given a penalty coefficient. The regularised information Gain is defined as:

$$Gain(h_i, y) = \begin{cases} \lambda_i . Gain(h_i, y), & h_i \notin F \\ Gain(h_i, y), & h_i \notin F \end{cases}$$ Equation 3.3

Where $\lambda_i \notin (0, 1)$ is the coefficient of regularisation for $y_i (i \in \{1, \dots, P\})$ and F is the set of features chosen in the preceding nodes. $\lambda_i \notin (0, 1)$ is computed based on the importance score of h_i from the traditional RF as follows:

$$\lambda_i = (1 - \gamma) + \gamma Imp_i$$ Equation 3.4

Where $\gamma \in [0,1]$ is the importance coeficient and $\mathrm{Imp}_i \in [0,1]$ is the base coefficient controlling regurlarisation. Regularisation allows the model to reduce redundancy associated with tree models of feature selection, by only choosing a new feature for spliting data in a tree node if it yields different information from the feature that was chosen in the earlier split. Unlike other feature selection methods, the reguralized framework allows for the construction of a single model at a time therefore reducing the time needed to train the model (Deng and Runger 2012). GRRF also has the ability to select the ideal subset of variables with the lowest misclassification error. In this study, GRRF was used to select the key wavelengths to accurately discriminate among non-sites, midden, vitrified dung and non-vitrified dung. This was done so as to reduce the high dimensionality inherent within the hyperspectral data (Abdel-Rahman et al. 2014; Chan and Paelinckx 2008; Mansour et al. 2012). The key wavelengths selected by GRRF were then utilised as input variables in the traditional RF algorithm to discriminate among the non-sites.

3.2.7 Random forest classifier

RF classifier was used to discriminate between non-sites, midden, vitrified dung and non-vitrified dung using key elements selected by FVS and their key wavelengths selected by GRRF. RF classification algorithm has been extensively employed in the classification of both hyperspectral and multispectral data (Abdel-Rahman et al. 2015; Akar and Güngör 2013; Chan and Paelinckx 2008; Rodriguez-Galiano et al. 2012a). Generally, RF can be described as an ensemble of classifiers which creates binary decision trees and assigns class basing on majority votes at each node (Chan and Paelinckx 2008). The decision trees are grown independently of each other using different samples, facilitated by bagging which randomly creates subsets of the original datasets, with replacement, for each node (Genuer et al. 2010). The variables which are not included in the bootstrap sample, which makes a third of the data, are called the out-of-bag (OOB) sample (Belgiu and Drăguţ 2016; Genuer et al. 2010). Each tree grows without

being pruned (Genuer et al. 2010). However, *Ntree*, the default number is 500 trees, and *Mtry*, the default is the square root of the total number of variables $\sqrt{P}$, are defined by the user (Chan and Paelinckx 2008). The *mtry* and *ntree* have to be optimised, in order to archive high classification accuracies (Mutanga et al. 2012). This study identified the best combination of *mtry* and *ntree* parameters using a grid search based on the OOB approximation of error (Tian et al. 2009). The optimisation of *Ntree* was done using values ranging between 500 and 10000 at the interval of 500, while the *mtry* was optimised using a multiplicative factor of its default.

RF has inherent measures of variable importance and the ability to estimate prediction accuracy (Belgiu and Drăguţ 2016). RF estimates prediction accuracy by cross-validating the bagging sample with a third of the data being excluded from the sample (Touw et al. 2012). The classification error from these accuracy predictions is called the OOB error. Variable importance helps in understanding the relevance of each variable predictor in data classification. Variable importance measures in RF comprise of mean variable importance/ mean decrease accuracy (MDA) and Gini importance (Archer and Kimes 2008). MDA was calculated using OOB observations and was used to rank elements used as input variables in the FVS model in this study. High MDA values indicate important variables in the classification, while low values represent variables which are less important in the classification. Gini index was used to assess the importance of different spectral bands in discriminating different archaeological sites. High Gini impurity indicates heterogeneity between classes while a lower Gini impurity indicates homogeneity within classes. Therefore, features with a less mean decrease in Gini index are of less importance in the classification because they do not play any role in splitting the data into classes.

3.2.8 Accuracy assessment

The accuracy assessment was done using a holdout dataset created by randomly dividing the laboratory data into 70% training and 30% testing before classifying it. Misclassification was assessed using the OOB error, which is an internal process of estimating RF error. An error matrix was done to calculate the user's accuracy, producer's accuracy and the overall accuracy for the assessment of classification accuracy of the RF classifier. Even though the cause of correct allocations or misclassifications have been deemed as a needless component of accuracy assessment, Kappa Coefficient was used in this study together with overall accuracy (Pontius Jr and Millones 2011; Stehman and Foody 2019). This is because, despite it containing data that is redundant to that of overall accuracy, it is still an important part of the accuracy

assessment (Stehman and Foody 2019). A perfect agreement is achieved if the kappa value is one or close to one (McHenry and Coffing 2000).

3.3 Results

3.3.1 Statistical analysis

This study used statistical methods to assess the concentration of elements within natural soils, midden, vitrified and non-vitrified dung. The soil analysis was done on samples taken from each of the abovementioned classes. The descriptive statistics for the concentration of different elements are summarized in Tables 3.1, 3.2, 3.3, 3.4 for natural soils, vitrified dung, non-vitrified dung and midden, respectively. Coefficient of variation (CV) is defined as a proportion of the standard deviation to the mean. A high CV value indicates a higher degree of variation between datasets while low CV values indicates less degree of variation. CV revealed high variability of the concentrations of most elements within each soil class with the variation between 12% and 50%. The concentrations of Zn and Cu within the midden were very highly variable with a coefficient variation of 53.6% and 56.9%, respectively. The concentrations of most elements across different classes are also highly variable. The mean concentrations of P, Mn, Ca, Mg, Zn and Ba were very high in vitrified dung. Non-vitrified dung and midden also had comparatively higher concentrations of the above-mentioned elements than non-sites (Tables 3.1, 3.2, 3.3, 3.4).

Table 3. 1 Summary statistics for the concentration of different chemical elements within natural soils

Element	1^{ST} qu.	median	3^{rd} qu.	mean	standard deviation	coefficient of variation
Ag	0.5	0.5	0.5	0.5	0.0	5.9
Al	3.7	4.2	4.5	4.1	0.5	12.5
As	5.0	5.0	5.0	5.0	0.0	0.0
Ba	375.0	400.0	500.0	430.0	65.3	15.2
Be	1.0	1.1	1.2	1.1	0.1	13.9
Bi	2.0	2.0	2.0	2.0	0.0	0.0
Ca	0.3	1.3	1.4	0.9	0.6	64.8
Cd	0.5	0.5	0.5	0.5	0.0	0.0
Co	4.0	8.0	12.0	8.0	4.1	50.9
Cr	24.5	43.0	62.0	50.5	32.4	64.0
Cu	13.5	25.0	30.5	24.7	12.0	48.3
Fe	1.0	1.8	2.5	1.9	0.9	49.3
Ga	10.0	10.0	10.0	10.0	0.0	0.0
K	1.0	1.2	1.3	1.2	0.2	15.8
La	25.0	30.0	30.0	27.3	4.7	17.1
Mg	0.3	0.6	0.7	0.5	0.2	46.0
Mn	251.5	388.0	504.0	387.9	144.0	37.1
Mo	1.0	1.0	1.0	1.0	0.0	0.0
Na	0.9	1.0	1.1	1.0	0.1	8.9
Ni	10.0	19.0	27.5	21.8	13.4	61.3
P	215.0	360.0	480.0	406.4	251.3	61.8
Pb	10.0	11.0	13.5	11.0	2.9	26.7
S	0.0	0.0	0.0	0.0	0.0	0.0
Sb	5.0	5.0	5.0	5.0	0.0	0.0
Sc	3.0	6.0	7.0	5.5	2.2	39.8
Sr	90.0	154.0	198.0	150.7	63.0	41.8
Th	20.0	20.0	20.0	20.0	0.0	0.0
Ti	0.3	0.4	0.7	0.5	0.4	71.2
Tl	10.0	10.0	10.0	10.0	0.0	0.0
U	10.0	10.0	10.0	10.0	0.0	0.0
V	30.0	51.0	79.5	59.3	36.1	61.0
W	10.0	10.0	10.0	10.0	0.0	0.0
Zn	20.5	37.0	44.5	35.8	14.5	40.5

Table 3. 2 Summary statistics for the concentration of different chemical elements within vitrified dung

Elements	1st qu.	median	3rd qu.	mean	standard deviation	coefficient of variation
Ag	0.5	0.5	0.5	0.5	0.0	0.0
Al	1.9	2.3	2.5	2.2	0.4	18.3
As	5.0	5.0	5.0	5.0	0.0	0.0
Ba	490.0	605.0	672.5	609.2	120.2	19.7
Be	0.5	0.6	0.6	0.6	0.1	18.8
Bi	2.0	2.0	2.0	2.0	0.0	0.0
Ca	7.1	8.8	11.5	9.0	2.8	31.4
Cd	0.5	0.5	0.5	0.5	0.0	0.0
Co	3.0	3.0	5.0	3.8	1.6	41.4
Cr	26.5	34.0	37.5	33.9	9.3	27.4
Cu	35.0	43.5	50.5	43.5	10.7	24.7
Fe	0.8	1.1	1.3	1.1	0.4	34.1
Ga	10.0	10.0	10.0	10.0	0.0	0.0
K	1.6	1.7	2.0	1.9	0.5	29.0
La	10.0	20.0	20.0	16.7	6.5	39.1
Mg	2.4	3.1	3.4	2.8	0.8	27.1
Mn	501.0	573.0	715.0	600.0	127.2	21.2
Mo	1.0	1.0	1.0	1.0	0.0	0.0
Na	0.4	0.5	0.6	0.5	0.1	28.3
Ni	17.0	21.0	24.5	21.7	5.5	25.4
P	9535.0	10000.0	10000.0	9279.2	1380.7	14.9
Pb	6.0	7.0	8.3	7.3	2.2	29.8
S	0.0	0.0	0.1	0.0	0.0	75.8
Sb	5.0	5.0	5.0	5.0	0.0	0.0
Sc	2.8	3.0	4.0	3.1	0.8	25.7
Sr	987.0	1527.5	1867.5	1471.3	571.2	38.8
Th	20.0	20.0	20.0	20.0	0.0	0.0
Ti	0.1	0.2	0.2	0.2	0.1	40.7
Tl	10.0	10.0	10.0	10.0	0.0	0.0
U	10.0	10.0	10.0	10.0	0.0	0.0
V	16.3	26.0	36.3	27.0	14.4	53.3
W	10.0	10.0	10.0	10.0	0.0	0.0
Zn	102.0	141.5	192.5	149.7	55.6	37.1

Table 3. 3 Summary statistics for the concentration of different chemical elements within non-vitrified dung

Elements	1st qu.	median	3rd qu.	mean	standard deviation	coefficient of variation
Ag	0.5	0.5	0.5	0.5	0.0	0.0
Al	2.9	3.0	3.7	3.6	1.0	28.6
As	5.0	5.0	5.0	5.0	0.0	0.0
Ba	450.0	490.0	560.0	517.1	79.4	15.4
Be	0.6	0.8	1.0	0.8	0.2	24.1
Bi	2.0	2.0	2.0	2.0	0.0	0.0
Ca	3.0	3.8	4.6	4.1	1.3	32.0
Cd	0.5	0.5	0.5	0.5	0.0	0.0
Co	5.0	7.0	10.0	7.7	3.3	43.2
Cr	57.0	78.0	83.0	75.2	25.7	34.2
Cu	30.0	35.0	40.0	37.6	13.0	34.6
Fe	1.4	1.7	2.5	1.9	0.6	32.0
Ga	10.0	10.0	10.0	11.2	3.3	29.7
K	1.1	1.3	1.4	1.3	0.3	19.1
La	20.0	20.0	20.0	22.4	4.4	19.6
Mg	1.1	1.6	1.9	1.6	0.5	33.4
Mn	477.0	504.0	587.0	533.4	97.0	18.2
Mo	1.0	1.0	1.0	1.0	0.0	0.0
Na	0.5	0.6	0.7	0.7	0.2	30.0
Ni	30.0	35.0	41.0	36.1	10.4	28.7
P	3260.0	5930.0	8580.0	5803.5	3099.1	53.4
Pb	8.0	10.0	12.0	10.2	2.9	28.3
S	0.0	0.0	0.0	0.0	0.0	41.6
Sb	5.0	5.0	5.0	5.0	0.0	0.0
Sc	4.0	5.0	6.0	5.5	1.8	32.0
Sr	431.0	552.0	675.0	573.4	194.6	33.9
Th	20.0	20.0	20.0	20.0	0.0	0.0
Ti	0.2	0.2	0.3	0.3	0.2	68.8
Tl	10.0	10.0	10.0	10.0	0.0	0.0
U	10.0	10.0	10.0	10.0	0.0	0.0
V	35.0	40.0	78.0	54.2	24.9	46.0
W	10.0	10.0	10.0	10.0	0.0	0.0
Zn	89.0	113.0	122.0	103.2	34.5	33.5

Table 3. 4 Summary statistics for the concentration of different chemical elements within midden deposits

Elements	1st qu.	median	3rd qu.	mean	standard deviation	coefficient of variation
Ag	0.5	0.5	0.5	0.5	0.0	0.0
Al	4.0	5.2	5.6	4.8	0.9	19.7
As	5.0	5.0	5.0	5.0	0.0	0.0
Ba	490.0	620.0	645.0	570.0	87.9	15.4
Be	0.9	1.1	1.2	1.1	0.2	14.7
Bi	2.0	2.0	2.0	2.0	0.0	0.0
Ca	2.8	3.3	3.6	3.2	1.1	34.7
Cd	0.5	0.5	0.5	0.5	0.0	0.0
Co	13.5	15.0	15.0	13.6	2.9	21.1
Cr	37.0	115.0	120.0	87.5	41.8	47.8
Cu	38.5	43.0	80.5	60.5	34.4	56.9
Fe	2.9	3.2	3.2	3.1	0.5	15.0
Ga	10.0	10.0	10.0	11.8	4.0	34.2
K	1.2	1.7	1.7	1.5	0.3	23.1
La	20.0	30.0	30.0	26.4	5.0	19.1
Mg	1.0	1.0	1.5	1.3	0.5	39.3
Mn	510.0	526.0	733.0	620.2	194.3	31.3
Mo	1.0	1.0	1.0	1.0	0.0	0.0
Na	0.7	1.0	1.1	0.9	0.2	19.0
Ni	31.5	46.0	61.0	46.1	15.0	32.6
P	1865.0	2020.0	3210.0	2552.7	1091.3	42.7
Pb	10.5	15.0	16.5	13.7	4.9	35.4
S	0.0	0.0	0.0	0.0	0.0	37.0
Sb	5.0	5.0	5.0	5.0	0.0	0.0
Sc	8.0	9.0	9.0	8.4	1.0	12.3
Sr	325.0	410.0	496.0	425.9	182.6	42.9
Th	20.0	20.0	20.0	20.0	0.0	0.0
Ti	0.4	0.7	0.7	0.6	0.2	28.1
Tl	10.0	10.0	10.0	10.0	0.0	0.0
U	10.0	10.0	10.0	10.0	0.0	0.0
V	86.5	93.0	97.5	92.1	17.8	19.4
W	10.0	10.0	10.0	10.0	0.0	0.0
Zn	57.5	62.0	115.5	88.3	47.3	53.6

The results obtained using Welch's ANOVA ($P < 0.05$) demonstrate that there are significant differences between the means of different elements across different soil classes. Comparisons of the average concentration of individual elements between pairs of soil classes have shown that only the concertation of phosphorus (P) was significantly different across all four classes vitrified dung, non-vitrified dung, midden and natural soils (Games-Howell, $p \leq 0.05$). P has shown significant *p* values, ranging from 0.004 between midden and non-vitrified dung to

0.000 between midden and non-site. Other elements such as Mg, Na, Be, Fe, Mn, S and Zn also recorded insignificant differences between two or more soil classes. For example, Mg has shown significant *p* values, ranging from 0.003 between midden and non-site to 0.000 between midden and vitrified dung. However, an insignificant *p*-value of 0.379 for Mg element was recorded between midden and non-vitrified dung.

3.3.2 Variable importance and measurement

MDA measure inbuilt within the RF classification algorithm was used to measure the importance of each element in discriminating amongst non-sites, midden, vitrified and non-vitrified dung sites. Generally, Ca, P and Sr were the top most important elements in discriminating among the aforementioned classes, as shown in Figure 3. 4. Ga, Bi, and Th were the least important elements in discriminating amongst non-sites, midden, vitrified and non-vitrified dung sites (Figure 3. 4).

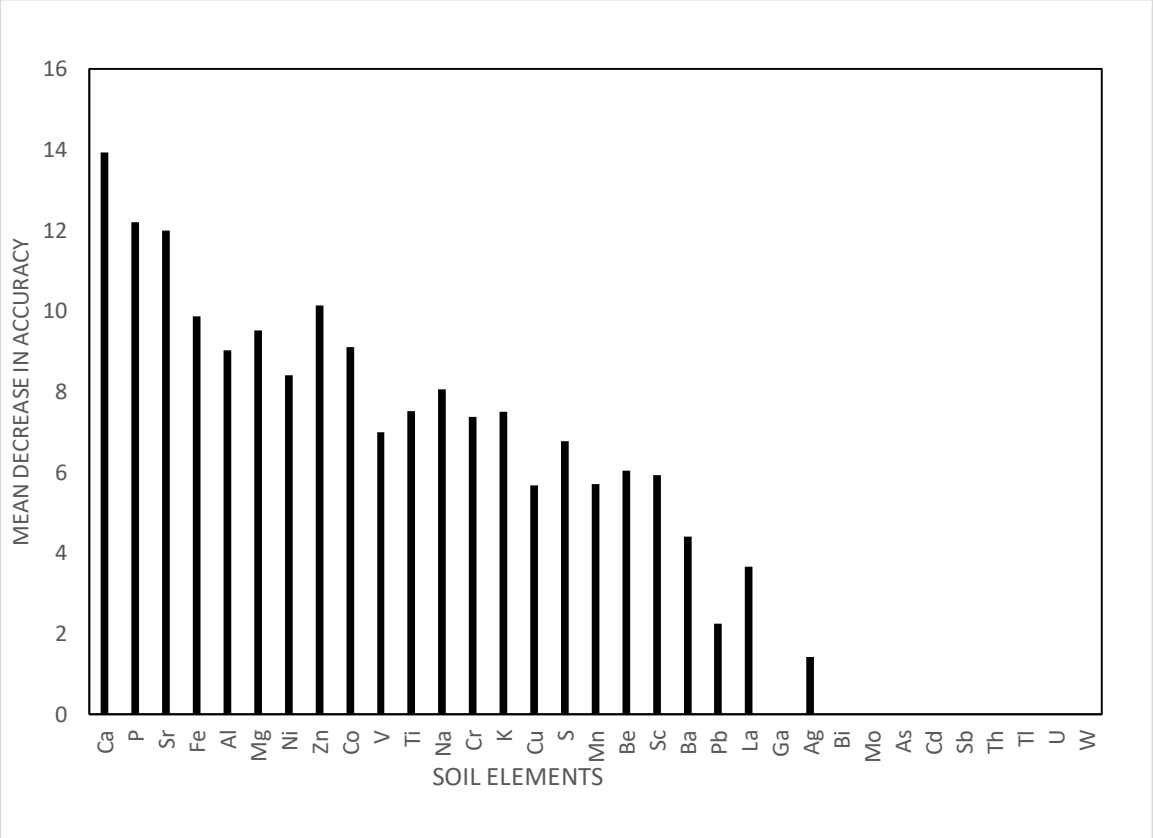

Figure 3. 4 Showing the variable importance computed by RF algorithm. The highest MDA indicates the most important elements

When assessing the importance of each element in discriminating among individual classes, Sr, Al and Ca were the most important elements in differentiating sites with vitrified dung from

the rest of the sites (Figure 3. 5). P and Mg were important in discriminating non-sites, middens, vitrified dung and non-vitrified dung.

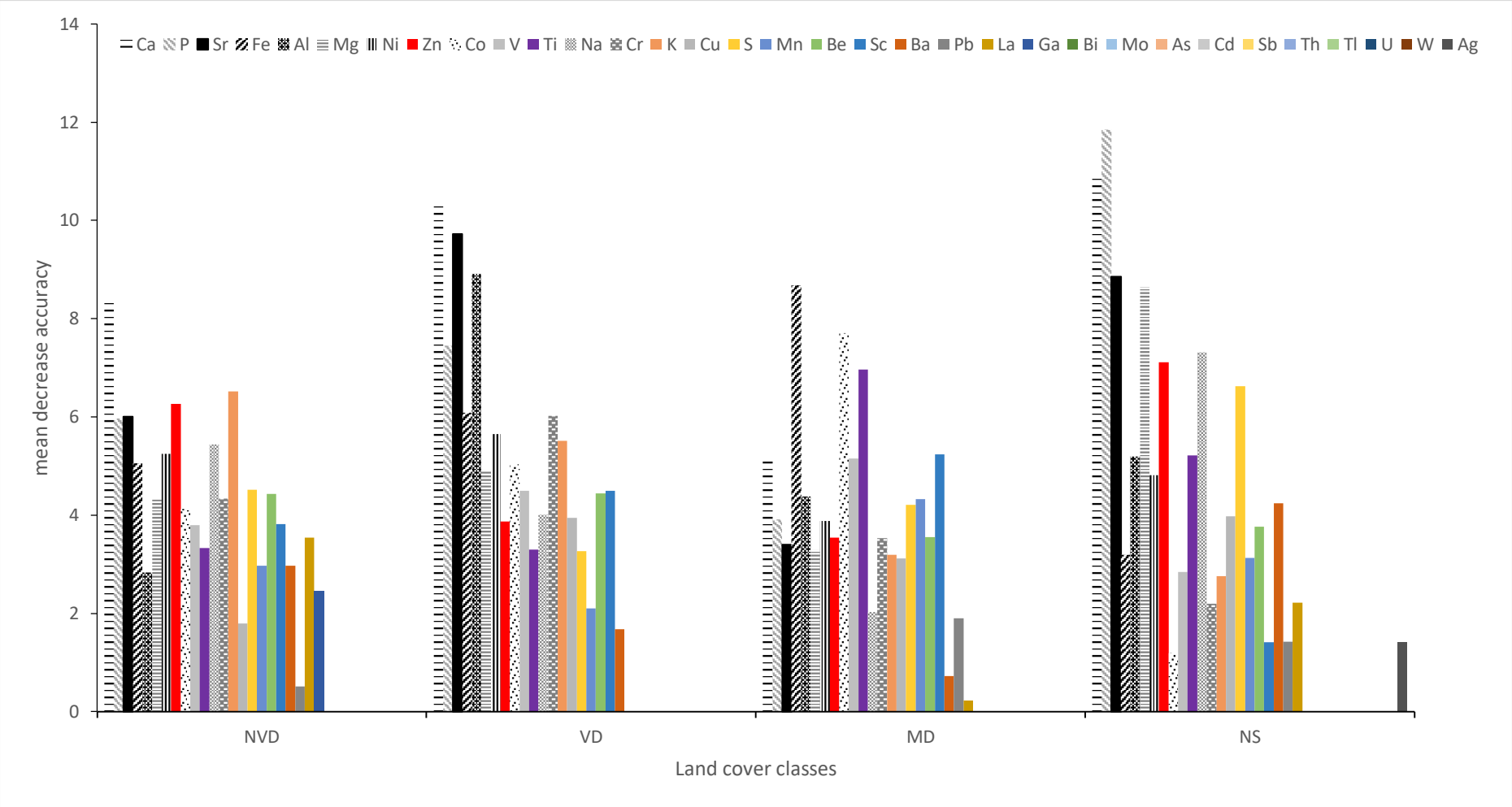

Figure 3. 5 Showing the importance of different elements in discriminating among the four soil classes; non-vitrified dung, vitrified dung, midden and non-sites. Elements with high MDA are the most important in the prediction model.

Basing on the measurements of variable importance (MDA) provided by RF, FVS procedure was used to find the smallest set of elements that resulted in the highest predictive accuracy in classifying non-sites, middens, vitrified dung and non-vitrified dung sites using RF. The optimal selected predictor variables (elements) with the lowest OOB error rate (15.38%) were P, Ca, Sr, Mg, Fe, Zn and Co. When using all elements the error rate increased to 17.31% (Figure 3. 6). The selected elements were then used as input variables in an RF classifier model for mapping non-sites, middens, vitrified dung and non-vitrified dung sites.

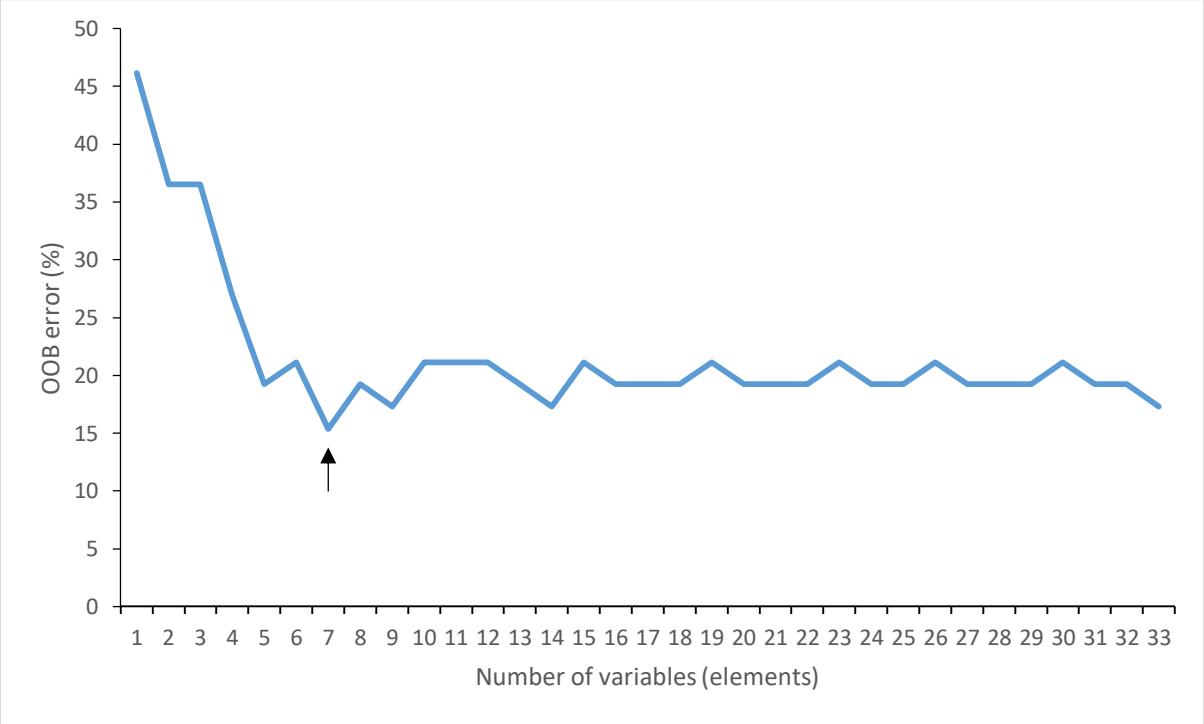

Figure 3. 6 Finding the best subset of classification variables for classifying non-sites, middens, vitrified dung and non-vitrified dung sites using FVS method based on the OOB error. The black arrow points to the optimal subgroup of elements with the lowest error.

All the wavelengths captured using the field spectrometer were input into an RF classification model. Mean decrease in Gini index in an ordinary RF was used to assess the importance of variables in differentiating between vitrified dung, natural soils, midden and non-vitrified dung sites. In general, the highest mean decrease in Gini Index occurred in the wavelengths within the visible spectrum (350-576 nm), with 513nm being the most important wavelength of them all. However, important variables cover a wide range of electromagnetic (EM) waves from visible wavelengths to the near-infrared wavelengths with notable peaks; between 350 and 576 nm, 1292nm-1380nm, 1575 and 1748nm, 1801 and 1808 nm (Figure 3. 7).

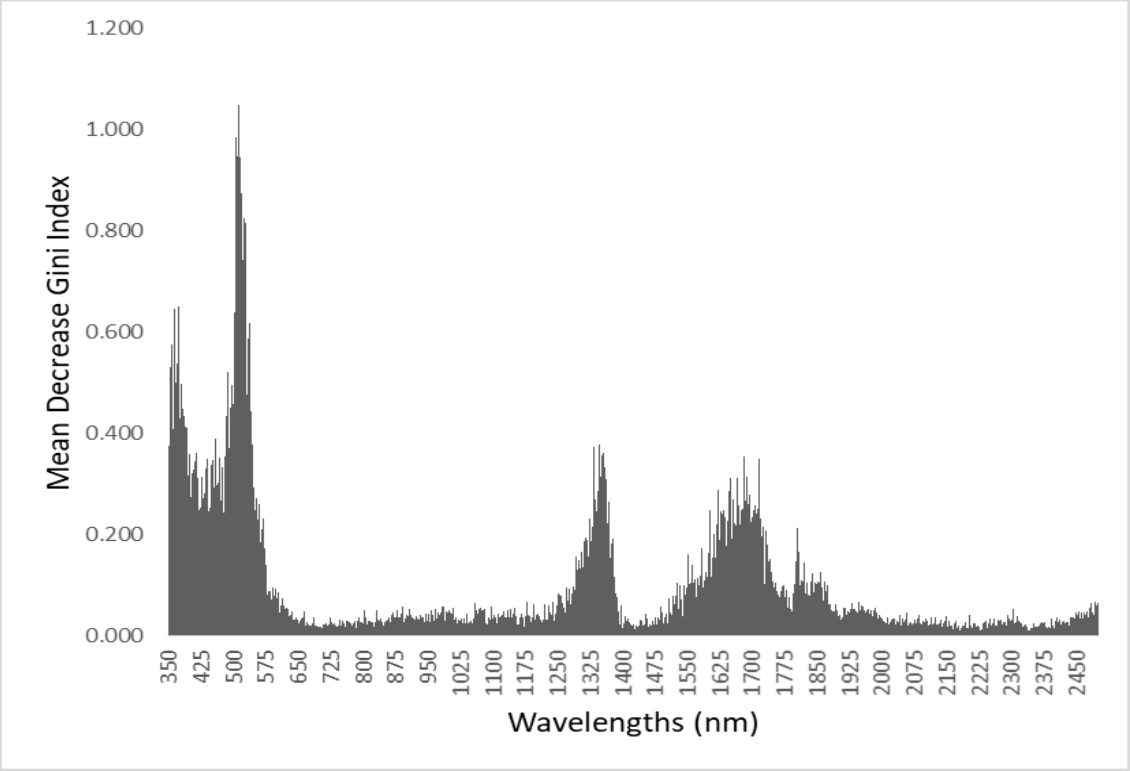

Figure 3. 7 Variable importance measurement produced by the RF algorithm for all variables (2151 wavelengths). The high mean decrease in Gini index reflects the most important variable.

The GRRF was used to select the best wavelengths for classifying vitrified dung, midden, non-vitrified dung and natural soils. This was done using variable importance scores for each wavelength obtained from the normal RF to guide the selection of features in a regularised RF. The best-selected wavelengths were 549 nm and 624nm within the visible spectrum while within the near infrared 996 nm, 1026nm, 1665nm, 1774nm, 1934nm and 2290nm were chosen, as shown in Figure 3. 8. The selected wavelengths were then inputted into RF classifier to map non-sites, middens, vitrified dung and non-vitrified dung sites.

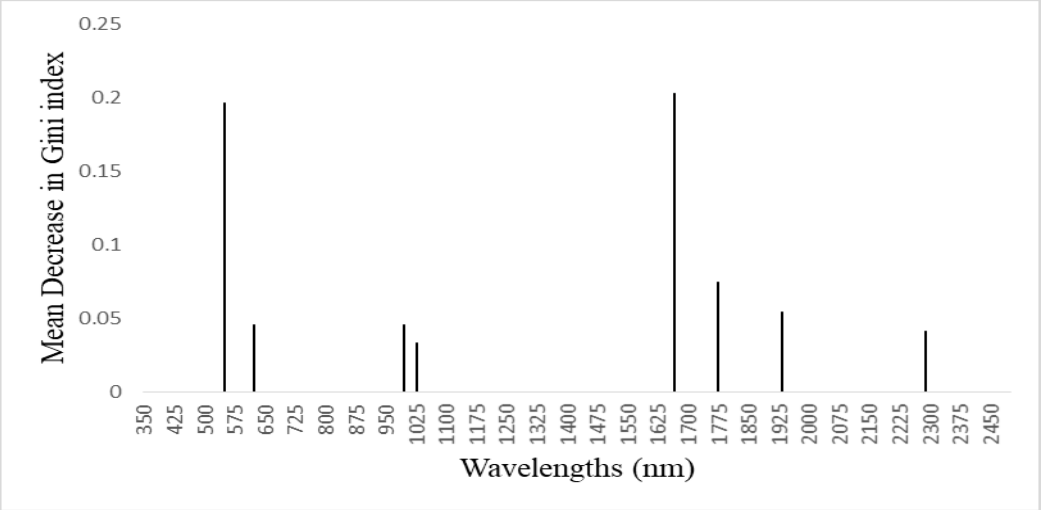

Figure 3. 8 The importance of optimum variables selected by GRRF calculated by the ordinary RF algorithm. The highest mean decrease in Gini index shows the most important variable.

3.3.3 Accuracy assessment

The prediction ability of RF was tested using optimal elements selected by FVS procedure and all elements. A holdout dataset, which was created by randomly dividing data into training (70%) and testing (30%), was used to test the accuracy of both models. RF was optimized using the grid search with the optimum combination of *mtry* and *ntree* achieving the lowest OOB error of about 15.38%. The findings demonstrate that the sites can be more accurately mapped using the selected seven bands than when using all the thirty-three elements (Table 3. 5). The overall accuracies of 84.62% was achieved when using the optimum variables while 82.69% was achieved when using 33 elements.

Table 3. 5 Error matrices showing the overall accuracy and Kappa for the classification of the four soil classes; non-vitrified dung (NVD), midden (MD), non-sites (NS), and vitrified dung (VD) using all variables (33 elements) and the optimum variables (7 elements)

Class	Thirty-three elements					Class	Seven elements				
	KR	MD	NS	VD	Total		KR	MD	NS	VD	Total
KR	14	2	0	1	17	KR	15	1	0	1	17
MD	1	8	2	0	11	MD	1	8	2	0	11
NS	0	2	10	0	12	NS	0	1	11	0	12
VD	1	0	0	11	12	VD	2	0	0	10	12
Total	16	12	12	12	52	Total	18	10	13	11	52
OA	82.69%					OA	84.62%				
Kappa	0.7674					Kappa	0.7921				

The user's and producer's accuracies of the two models are compared in Table 3. 6. Vitrified dung had higher producer's accuracy of 90.91% when using the most important variables (7 elements) while producer's accuracy of 91.67% was achieved when using 33 elements. Vitrified dung achieved high user's accuracy (91.67%) when using 33 elements and a lower user's accuracy when using the most important elements. Midden achieved lowest producers and users accuracies for both 33 elements and the most important elements (Table 3. 6).

Table 3. 6 Producer's and user's accuracies for the classification of the four soil classes; non-vitrified dung (NVD), midden (MD), non-sites (NS), and vitrified dung (VD) derived using all variables (33 elements) and the most important variables (7 elements)

Class	Thirty-three elements		Class	Seven elements	
	Producer's Accuracy (%)	User's Accuracy (%)		Producer's Accuracy (%)	User's Accuracy (%)
KR	87.50	82.35	KR	83.33	88.24
MD	66.67	72.73	MD	80.00	72.73
NS	83.33	83.33	NS	84.62	91.67
VD	91.67	91.67	VD	90.91	83.33

Classifications on ordinary RF algorithm were also done using optimal bands selected by the GRRF model. The optimum combination of *mtry* and *ntree* yielded the lowest OOB error of about 0.11. In overall, the classification model achieved an accuracy of 84.76% when using all wavelengths. However, a higher overall accuracy of 87% was achieved when using the optimal bands selected by GRRF (Table 3. 7).

Table 3. 7 Error matrices showing the overall accuracy and Kappa for the classification of the four soil classes; non-vitrified dung (NVD), midden (MD), non-sites (NS), and vitrified dung (VD) using all variables (2151 bands) and the optimum variables (8 bands).

Class	using 2151 bands					Class	using 8 bands				
	NVD	MD	NS	VD	Total		NVD	MD	NS	VD	Total
NVD	30	4	0	0	34	NVD	30	6	0	0	36
MD	4	18	0	4	26	MD	4	17	0	0	21
NS	1	2	27	0	30	NS	1	2	27	0	30
VD	0	1	0	14	15	VD	0	0	0	18	18
Total	35	25	27	18	105	Total	35	25	27	18	105
OA	84.76%					OA	87.62%				
Kappa	0.7927					Kappa	0.8316				

Table 3. 8 shows a comparison between the user's and producer's accuracies of the aforementioned datasets. Vitrified dung achieved high producer's and user's accuracies of 100% when using the optimum variables. The producer's and user's accuracies achieved for vitrified dung, which are 77.78% and 93.33% respectively, were lower than those achieved when using optimum bands. Midden achieved lowest user's and producer's accuracies when using 2151 bands and optimum bands respectively (Table 3. 8).

Table 3. 8 Producer's and user's accuracies for the classification of the four soil classes; non-vitrified dung (NVD), midden (MD), non-sites (NS), and vitrified dung (VD) using all variables (2151 bands) and the optimum variables (8 bands).

Class	using 2151 bands		Class	using 8 bands	
	Producer's Accuracy (%)	User's Accuracy (%)		Producer's Accuracy (%)	User's Accuracy (%)
NVD	85.71	88.24	NVD	85.71	83.33
MD	72.00	69.23	MD	68.00	80.95
NS	100.00	90.00	NS	100.00	90.00
VD	77.78	93.33	VD	100.00	100.00

A combination of optimum elements and bands were also put into ordinary RF classifier to see if they can improve the classification accuracy. The results show that a combination of optimal elements and bands produce a better classification accuracy than predictive models for all bands, all elements and when only selected elements are used. The model achieved an overall accuracy of 85.71% (Table 3. 9). The optimal *mtry* and *ntree* for the model produced the lowest OOB error of about 14.29%. High producer's accuracies of 100% were achieved for non-

vitrified dung and vitrified dung while midden and non-site achieved the lowest producer's accuracies of 66.67%. The user's accuracies of 100% were achieved for vitrified dung, midden and non-site while 71.43% was achieved for non-vitrified dung.

Table 3. 9 Error matrices showing the overall accuracy and Kappa for the classification of the four soil classes; non-vitrified dung, midden, non-sites and vitrified dung using a combination of optimum elements (n=7) and the optimum bands (n=8)

Class	NVD	MD	NS	VD	Total	UA (%)
NVD	5	1	1	0	7	71.43
MD	0	2	0	0	2	100.00
NS	0	0	2	0	2	100.00
VD	0	0	0	3	3	100.00
Total	5	3	3	3	14	
PA (%)	100.00	66.67	66.67	100.00		
OA	85.71%					
Kappa	0.7999					

PA= Producer's accuracy, UA= User's accuracy

3.4 Discussion

The main aim of this study was to assess the possibility of using hyperspectral data to discriminate non-sites, middens, non-vitrified and vitrified dung sites characteristic of areas previously occupied by farming communities. It also assessed if the aforementioned classes can be distinguished based on their chemical composition. The findings of this study have shown that there is a significant difference in the composition of elements characterising archaeological features. Most importantly, it has also shown that remote sensing techniques can be used to map surface archaeological features. This is an important development in the archaeological survey because the use of remote sensing techniques will enable the fast and cheaper documentation of sites over large areas.

Overall, the results for statistical analysis indicates that there is a significant difference in the concentration of elements in non-sites, middens, vitrified dung and non-vitrified dung sites. This is because different anthropogenic activities have different effects on the composition of soil elements (Entwistle et al. 2000; Fleisher and Sulas 2015). The concentration of P was significantly different across the non-sites, midden, vitrified dung and non-vitrified dung byre. On average vitrified dung had high concentrations of P followed by non-vitrified dung, midden and non-sites. This is unsurprising since phosphorus is widely used in archaeological research

as an indicator of different human activities (Holliday and Gartner 2007; Hutson et al. 2009). Phosphorous is incorporated into the soil by a number of human activities, which includes food preparation, garbage disposal and animal dung deposits, therefore, there is a need to analyse its concentration in combination with that of other elements in order to identify different activity areas (Entwistle et al. 2000; Middleton 2004). In this study, phosphorus was incorporated into the soil by deposits of animal dung in byres and ash and organic deposits in middens. Other elements such as Ca and Mg were significantly different among vitrified dung and the non-sites but were not significantly different between midden and non-vitrified dung. Generally, Mg and Ca were highly concentrated in activity areas with vitrified dung, non-vitrified dung, midden than in non-activity areas characterised by non-sites. The concentrations of the aforementioned elements within soil classes were also highly variable. This is also supported by the findings from Luzzadder-Beach et al. (2011) on the concentration of elements on anthropogenic activity areas in Turkey and Mexico, and Huffman et al. (2013) on the concentrations of Ca in vitrified dung deposits within the study area. This is influenced by the differences in the concertation of Ca and Mg in grasses consumed by animals and wood ash, which increase their levels in the soil (Griffith 1980; Hejcman et al. 2011; Huffman et al. 2013; Mashimbye 2013; Middleton and Price 1996). The differences in concentrations of elements within the same class can also be a result of depositional and post-depositional processes, which affects the overall concentration of elements in the soil, such as human activities, erosion and leaching (Huffman et al. 2013; Middleton and Price 1996; Wilson et al. 2009). On the other hand, potassium (K) is insignificantly different across all the classes except vitrified dung. This supports Huffman et al. (2013) findings that K_2O was significantly higher in vitrified dung than in non-vitrified dung. It is still not yet clear as to what causes the high levels of K in the vitrified dung deposits, however, Huffman et al. (2013) attribute some of it to mopane logs used to construct the fence around the kraal.

FVS procedure basing on the importance score of features calculated by ordinary RF was used to select a subset of key elements that can accurately discriminate among different archaeological sites. P, Ca, Sr, Mg, Fe, Zn and Co were chosen as the optimal elements for discriminating among middens, non-sites, non-vitrified dung and vitrified dung sites. This is in line with studies by Wilson and Davidson (2008) who found out that the composition of the aforementioned elements is affected by the presence of human activity areas such as middens and kraals. The concentration of the selected elements was also significantly different across different classes as discussed above. The classification done on RF classifier using chosen

optimal elements as input variables in RF classifier yielded high classification accuracy. This demonstrated that classification algorithms can also be used to predict the sites using their chemical composition. This also confirms findings by Oonk and Spijker (2015) that archaeological sites can be predicted by using elements as input variables in classification algorithms.

The spectral analysis results obtained from this study has shown that field spectroscopy data can be utilised to discriminating non-sites, midden, non-vitrified dung and vitrified dung from each other. GRRF model was used to reduce high dimensionality in the dataset (Deng and Runger 2013; Mureriwa et al. 2016). This algorithm has produced good results in vegetation mapping but has never been tested in soil analysis (Adam et al. 2017; Mureriwa et al. 2016). The algorithm selected eight important wavelengths across VIS/IR spectrum, 549 nm, 624nm, 996 nm, 1026nm, 1665nm, 1774nm, 1934nm and 2290nm, for discriminating among non-sites, midden, non-vitrified dung and vitrified dung. The selection of wavelengths from the visible spectrum (549 nm and 624nm) might be influenced by differences in soil organic content. This is consistent with the results of Bartholomeus et al. (2008) and Nolet et al. (2014) who found that there is a correlation between the absorption of wavelengths within the visible spectrum and the amount of organic matter in the soil. Soil organic content is also associated with soil colour. This is because a high concentration of organic matter results in dark soils and high wavelength absorption (He et al. 2009). Wavelengths 996nm and 1026nm in the near infrared region can be correlated with the concentration of elements such as Mg and Ca. This result is supported by Thomasson et al. (2001) who found out that concentration Ca and Mg levels in the soil are sensitive to spectral regions between 950-1500nm. The absorptions at other four selected wavelengths; 1665nm, 1774nm, 1934nm and 2290nm can be associated with the concentration of phosphorus in the samples. The increased levels of phosphorous highly correlate with the absorption of wavelengths between 1500nm and 2500nm (Bogrekci and Lee 2005a). Concentrations of calcium phosphate and magnesium phosphates in the soil also show high correlation with reflectance spectra in the aforementioned wavelength regions (Bogrekci and Lee 2005b). However, it has to be noted that different wavelengths within the same spectral region from those chosen by other models in other researches might have been chosen because the model was trained to remove correlation within the bands.

In general, high classification accuracies were achieved when using optimal bands selected by GRRF than when using all the 2151 bands. Low classification accuracy achieved when using all the 2151 bands is caused by high auto-correlation inherent within the field spectroscopy

data, which affects the performance of the prediction models (Adam et al. 2009; Mansour et al. 2012; Serpico and Moser 2007). The results of this study demonstrate that removing correlated variables improves classifiers prediction accuracy. Most importantly, high classification accuracies achieved using a subset of optimal wavelengths selected by the GRRF affirms its ability to select important wavelengths that improves the prediction accuracies of RF in classifying archaeological sites (Adam et al. 2017; Mureriwa et al. 2016). The combination of key elements (n= 7) and key wavelengths (n = 8), has yielded lower classification accuracy compared to the use of key elements (n= 7) and key wavelengths (n = 8) separately. Low classification accuracy achieved when combining key elements with key wavelengths was caused by data redundancy which resulted in noisy classification output (Adam et al. 2009; Bajcsy and Groves 2004; Mansour et al. 2012). The redundancy comes from the fact that wavelengths provide information about both the physical and chemical properties of the soil (Ben-Dor et al. 1997; Bogrekci and Lee 2005a), which means that combining the elements and spectral data in this study produced redundant data.

Generally, high classification accuracies achieved in this study show that it is possible to directly detect archaeological features such as middens, vitrified and non-vitrified byres using field spectroscopy data. This, therefore, promises a cost-effective method, which can be used to carry out archaeological surveys over large areas within a short period when compared to the use of element data and fieldwalking surveys. Surveying using remote sensing techniques will also make documentation and monitoring of archaeological sites located in inaccessible areas such as war zones and places with dangerous wild animals easy. In summary, this study followed the common geoarchaeological approach of identifying activity areas/sites based on the differences in the composition of elements and the possibility of identifying different sites basing on their spectral properties. Moreover, this study recommends the analysis of mineralogical constituents of the middens, non-sites, non-vitrified dung and vitrified dung sites and correlating them with their spectral properties.

3.5 Conclusion

The focus of this study was to investigate whether field spectra measurement can discriminate amongst archaeological sites using soil properties as indicators and identify the important bands for doing so. Statistical methods were used to assess if there is a significant difference in the concentration of elements between archaeological features and natural soils. Based on the outcomes of this study, the following inferences can be made:

1. There is a significant difference in the concentration of elements between non-sites, middens, non-vitrified dung and vitrified dung sites. This difference in the composition of elements within the aforementioned features can be used to discriminate among them when input into a classification algorithm. P, Ca, Sr, Mg, Fe, Zn and Co were identified as the important elements for discriminating among non-sites, middens, non-vitrified dung and vitrified dung sites when used as input variables in a classification model.

2. Field spectroscopy data has the ability to discriminate between non-sites, middens, non-vitrified dung and vitrified dung sites. This means that non-vitrified dung, vitrified dung, midden and non-sites have different spectral signatures.

3. Wavelengths within the visible-near infrared spectrum can be used to discriminate among natural soils, middens, vitrified dung and non-vitrified dung byres. A subset of eight important bands that gave the highest classification accuracy when discriminating among the aforementioned classes was identified across the visible-near infrared spectrum using GRRF. These were 549 nm and 624nm within the visible spectrum while within the near-infrared wavelengths 996 nm, 1026nm, 1665nm, 1774nm, 1934nm and 2290nm were chosen.

In summary, the results of this study have shown that there is chemical contrast between archaeological features such as middens, vitrified and non-vitrified dung byres and natural soils which makes it possible for field spectroscopy to discriminate among them. As such, the potential of remote sensing in detecting and mapping archaeological features with distinct soil physical and chemical characteristics such as the ones used in this study is present. Although the potential is present, further studies are needed to upscale field spectral measurements to different sensor spectral resolutions to ascertain which satellite sensor has the optimum wavelengths for detecting the archaeological sites characterised by middens, vitrified dung and non-vitrified dung.

Funding: This work was funded by the University of Botswana and the University of the Witwatersrand.

Conflicts of interest: The authors declare no conflict of interest

Acknowledgements

Thanks to the training department at the University of Botswana, for supporting this research. Gratitude is also given to SANParks for allowing access to Mapungubwe National Park and the DeBeers Group (through Duncan MacFadyen) for allowing access to Venetia Nature Reserve and use the research facility. The authors are also grateful to Prof. Thomas Huffman for availing his data and devoting his time by taking us through the study area, and Ihnos Dhau for his assistance in fieldwork during data collection and data processing in the lab. Special thanks to Lesego Madisha (former archaeologist at SANParks, Mapungubwe) for her kind assistance, SANParks' Cultural Heritage Manager Crispen Chauke and the Venetia Nature Reserve staff for their help.

CHAPTER FOUR

4. Examining the spectral ability of multispectral sensors to detect surface archaeological deposits, a case of the Shashi-Limpopo confluence area

The results of this chapter have been published as:

Thabeng, O. L., Merlo, S. and Adam, E., 2020. "From the Bottom Up: Assessing the Spectral Ability of Common Multispectral Sensors to Detect Surface Archaeological Deposits Using Field Spectrometry and Advanced Classifiers in the Shashi-Limpopo Confluence Area." *African Archaeological Review* 37: 25-49.

Abstract

This paper presents original research conducted in the Shashi-Limpopo confluence (Southern Africa) to identify the most suitable multispectral sensors for mapping archaeological sites typically inhabited by the farming communities of Southern Africa and characterised by surface features, such as ash middens, non-vitrified dung and vitrified dung. To achieve this, hyperspectral data were collected in the field using GER-1500 field spectroradiometer under laboratory conditions. The data were then resampled to the spectral resolutions of six common multispectral sensors (GeoEye, Landsat 8 OLI, RapidEye, Sentinel-2, SPOT 5 and WorldView-2) using the spectral library resampling tool in Environment for Visualizing Images (ENVI) v. 5.4 software. Mean decrease in accuracy, which is a measure of importance in RF classifier, was used to assess the importance of both hyperspectral wavelengths and each band allocated to a multispectral sensor in discriminating the above-mentioned archaeological classes. Two predictive models based on the resampled hyperspectral data were developed in R statistical packages version 3.4.1 using algorithms for support vector machine (SVM) and random forest (RF) classifiers. The results demonstrated that data resampled to the resolution of common multispectral sensors have the ability to predict surface archaeological features using RF and SVM classifiers. The important bands for predicting the sites were mostly in the visible and shortwave infrared regions of the electromagnetic spectrum. The best performance was achieved with data resampled to the resolution of the Sentinel-2 sensor, which attained 81.90% and 92.38% accuracy in both RF and SVM classifiers. Both classifiers achieved relatively low classification accuracies when using hyperspectral data resampled to the resolutions of satellite sensors which do not capture data in the shortwave infrared region (SWIR) such as WorldView-2, GeoEye and RapidEye sensors.

Résumé

Cet article présente des recherches originales réalisées dans la confluence de Shashi-Limpopo (Afrique australe) afin d'identifier les capteurs multispectraux les plus appropriés pour la cartographie des sites archéologiques habités par les communautés agricoles de l'Afrique australe. Ces sites sont caractérisés par des caractéristiques de surface spécifiques, telles que des amas de cendres, de bouse non vitrifiée et de bouse vitrifiée. Pour y parvenir, des données hyperspectrales ont été recueillies sur le terrain à l'aide d'un spectroradiomètre de champ GER-1500 dans des conditions de laboratoire. Les données ont ensuite été rééchantillonnées aux résolutions spectrales de six capteurs multispectraux courants (GeoEye, Landsat 8 OLI, RapidEye, Sentinel-2, SPOT 5 et WorldView-2). Cela s'est fait à l'aide de l'outil de

rééchantillonnage des bibliothèques spectrales integré dans l'outil Environnement de visualisation des images du logiciel ENVI v. 5.4. La diminution moyenne de la précision, qui est une mesure d'importance dans le classificateur random forest (RF), a été utilisée pour évaluer l'importance des longueurs d'onde hyperspectrales et de chaque bande attribuée à un capteur multispectral, afin de distinguer les classes archéologiques susmentionnées. Deux modèles prédictifs basés sur les données hyperspectrales rééchantillonnées ont été développés dans les logicel statistique R version 3.4.1, en utilisant des algorithmes 'support vector machine' (SVM) et les classificateurs RF. Les résultats ont montré que les données rééchantillonnées à la résolution des capteurs multispectraux courants permettent de prédire les caractéristiques archéologiques de surface à l'aide de classificateurs RF et SVM. Les bandes importantes pour la prédiction des sites étaient principalement dans les régions de l'infrarouge visible et à ondes courtes du spectre électromagnétique. Les meilleures performances ont été obtenues avec des données rééchantillonnées à la résolution du capteur Sentinel-2, qui ont atteint une précision de 81,90% et 92,38% dans les classificateurs RF et SVM. Les deux classificateurs ont obtenu une précision de classification relativement faible lors de l'utilisation de données hyperspectrales rééchantillonnées aux résolutions des capteurs satellites qui ne capturent pas de données dans la région infrarouge à ondes courtes (SWIR), telles que les capteurs WorldView-2, GeoEye et RapidEye.

Keywords Field spectral data, Spectral resampling, Variable importance, Farming communities

Archaeological time period: 900AD-1800'S

Country and region discussed: Botswana, South Africa and Zimbabwe, Southern Africa

4.1 Introduction

Africa is rich with heritage which documents human history from early primates up to recent complex societies (Connah 2004; Haaland 1995; Lange 2007; MacDonald 2013; Mattingly et al. 2007; Phillipson 2005; Shaw et al. 1993; Stahl 1994). Heritage sites on the continent are faced with dangers posed by both anthropogenic and natural threats such as mining activities, urban development, looting, flooding, erosion and fires (Chirikure 2013; Kankpeyeng and DeCorse 2004; Khandlhela and May 2006; Lasaponara et al. 2016a; Musyoki et al. 2016; Nienaber et al. 2008; Parcak 2015; Smith 2012). In addition to this, heritage management institutions in Africa are facing a number of challenges, which include, among others, lack of funds often leading to inadequate surveying, documentation and monitoring of heritage sites (Chirikure 2013; Mabulla 2001; Mcintosh 1993). Site surveying, documentation and monitoring in some parts of the sub-continent is also hampered by inaccessibility due to factors such as the presence of dangerous wild animals, conflicts, and property rights (Biagetti et al. 2017; Mabulla 2001; Thabeng et al. 2019).

The documentation of archaeological features in Africa has traditionally been done through fieldwalking surveys (Fleisher and LaViolette 1999; Hitchner 1995; Huffman 2009b, 2011; McIntosh and McIntosh 1993). Field walking survey offers the surveyor an opportunity to identify, appreciate and record finer details of different types of archaeological sites on the ground (Foard 1977; Reid and Segobye 2000). Even though fieldwalking surveys offer detailed contextual records of archaeological materials on the ground, they are time-consuming, costly and difficult to carry out over large areas (Banning et al. 2006; Corrie 2011; Hitchings et al. 2013). More recently, remote sensing has offered a relatively cheap, fast, systematic and reproducible method of survey, which can be used to document and monitor archaeological sites over large and/or inaccessible areas within a short period of time (Keay et al. 2014; Lasaponara et al. 2014).

The potential of remote sensing techniques in the archaeological survey has been demonstrated in various contexts since the 1920s (Agapiou et al. 2014a; Beck 2007; Crawford 1923; Mason 1968; Opitz and Herrmann 2018; Parcak 2007). Remote sensing in archaeology exploits the spectral contrast between areas of archaeological interest and their surroundings (Corrie 2011). This is because different anthropogenic activities have localised impact on the soil's physical and chemical properties, thus making it different from its surroundings (Oonk et al. 2009; Wilson et al. 2008). As a result, several studies (Agapiou et al. 2012b; Altaweel 2005; Crawford

1923) employed remote sensing techniques in archaeology and identified a number of archaeological site indicators. For example, negative vegetation marks have been identified as indicators of the presence of subsurface archaeological features such as walls (Hejcman and Smrž 2010). This is because the presence of walls in the soil makes it more compact and less moisture retentive therefore resulting in stunted vegetation growth over them (Gojda and Hejcman 2012). High moisture retentive features such as ditches have been linked with positive vegetation marks (Featherstone et al. 1999; Reeves 1936). On the other hand surface, archaeological features can be identified based on their physical features such as form (De Laet et al. 2007; Mason 1968; Sadr 2016b) and ecological indicators (Denbow 1979; Reid 2016).

Remote sensing data can be captured using broadband (multispectral) and narrowband (hyperspectral) sensors housed on a handheld, airborne and spaceborne platforms (Bradbury et al. 2013; Cavalli et al. 2013; Doneus et al. 2014; Mutanga et al. 2015; Schmidt and Skidmore 2003). Although of recent, there are many multispectral satellite sensors with different spatial and spectral characteristics providing large volumes of dataset, the challenge now is to identify the suitable sensors for studying different archaeological features (Agapiou et al. 2014a; Parcak 2007). This is because, in addition to optimum environmental conditions, the ability to detect archaeological material using remote sensing depends on the spectral and spatial resolutions of the sensor (Beck 2007). As a result, a number of studies have compared the accuracies of different satellites in detecting archaeological features (Fowler 2002; Parcak 2007). Consequently, this approach is time-consuming and expensive, especially when using commercial satellite images.

On the other hand, hyperspectral data offer high spectral resolution by capturing narrow bands across visible, near infrared and shortwave infrared portions of the electromagnetic spectrum. This high spectral resolution permits the identification of distinctive attributes of different features (Agapiou et al. 2012b; Cavalli et al. 2007; Cerra et al. 2018). As a result, many studies have used field and laboratory hyperspectral data to pilot investigations on the potential application of remote sensing principles in various fields including the analysis of soil physical and chemical properties (Cozzolino and Moron 2003; Nocita et al. 2014; Sørensen and Dalsgaard 2005), vegetation health (Dhau et al. 2018b; Kokaly 2001), spectral identification of different vegetation species (Adam et al. 2009; Cochrane 2000), and spectral discrimination of archaeological sites (Agapiou et al. 2010, 2012b; Melillos et al. 2018). Hyperspectral data has also been used to investigate the ability of planned multispectral satellite sensors to detect vegetation indices associated with buried archaeological features (Agapiou et al. 2014b).

Currently, there are very few studies aimed at identifying spectral bands suitable for discriminating surface archaeological features in current operational multispectral sensors (Thabeng et al. 2019). However, even though the use of hyperspectral sensors in discriminating against archaeological features has been successful, there are some limitations to it.

Some of the major limitations of hyperspectral data are high computational demands and the large data redundancy due to the strong correlation between the spectral features (Burger and Gowen 2011; Doneus et al. 2014; Feng et al. 2016; Metternicht et al. 2010; Sibanda et al. 2016). Additionally, even though hand-held spectrometers have been widely used in preliminary studies investigating applications of remote sensing in many applications, there are no operational airborne and spaceborne sensors matching its very high spectral resolution. As a result numerous studies have resampled field and laboratory hyperspectral data acquired over small areas to the spectral resolutions of existing multispectral and hyperspectral sensors in order to investigate their possible use in different applications including soil analysis (Nawar et al. 2014), vegetation studies (Adam et al. 2012; Mansour et al. 2012) and archaeology (Agapiou et al. 2014a). The major limitation of resampling using field and lab spectroscopy data is that it has a high signal to noise ratio (the amount of useful information against the unwanted data), which is impossible to achieve with imagery from airborne and spaceborne sensors (Mutanga et al. 2015). However, studies (Mansour et al. 2012; Mutanga et al. 2015) have found no significant difference between the results obtained from resampling fine resolution data and those from the actual image. Therefore, there is a need to test this technique in archaeological applications focusing on surface deposits, where according to our knowledge, it has never been tested before. If the results are positive, the mapping of archaeological surface deposits could be possible on satellite platforms.

To this end, this study seeks to evaluate the ability of in *situ* hyperspectral data resampled to the spectral resolutions of the most common multispectral sensors (namely GeoEye, Landsat 8 OLI, RapidEye, Sentinel-2, SPOT 5 and WorldView-2), to detect surface archaeological deposits. The specific objectives of the paper are: (i) to identify the optimum spectral resolution for predicting archaeological sites (ash middens, non-vitrified dung and vitrified dung) using in *situ* hyperspectral data resampled to different remote sensing multispectral platforms; (ii) to compare the prediction accuracies of ash middens, non-vitrified dung and vitrified dung achieved using resampled data, RF and SVM classifiers; and (iii) to identify the importance of the different bands allocated in different multispectral sensors in predicting archaeological sites (ash middens, non-vitrified dung and vitrified dung) using RF algorithm.

4.2 Materials and Methods

4.2.1 Study area and archaeological context

The Mapungubwe cultural landscape is a UNESCO listed heritage area situated where the Shashi and Limpopo rivers meet in the province of Limpopo, South Africa (Figure 4. 1). The Shashi-Limpopo Confluence Area (SLCA) forms the boundaries of three countries; Botswana to the west, South Africa to the south and Zimbabwe to the north. The soils in the study area are dominated by cambisols, leptosols, and luvisols originating from the Karoo system (Bangira and Manyevere 2009; Götze et al. 2003).

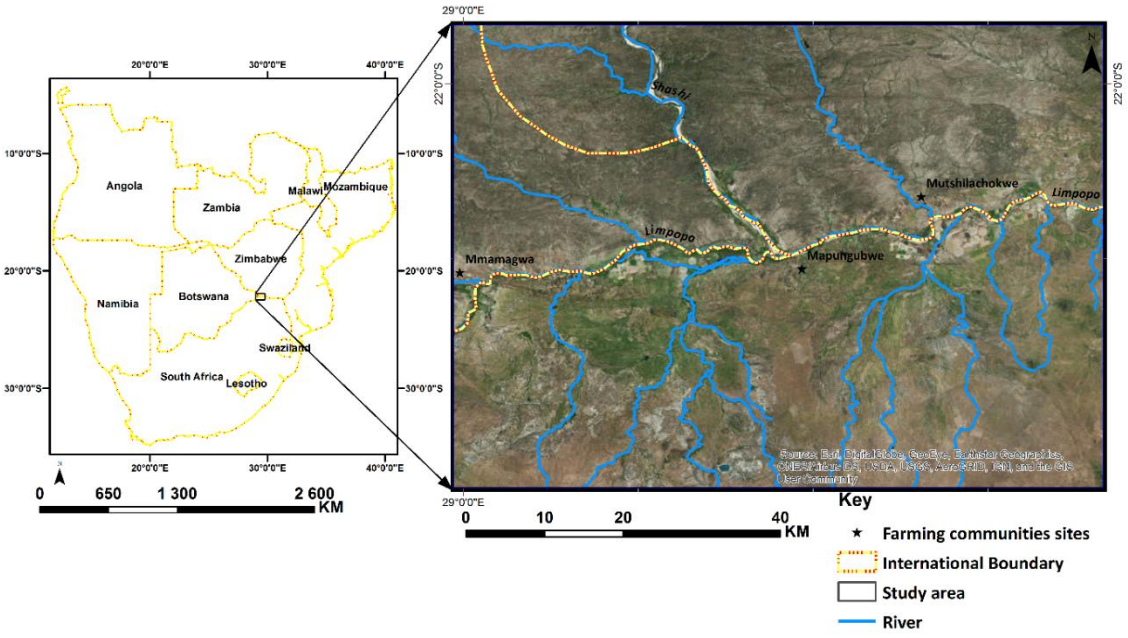

Figure 4. 1 Location of the study area in southern Africa

Mapungubwe cultural landscape has been occupied by different groups of farming communities in two distinctive periods. The first occupation of the Mapungubwe cultural landscape by farming communities temporarily occurred during the early centuries of the first millennium AD (Huffman 2008; Huffman and Du Piesanie 2011). The second occupation of the Mapungubwe cultural landscape by different groups of farming communities occurred from 900 AD onwards (Calabrese 2000; Eloff and Meyer 1981; Huffman 2000; Vogel and Calabrese 2000). These societies practised the central cattle pattern (CCP) settlement system (Hanisch 2002). The main features of this spatial organisation are:(1) a central cattle kraal with elite burials and storage pits for grains; (2) a men gathering area next to the kraal; (3) an outer

residential zone characterised by huts which are arranged according to left/right seniority, with the one upslope behind the court being most senior; (4) the demarcation of space within the house into right for male and left for female (Fagan 1964; Huffman 2000, 2001, 2009a). Social and political changes in the Mapungubwe cultural landscape took place during the early centuries (AD1000- AD1300) of its occupation, with the development of class distinction and sacred leadership (Huffman 2000; Meyer 2000). The chief/king was physically separated from the commoners in the twelfth century with the occupation of the Mapungubwe hill (Huffman 2009a). This led to changes in the organisation of the settlements whereby the traditional CCP was abandoned and some stonewalls were built to seclude rulers from the commoners in major settlements (Huffman 2000; Meyer 2000). However, the CCP continued in the satellite settlements occupied by commoners (Huffman 2000). At the peak of its power the leadership of Mapungubwe is believed to have dominated societies about 200 km away. Mapungubwe societies traded glass beads, marine shells with the merchants along the Indian Ocean coast, and exchanged these goods with metals, salt, ivory and animal skins from the interior polities such as Toutswe and Bosutswe. This was before the shift of power and trade to the Great Zimbabwe kingdom after the collapse of the Mapungubwe kingdom in the 13th century AD (Calabrese 2000; Denbow 1990; Huffman 2009a; Klehm et al. 2019). Nevertheless, the trading between the societies which occupied the Mapungubwe cultural landscape and the east coast merchants continued into the historic periods (Huffman 2012).

Archaeological sites previously occupied by farming communities in southern Africa, including SLCA, are generally characterized by features such as byres and middens (Denbow 1979; Huffman 2009a; Huffman et al. 2013; Jacobson et al. 2003; Reid and Segobye 2000; Thy et al. 1995). The locations of byres within the settlement are normally marked by the deposits of vitrified dung and/or non-vitrified dung deposits (Huffman 2009a; Meyer 2000). Non-vitrified dung deposits consist of unburned dung (Huffman et al. 2013). Vitrified dung is a glassy biomass slag with high deposits of nitrates and phosphates formed by burning thick dung deposits at very high temperatures (in the region of 1100^{o}C) (Peter 2001; Thy et al. 1995). The burning of dung has been associated with cleansing practices (Huffman et al. 2013; Peter 2001). Middens are areas where the general waste of a household, including remains of unused materials such as broken potsherds, animal bones, beads and other utensils and ashes from fireplaces were discarded (Chirikure et al. 2014; Huffman 2012). Middens differ in size depending on the duration and density of site occupation (Eloff and Meyer 1981). Generally, the sites previously occupied by the farming communities appear as bare patches within the

savanna woody vegetation which is, in most cases, covered by grass (Denbow 1979; Mothulatshipi 2008). Some of the common grasses are cenchrus cilliaris which has been identified as an ecological indicator of similar sites in central eastern Botswana (Denbow 1979). This environment creates ideal conditions for testing the applicability of airborne and spaceborne remote sensing in archaeological survey. Although Cenchrus cilliaris as an ecological indicator of similar sites in central eastern Botswana by Denbow (1979), it is too widely spread to be used for archaeological sites prospection in Mapungubwe cultural landscape (Götze et al. 2008; Mothulatshipi 2008). If successful the models will only map archaeological features which are large enough to be captured by the sensor used for data gathering. Additionally, these models will also allow archaeologists and researchers to explore for archaeological sites with similar characteristics in the new environments.

Documenting the locations of byres and middens within the Mapungubwe cultural landscape is important for understanding their intra- and inter-settlement patterns because they form the central part of the settlements occupied by the farming communities as discussed above (Huffman 2000, 2009a; Meyer 2000). Furthermore, using spaceborne sensors to document the aforementioned features will deepen the understanding of their spatial organisation by providing their panoramic view within the landscape, thus revealing patterns which may be invisible on the ground through field walking. In-depth archaeological fieldwork spanning a period of close to four decades has been carried out on the South African side of the confluence by different researchers (Hanisch 1980; Huffman 1989b, 2009b, 2011; Huffman et al. 2004; Huffman and Du Piesanie 2011). In other areas of the confluence sporadic systematic surveys have been carried by Manyanga (2007) in Zimbabwe and Mothulatshipi (2008) in Botswana. The aforementioned unevenness in research creates imbalances in the understanding and interpretation of the archaeology of the confluence. Using this well-documented study area will help in testing the predictive ability of this remote sensing model and if successful it will enable the archaeologists and researchers to broaden their archaeological knowledge of the SLCA by deploying the model with confidence in areas where very few researches have been done especially in the Zimbabwe and Botswana side of the confluence. Above all, the archival nature

of satellite data will be of paramount importance in preserving the layout and locations of sites in the face of destruction emanating from natural phenomena and developments.

4.2.2 Field data collection

A total of 356 soil surface samples (at a depth of 0-20cm) were collected in February 2017 and packed in zip-lock plastic bags for field spectral measurements in the laboratory. This procedure corresponds with the traditional method of acquiring reproducible, stable and accurate spectral measurements (Ben-Dor et al. 2017; Stevens et al. 2010). Between 60 and 117 samples were collected for each category: non-sites (natural soil) and archaeological soils characterised by ash middens, vitrified dung and non-vitrified dung deposits. A purposive sampling method was used during the fieldwork data collection by visiting archaeological sites which were noted in the literature as characterised by dung deposits and ash middens (Huffman 2009b, 2011). Bare soil samples were collected from areas far away from the archaeological sites in order to avoid possible contamination from the archaeological soils caused by wind and water erosion.

4.2.3 Lab spectral measurements and resampling

A portable field spectrometer (FieldSpec® 4) was used to measure the reflectance spectra of vitrified dung, non-vitrified dung, midden and non-site soils in a controlled environment. This was done in order to minimise the atmospheric effects caused by weather conditions. The Analytical Spectral Devices (ASD) spectral offers very narrow spectral channels which have been successfully resampled to the resolution of broadband sensors (Castaldi et al. 2016; Mutanga et al. 2015). It captures visible-near infrared and short wave infrared spectral data between 350-2500nm, at a bandwidth of 1.4 nm in the visible-near infrared region (350-1000nm) and 1.1 nm in short wave infrared region (1001-2500nm) (Analytical Spectral Devices, Inc. 2018). The spectrometer was calibrated using a white spectrolon reference panel before taking measurements of a new sample and thereafter every 10 to 15 measurements in order to minimise atmospheric effects. Soil samples were flattened on a black plastic plate to create a smooth surface. The spectral measurements were then taken directly from the soil surface of each sample at nadir position with 10mm field of view using Hi-Brite contact probe fitted with 100W halogen reflector lamp (Ben-Dor et al. 2015; Ogen et al. 2017). Between 60 and 117 samples were collected from non-sites, middens, vitrified dung and non-vitrified dung sites in the field, see Table 4. 2 below. Three spectral measurements were taken per sample by randomly moving the probe over the soil surface, in an attempt to obtain a representative

reflectance spectrum for the sample. The spectral measurements were then averaged to represent the absolute spectral reading of the soil class of interest (Figure 4. 2).

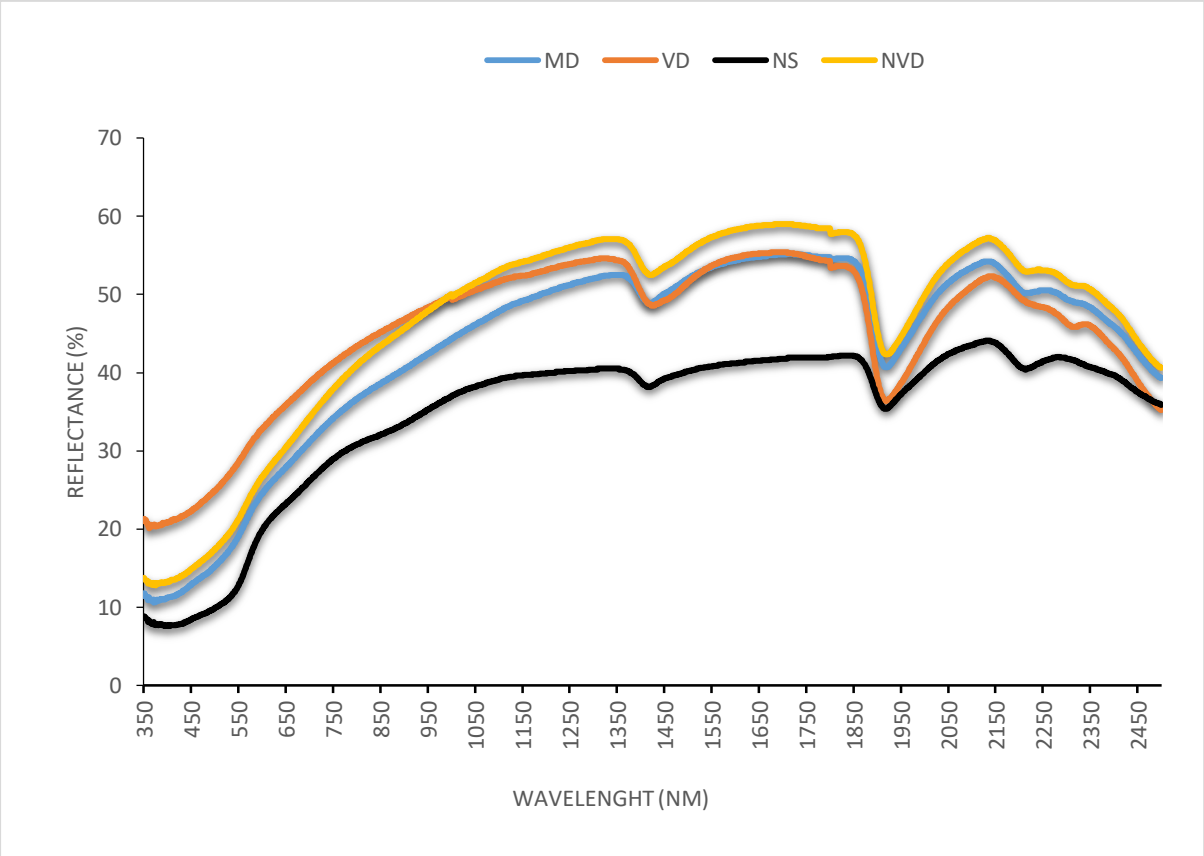

Figure 4. 2 Visualisation of the average lab spectral measurements of different soil classes. The classes are non-vitrified dung (NVD), midden (MD), non-site (NS) and vitrified dung (VD).

Hyperspectral data measured in the lab were then converted to an ASCII file containing 10-nm-wide band spacing using wavelengths between 350-2500 nm. The resultant hyperspectral data contained in the ASCII file was averaged to resample the spectral resolutions of common multispectral sensors using the resampling spectral library function inherent within Environment for Visualizing Images (ENVI) v. 5.4 software. The resampling tool in ENVI employs a Gaussian model with a spectral resolution (Full Width at Half Maximum) set to the provided band spacing. The Gaussian model has been successfully used to resample the spectral resolutions of various multispectral sensors using hyperspectral data (Dhau et al. 2018a; Oumar and Mutanga 2010; Verrelst et al. 2013). The hyperspectral data were resampled to the spectral resolutions of a selection of popular multispectral sensors (GeoEye, Landsat 8 OLI, RapidEye, Sentinel-2, SPOT 5 and WorldView-2) using band centres in Table 4. 1. Bands between 350-400nm and 2400-2500nm were removed from the data before resampling, as these bands are affected by noise (Castaldi et al. 2016).

Table 4. 1 Spatial resolutions and spectral characteristics of the different multispectral sensors (GeoEye, Landsat 8 OLI, RapidEye, Sentinel-2, Spot 5 and WorldView-2) showing band description, bandwidth and band centre

Sensor	Band description	Bandwidth	Band centre	Spatial resolution (nadir)
GeoEye	Blue	450-510	480	0.46m pan
	Green	510-580	545	1.84m MS
	Red	655-690	672.5	
	Near Infrared	780-920	850	
Landsat 8	Coastal	430-450	440	15m pan
	Blue	450-510	480	30m MS
	Green	530-590	560	
	Red	630-670	650	
	Near Infrared	850-880	865	
	SWIR 1	1570-1650	1610	
	SWIR 2	2110-2290	2200	
RapidEye	Blue	440-510	475	6.5m MS
	Green	520-590	555	
	Red	630-685	657.5	
	Red Edge	690-730	710	
	Near Infrared	760-850	805	
Sentinel-2	Aerosols	433-533	483	10m, 20m, and 30m MS and SWIR
	blue	458-523	490.5	
	green	542-578	560	

	red	650-680	665	
	vegetation red edge	695-713	704	
	vegetation red edge	733-748	740.5	
	vegetation red edge	733-793	763	
	Near Infrared	855-875	865	
	vegetation red edge	785-900	842.5	
	Water vapour	935-955	945	
	Short Wave Infrared-Cirrus	1360-1390	1375	
	Short Wave Infrared	1565-1655	1610	
	Short Wave Infrared	2100-2280	2240	
Spot 5	Green	500-590	545	5m pan
	Red	610-680	645	10m MS
	Near Infrared	780-890	835	20m SWIR
	SWIR	1580-1750	1665	
Worldview-2	Coastal	400-450	425	0.46m pan
	Blue	450-510	480	1.84 MS
	Green	510-580	545	
	Yellow	585-625	605	
	Red	630-690	660	
	Red Edge	705-745	725	
	Near Infrared 1	770-895	832.5	
	Near Infrared 2	860-1040	950	

The resulting resampled satellite datasets were divided into training (70%) and test (30%)

datasets (Table 4. 2). Thereafter the datasets were used as input variables in RF and SVM classifiers to test if their spectral resolutions are suitable for predicting archaeological sites.

Table 4. 2 Training and validation dataset for all the soil classes created by splitting the field data into 70:30.

Archaeological classes	Code	Training dataset	Validation dataset	Total number of spectral samples
Midden	MD	61	25	86
Non-vitrified dung	NVD	82	35	117
Vitrified dung	VD	42	18	60
Non-sites	NS	66	27	93

4.2.4 Data classification

RF and SVM were used to classify archaeological and non-archaeological data. In recent time, RF and SVM have been widely applied on remotely sensed data for land use and land cover classifications and dependable results has been attained (Ahmad et al. 2010; Chagas et al. 2016; Grimm et al. 2008). Furthermore RF and SVM has the ability to handle unwanted distortions in remote sensing (Rodriguez-Galiano and Chica-Rivas 2014). Their reliability would, therefore, be an advantage for archaeological site prediction, in particular in areas of limited accessibility.

4.2.4.1 Random forest

RF is a non-parametric machine learning classification algorithm developed by Breiman (2001). The algorithm uses an ensemble of classification and regression trees for prediction. The algorithm grows each tree, without trimming it until its nodes reach purity, using a random subset of predictor variables (Adam et al. 2017). Each tree from the forest then contributes a single vote for the prediction class with the majority votes deciding the class. RF needs the optimisation of the number of trees (ntree) and the number of the predictive variables taken into consideration at each node (*mtry*) in order to improve the classification accuracy (Genuer et al. 2010; Mureriwa et al. 2016). The bootstrap sampling of variables at random carried out in building each tree was performed with replacement from the population (Breiman 1996; Rodriguez-Galiano et al. 2012b). This sampling technique divides the variables into two-thirds training data and uses the remaining third to asses the importance of each variable in classification and generalisation error (Belgiu and Drăguţ 2016). The testing data is defined as the Out-Of-Bag (OOB) sample.

One major advantage of the RF over other machine learning algorithms, such as artificial neural networks and SVM, is its inherent ability to measure the importance of each candidate predictor in the classification process. This advantage has been demonstrated in a number studies where RF was used for reduction of dimensionality and variable selection in various domains like bioinformatics (Díaz-Uriarte and De Andres 2006; Farhat et al. 2016; Wu et al. 2008), ecology (Brieuc et al. 2015; Wei et al. 2010), remote sensing (Mutanga et al. 2012) and medical imaging (Lebedev et al. 2014). Gini importance measures the contribution of each predictor in keeping the nodes pure in a forest. The second measure of importance, mean decrease in accuracy, is calculated using the RF internal measure of accuracy. RF asses the importance of each variable in the final model by measuring the decrease in accuracy by means of OOB error, when its values are removed from the sample with other variables remaining constant (Breiman 2001). The error is expected to rise if the variable is important in the prediction of the forest. The importance of predictor variable y_j can be defined as:

$$MDA(y_j) = \frac{1}{ntree} \sum_{t=1}^{ntree} (ap_{tj} - a_{tj}) \qquad \text{Equation 4.1}$$

Whereby:

1. ntree is the number of trees of the RF,
2. ap_{tb} is the OOB error of tree *t* after randomly permuting the values of the predictor variable y_j , and,
3. a_{tb} is the OOB error of tree *t* before randomly permuting the values of the predictor variable y_j

The end results for each predictor variable can then be used to asses its importance in relation to others in the prediction process. In this study, MDA was used to measure the importance of hyperspectral data and resampled satellite bands in predicting non-sites, ash middens, non-vitrified dung and vitrified dung. The *mtry* and *ntree* were optimised using grid search and 10-fold cross-validation in the e1071 library (Meyer et al. 2017) of R statistical packages version 3.4.1. The resampled hyperspectral data was then classified in R using the randomForest package which is based on the original RF algorithm developed by Breiman and Cutler (2007).

4.2.4.2 Support vector machines

SVM classification algorithm has previously been used to classify land cover data from satellite sensors (Adam et al. 2014; Ustuner et al. 2015). This is because of its robust generalisation ability, capacity to deal with noise effects and achieve high classification accuracies (Shao and Lunetta 2012). SVM are non-parametric classifiers, therefore they do not assume normality within training statistics. In this study, SVM was used to predict the soil classes using resampled satellite bands. SVM is a kernel-based algorithm which predicts classes by finding the hyperplane that optimally separates two classes in a high dimensional feature space (Chen and Lin 2006; Zhu and Blumberg 2002). The most commonly used SVM kernels are the polynomial, sigmoid, linear and radial basis function (RBF) (Ben-Hur and Weston 2010; Lin and Lin 2003; Pal and Mather 2005). A radial basis kernel function was used to classify the data in this study because of its ability to handle nonlinear relations between class labels and attributes (Hsu et al. 2003). The RBF defined as:

$$k(x, x^1) = \exp(-\gamma||x - x^1||^2) \qquad \text{Equation 4.2}$$

Whereby x and x^1 represent two points from training data with default kernel function parameter (γ) which is (1/(data dimension)). RBF requires two user-defined parameters, which are the regularization parameter (C) and kernel function parameter (γ) to run the SVM model. The regularisation parameter regulates the accepted level of misclassification errors by determining the margin between class boundaries (Li et al. 2015b). Kernel function parameter defines the width of the Gaussian kernel. In general, the aforementioned parameters have an influence on the overall classification accuracy hence a need to carry out a search for optimum parameters to run the model for good classification accuracy to be attained (Hsu et al. 2003). In this study, pairs of C and γ parameters were optimised using a 10 fold cross-validation and gird search. This method tests various combinations of C and γ parameters and chooses the one which attained the best cross-validation accuracy. The model follows the procedure described below:

1. Consider a grid space of (C, γ) with log_2C ∈ {-5,-3, . . , 13} and $log_2\gamma$ ∈ {-13,-11, . , 3}.
2. For each pair of C and γ parameters in the search space, do 10-fold cross-validation on the training set.
3. Select a pair of C and γ, which will result in the best overall cross-validation classification rate.

4. Train a model using the selected best combination of parameters (C, γ)

The optimisation of parameters and classification of the resampled hyperspectral data were done using the e1071 library (Meyer et al. 2017) of R statistical packages version 3.4.1.

4.2.5 Accuracy assessment

Classification accuracy was assessed by means of the confusion matrix, which was constructed using a holdout dataset created by randomly dividing the resampled data into 70% (training data) and 30% (test data), see Table 4. 2 above. The confusion matrix enables the assessment of the classification of each class by giving the user's accuracy and the producer's accuracy (Congalton 1991). User's accuracy shows the proportion of predictor variables correctly predicted as they are in reality. This measure is achieved by dividing the number of correctly predicted variables by the row total. Producer's accuracy, on the other hand, measures the proportion of predictor variables, which were correctly predicted within a class. Producer's accuracy is attained by dividing the number of correctly predicted variables by the column total. Above all, the confusion also offers the overall accuracy, which is the percentage of correctly classified test pixels across all classes. Even though the cause of correct allocations or misclassifications have been deemed as a needless component of accuracy assessment, Kappa Coefficient was used in this study together with overall accuracy (Pontius Jr and Millones 2011; Stehman and Foody 2019). This is because, despite it containing data that is redundant to that of overall accuracy, it is still an important part of the accuracy assessment (Stehman and Foody 2019). Cohen's kappa coefficient is defined as:

$$K = \frac{\Pr(o) - \Pr(c)}{1 - \Pr(c)} \qquad \text{Equation 4.3}$$

Where $\Pr(o)$ is the observed agreement and $\Pr(c)$ is the expected agreement. A perfect agreement is achieved if the kappa value (K) is one or close to one (McHugh 2012; Rosenfield and Fitzpatrick-Lins 1986).

4.3 Results

4.3.1 Optimisation of RF and SVM

The optimisation results of RF parameters (*mtry* and *ntree*) for different sensors are shown in Figure 4. 3. In general, the lowest error rates achieved by the different optimum *mtry* and *ntree* combinations for spectral data resampled to resolutions of various sensors ranges between 0.12 and 0.168 (Figure 4. 3). The optimum *mtry* and *ntree* parameter combinations for Sentinel-2 achieved the lowest OOB error rate at the value of 0.12. The best *mtry* and *ntree* parameter

combination for hyperspectral data resampled to resolution each satellite sensor was used to classify its related data in the RF algorithm.

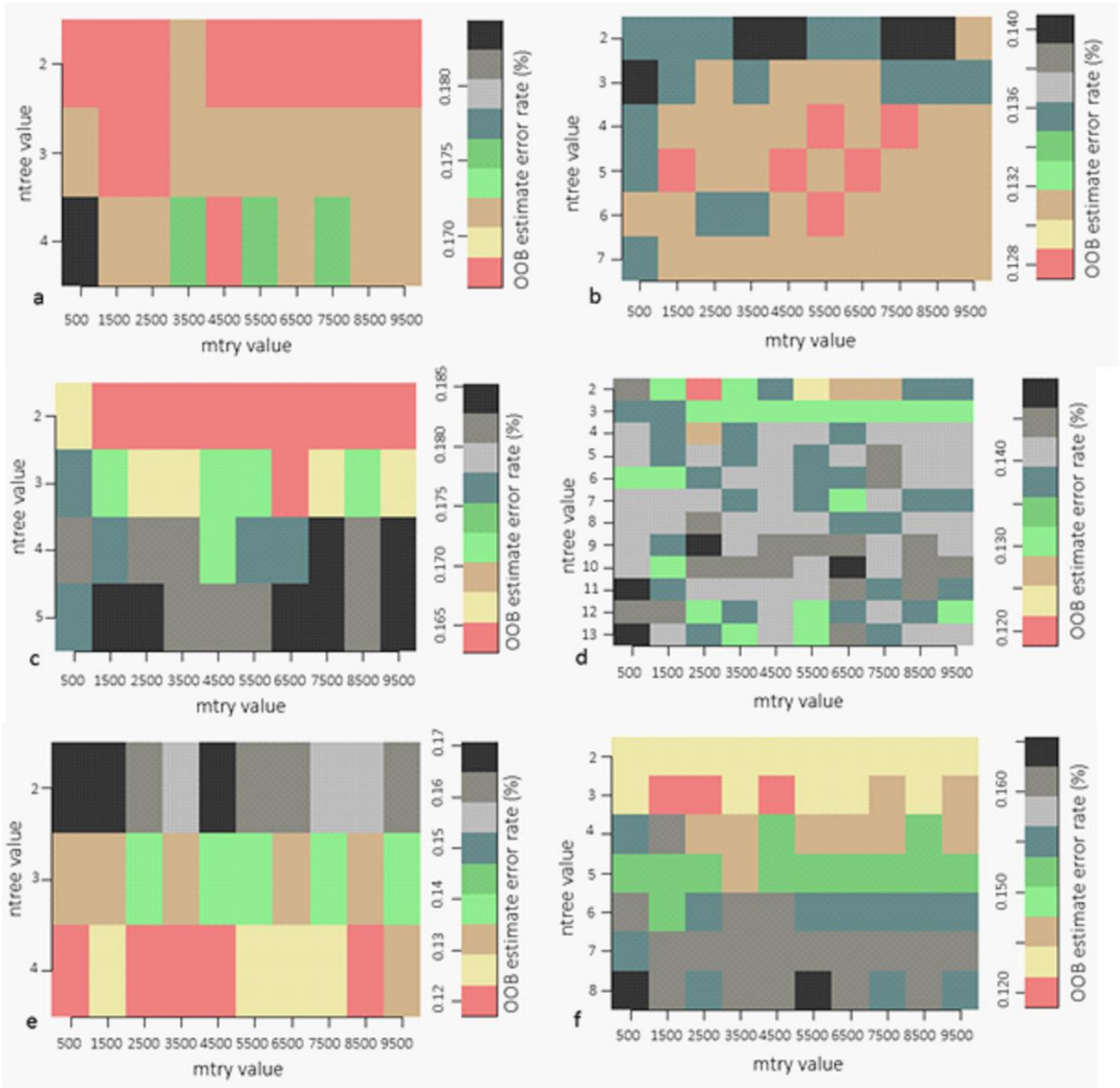

Figure 4. 3 OOB errors of optimised RF parameters (mtry and ntree) using grid search procedure. The OOB method was used to identify the error rates for different sets of mtry and ntree; 30 sets for GeoEye (a), 60 sets for Landsat 8 OLI (b), 40 sets for RapidEye (c), 120 sets for Sentinel-2 (d), 30 sets for SPOT 5 (e), and 70 sets for WorldView-2 (f)

The exponentially growing sequence of C and γ values were assessed using grid search in an attempt to select the best parameter combinations for classifying dataset resampled to the spectral resolutions of different sensors. The optimisation model achieved varying optimum combinations of C and γ for classifying data resampled to resolutions of GeoEye (C= 1000 and γ= 1), Landsat 8 OLI (C= 100 and γ= 1), RapidEye (C= 100 and γ=1), Sentinel-2 (C= 1000 and γ= 0.1), SPOT 5 (C= 1000 and γ= 1), and WorldView-2 (C= 100 and γ=1) sensors, in SVM classifier using RBF.

4.3.2 Band importance

RF algorithm was used to assess the relative importance of each resampled band in predicting midden, non-vitrified dung, non-sites and vitrified dung. Different sensors have their most important bands situated at different portions of the electromagnetic spectrum (Figure 4. 4). However, the majority of sensors have their most important bands located within the visible spectrum. The green band (545 nm) in the SPOT 5 satellite sensor was the most important band in discriminating midden, vitrified dung, non-vitrified dung and non-sites. This band combines the wavelengths in the blue with those in the green part of the electromagnetic spectrum (Figure 4. 4). SWIR band in the SPOT 5 sensor was the second most important band. However, blue band was the most important band for satellites which have the ability to capture data in the blue portion of the electromagnetic spectrum such as GeoEye (480nm), RapidEye (470 nm), Sentinel-2 (490 nm), and WorldView-2 (480 nm). Landsat 8 OLI was the only satellite which, despite having a blue band, had its most important band in discriminating midden, non-vitrified dung, non-sites and vitrified dung located in the SWIR (1610 nm). The red band was the least important band for discriminating midden, vitrified dung, non-vitrified dung and non-sites for satellite sensors Landsat 8 OLI, SPOT 5 and GeoEye. The red edge bands were the least important in discriminating the aforementioned archaeological classes for satellite sensors WorldView-2, Sentinel-2 and RapidEye, which capture data in the red edge wavelengths. Overall, SPOT 5 had the most important bands for discriminating midden, vitrified dung, non-vitrified dung and non-sites. Majority of bands of the Sentinel-2 sensor, which captures data in most regions of the magnetic spectrum, have low values in mean decrease of accuracy as compared to other sensors (Figure 4. 4).

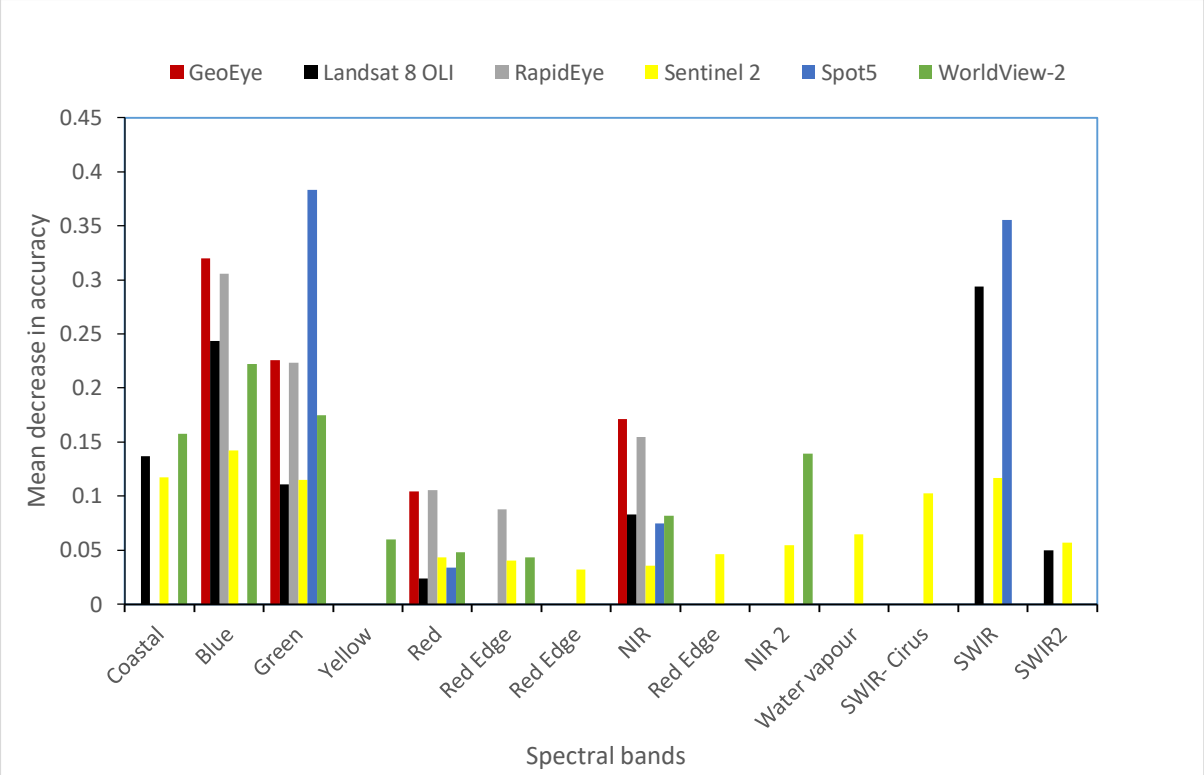

Figure 4. 4 Relative importance of each band for different sensors used in this study for predicting midden, non-vitrified dung, non-sites and vitrified dung using RF. The spectral bands are distributed as follows: blue, green, red, and near-infrared for GeoEye; coastal, blue, green, red, near infrared, SWIR1, and SWIR 2 for Landsat 8 OLI; blue, green, red, red edge, and near infrared for RapidEye; aerosols, blue, green, red, red edge, red edge, red edge, near infrared, red edge, water vapour, SWIRI-Cirus, SWIR 1, and SWIR 2 for Sentinel-2; green, red, near infrared, and SWIR for SPOT 5; coastal, blue, green, yellow, red, red edge, NIR1, and NIR2 for WorldView-2. The most important variables are those with highest MDA.

The relationship between the important bands for discriminating midden, non-vitrified dung, non-sites and vitrified dung using hyperspectral data and the location of bands for different sensors was assessed using the mean decrease in accuracy in RF. The most important bands for classifying the aforementioned features using hyperspectral data are spread across visible, near infrared and short wave infrared portions of the electromagnetic spectrum (350-2500nm), see Figure 4. 5. However, there are notable peaks in the visible and the short wave infrared portions of the electromagnetic spectrum between 350-576 nm, 1292nm-1380nm, 1575-1748nm, and 1801-1808 nm. All the satellite sensors have their bands located in the different areas of the visible spectrum. On the contrary, new satellite sensors with a spatial resolution less than 5 m do not have bands covering the short wave infrared region, which also possess some important bands in classifying the aforementioned features (Figure 4. 5). Only medium resolution sensors (Landsat 8 OLI, Sentinel-2, and SPOT 5) have bands located within the short

wave infrared portion of the electromagnetic spectrum. The short wave infrared band from the previously mentioned sensors is in line with the location of hyperspectral bands, which are important for discriminating midden, non-vitrified dung, non-sites and vitrified dung, see Figure 4. 5. This, therefore, corroborates the importance of this band in the classification of the aforementioned features as shown in Figure 4. 4.

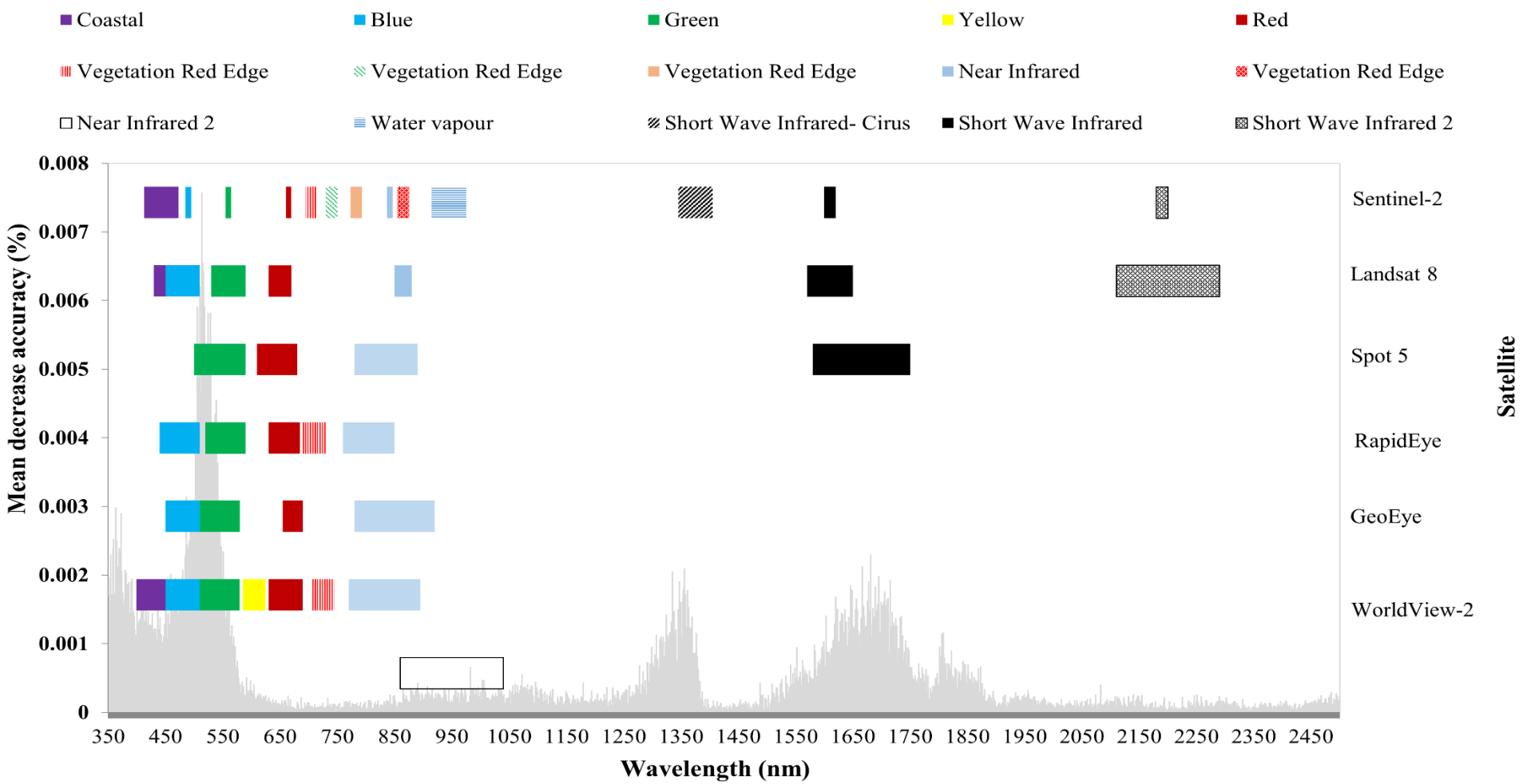

Figure 4. 5 The location of different bands of satellite sensors across the visible, near infrared and shortwave infrared portion of the electromagnetic spectrum (350-2500nm) in relation to the relative importance of spectral bands collected using field spectrometer in predicting midden, non-vitrified dung, non-sites and vitrified dung using RF algorithm. The important bands are those with a high MDA.

4.3.3 Classification accuracy

The classification of the midden, non-vitrified dung, non-sites and vitrified dung sites was performed using RF and SVM on the hyperspectral data resampled to the spectral resolution of GeoEye, Landsat 8 OLI RapidEye, Sentinel-2, SPOT 5 and WorldView-2 sensors, respectively. The error matrices for the output of each classifier was created using a holdout sample created by randomly dividing resampled laboratory data into 70% and 30% for training and validation respectively. SVM achieved higher classification accuracies than RF for all datasets.

Accuracy assessment of the RF classifier, which was done using the validation data, achieved overall accuracies of 78.10%, 80.00%, 72.38%, 81.90%, 77.14%, and 77.14% and Kappa coefficients of 0.7030, 0.7276, 0.6262, 0.7529, 0.6877, and 0.6905 when classifying hyperspectral data resampled to the spectral resolutions of GeoEye, Landsat 8 OLI, RapidEye, Sentinel-2, SPOT 5, and WorldView-2, respectively (Figure 4. 6). Generally, a lower classification accuracy of 72.38% and Kappa coefficient of 0.6262 were attained with the data resampled to the spectral resolution of RapidEye sensor while Sentinel-2 achieved a very high classification accuracy of 81.90% and a kappa coefficient of 0.7529 (Table 4. 5 and Figure 4. 6). Sentinel-2 attained high producer's and user's accuracies of 82.86% and 78.38, respectively, for NVD while RapidEye attained producer's accuracy of 60.00% and user's accuracy of 75.00% for the same class (Table 4. 3 and 4. 5). However, mixed results were attained when classifying MD, with data resampled to RapidEye sensor resolution achieving high producer's accuracy of 64.00% as compared to 60.00% for Sentinel-2, while on the other hand Sentinel-2 achieved higher user's accuracy of 65.22% as compared to 50.00% (Table 4. 3 and 4. 5). However, mixed results were attained when classifying MD, with data resampled to RapidEye sensor resolution achieving high producer's accuracy of 64.00% as compared to 60.00% for Sentinel-2, while on the other hand Sentinel-2 achieved higher user's accuracy of 65.22% as compared to 50.00% (Table 4. 3 and 4. 5).

Table 4. 3 Error matrices of RF classification algorithm based on the holdout sample for hyperspectral data resampled to the spectral resolutions of RapidEye and Sentinel-2 sensors.

Class	RapidEye					Class	Sentinel-2				
	NVD	MD	NS	VD	Total		NVD	MD	NS	VD	Total
NVD	21	6	0	1	28	NVD	29	8	0	0	37
MD	11	16	1	4	32	MD	5	15	0	3	23
NS	3	3	26	0	32	NS	1	2	27	0	30
VD	0	0	0	13	13	VD	0	0	0	15	15
Total	35	25	27	18	105	Total	35	25	27	18	105
OA	72.38%					OA	81.90%				
Kappa	0.6262					Kappa	0.7529				

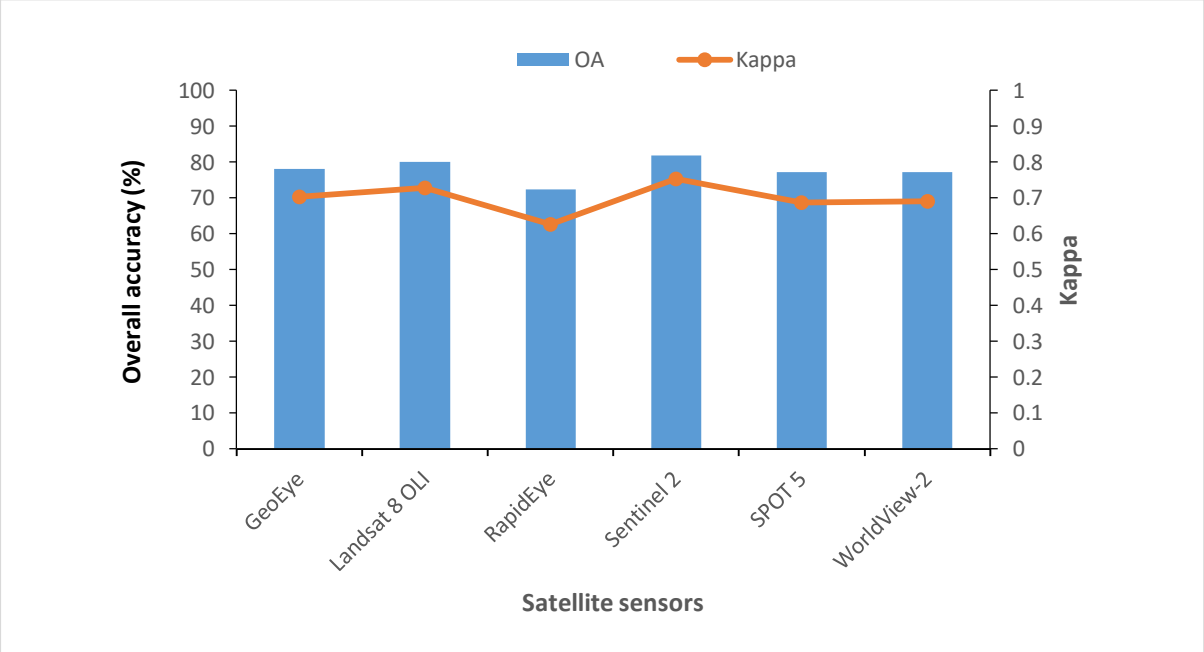

Figure 4. 6 The OA (%) and Kappa coefficients for RF classification of the midden, non-vitrified dung, non-sites and vitrified dung achieved using a holdout sample from hyperspectral data resampled to resolutions of different multispectral sensors

SVM classifier achieved overall accuracies of 86.67%, 92.38%, 82.86%, 92.38%, 91.43%, and 86.67% and kappa coefficients of 0.8188, 0.8967, 0.7663, 0.8963, 0.8836, and 0.8192 when using a holdout sample from the data resampled to spectral resolutions of GeoEye, Landsat 8 OLI, RapidEye, Sentinel-2, SPOT 5, and WorldView-2 sensors, respectively (Figure 4. 7 and

Table 4. 6). In overall, Sentinel-2 achieved a high overall classification accuracy of 92.38% and a kappa coefficient of 0.8963 while RapidEye attained the lowest overall classification of 82.86% and a kappa coefficient of 0.7663. MD achieved producer's accuracy of 68.00% and user's accuracy of 68.00% for hyperspectral data resampled to RapidEye sensor while user's and producer's accuracies of 84.00% and 87.50% were achieved for the one resampled to a spectral resolution of Sentinel-2 sensor. Similar user's accuracies of 100% were archived for VD from the data resampled to the spectral resolutions of RapidEye and Sentinel-2 while varying producer's accuracies of 83.33% and 94.44% were attained for the same datasets, respectively (Table 4. 4 and 4. 6). Landsat 8 OLI also achieved a very high overall classification accuracy of 92.38%, which was similar to that of Sentinel-2 when using SVM classifier (Table 4. 6 and Figure 4. 7). However, their producer's and user's accuracy for NVD and MD were different (Table 4. 6). Further results on producer's and user's accuracies for SVM classifiers are provided in Table 4. 6.

Table 4. 4 Error matrices of SVM classification based on the holdout sample for hyperspectral data resampled to the spectral resolutions of RapidEye and Sentinel-2 sensors

Class	RapidEye					Class	Sentinel-2				
	NVD	MD	NS	VD	Total		NVD	MD	NS	VD	Total
NVD	29	6	0	1	36	NVD	32	4	0	0	36
MD	5	17	1	2	25	MD	2	21	0	1	24
NS	1	2	26	0	29	NS	1	0	27	0	28
VD	0	0	0	15	15	VD	0	0	0	17	17
Total	35	25	27	18	105	Total	35	25	27	18	105
OA	82.86%					OA	92.38%				
Kappa	0.7663					Kappa	0.8963				

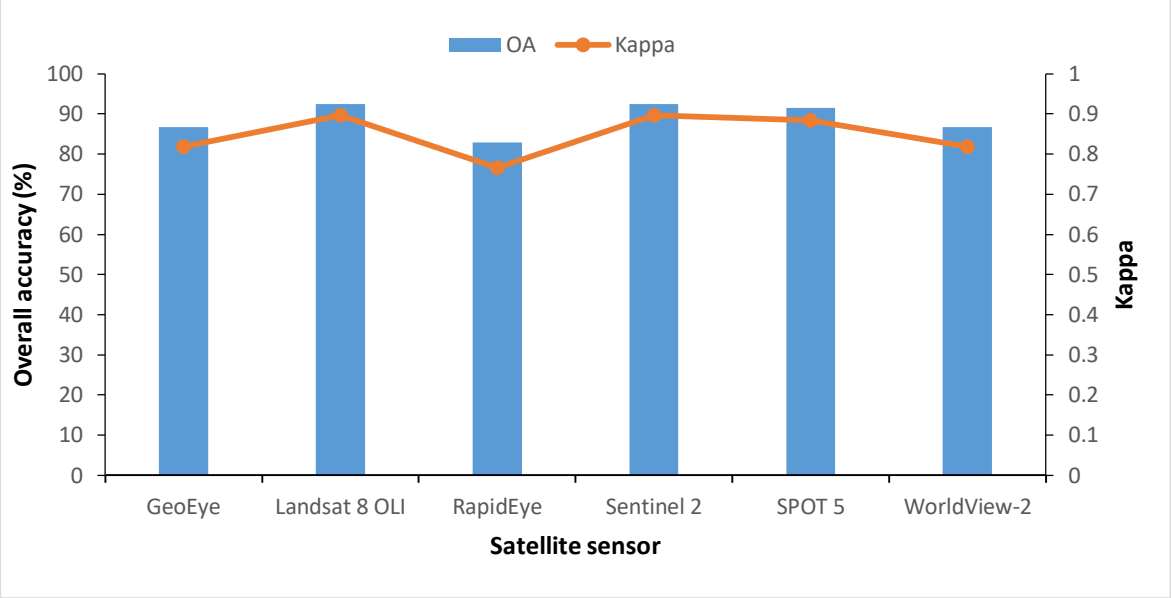

Figure 4. 7 The OA (%) and kappa coefficients for SVM classification of the midden, non-vitrified dung, non-sites and vitrified dung achieved using a holdout sample from hyperspectral data resampled to resolutions of different multispectral sensors

Table 4. 5 RF classification accuracy of the midden, non-vitrified dung, non-sites and vitrified dung achieved using a holdout sample from hyperspectral data resampled to resolutions of different multispectral sensors

	GeoEye		Landsat 8 OLI		RapidEye		Sentinel-2		SPOT 5		WorldView-2	
	PA (%)	UA (%)	PA (%)	UA (%)	PA (%)	UA (%)	PA (%)	UA (%)	PA (%)	UA (%)	PA (%)	UA (%)
NVD	71.43	80.65	77.14	77.14	60.00	75.00	82.86	78.38	77.14	72.97	68.57	80.00
MD	64.00	59.26	60.00	60.00	64.00	50.00	60.00	65.22	52.00	54.17	64.00	57.14
NS	96.30	81.25	100.00	90.00	96.30	81.25	100.00	90.00	100.00	90.00	96.30	81.25
VD	83.33	100.00	83.33	100.00	72.22	100.00	83.33	100.00	77.78	100.00	83.33	100.00
OA (%)	78.10		80.00		72.38		81.90		77.14		77.14	
Kappa	0.7030		0.7276		0.6262		0.7529		0.6877		0.6905	

PA= producer's accuracy, UA=User's accuracy, OA=Overall accuracy

Table 4. 6 SVM classification accuracy of the midden, non-vitrified dung, non-sites and vitrified dung achieved using a holdout sample from hyperspectral data resampled to resolutions of different multispectral sensors

	GeoEye		Landsat 8 OLI		RapidEye		Sentinel-2		SPOT 5		WorldView-2	
	PA (%)	UA (%)	PA (%)	UA (%)	PA (%)	UA (%)	PA (%)	UA (%)	PA (%)	UA (%)	PA (%)	UA (%)
NVD	85.71	88.24	88.57	93.94	82.86	80.56	91.43	88.89	88.57	91.18	82.86	90.63
MD	80.00	71.43	88.00	84.62	68.00	68.00	84.00	87.50	88.00	81.48	84.00	70.00
NS	96.30	92.86	100.00	93.10	96.30	89.66	100.00	96.43	100.00	96.43	96.30	92.86
VD	83.33	100.00	94.44	100.00	83.33	100.00	94.44	100.00	88.89	100.00	83.33	100.00
OA (%)	86.67		92.38		82.86		92.38		91.43		86.67	
Kappa	0.8188		0.8967		0.7663		0.8963		0.8836		0.8192	

PA= producer's accuracy, UA=User's accuracy, OA=Overall accuracy

4.4 Discussion

Due to improvement of both spatial and spectral resolution of satellite sensors, successful prediction of sub-surface and surface archaeological material using various multispectral remote sensing data has been reported in numerous studies (Agapiou et al. 2012a; Beck et al. 2007; Lasaponara and Masini 2006; Masini and Lasaponara 2007; Melillos et al. 2018; Parcak 2007; Schuetter et al. 2013; Thabeng et al. 2019). Consequently, archaeological materials produce localised signatures which cannot generally be used to predict archaeological sites in other parts of the world. As such, there is a need to vigorously test the potential of the sensors under various archaeological contexts. This study optimised for the best multispectral sensors suitable for detecting archaeological sites characterised by surface features, which include ash middens, vitrified dung and non-vitrified dung, within the southern African context.

This study has shown that a range of multispectral satellite sensors possesses bands which are important in discriminating natural soils and archaeological sites characterised by ash middens, non-vitrified dung, and vitrified dung deposits using RF and SVM classifiers. Generally, the visible bands are the most important in the discrimination of the above-mentioned soil classes in all the resampled multispectral sensor data. The blue band is the most important variable for predicting the aforementioned archaeological classes using hyperspectral data resampled to GeoEye, RapidEye Sentinel-2 and WorldView-2. However, overall, the green band in the SPOT 5 sensor was the most important across all bands. This is because it combines the wavelengths from the blue and the green sections of the electromagnetic spectrum, which covers the most important bands for discriminating ash midden, non-vitrified dung, and vitrified dung deposits (Figure 4. 5). The aforementioned wavelengths are commonly associated with soil colour, which is normally influenced by organic matter content (Ben-Dor et al. 1997). The other important bands are in the SWIR which are sensitive to soil chromosomes (Castaldi et al. 2016). Generally, the resampled bands in the red, red edge and near-infrared regions were least important in the classification of the aforementioned soils. This is because they have been found to be highly sensitive to chlorophyll content and leaf structure in vegetation (Adam et al. 2017; Fernández-Manso et al. 2016; Glenn et al. 2008). This also is in line with the results of Ben-Dor et al (1997), who observed that chlorophyll is not sensitive to the spectra in its late stages of decomposition because of its rapid decomposition. Furthermore, the additional bands in the new Very High Resolution (VHR) satellites such as yellow band in WorldView-2 were also of less importance (Figure 4. 4).

The importance of each wavelength (350-2500nm) in hyperspectral data was effectively assessed using a mean decrease in accuracy in RF. The wavelengths in the visible and shortwave infrared regions were found to be the most important discriminating natural soils and archaeological sites characterised by ash midden, non-vitrified dung, and vitrified dung deposits. These wavelengths are in line with the spectral resolutions of Sentinel-2, SPOT 5 and Landsat 8 OLI. This, in turn, makes the aforementioned satellite sensors most suitable in discriminating the surface archaeological sites characterised by a midden, non-vitrified dung, vitrified dung deposits and their surrounding natural soils. This is also supported by the high prediction accuracies of 91.43% - 92.38% and 77.14%-81.90% they attained when using SVM and RF classifiers, respectively, to predict the above-mentioned features. Sentinel-2 achieved the highest classification accuracies of 92.38% and 81.90% in SVM and RF, in that sequence. This is largely because of its high spectral resolution, which captures data across wide portions of the electromagnetic spectrum. As a result, enabling it to detect subtle differences in the properties of the above-mentioned features. This is in line with the findings of Cavalli et al. (2007) who found out that bands in SWIR are important in detecting soil characteristics related to archaeological remains. Despite their high spatial resolution, the results in this study show that new VHR multispectral sensors (GeoEye and WorldView-2) do not have all the best bands for detecting the abovementioned archaeological deposits. These sensors capture data in visible and near infrared regions only and do not have bands in the SWIR which are sensitive to some important soil characteristics as discussed above.

The high classification accuracy achieved, when using Landsat 8 OLI, Sentinel-2, and SPOT 5, is an important development for archaeological heritage managers and researchers in general, and in particular in the African continent where there is limited funding. Importantly, imagery captured by Sentinel-2 and Landsat 8 OLI is free and readily available to acquire via world wide web portals. As a result, survey, documentation and monitoring of archaeological sites over large areas using these sensors is potentially cost-effective. However, although SPOT 5, Sentinel-2 and Landsat 8 OLI possess spectral resolutions required to detect archaeological features in the study area, their lower spatial resolution (2.5m to 15m panchromatic and 10 to 60 m multispectral) might prove to be a challenge when the models are up-scaled to satellite sensors. This is because middens and byres in the study area are oftentimes located in close proximity (Calabrese 2000; Huffman 2009a), as such they can be captured in a single cell causing spectra confusion. Furthermore, on average, the size of individual byres and middens ranges between 3 and 18 meters in diameter (Huffman pers comm.). This is smaller than the

minimum size of features that can be meaningfully discriminated by the aforementioned satellites, which ranges between 20m and 30m (Myint et al. 2011; Thabeng et al. 2019). As such, this study recommends further research with the use of actual images to assess the two approaches suggested below. The first approach will be to compare the potential of very high spatial resolution multispectral satellites (WorldView-2 and GeoEye) and that of low spatial resolution satellites sensors (Landsat 8 OLI and Sentinel-2) in detecting archaeological sites characterised by surface features. This is because, generally, the spatial resolutions (0.46 panchromatic and 1.84 multispectral) for VHR satellite sensors have the potential to capture individual features with diameters of about 4m upwards (Thabeng et al. 2019). On the other hand, low spatial resolution satellite sensors have the spectral ability to detect soil characteristics which shows reflectance differences within visible and SWIR bands as discussed above. The second approach will be to assess the potential of data fusion created by merging images with different spectral and spatial resolutions in detecting the non-sites ash middens, non-vitrified dung and vitrified dung deposits. The main reason for data fusion is to create an image that combines the spectral abilities of low spatial resolution satellite sensors and the spatial abilities of very high spatial resolution satellite sensors.

Generally, the results from this study showed that RF and SVM classifiers have the ability to accurately predict ash midden, non-vitrified dung, and vitrified dung materials basing on their spectral data. These results agree with those of other research which achieved good results when using RF and SVM together in a number of spectral mapping applications including that of vegetation species (Ghosh et al. 2014; Sesnie et al. 2010), vegetation health (Abdel-Rahman et al. 2014), agriculture (Duro et al. 2012), land cover (Adam et al. 2014; Noi and Kappas 2018) and archaeology (Thabeng et al. 2019). However, comparison of the accuracies achieved by the two classifiers has shown some variation on how they performed in this study. In general, SVM achieved higher overall classification accuracies than RF in all datasets. RF classifier achieved 78.10%, 80.00%, 72.38%, 81.90%, 77.14%, and 77.14% when classifying hyperspectral data resampled to the spectral resolutions of GeoEye, Landsat 8 OLI, RapidEye, Sentinel-2, SPOT 5, and WorldView-2, respectively, while SVM classifier achieved overall accuracies of 86.67%, 92.38%, 82.86%, 92.38%, 91.43%, and 86.67% for the similar datasets, respectively. This is in line with the results from other studies (Adam et al. 2014; Sesnie et al. 2010) which attained varying overall classification accuracies between the two classifiers when dealing with similar data samples. However, researchers (Pelletier et al. 2016; Thabeng et al. 2019) found out that even though there may be variations in their results, RF and SVM

classifiers complement each other because of their different classification abilities. There was also a variation on how RF and SVM predicted individual classes. In general, RF classifier picked a lot of confusion between MD and NVD than SVM classifier (Table 4. 3 and 4. 4). RF achieved lowest producers accuracy (52.00%) and user's accuracy (54.17%) for hyperspectral data resampled to the resolution of SPOT 5 sensor while the lowest producer's and user's accuracies attained by SVM classifier stood at 68.00% each and were from hyperspectral data resampled to RapidEye sensor. The confusion between MD and NVD might be a result of chemical similarities between the two of them (Thabeng et al. 2019). The other reason might be signature confusion influenced by the post-depositional processes such as erosion, which is rampant in the study area, mixing the two deposits because as discussed above MDs are located in close proximity to byres. This, therefore, supports results from Sesnie (2010) who posits that SVM is a superior method for solving complex classification problems. In consequence, this result makes SVM a better predictor of archaeological sites in the study area more especially those characterised by MD and NVD. However, both classifiers achieved the highest user's accuracy (100%) for VD across all the datasets.

Above all the ability to use classifiers in predicting archaeological sites is a good development because it broadens the use of spectral data of archaeological features from the traditional visible bands to bands beyond the visible spectrum. It also helped to identify different archaeological features across the landscape based on the spectral signatures resulting from their geochemical contrast without necessarily doing extensive fieldwork. Thus giving researchers the much needed preliminary idea on the type of archaeological sites characterising the landscape and their distribution which will assist in planning field surveys and excavations.

In summary, the positive results attained from this study are a step in the right direction in improving archaeological survey techniques. This is important more especially within the risky environments of the resource-strapped African continent. The use of multispectral satellite data will help to advance archaeological heritage management. It will also improve the knowledge of the archaeological record in the continent by balancing the archaeological research and giving new aerial perspectives of archaeological landscapes. There is some commonality in the majority of archaeological sites in Southern Africa such as the presence of byres and middens (Denbow 1979; Huffman et al. 2013; Jacobson et al. 2003; Peter 2001). Therefore, the results of this study need to be up-scaled to actual images from satellites which are in operation and tested in the sub-continent. Most importantly, it should also be indicated that the method can be applied anywhere in the world as a cheap way of identifying sensors with spectral abilities

to predict the archaeological material of interest. This is because there are many remote sensing sensors which are now available with different spectral and spatial resolutions and the selection of the appropriate data for archaeological applications is challenging. If the results are positive, the mapping of archaeological sites could be up-scaled to data from operational sensors on satellite platforms. Despite the abovementioned successes and potentials, lack of archaeologists with remote sensing expertise remains a challenge to the application of remote sensing techniques in the African continent and the world.

4.5 Conclusions

This study investigates the possibility of discriminating archaeological features using hyperspectral data resampled to the spectral resolutions most widely used multispectral sensors. The following findings can be concluded:

- The bands within the visible and SWIR portions of the electromagnetic spectrum are the most important for predicting the natural soils and archaeological sites characterised by ash middens, vitrified dung and non-vitrified dung. The aforementioned regions are in line with the spectral resolutions of the Sentinel-2, SPOT 5 and Landsat 8 OLI sensors. This, therefore, makes them the most suitable sensors for detecting archaeological sites even though they have a low spatial resolution which is a limitation.
- High classification accuracies which were achieved in this study, demonstrates that the multispectral sensors have the ability to detect ash middens, non-vitrified dung and vitrified dung. In general, high classification accuracies were achieved when using SVM as compared to the RF classifier. The highest classification accuracies were achieved when classifying data resampled to the resolution of the Sentinel-2 sensor using both RF (81.90%) and SVM (92.38%). Landsat 8 OLI also achieved the highest classification accuracy similar to that of Sentinel-2 when using SVM classifier.
- The green band and SWIR bands in SPOT 5 satellite sensor were the most important bands in discriminating against midden, vitrified dung, non-vitrified dung and non-sites. However, the blue band was the most important band in sensors; GeoEye, RapidEye, Sentinel-2, and WorldView-2, with the ability to capture it. Other important bands included the SWIR bands in Landsat 8 OLI and Sentinel-2 and NIR bands in sensors without SWIR bands.

The results of this study have revealed the prospects of discriminating ash middens, natural soils, vitrified dung and non-vitrified dung by means of hyperspectral data resampled to the resolutions of multispectral satellite sensors. This, in turn, offers the opportunity to upscale this approach to spaceborne sensors for mapping and monitoring archaeological features. This is an important development for archaeological researchers and heritage managers because it will reduce the difficulties encountered during fieldwalking surveys. The difficulties include cost, access rights in private properties, long surveying periods, areas characterised by the presence of wild animals and active war zones. This is one of the earliest studies whereby the potential of several sensors to detect surface archaeological material is being assessed. Although, hyperspectral data resampled to the spectral resolutions of low spatial resolution sensors (Landsat 8 OLI, Sentinel-2, and SPOT 5) achieved relatively high classification accuracies, this study recommends more research using actual images to assess the potential of very high spatial resolution satellites (GeoEye or WorldView-2) in detecting archaeological sites characterised by surface features. This is because the middens and byres in the study area are closely located to each other, therefore, the spatial resolutions for VHR satellite sensors have the potential to reduce within cell spectral mixing by capturing individual archaeological features. Additionally, VHR satellite sensors also have bands, which are important for discriminating archaeological and non-archaeological features and they achieved high classification accuracies in this study.

Acknowledgements

We would like to thank Inos Dhau, Tshekiso Kgosietsile and Andani Gangashe for their assistance during data collection. Gratitude is also given to SANParks for allowing access to the Mapungubwe National Park and the DeBeers Group (through Duncan MacFadyen) for allowing access to the Venetia Nature Reserve and use of the research facility. The authors are also grateful to Prof. Thomas Huffman for availing his data and devoting his time by taking us through the study area. Special thanks to Lesego Madisha (former archaeologist at SANParks, Mapungubwe) for her kind assistance, SANParks' Cultural Heritage Manager Crispen Chauke and the Venetia Nature Reserve staff for their help.

Funding information

This study was funded by the University of Botswana training department.

Conflict of interest

The authors declare that they have no conflict of interest

CHAPTER FIVE

5. High-resolution remote sensing and advanced classification techniques for the prospection of archaeological sites' markers: the case of dung deposits in the Shashi-Limpopo Confluence area (Southern Africa)

This chapter is based on:

Thabeng, O. L., Merlo, S. and Adam, E., 2019. "High-Resolution Remote Sensing and Advanced Classification Techniques for the Prospection of Archaeological Sites' Markers: The Case of Dung Deposits in the Shashi-Limpopo Confluence Area (Southern Africa)." *Journal of Archaeological Science* 102:48–60.

Abstract

Archaeological prospection through remote sensing is based on the contrast between areas of archaeological interest and their surroundings. It has been used as the cheapest and the fastest way of locating and documenting areas of archaeological interest since the 1920s, initially with the aid of film-based aerial photographs. In recent years, there has been a shift towards the use of multispectral satellite data in prospecting for archaeological sites because of their ability to give information on spectral characteristics of archaeological material beyond the visible spectrum. However, spectral signatures for identifying archaeological sites are not universal, and an assessment of the applicability of remote sensing techniques in different archaeological landscapes is needed. This study tests the feasibility of prospecting for archaeological sites previously occupied by farming communities in the Shashi-Limpopo Confluence Area of southern Africa, using very high-resolution satellite WorldView-2 images. It also assesses the performance of advanced classification algorithms (support vector machine and random forest) and the contribution of new WorldView-2 bands in detecting archaeological sites. Two independent accuracy assessments were carried out, using a data set collected by Huffman (2009b, 2011) and a randomly generated holdout test dataset, respectively. The results demonstrate the potential of remote sensing methods in prospecting for archaeological sites previously occupied by farming communities using very high-resolution satellite images and advanced classification algorithms. Very high overall accuracies were achieved by: random forest, 95.29% using holdout sample and 97.71 using independent dataset; support vector machine, 88.82% using holdout sample and 95.88 using independent dataset, respectively. The new WorldView-2 bands were of least importance (compared to traditional bands) in detecting sites in Shashi-Limpopo Confluence Area. Despite high classification accuracies achieved by both classifiers, there were some misclassifications between vitrified dung sites and river sand. Therefore, to address this problem, this study recommends the use of robust classifiers such as object-based algorithms because of their ability to segment an image into homogenous objects and classify them using a combination of spectral, textual, sub-pixels, spatial, relational and contextual methods.

Keywords: Remote sensing, farming communities, vitrified dung, non-vitrified dung, survey, prospection, advanced classification

5.1 Introduction

Archaeological prospection through remote sensing offers a practical and economical means to detect and characterise different types of archaeological sites, over traditional field walking survey methods (Beck 2007). It also reduces the biases inherent in fieldwalking survey methods, which can be influenced by the researcher's tendency to sample hotspots, leaving out other parts of the study area, whereas remote sensing can offer more comprehensive coverage of an area (Bintliff 2000; Hawkins et al. 2003; Renfrew and Bahn 2012). Most importantly, the use of aerial and satellite images gives archaeologists a synoptic view of archaeological landscapes and helps them understand patterns which may not be visible when on the ground (Crawford 1923; Hritz 2010). The increased spatial, temporal and spectral resolutions of satellite remotely sensed data offer opportunities for discriminating different archaeological traces and detecting their change over time (Agapiou et al. 2015; Doneus et al. 2014; Hadjimitsis et al. 2009; Verhoeven and Vermeulen 2016), including the monitoring of looting activities (Hesse 2015; Parcak 2015; Van Ess et al. 2006). Additionally, remotely sensed digital data can be integrated with various other datasets for advanced analysis (Hesse 2015; Megarry et al. 2016; Parcak 2007). For example, researchers such as Chen et al. (2013a; b) and Megarry et al (2016) integrated satellite image data and topographic data to directly predict the possible locations of archaeological sites using statistical methods.

Early studies, which employed aerial photography and early satellite images for archaeological prospection and prediction, visually identified soil marks, vegetation marks, surface features and other proxies for buried and semi-buried archaeological features based on tonal and textural differences in the images (Crawford 1923; Evans and Jones 1977; Fowler 2002; Gojda and Hejcman 2012). More recently Normalized Difference Vegetation Index (NDVI) and other image processing techniques on multispectral satellite imagery have been employed to assess the types and health of vegetation that may indicate the presence of archaeological features (Agapiou et al. 2014a; Aqdus et al. 2008; Doneus et al. 2014; Keay et al. 2014; Keeney and Hickey 2015; Lasaponara and Masini 2006, 2007; Masini and Lasaponara 2007). The use of remote sensing techniques in African archaeology has followed similar trajectories of development. It begun with the visual inspection of aerial photographs to detect archaeological sites (Denbow 1979; Lightfoot and Miller 1996; Mason 1968; Seddon 1968a) and is now exploiting satellite images and their improved spatial resolution for the mapping of settlement patterns (Sadr 2016b; Sadr and Rodier 2012). More recently, multispectral data has been

digitally processed to identify proxy archaeological indicators such as vegetation (Biagetti et al. 2017; Clark et al. 1998; Reid 2016).

Few studies (De Laet et al. 2007; Parcak 2007) in Africa and beyond have focused on the possibility of directly detecting the presence of archaeological materials using their spectral signatures. In fact, despite its potential advantage for identifying archaeological sites, early remote sensing imagery was challenging to use for a number of reasons, including the low spatial resolution of platforms such as Landsat and SPOT, which hampered the ability to map landscape complexity and to distinguish subtle spectral differences of archaeological sites and the surrounding areas (De Laet et al. 2007; Lasaponara and Masini 2006; Masini and Lasaponara 2007). The advent of new generation satellites with Very High Resolution (VHR) spatial images such as WorldView-2, Quick Bird and IKONOS, availed new avenues which can be harnessed for this approach. VHR satellite images offer a synoptic view which provides invaluable insight into complex archaeological environments at a high spatial and spectral detail (Masini and Lasaponara 2007). For example, WorldView-2 has a very high spatial resolution (0.46m panchromatic and 1.84m multispectral) and a relatively narrow bandwidth, together with new spectral bands such as coastal, yellow, red-edge and NIR2 (DigitalGlobe 2010). These new spectral bands combined with high spatial resolution sensors have the ability to detect and characterise small (sub-meter) and spectrally less evident archaeological features compared to the traditional multispectral data such as SPOT and Landsat TM (Aqdus et al. 2012; DigitalGlobe 2010; Keay et al. 2014; Lasaponara et al. 2016b).

In recent years, computer software and algorithms for processing and classifying satellite images have significantly improved (Lu and Weng 2007; Rodriguez-Galiano et al. 2012b). Computer software includes advanced machine learning classifiers such as random forest (RF) and support vector machine (SVM) (Breiman 2001; Huang et al. 2002; Zhu and Blumberg 2002). The aforementioned classifiers use training samples to learn patterns in data and use them to make predictions for similar occurrences (Belgiu and Drăguţ 2016). The SVM and RF classifiers have been used for different applications such as land cover/use classifications of urban environments (Zhu and Blumberg 2002), vegetation (Huang et al. 2008a; Lawrence et al. 2006; Raczko and Zagajewski 2017), discrimination of heterogeneous landscapes (Adam et al. 2014; Rodriguez-Galiano et al. 2012b) and biophysical studies, including the estimation of biomass (Mutanga et al. 2012). The use of advanced classification algorithms helped in increasing the reliability and accuracy of classifications performed on images, even with limited training data sets (Rodriguez-Galiano et al. 2012b; Shao and Lunetta 2012). The use of

machine learning algorithms in archaeology has been neglected. The aim of this study is threefold: (i) to test the feasibility of directly detecting archaeological sites characterised by animal byres through the use of high spatial resolution satellite images; (ii) assess the contribution of new bands from VHR satellites, more specifically WorldView-2, in detecting archaeological sites; and (iii) test the performance of advanced machine learning classifiers (RF and SVM) in archaeological applications. To achieve its aim, the research makes use of a case study from the southern African Shashi-Limpopo Confluence Area (SLCA), where animal byres are a common characteristic feature of archaeological sites from the early Zhizo periods up to the historic past (Hanisch 1980; Huffman 2012).

5.2 Archaeological Context

The SLCA, which forms the boundary of three countries, Botswana to the west, South Africa to the south and Zimbabwe to the north (Figure 5. 1), has been permanently occupied by groups of farming communities from 900 AD onwards (Calabrese 2000; Eloff and Meyer 1981; Huffman 2000; Vogel and Calabrese 2000). These societies practised the so-called Central Cattle Pattern (CCP) settlement system, whereby an animal byre (kraal) was located at the centre of the settlement, close to the male gathering area (Hanisch 2002; Huffman 2009a). As a result, remains of animal byres in the form of dung deposits are some of the major characteristic features of settlements across the confluence area (Hanisch 1980; Huffman 2009b, 2011; Huffman et al. 2004). These features can be further divided into vitrified and non-vitrified deposits (Huffman et al. 2013; Meyer 2000). Non-vitrified dung deposits consist of unburned dung (Huffman et al. 2013). Vitrified dung is a glassy biomass slag with high deposits of nitrates and phosphates formed by burning thick dung deposits at very high temperatures (in the region of 1100^{o} C)(Peter 2001; Thy et al. 1995). The causes of dung vitrification are debated. Thy et al. (1995) posits that, for vitrification to occur, dung may have been burned by veld fires or lightning at very high temperatures, in an environment conducive to internal combustion. Other researchers (Huffman et al. 2013; Peter 2001) argue that vitrification is a result of the intentional burning of byres, most likely for cleansing purposes. These sites appear as cleared patches within the savannah woody vegetation. In some cases, they are covered by some grass species including *cenchrus ciliaris*, which has been identified by Denbow (1979) as an indicator of archaeological middens and byres. Nevertheless, this grass is ubiquitous in the SLCA.

Substantial excavations and intensive fieldwalking survey, spanning a period of close to four decades, were carried out on the South African side of the confluence by different researchers (Hanisch, 1980, Huffman, 1989, Huffman et al., 2004, Huffman, 2009b, Huffman, 2011). These surveys resulted in the identification of about 1160 farming community sites dating from as early as 450AD (Huffman and Du Piesanie, 2011). Various approaches were used to document the site locations at different periods of the survey. Sites found before the late 1990s were documented in 1: 50,000 topographic maps while those found after this date were recorded using Global Positioning System (GPS) by capturing the coordinates at their centre (Huffman, 2011). In other areas of the confluence sporadic systematic surveys have been carried by Manyanga (2007) in Zimbabwe and Mothulatshipi (2008) in Botswana. Surveying for archaeological sites in the SLCA through fieldwalking is a challenge due to the complexity of the landscape, the presence of dangerous wild animals (including lions and elephants), and ownership accessibility. Remotely sensed based survey of the broader confluence area is a viable approach to complete the patchy prospection of this important landscape beyond the borders of South Africa.

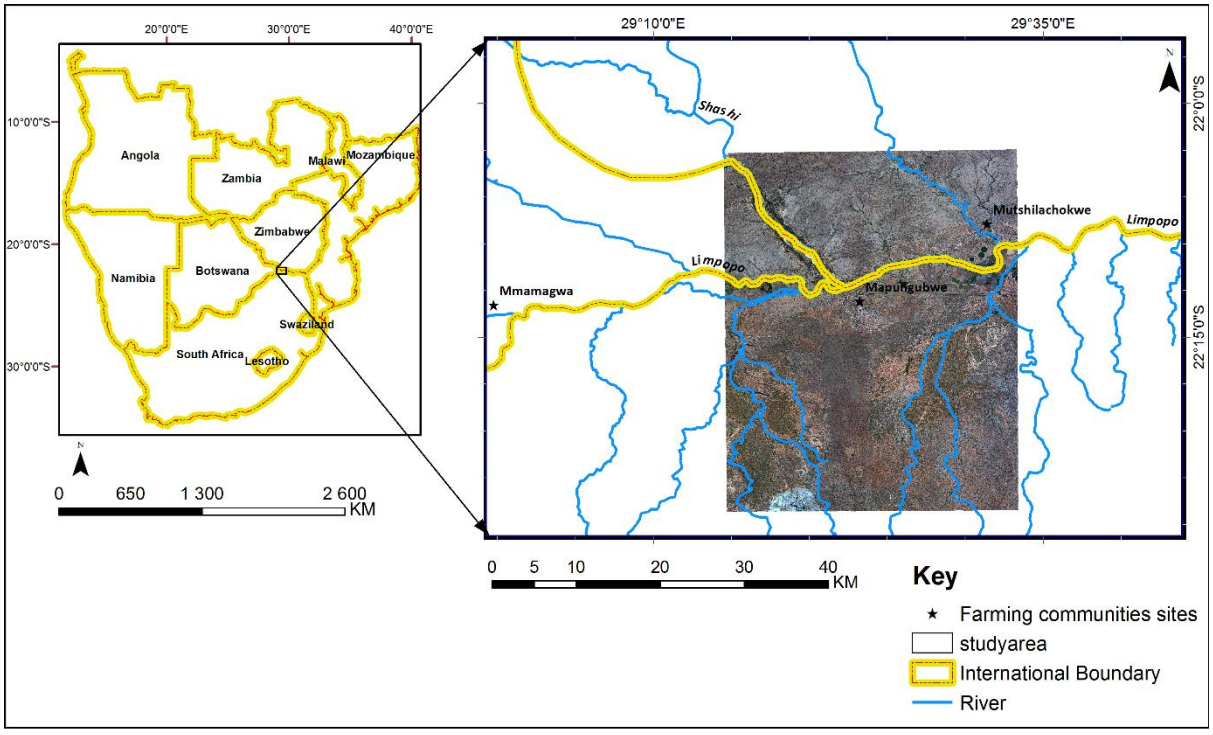

Figure 5. 1 Location of the Shashi-Limpopo confluence area showing sites mentioned in the text and the footprint of the WorldView-2 image used in the study

5.3 Materials and Methods

5.3.1 Remote sensing data acquisition and pre-processing

Cloud-free multispectral WorldView-2 images dated August 5, 2014, and covering 1388 km^2 of the entire study area were acquired free of charge from Digital Globe under their image grant programme. The date of acquisition was based on the images' availability and took into consideration the landscape dynamics. In fact, from August to October (Southern hemisphere spring season), the savannah canopy is very dry and open with most of the archaeological dung deposits exposed. WorldView-2 has one panchromatic and eight multispectral bands distributed from the visible to the near-infrared region of the spectrum, with a spatial resolution of 0.5 m and 2 m respectively. It has a swath width of 16.4 km at nadir. The spectral ranges of the eight multispectral bands are 400–450 nm (B1-coastal), 450–510 nm (B2-blue), 510–581 nm (B3-green), 585–625 nm (B4-yellow), 630–690 nm (B5-red), 705–745 nm (B6-red edge), 770–895 nm (B7-near infrared-1), and 860–1040 nm (B8-near-infrared-2). These provide the WorldView-2 images with both high spectral and spatial resolutions which are vital in detecting dung remains.

The images were geometrically corrected by DigitalGlobe Foundation (www.digitalglobefoundation.org). The radiometric corrections were done on each image using Fast Line-of-Sight Atmospheric Analysis of Hypercubes (FLAASH). FLAASH has the ability to correct atmospheric effects on the image and give radiance values leading to the recovery of accurate reflectance spectra (Matthew et al. 2002). To prepare the images for radiance calibration in FLAASH, they were first converted to top-of-atmosphere (TOA) radiance, using radiometric calibration coefficients supplied in the metadata file. Radiance calibration was then performed on the FLAASH model using standard parameters without aerosol retrieval at an average altitude of 540 m.

5.3.2 Land-cover categories and reference data collection

Following a first visit to the confluence area in September 2015 with an archaeological expert who provided vital information on site locations and characteristics, fieldwork data collection was conducted in September 2016 with the purpose of acquiring ground reference points to classify the WorldView-2 image. Even though data collection was completed two years after the image was captured, this will not have an effect on the classification results because the structure and chemical composition of the study material (vitrified dung and non-vitrified dung) does not change within such a short period (Huffman et al., 2013). The period that was

chosen for data collection also coincides with the spring season, which is the time when the image was acquired. The two visits revealed that the land is normally bare in the study area during the spring season, exposing surface archaeological remains. Moreover, most of the area chosen falls within a national park and world heritage site and a private game reserve. Changes in land use are minimal since the areas are protected against changes by legislation. The visits, therefore, confirmed that land cover and land use (LULC) changes did not occur and cannot have significant effects on the prediction model.

A purposive sampling method was used during the fieldwork data collection by visiting sites which appear in the literature and have been dated to the period of interest. A global positioning system device (GPS) was used to navigate to these sites, whose coordinates were extracted from the site inventory constructed by Huffman (2009b, 2011). Although a variety of different remains characterise the farming communities' period in the Shashi-Limpopo confluence, the survey targeted only three archaeological classes: vitrified and non-vitrified dung deposits and middens. This latter class will not be further explored in this paper. Three additional land use and land cover classes including bare land (natural soils), savannah woody vegetation, and irrigated agriculture (pivot agriculture) were extracted from the WorldView-2 data using collected ground reference points and were considered as variables during the image classification process. The natural vegetation in the study area was grouped into a single savannah woody vegetation class. The commercial farms were grouped into irrigated agriculture because of their pivot irrigation systems. This broad categorisation of the vegetation was deemed acceptable for the study which was aimed at distinguishing barren soil (archaeological and non-archaeological) from the surrounding vegetation classes and not at mapping different vegetation types in the area. Furthermore, even though different types of vegetation have distinct spectral signatures that may be used to discriminate amongst them, in the context of this study there are no vegetation proxies related to archaeological remains. An unclassified category was created by grouping features such as rivers, roads and the Venetia mine. This category was excluded from the classification to avoid unnecessary confusion. These features have potentially a similar spectral reflectance to that of archaeological sites. For general land cover and land use, additional points were digitised using a pan-sharpened version of the WV image. In total 565 reference points were created with different class sizes ranging between 45 and 205 points. Spectral curves (Table 5. 1) were generated using averages of reflectance values of each class extracted from the WorldView-2 image. The reference data was then randomly divided into training (70%) and validation (30%) datasets.

No	Archaeological and land cover classes	Field observation photograph	Earth observation (as seen in WV imagery – 2 m. resolution)	Spectral reflectance curves	Total ground data
1	Vitrified dung		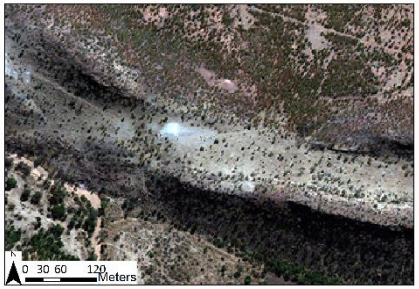	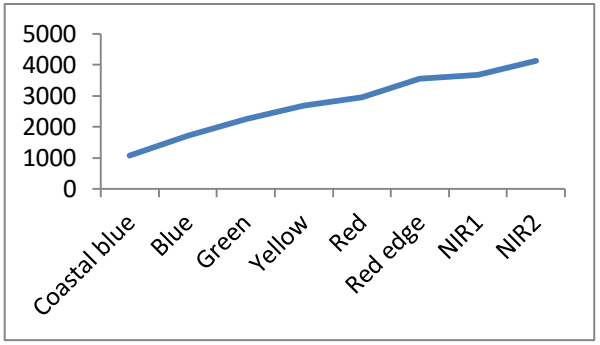	60
2	Non-vitrified dung		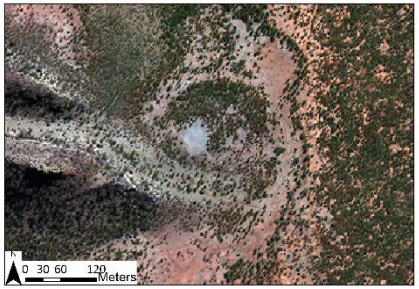	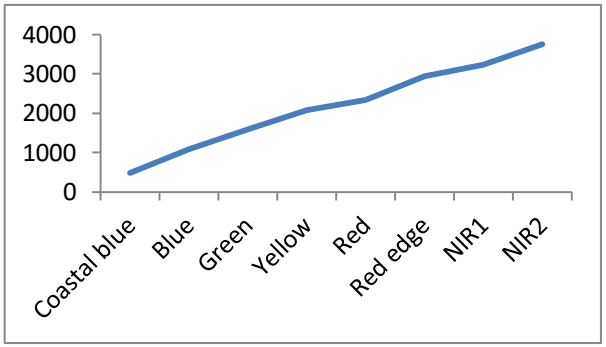	49
3	Irrigated agriculture		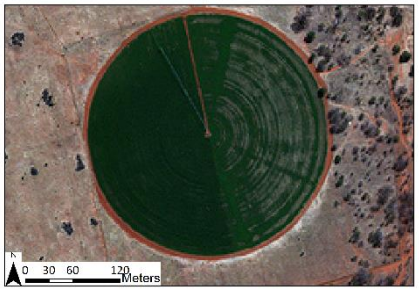	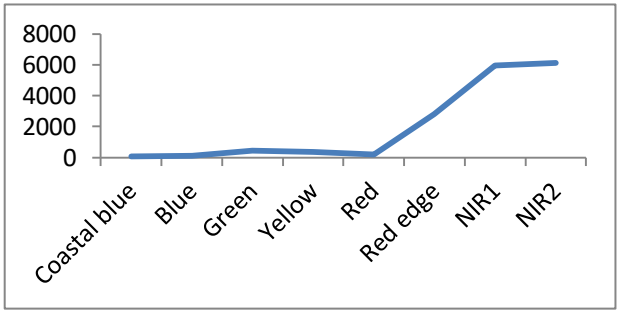	205

4	Bare soil		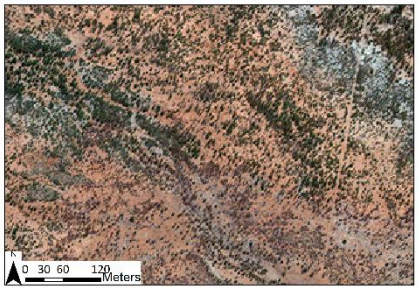	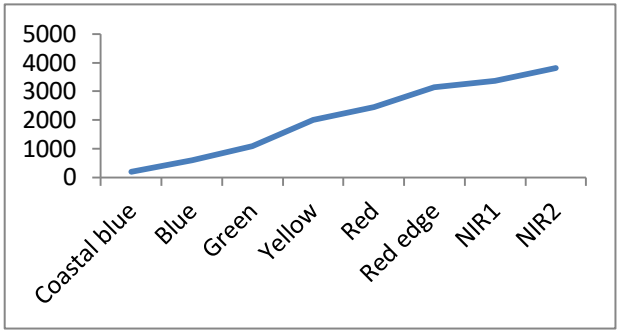	116
5	Savannah woody vegetation		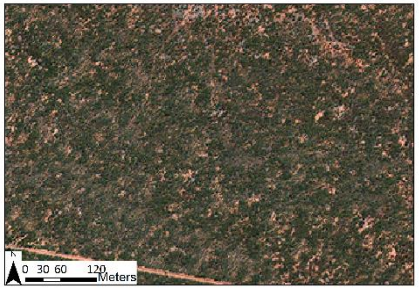	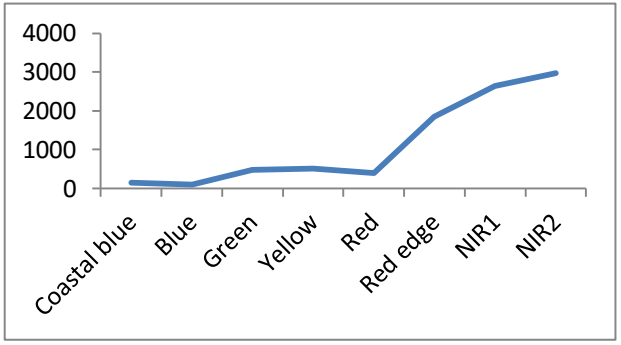	135

Table 5. 1 . Reference data for archaeological sites and land cover land use classes. The mean reflectance curves were constructed using spectral data extracted from WorldView-2 image using reference points

5.3.3 Image classification

Two machine-learning classifiers (random forest and support vector machine) were tested in this study. Random forest (RF) and support vector machine (SVM) algorithms were implemented on the images using R and ENVI software respectively. RF and SVM have received increasing attention in remote sensing applications, and good results have been achieved (Archer and Kimes 2008). One of the advantages of the machine learning classifiers such as SVM and RF is that they can produce reliable results with a small number of training samples (Mountrakis et al. 2011; Pal and Mather 2005; Rodriguez-Galiano et al. 2012b). Their reliability would, therefore, be an advantage for archaeological research, in particular in areas of limited accessibility.

5.3.3.1 Random forest

The RF classification algorithm uses an ensemble of non-pruned binary decision trees constructed using several bootstrap samples taken from learning sample using a randomly selected subset of variables (Archer and Kimes 2008; Breiman 2001). The bootstrap process, which uses two-thirds of the original data, offers an opportunity to estimate classification error using data withheld from the random dataset, about one-third of the original data, used in growing a tree (out-of-bag) (Breiman 2001; Genuer et al. 2010). An Out-Of-Bag (OOB) sample is also used in the estimation of variable importance. To minimise the correlation between classifiers in the ensemble, the algorithm uses the best split of a random subset of predictive variables at each node to grow the tree (Archer and Kimes 2008). Normally, the number of the predictive variables taken into consideration at each node (*mtry*) is defined by the user, with the default value being the square root of the number of variables. The tree is grown to its full extent without being pruned (Breiman 2001). The classification decision is then voted for by each tree from *ntree* with the majority vote determining the predicted class of observation. Since no tree pruning is done and only a sample of variables being trained on data, RF is less computationally demanding than other ensemble methods (Svetnik et al. 2003). The RF classification algorithm also provides a measure of the variables' importance as part of the classification process. These are *Gini* importance, mean decrease accuracy (MDA) and the number of times each variable is selected by each tree in the ensemble (Strobl et al. 2007). In this study, MDA was chosen as a measure of variable importance. MDA is measured by the average difference between prediction accuracies observed for each tree before and after the predictor variable is randomly permuted (Archer and Kimes 2008). Relatively large values

indicate the most important predictor variable while small values indicate the predictor is of less or no importance. As a result, in this study MDA was used to measure the contribution of each WorldView-2 band in discriminating LULC classes.

The optimisation of *mtry* and *ntree* was done using a *randomForest* library of R statistical packages version 3.4.1. The optimal combination of both *mtry* and *ntree* parameters was found using a grid search approach based on the OOB estimate of error. The grid search value for *mtry* was varied from 1 to 8, while the range of the grid search value for the *ntree* parameter was varied from 500 to 10,000 with an interval of 500. RF classification was carried out on the image using the *randomForest* classification package in R software. This package is based on the original RF algorithm developed by Breiman and Cutler (2007).

5.3.3.2 Support vector machine

SVM classifiers are designated to find the hyperplane that will optimally differentiate two classes (Mountrakis et al. 2011; Zhu and Blumberg 2002). The optimal separating hyperplane is the one with a maximum distance between it and the closest point without incurring some classification errors (Zhu and Blumberg 2002). The points closer to optimal separating hyperplane are classified as support vectors (Pal and Mather 2005). In a case where it is impossible to separate the two classes linearly, the SVM algorithm finds a location which maximises the margins while simultaneously minimising the number of errors (Pal and Mather 2005). SVM also uses kernel density to generate boundaries on non-linear surfaces. This is because kernel density gives the user an opportunity to classify data which does not have representation with clear fixed-dimensional vector space (Ben-Hur and Weston 2010). Generally, the most common kernel functions used in SVMs can be categorised into four groups; namely, polynomial, sigmoid, radial basis function and linear (Ben-Hur and Weston 2010; Lin and Lin 2003; Pal and Mather 2005). However, the majority of the remote sensing studies have used polynomial and radial basis function kernels for image classification (Huang et al., 2002; Otukei and Blaschke, 2010; Zhu and Blumberg, 2002). In cases where the two classifiers were compared, radial basis function outperformed polynomial function (Kavzoglu and Colkesen 2009). As a result, the radial basis function (RBF) was used to classify the dataset in this study. RBF requires the optimisation of two parameters: *sigma* (C) the regularisation factor, and *gamma* (γ) the width of the kernel (Hsu et al. 2003; Huang et al. 2002). The optimisation was performed using a 10-fold cross-validation and grid search. The grid search method tests different pairs of cost and gamma parameters and the one with the highest cross-

validation accuracy is selected (Hsu et al. 2003). RBF parameters were optimised using the e1071 library (Meyer et al. 2017) of R statistical packages version 3.4.1.

5.3.4 Accuracy Assessment

A holdout test dataset was generated by randomly dividing the ground-referenced data for the study area into 70% and 30% for training and testing for the accuracy assessment of the SVM and RF classifiers. The divisions mentioned above were done before classifying the data. An independent test data set constituting 278 non-vitrified and 23 vitrified dung sites mapped by Huffman (2009b, 2011) was also used for accuracy assessment of the SVM and RF classifiers. A confusion matrix was subsequently constructed to compute the kappa statistic, overall accuracy, user's accuracy and producer's accuracy as criteria for evaluating the level of accuracy and reliability of the generated surveying maps in site identification. Mcnemar's test was also used to test whether there is any significant difference in the way the two classifiers predicted the classes. Mcnemar's test is a non-parametric test that is based upon confusion matrices that are two by two dimensions (de Leeuw et al. 2006). This test is based on the standardised normal test statistic defined as:

$$Z = \frac{f_1 - f_5}{\sqrt{f_1 + f_5}} \qquad \text{Equation 5.1}$$

by which f_1 and $f_5$represent the off-diagonal entries in the matrix. Simply put f_1 and f_5 represents the number of cells correctly classified by one algorithm and misclassified by the other. The significance level was set at 0.05, with the difference being assumed to be significant if the Z is greater than the critical value 1.96.

5.4 Results

5.4.1 Tuning RF and SVM parameters

Results from the grid search indicated that the default *mtry* values between 4 and 6 combined with *ntree* values between 500 and 9500 produced the lowest OOB error rate (2.8%). The highest OOB error was attained when the number of predictors sampled for splitting at each node (*mtry*) is set at 2 with a number of trees grown set at 500, 2000-3500, 4500, 5500-8000, 9000-10000 and when *mtry* is set at 8 with *ntree* set at 500 and 9500 (Figure 5. 2). As a result, *mtry* value of 4 and *ntree* value of 500 were used as input parameters to train the RF algorithm

to classify the LULC classes. On the other hand, grid search gave 0.01 and 10 as a combination of gamma and cost values giving the highest prediction accuracy for the SVM classifier.

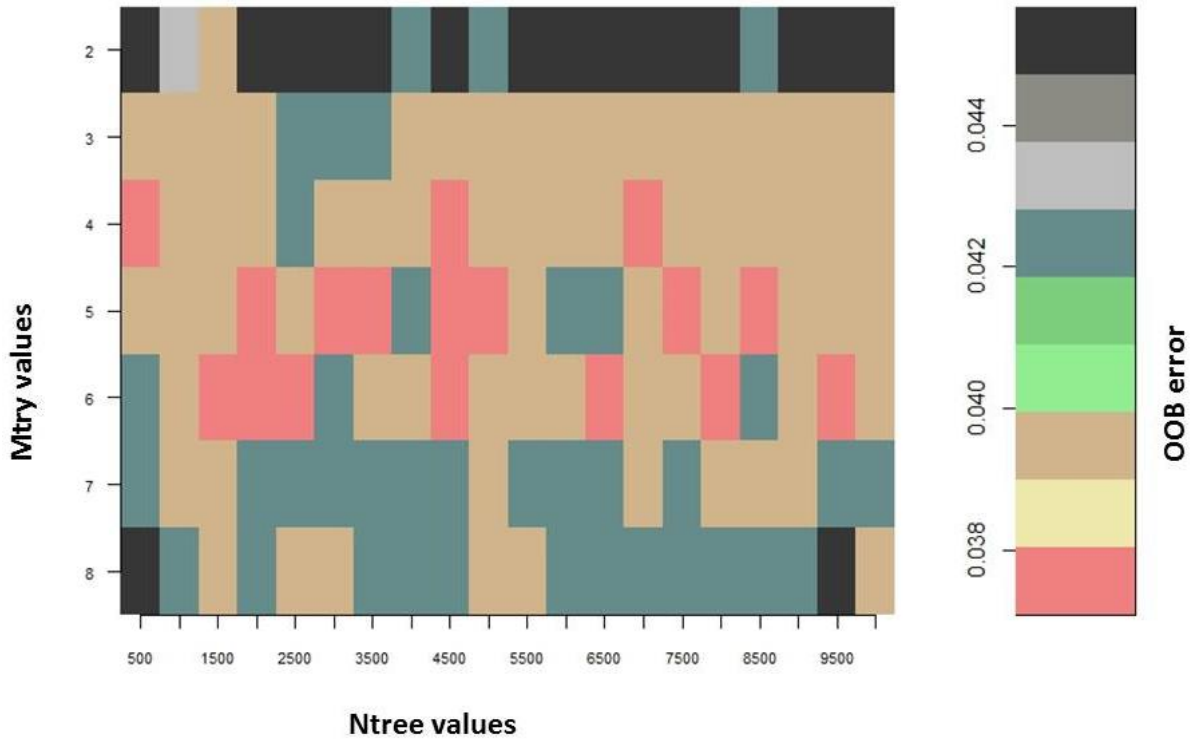

Figure 5. 2 OOB errors of random forest parameters (*mtry* and *ntree*) optimised using grid search method.

The RF classifier was able to determine the relative importance of WorldView-2 bands in discriminating the archaeological sites from other LULC classes. The mean decrease in accuracy with the RF algorithm has shown that generally, the red band, near-infrared and the blue bands were the most important in predicting the land cover classes (Figure 5. 3). For individual classes, the blue, red and green bands were most influential in detecting vitrified dung deposits, while the blue, red and near-infrared bands were instrumental in detecting non-vitrified dung (Figure 5. 4). Amongst the four new WorldView-2 bands, only the yellow one was important in detecting both vitrified and non-vitrified dung sites. Red edge and NIR2 formed part of the most important bands in detecting savannah woody vegetation. This is an important result, which highlights the usability of imagery with limited spectral bands in the detection of dung deposits in archaeological landscapes.

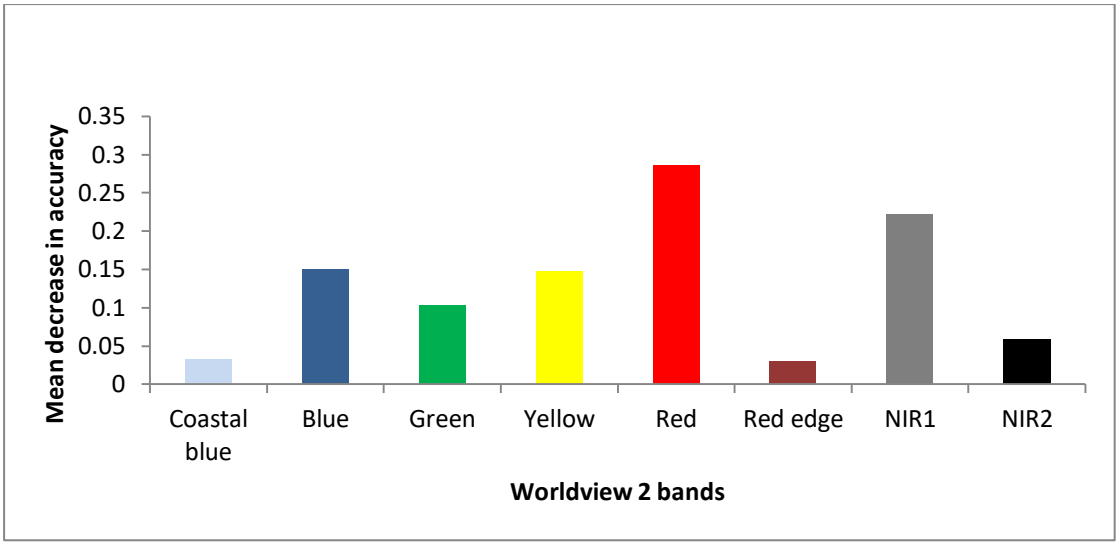

Figure 5. 3 Histogram showing the overall importance of different WV2 bands in detecting the different land cover classes reported in Table 5.1

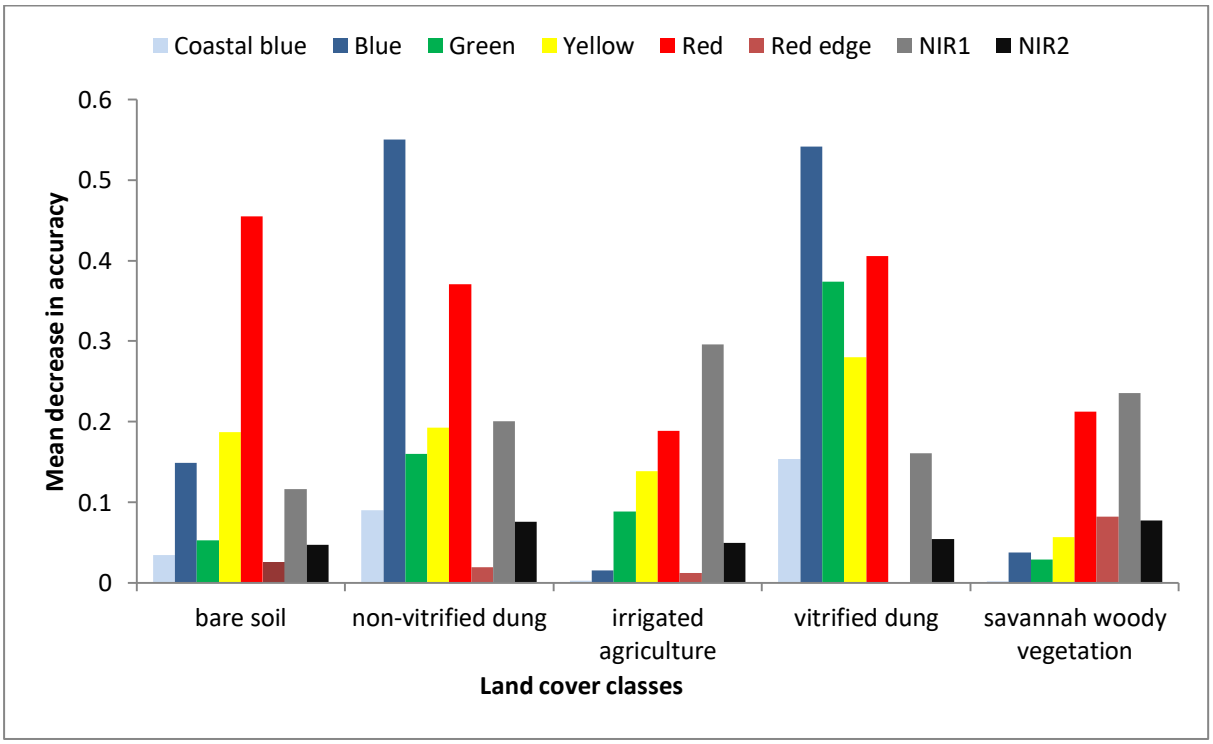

Figure 5. 4 Histogram showing the importance of different WV2 bands in detecting each land cover class considered in the study

5.4.2 Image classification and site prediction

The classification of the image using both RF and SVM algorithms was done to discriminate between bare soil, savannah woody vegetation, irrigated agricultural fields, archaeological sites with vitrified dung and those with non-vitrified dung. The main visual difference on the

thematic maps produced by the two algorithms was the amount of non-vitrified dung land cover class in the northern part of the study area (Figure 5. 5). The map produced by SVM algorithm shows that the aforementioned area is dominated by non-vitrified dung and savannah woody vegetation while the map produced by RF classifier shows the dominance of bare soil with some strips of savannah woody vegetation in the same area (Figure 5. 5). Statistically, SVM assigned 6.64 km^2 of the study area to vitrified dung sites while RF assigned only 3.46 km^2 of the study area to the same class (Table 5. 2).

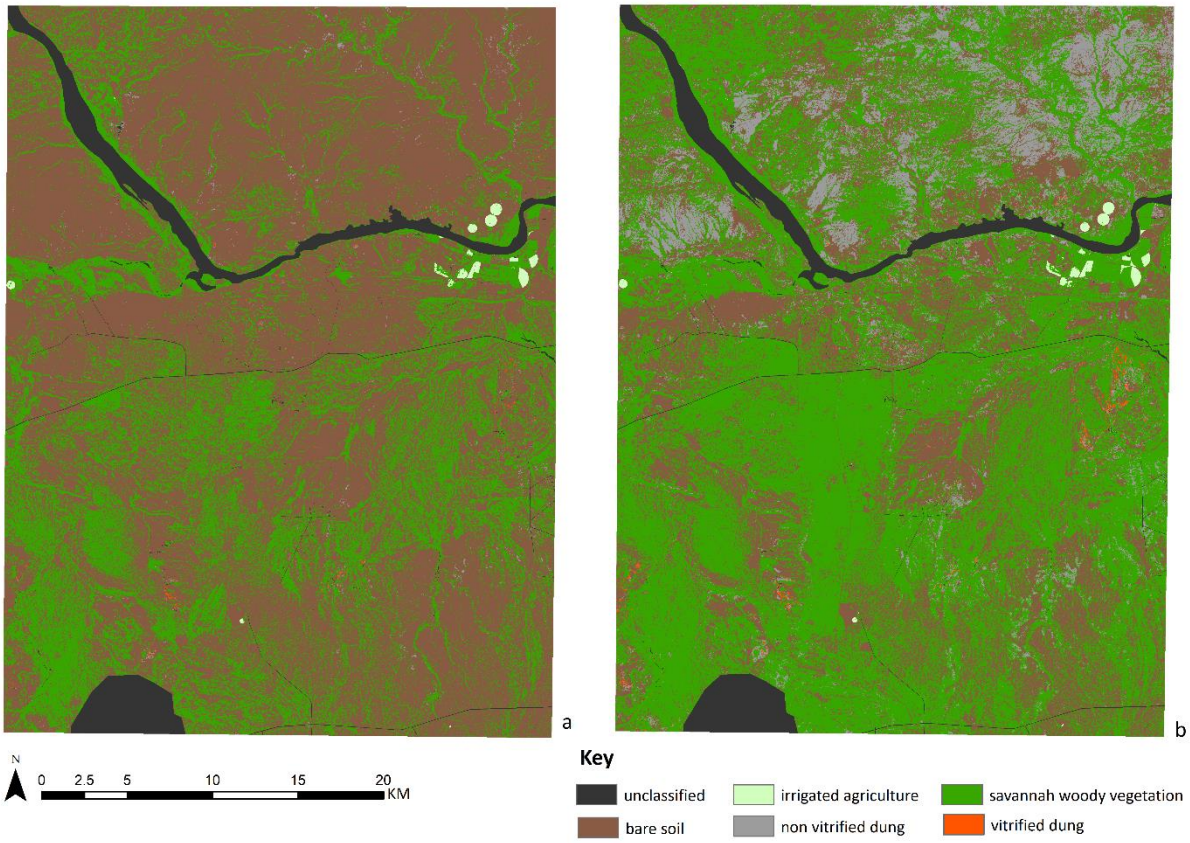

Figure 5. 5 Classification maps obtained using RF (a) and SVM (b) algorithms

Table 5. 2 Area (km2) covered by different LULC classes as predicted by RF and SVM classifier

Class	SVM	Random forest
Unclassified	52.82	52.82
BS	493.59	775.25
IA	5.97	3.53
NVD	145.28	24.37
SWV	667.53	512.39
VD	6.64	3.46
Total	1371.83	1371.83

5.4.3 Accuracy assessment

Two sets of data, a holdout sample and independent data, were used for assessing the classification accuracies of both RF and SVM classifiers by employing error matrices as shown in tables 5.3, 5.4, 5.6 and 5.7 respectively. Generally, the RF classifier had a higher overall accuracy than SVM classifier.

An accuracy assessment for the SVM algorithm using a holdout sample produced 88.82% overall accuracy and a kappa coefficient of 0.84. Vitrified dung had the highest producer's accuracy of 100% while non-vitrified dung had 87% (Table 5. 3). Non-vitrified had 93% user's accuracy while vitrified dung had 89%. An accuracy assessment which was done with an independent data set produced higher accuracies for non-vitrified dung sites (Table 5. 4). Non-vitrified dung recorded 100% producer's accuracy and 99% user's accuracy while vitrified dung recorded producer's and user's accuracies value of 96% and 92% respectively. A single vitrified dung site was confused as a non-vitrified dung site. Sites mapped by Huffman (2009b, 2011) were then overlaid on the classified image. It was found that 19.35% of vitrified dung sites and 61.94% of the non-vitrified dung sites were located their exact predicted locations. Some of the sites were located away from their predicted locations with 19.35% of vitrified dung sites and 34.84 % of non-vitrified dung sites being within 10 meters from their expected positions (Table 5. 5).

The RF classifier yielded 95.29% overall accuracy and a kappa coefficient of 0.84. A 100% user's accuracy was attained for vitrified dung, non-vitrified and bare soil when using RF classifier (Table 5. 6). Savannah woody vegetation and irrigated agriculture attained user's accuracy less than 100%, which was 88% and 97% respectively. Vitrified and non-vitrified

dung classes had 100% producer's accuracy and there was no confusion between them and other classes. However, a confusion occurred between vitrified dung sites and non-vitrified dung sites when using an independent dataset taken from a list of archaeological sites compiled by Huffman (2009b, 2011) for accuracy assessment (Table 5. 6). Two vitrified dung sites were confused as non-vitrified dung sites. Vitrified dung sites had the highest user's accuracy of about 100 % while non-vitrified dung had the highest producer's accuracy value of 100%. When assessing the prediction accuracy of the model using an independent dataset, taken from a list of 278 non-vitrified dung sites and 23 vitrified sites compiled by Huffman (2009b, 2011), 19.35% of vitrified and 29.03% of non-vitrified dung sites were located on their predicted locations (Table 5. 8). Three vitrified dung sites were confused as non-vitrified dung sites.

Even though the classifiers had different classification accuracies, an assessment done on their prediction accuracies using Mcnemar's test showed that there is no significant difference ($Z \leq 1.96$) at 5% significance level in the way they discriminated the LULC classes (Table 5. 9).

Table 5. 3 Confusion matrix showing overall classification accuracy and kappa for discriminating the five land cover classes; Vitrified Dung (VD), Savannah Woody Vegetation (SWV), Non-Vitrified Dung (NVD), Irrigated Agriculture (IA) and Bare Soil (BS) using SVM

	VD	SWV	NVD	IA	BS	Total	UA
VD	17	0	0	0	2	19	89.47
SWV	0	40	0	2	2	44	90.91
NVD	0	0	13	0	1	14	92.86
IA	0	8	0	57	0	65	87.69
BS	0	2	2	0	24	28	85.71
Total	17	50	15	59	29	170	
PA	100	80	86.67	96.61	82.76		
OA	88.82%						
Kappa	0.84						

Table 5. 4 Confusion matrix showing user's and producers accuracy for sites identified by Huffman (2009b, 2011) on an image classified using SVM classifier

	VD	SWV	NVD	IA	BS	Total	UA
VD	22	0	0	0	2	24	91.67
SWV	0	40	0	2	2	44	90.91
NVD	1	0	276	0	1	278	99.28
IA	0	8	0	57	0	65	87.69
BS	0	2	0	0	24	26	92.31
Total	23	50	276	59	29	437	
PA	95.65	80.00	100	96.61	82.76		
OA	95.88%						
Kappa	0.93						

Table 5. 5 The distance (m) between site locations predicted by SVM algorithm and sites locations mapped by Huffman (2009b, 2011)

Distance (m)	0	10	20	30	40	50	60 and above
VD	19.35	19.35	16.13	6.45	6.45	3.23	29.03
NVD	61.94	34.84	1.61	0.65	0.32	0.00	0.65

Table 5. 6 Confusion matrix showing overall classification accuracy and kappa for discriminating the five land cover classes; Vitrified Dung (VD), Savannah Woody Vegetation (SWV), Non-Vitrified Dung (NVD), Irrigated Agriculture (IA) and Bare Soil (BS) using RF

	VD	SWV	NVD	IA	BS	Total	UA
VD	17	0	0	0	0	17	100
SWV	0	44	0	2	0	46	95.65
NVD	0	0	15	0	0	15	100
IA	0	5	0	57	0	62	91.94
BS	0	1	0	0	29	30	96.67
Total	17	50	15	59	29	170	
PA	100	88.00	100	96.61	100		
OA	95.29%						
Kappa	0.93						

Table 5. 7 Confusion matrix showing user's and producers accuracy for sites identified by Huffman (2009b, 2011) on an image classified using RF classifier

	VD	SWV	NVD	IA	BS	Total	UA
VD	21	0	0	0	0	21	100
SWV	0	44	0	2	0	46	95.65
NVD	2	0	276	0	0	278	99.28
IA	0	5	0	57	0	62	91.94
BS	0	1	0	0	29	30	96.67
Total	23	50	276	59	29	437	
PA	91.30	88.00	100	96.61	100		
OA	97.71%						
Kappa	0.96						

Table 5. 8 The distance (m) between site locations predicted by RF algorithm and site locations mapped by Huffman (2009b, 2011).

Distance (m)	0	10	20	30	40	50	60 and above
VD	19.35	22.58	9.68	12.90	6.45	3.23	25.81
NVD	29.03	55.81	7.10	1.61	2.26	0.32	3.87

Table 5. 9 Cross-tabulation of a number of correctly classified and misclassified pixels for both SVM and RF.

	Random forest		
Support vector machine	correct classified	misclassified	**Total**
correct classified	165	0	**165**
misclassified	0	5	**5**
Total	**165**	**5**	**170**
Z-value	0		

5.5 Discussion

The main aim of this study was to test the possibility of prospecting for archaeological sites previously occupied by farming communities using VHR satellite images, a method which is significantly cheaper and less labour intensive than traditional field surveys. This was done through the use of VHR WorldView-2 satellite imagery and RF and SVM advanced classification algorithms. All the archaeological sites which had been identified during the field

survey were correctly predicted by the model, confirming the ability of satellite sensors to detect both vitrified dung and non-vitrified dung sites. These include sites mapped by another researcher (Huffman 2009b, 2011). This is a significant development because the use of remote sensing for archaeological survey in the SLCA region will help in developing a timely and systematic approach to documenting its archaeological sites at low cost. Moreover, it will provide the much-needed synoptic view of settlement patterns in a broader regional context, beyond the setting of the Mapungubwe cultural landscape.

The importance of each WorldView-2 band in discriminating between vitrified dung, non-vitrified dung and other LULC classes was assessed using the *randomForest* algorithm. Different WorldView-2 bands contributed differently to the detection of both vitrified dung and non-vitrified dung sites. This might have been caused by the differences in the physical and chemical makeup of the two sites (Rossel et al. 2006). Bands within the visible spectrum were the most important bands in detecting archaeological sites with vitrified dung (Figure 5. 4). This might have been influenced by the whitish colour of the vitrified dung which makes it appear brighter than its surroundings (Rossel et al. 2006; Todd et al. 1998). The red band and NIR1, which have the ability to discriminate different soil types (DigitalGlobe 2010), were important in distinguishing non-vitrified sites from vitrified sites, which has not been the case when using aerial photographs (Denbow 1979). This is a remarkable achievement because it will give researchers an idea on the types of sites, their distribution and relationship to their surroundings before engaging in fieldwork. It also extends the types of characteristics that can be used to identify archaeological sites in SLCA to those beyond the visible spectrum. The importance of the new yellow band in detecting both vitrified and non-vitrified dung sites confirms its sensitivity to soil types as observed in other studies (Alexakis et al. 2016; Wolf 2012). Above all, the ability of WorldView-2 multispectral bands to discriminate between different types of soil makes it a viable tool for detecting archaeological sites characterised by surface features, where the use of ecological indicators is not possible or desirable. This includes the current study area where the grass species *Cenchrus cilliaris* identified by Denbow (1979) as an ecological indicator for archaeological sites characterised by vitrified dung deposits in eastern Botswana, is too widely spread (Götze et al. 2008; Mothulatshipi 2008) to be used for archaeological sites prospection.

High classification accuracies were achieved using SVM and RF machine learning algorithms to map archaeological sites in SLCA. This is also supported by other research (Akar and Güngör 2013; Na et al. 2010; Rodriguez-Galiano et al. 2012a; Ustuner et al. 2015) where

machine-learning algorithms outperformed other traditional classifiers such as maximum likelihood in land cover classifications and achieved very high mapping accuracies. This is because machine-learning algorithms are powerful non-parametric algorithms which have the ability to handle high-dimensional and complex data more accurately than parametric algorithms (Knorn et al. 2009; Mas and Flores 2008; Na et al. 2010; Wang et al. 2016). A comparative analysis of the results obtained by RF and SVM classifiers shows that they both have an outstanding ability to discriminate archaeological sites against other LULC classes. In fact RF achieved 95.29% overall accuracy while SVM achieved 88.62%. Mcnemar's test of significance done on the prediction accuracies of the two classifiers has indicated that the differences in their predictions are statistically insignificant. This is in line with other studies (Abdel-Rahman et al. 2014; Ghosh et al. 2014) where no significant difference in mapping accuracies of the two above-mentioned classifiers was observed. However, there were some differences in the producers and users accuracies achieved by both classifiers in predicting the vitrified dung and the non-vitrified dung deposits with random forest showing better performances. SVM achieved 89.47% and 92.86% user's accuracies while random forest achieved 100% user's accuracy for both vitrified dung and non-vitrified dung respectively. Random forest achieved 100% producer's accuracies while SVM achieved 95.65% and 100% for vitrified dung and non-vitrified dung, respectively. Visual inspection of the images proves that both algorithms have different strengths, which can be of great use at different scales of archaeological survey. The RF classifier has a better ability to handle areas where there is an erosion of material. This makes it a good predictor of possible site locations as it will likely pick areas with high concentrations of dung and leave out those with thin layers of eroded dung (Figure 5. 5 and 5. 6). This will help in planning and directing field-walking survey, which is expensive and in most cases biased to hotspot areas. However, when mapping site extent the SVM classifier becomes handy because it can pick areas covered with thin layers of both vitrified and non-vitrified dung even though it mostly misclassified areas covered with bare soil as non-vitrified dung sites. This is in agreement with other studies (Burai et al. 2015) where SVM misclassified pixels generally belonging to the same vegetation category. As a result, the uses of the aforementioned algorithms is recommended in combination since they complement each (Ghosh et al. 2014; Pelletier et al. 2016).

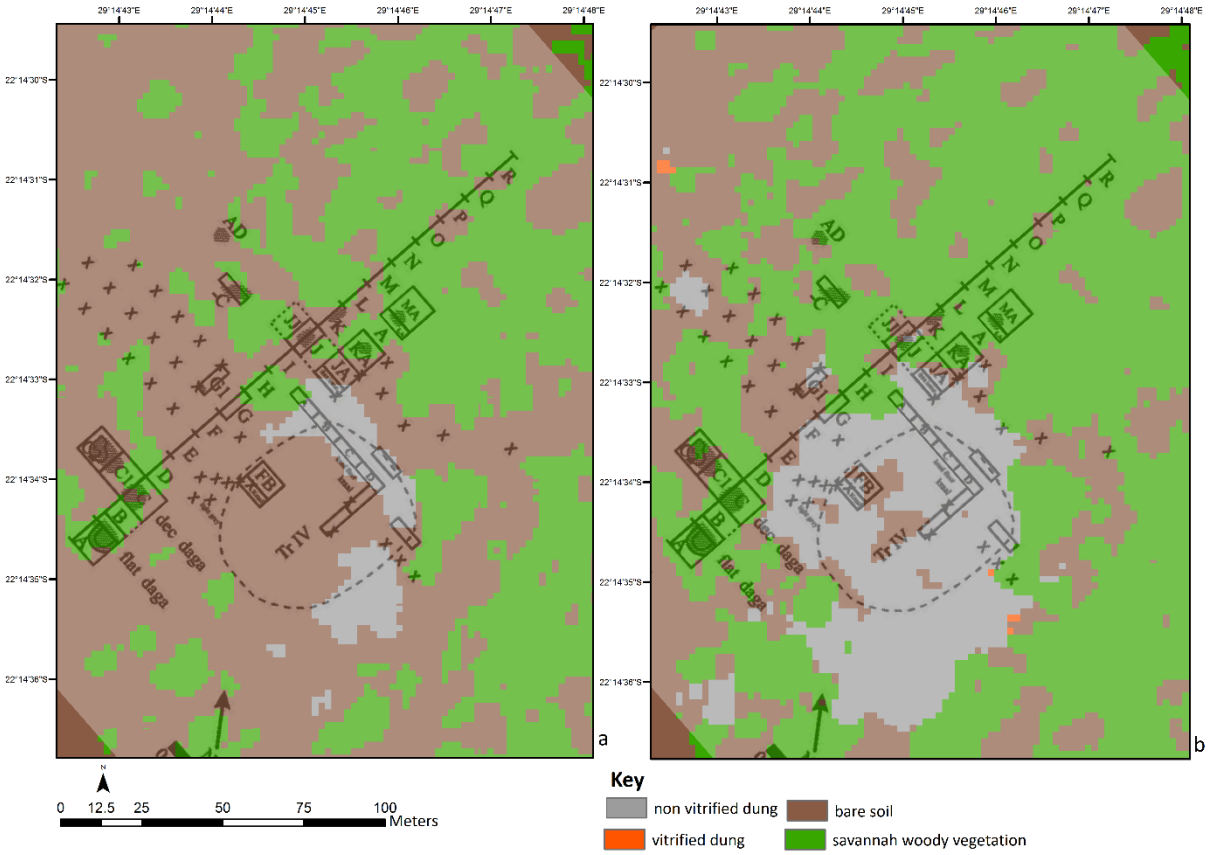

Figure 5. 6 A plan of site AA 14B drawn by Huffman (2004) overlaid on both random (a) forest and SVM (b) classified images

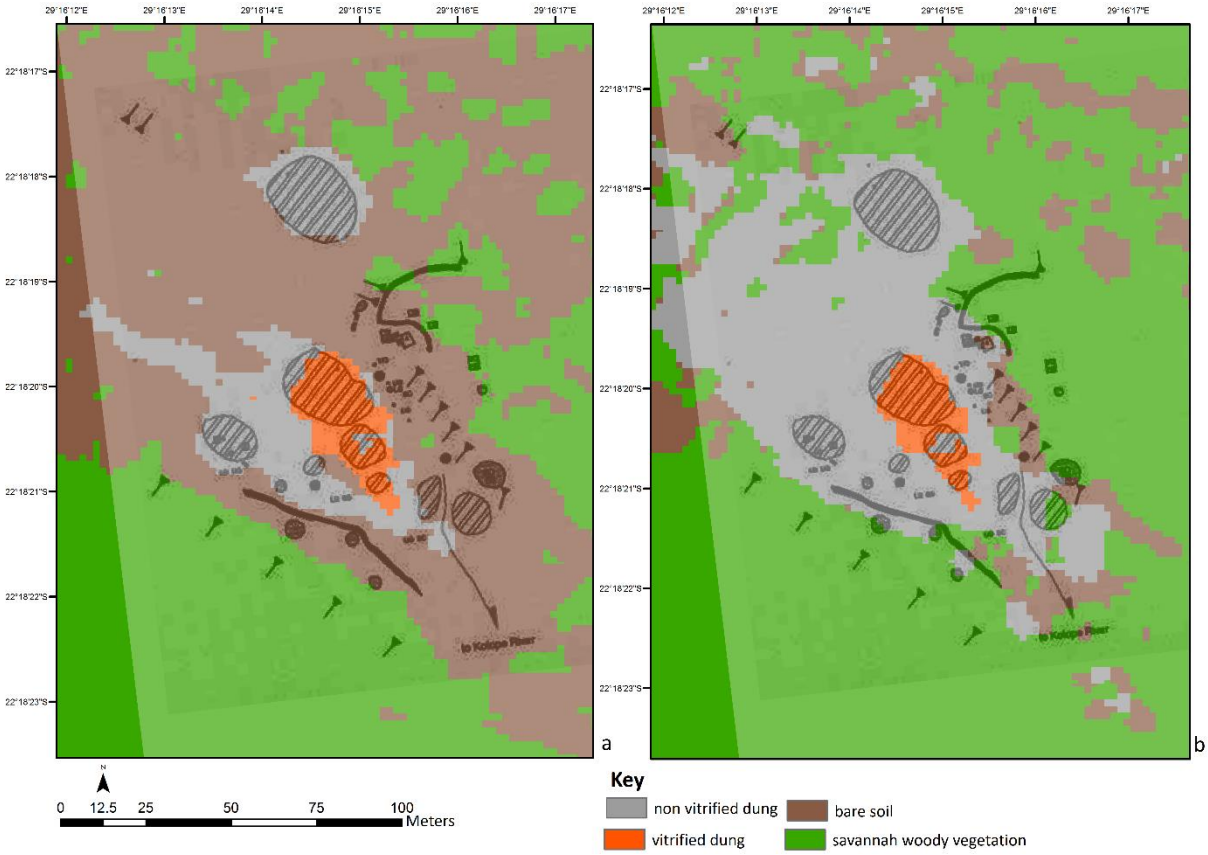

Figure 5. 7 A plan of site AD4 drawn by Calabrese (1997) overlaid on both RF (a) and SVM (b) classified images. Dark circles represent possible midden areas, solid lines represent stone walls while circular features with lines across represent kraals

There were some challenges to this study. Vitrified dung had similar spectral characteristics to river sand. This may be due to their similar whitish colour (Rossel et al. 2006). This similarity made it difficult for the classifiers to differentiate between the two aforementioned features. The other challenge is posed by erosion, which is rampant in the study area. Erosion can lead to disappearing of archaeological sites either because they are buried deep under soil deposits, or washed away and deposited on a different location where they might be detected as sites while in actual fact they are not. Object-based classification is recommended as an attempt to curb this limitation because of its ability to discriminate against different land cover classes using their spectral properties, texture, and shape (Whiteside et al. 2011).

Overall, high prediction accuracies attained in this study show the potential of using very high-resolution satellite images in conjunction with advanced classification algorithms to map surface archaeological features with distinct spectral signatures. Although dung deposits mainly characterise farming communities sites in Africa and India, the prediction techniques are applicable to a number of archaeological features such as middens, house floors, hearths

and other past anthropogenic activity areas that have a distinct chemical signature from their surroundings due to the presence of elements such as iron oxides and phosphates (Hejcman et al. 2011; Huffman et al. 2013; Luzzadder-Beach et al. 2011; Middleton 2004; Oonk et al. 2009; Wilson et al. 2009). Iron oxides and phosphates in the soil are sensitive to wavelengths between 0.4-1µm (Rossel and Behrens 2010) and 0.225-2.550 µm (Bogrekci and Lee 2005b), respectively. In this research, spectral bands in the visible and NIR regions have emerged as the most important in discriminating between archaeological features and surrounding soils. This spectral range is present in most satellite sensors, including non-commercial ones and can be exploited for archaeological site prediction. Spatial resolution remains a critical factor in the identification of archaeological features. The minimum size of features that can be undoubtedly mapped using satellite images needs to be one-half the diameter of the smallest object of interest (Cowen et al. 1995; Myint et al. 2011). For example, in order to identify a roundhouse or a midden that is 4 m wide, the minimum spatial resolution of high-quality imagery would be 2 by 2 m. In addition to this, in a real-world situation, a 4 m wide object to be identified in an image is unlikely to be perfectly contained by 4 pixels of a 2x2 m. resolution. As such, pixel sizes that are remarkable smaller than an object to identify are needed (Cowen et al. 1995; Myint et al. 2011). Imagery such as Sentinel and Landsat, which has the necessary spectral resolution, may not be able to detect a number of archaeological features of small sizes (furnaces, grain bins, small dwellings) due to their spatial resolutions that range between 10m and 60m (in the visible and IR bands).

5.6 Conclusion

Whilst most of the remote sensing based prospection for archaeological sites has been based so far on the use of image enhancement and vegetation indexes to detect archaeological sites or their proxy indicators, this study has demonstrated that advanced classification can assist the direct detection of archaeological features, provided they are not obscured by dense vegetation and possess characteristic properties distinct from those of their surroundings. This study has demonstrated that very high spatial resolution satellite images can be used to detect surface archaeological features directly. In general, this study has also proven that the contribution of new bands in WorldView-2 is of less importance in discriminating against sites characterised by byres. Very high classification accuracies achieved by advanced classification algorithms using limited training datasets in this study demonstrates the suitability of using them for archaeological applications.

Following this pilot study, which used very high-resolution images from a commercial satellite, there is a need to assess the possibility of using high-resolution images from non-commercial (and therefore free of charge) satellites which could be more accessible to archaeologists. Most importantly, even though the study was piloted in the Shashi-Limpopo Confluence area, the method can be applied elsewhere in the world to carry out systematic, cost-effective and repetitive surveys of surface features over large areas and in restricted and inaccessible regions.

CHAPTER SIX

6. Evaluating the performance of geographic object-based image analysis in mapping archaeological landscape previously occupied by farming communities: A case of Shashi-Limpopo Confluence Area

This chapter is based on:

Thabeng, O. L., Adam, E. and Merlo, S., (In Preparation). "Evaluating the performance of geographic object-based image analysis in mapping archaeological landscape previously occupied by farming communities: A case of Shashi-Limpopo Confluence Area."

Abstract

The application of pixel-based remote sensing techniques in archaeology is usually limited by spectral confusion between archaeological material and the surrounding environment because of their reliance on the spectral contrast between features. The aforementioned limitation is most common in areas where archaeological features were constructed using the same material from their surroundings or archaeological material have been eroded to other areas. To address this issue, we investigated the possibility of using the geographic object-based image analysis (GEOBIA) to predict archaeological and non-archaeological features. The chosen study area was previously occupied by farming communities and is characterised by natural soils (non-sites), vitrified dung, non-vitrified dung and savannah woody vegetation. The study used three stage GEOBIA that comprises of (1) image object segmentation, (2) feature selection, and (3) object classification. The spectral mean of each band and area extent of an object were selected as input variables for object classifications in support vector machines (SVM) and random forest (RF) classifiers. The results of this study have shown that GEOBIA approaches have the potential to map archaeological landscapes. The SVM and RF classifiers achieved high classification accuracies of 96.58% and 94.87%, respectively. Visual inspection of the classified images has demonstrated the importance of the aforementioned models in mapping archaeological and non-archaeological features because of their ability to manage the spectral confusion between non-sites and vitrified dung sites. In summary, the results have demonstrated that the robust ability of the GEOBIA to integrate spatial attributes into the classification model improves the chances of separating materials with limited spectral contrast.

Keywords: Advanced classification algorithms, Vitrified dung, Non-vitrified dung, Remote sensing, Image segmentation, Very high spatial resolution

6.1 Introduction

Heritage sites are important to understanding human social development because they give an account of the past civilisations, cultures and their evolution to the contemporary (Hassani 2015; Keitumetse 2011). However, heritage sites are faced with dangers posed by both anthropogenic and natural threats such as mining activities, urban development, looting, flooding, erosion and fires (Casana and Laugier 2017; Chirikure 2013; Durand et al. 2010; Khandlhela and May 2006; Lanza 2003; Lasaponara et al. 2016a; Musyoki et al. 2016; Nienaber et al. 2008; Parcak 2015; Smith 2012). In addition to this, heritage management institutions in most developing countries are also faced with a number of challenges, which includes among others a lack of funds often leading to inadequate surveying, documentation and monitoring of heritage sites (Chirikure 2013; Mabulla 2001; Mcintosh 1993). Site surveying, documentation and monitoring in some parts of the world are also hampered by their inaccessibility due to a range of factors including dangerous wild animals and dense vegetation, conflicts and property rights (Biagetti et al. 2017; Casana and Laugier 2017; Mabulla 2001; Thabeng et al. 2019). Hence, there is a need to develop a system which can enable cost-effective documentation and rapid monitoring of the status of archaeological sites in order to enable effective preservation and management (Lasaponara et al. 2007; Parcak 2007).

The documentation of archaeological features has traditionally been done through fieldwalking surveys (Fleisher and LaViolette 1999; Hitchner 1995; Huffman 2009b, 2011; McIntosh and McIntosh 1993). Fieldwalking survey offers the surveyor an opportunity to identify, appreciate and record finer details of different types of archaeological sites on the ground (Foard 1977; Reid and Segobye 2000). Although fieldwalking surveys offer detailed contextual records of archaeological materials on the ground and can be done in a comprehensive, systematic fashion, they are time-consuming, costly and can be difficult to carry out over large areas (Banning et al. 2006; Corrie 2011; Hitchings et al. 2013). More recently, with the advent of high-resolution multi-spectral satellites, remote sensing has offered a relatively cheap, fast, systematic and reproducible method of survey, which can be used to document and monitor archaeological sites over large and/or inaccessible areas within a short period (Keay et al. 2014; Lasaponara et al. 2014; Lasaponara and Masini 2005). However, there are challenges arising from the use of high-resolution multi-spectral satellite data which includes within class spectral variability and increased spectral confusion between classes (Blaschke et al. 2014; Pu et al.

2011; Wu 2009). Additionally, the use of remote sensing needs specialised expertise which is more expensive to acquire as compared to training required for surveyors employed in field walking surveys (Davis and Douglass 2020; Klehm and Gokee 2020).

Remote sensing in archaeology commonly exploits the spectral contrast between areas of archaeological interest and their surroundings (Beck 2007; Corrie 2011). This is largely because past anthropogenic activities have localised impact on the soil's physical and chemical properties, thus making it different from its surroundings (Oonk et al. 2009; Wilson et al. 2008). A key requirement in remote sensing image analysis is the decision on the basic unit of classification, which can either be an image pixel or an image object (Li et al. 2016; Toure et al. 2018; Witharana and Lynch 2016; Zhang et al. 2017). Image pixel is the smallest discrete area within a two-dimensional array of cells that forms an image (Lillesand et al. 2008). The image object is created by grouping spatially connected pixels with homogeneous properties using segmentation analysis (Belgiu and Drăguţ 2014; Li et al. 2016; Myint et al. 2011).

Different pixel-based image classification approaches have been tested in archaeological applications using imagery captured by hyperspectral and multispectral sensors (Aqdus et al. 2012; Cavalli et al. 2007; Doneus et al. 2014; Lasaponara and Masini 2006; Thabeng et al. 2019). Image enhancement techniques have been mainly employed to increase the prominence and identification of archaeological features in an image (Lasaponara and Masini 2006; Pan et al. 2017). For example, the principal component analysis was used to enhance spectral differences of cropmarks associated with archaeological sites in southern Scotland, improving the visibility and identification of archaeological features in the landscape (Aqdus et al. 2012). Bennett et al. (2012) used normalised vegetation indices to identify archaeological sites in the grasslands of Salisbury Plain, Wiltshire. On the other hand, some researchers used unsupervised pixel based classifiers to assess the possibility of spectrally separating archaeological features from their surroundings and identifying unknown classes (Clark et al. 1998; Harrower and D'Andrea 2014; Lasaponara et al. 2014; Parcak 2007). Criminale et al. (2009) used ISODATA unsupervised classifier to identify palaeoriverbeds which cut through the ditches of the Neolithic village of Schifata in northern Italy. The main challenge of using unsupervised classifiers is that an analyst does not develop reference data classes to be used in training the classification model (Yang and Yang 2004). As a result, the classifiers produce meaningless classes of data which can be challenging to merge into meaningful classes (Lu and Weng 2007). Supervised pixel based classifiers have been used to predict areas of archaeological interest (De Laet et al. 2007; Siart et al. 2008; Thabeng et al. 2019).

The pixel-based methods have produced high classification accuracies in detecting most of the archaeological sites. However, some limitations associated with the pixel-based method in archaeological applications have been reported by some recent studies (Thabeng et al. 2019; Verhagen and Drăguţ 2012). Pixel-based classifiers cannot handle the within-class spectral variability (Blaschke et al. 2014). Above all, the main problem with the application of the aforementioned classification methods is that they assume pixel as the spatial unit of analysis and depends solely on its spectral properties for classification (Myint et al. 2011). This becomes problematic in archaeological sites and environments characterised by features with variance in material composition and spatial attributes but having similar spectral signatures (Blaschke et al. 2014; Whiteside et al. 2011). For example, despite the difference in their spatial attributes, Thabeng et al. (2019) found out that there is no spectral difference between vitrified dung deposits and non-sites. The confusion between the two features might be because of their similar whitish colour or the washing down of dung deposits into the river by water erosion which is rampant in the area. As a result, this calls for the classification process which will incorporate spatial attributes of the aforementioned features such as size and texture, in addition to spectral properties, in order to improve the accuracy.

The geographic object-based image analysis (GEOBIA) has been used to differentiate features with similar spectral characteristics and different spatial attributes, contextual and texture (Blaschke and Strobl 2001; Hu et al. 2013; Myint et al. 2011; Whiteside et al. 2011). Furthermore, GEOBIA attained higher classification accuracies in high spatial resolution images when compared to pixel-based classifications which are prone to salt and paper effect (Ouyang et al. 2011; Weih and Riggan 2010). Research has also shown that GEOBIA is superior to pixel-based classifications especially in complex environments (Pu et al. 2011; Whiteside et al. 2011). For example, Myint et al. (2011) proved that GEOBIA outclassed pixel-based analysis when mapping the central part of the city of Phoenix in Arizona, which was characterised by spectrally similar feature classes such as buildings, unmanaged soils and impervious surfaces (roads and pavements).

In their study, object-based classifier outperformed pixel-based maximum likelihood classifier by 22.8% as they achieved an overall accuracy of 90.40% and 67.60% respectively. Furthermore, GEOBIA has been used for classification in a number of land use and land cover studies, which include mapping croplands (Li et al. 2016, 2015a; Vogels et al. 2017) and biomass in the Atlantic forest biome characterised by eucalyptus, pinus, rupestrian fields, shrub savannas, grassland and in semi-deciduous forest (Silveira et al. 2019) where it achieved

excellent results. Lately, object-based classification has been used to delineate landforms for the prediction of archaeological sites (Verhagen and Drăguț 2012) and the detection of looting activities (Van Ess et al. 2006). Conversely, this method has not been tested in discriminating between surface archaeological deposits of vitrified dung, non-vitrified dung and non-sites (natural soils), which are the major characteristic features of archaeological sites previously occupied by farming communities in the south central part of southern Africa. Furthermore, the aforementioned features (midden, vitrified dung and non-vitrified dung) form the central part of farming communities settlements and therefore are important for understanding their intra and inter settlement patterns (Huffman 2000, 2009a; Meyer 2000).

However, mapping features using GEOBIA requires an image with high spatial resolution to reveal the spatial and contextual properties of individual features (Blaschke 2010; Myint et al. 2011; Toure et al. 2018). Myint et al. (2011) posit that for the object to be effectively delineated, it must be at least twice the size of the spatial resolution of the image or more. Additionally, Thabeng et al (2019) report that an archaeological feature has to be at least 4m in diameter for it to be clearly discriminated when using Worldview-2 images. This, therefore, means that very high-resolution satellite images such as WorldView-2 and GeoEye has spatial accuracy to capture the spatial and contextual attributes of byres in the study area because they range between 3m and 18m in diameter (Huffman, pers comm., 2018). Hence, the objective of this study is to investigate whether the use of GEOBIA based on advanced classification algorithms, random forest and support vector machines, can accurately discriminate between the archaeological deposits and non-archaeological deposits in the Shashi-Limpopo Confluence Area (SLCA) using a high-resolution WorldView-2 satellite image.

6.2 Materials and methods

6.2.1 The study area and archaeological context

This study was carried out in the Mapungubwe Cultural Landscape, which is located at the confluence of Shashi and Limpopo rivers in southern Africa (Figure 6. 1). The landscape is listed under UNESCO World Heritage and is believed to have been occupied by one of the earliest complex societies in Southern Africa (Huffman 2009a). Mapungubwe cultural landscape has been inundated with archaeological research since the early 1930s with the discovery of the golden rhinoceros on the Mapungubwe hill (Huffman and Du Piesanie 2011; Meyer 2000). These include one of the most extended systematic field walking surveys in the

Mapungubwe landscape under the 'Origins of Mapungubwe Project' spanning more than two decades and discovering over 1100 farming community sites in the process (Huffman and Du Piesanie 2011). Research has also revealed a lot of the archaeological materials that formed an integral part of everyday life and social patterns within the settlement. These include artefacts such as glass beads, bangles, ceramic figurines and pots together with features such as middens and byres (Hanisch 1980; Huffman 2009b, 2011; Huffman et al. 2004). The byres are likely to show the centre of the settlement. This is because research has shown that the societies which occupied the Mapungubwe landscape practised the Central Cattle Pattern (CCP) settlement system, whereby an animal byre (kraal) was located at the centre of the settlement, close to the male gathering area (Hanisch 2002; Huffman 2009a). The byres can be further divided into vitrified and non-vitrified deposits (Huffman et al. 2013; Meyer 2000). Non-vitrified dung deposits consist of unburned dung (Huffman et al. 2013). Vitrified dung is a glassy biomass slag formed by burning thick dung deposits at very high temperatures (in the region of 1100^{o} C) (Peter 2001; Thy et al. 1995). However, there is no consensus on the cause of the above-mentioned burning — some researchers (Huffman et al. 2013; Peter 2001) attributing it to intentional causes while others posit that it was accidental occurrences such as veld fires or lightning at very high temperatures (Thy et al. 1995). This study, therefore, will assess the feasibility of using GEOBIA to detect archaeological sites characterised by vitrified dung and non-vitrified dung within the SLCA. Although *Cenchrus cilliaris* has been previously used as an indicator of the aforementioned sites in central eastern Botswana by Denbow (1979), it is not a diagnostic feature of the sites in SLCA, as such, this study targeted barren dung deposits directly.

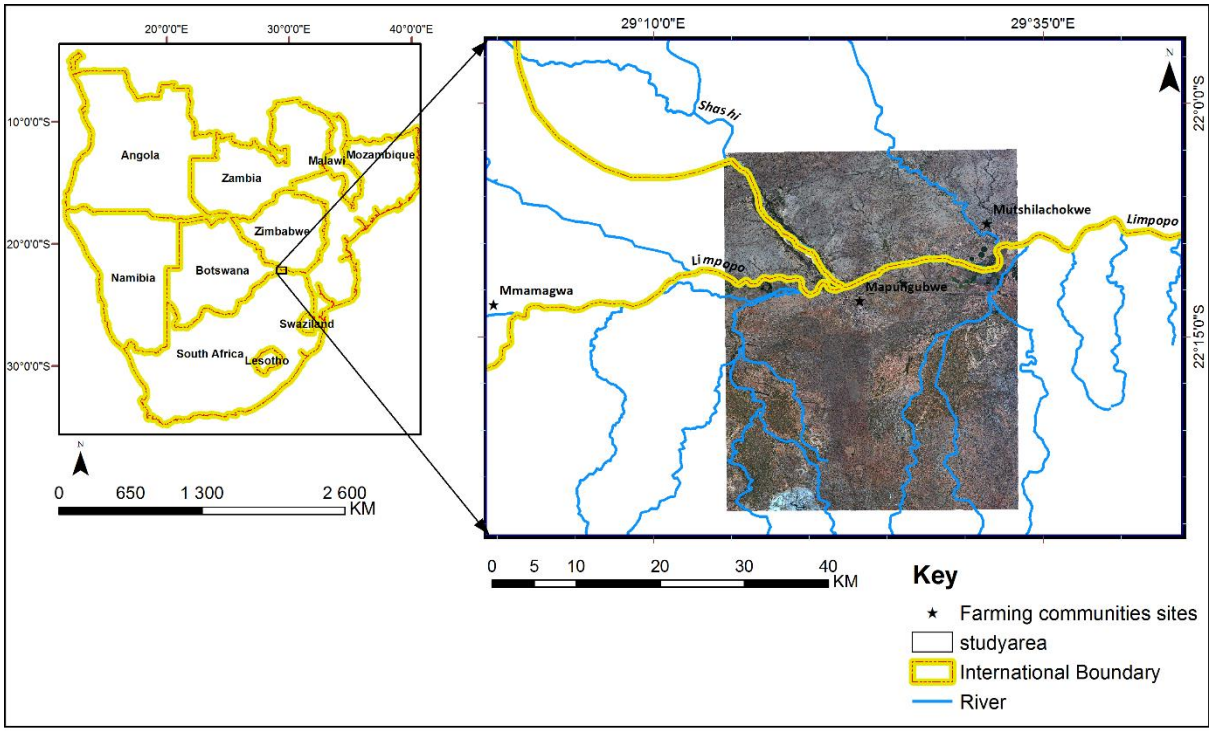

Figure 6. 1 Location of the study area in southern Africa with a true colour WorldView-2 image used in this study

6.2.2 Worldview-2

Two cloud-free WorldView-2 images captured on August 5, 2014, covering 1388 km^2 of the study area, at spatial resolutions of 0.5 m for the panchromatic band and 2 m for multispectral bands was used in this study. This is the best period to identify the surface archaeological features because the savannah canopy is very dry and open with most of the archaeological dung deposits exposed during that period (Southern hemisphere spring season). The images were obtained as a grant from Digital Globe and were geometrically corrected on supply. WorldView-2 satellite collects images in one panchromatic (450-800nm) and eight multispectral bands at 400–450 nm (B1-coastal), 450–510 nm (B2-blue), 510–581 nm (B3-green), 585–625 nm (B4-yellow), 630–690 nm (B5-red), 705–745 nm (B6-red edge), 770–895 nm (B7-near infrared-1), and 860–1040 nm (B8-near-infrared-2). Nonetheless, the panchromatic band was excluded from analysis in this study. The radiometric corrections were done on each image using Fast Line-of-Sight Atmospheric Analysis of Hypercubes (FLAASH) in Envi 4.8, before merging the images. FLAASH has the ability to correct atmospheric effects on the image and give radiance values leading to the recovery of accurate reflectance spectra (Matthew et al. 2002).

6.2.3 Segmentation and feature selection

Image segmentation create the objects, which are the basic spatial unit of analysis in GEOBIA (Whiteside et al. 2011). The created objects relate to natural spatial units, therefore, they should form a more meaningful spatial unit for land cover mapping (Costa et al. 2017; Pu et al. 2011). Additionally, the quality of demarcation of target objects has a direct impact on the prediction accuracy of the classes in an image (Whiteside et al. 2011). Multi-resolution segmentation (MRS) algorithm in 64-bit Ecognition developer v.9 software, was used in this study. This is the most regularly used segmentation technique (Belgiu and Csillik 2018) and researchers (Aguilar et al. 2017; Li et al. 2016; Witharana and Civco 2014) have held it as one of the best segmentation methods in GEOBIA. MRS employs a bottom-up region method whereby a pixel is identified as a single object before being paired with other spatially adjacent objects to form bigger objects depending mainly on the defined scale heterogeneity level (Li et al. 2016; Mathieu et al. 2007). The object pairing is based on the pairwise clustering procedure (Van Coillie et al. 2007). The MRS allows the user to regulate the level of homogeneity within the objects by setting the scale, shape and colour parameters (Luo et al. 2015).

The scale parameter plays a major role in influencing the quality of segmentation process because it determines the size of the object which can, in turn, lead to under-segmentation or over-segmentation error (Myint et al. 2011). The large values for scale parameter allow for the creation of large objects and more heterogeneity within the objects while small values for scale creates small homogeneous objects. The impact of segmentation scale on class distinction was investigated at 10 different scales (10, 20, 30, 40, 50, 60, 70, 80, 90, and 100) in this study. After finding the suitable scale factor, the shape and colour parameters were adjusted to improve the features of output image objects (Mathieu et al. 2007; Pu et al. 2011). The shape is based on the geometric characteristics of the archaeological and non-archaeological features. The shape of an object is influenced by two inversely proportional properties, which are smoothness and compactness (Esch et al. 2008; Platt and Rapoza 2008). The colour parameter deals with spectral heterogeneity of archaeological and non-archaeological features, as a result, it is affected by the weight assigned to each band in segmentation (Li et al. 2016; Mathieu et al. 2007). However, the weight value of each band was left at one, which is the default, in order to avoid the biases in the classification. The combined weighted values of shape and colour parameters add up to a total of one (Li et al. 2016; Platt and Rapoza 2008). Studies by Costa et al. (2017) and Mathieu et al. (2007) have shown that in most cases desired results are achieved when the shape is given less weight than colour. As a result, in tuning the parameters

for segmentation in this study, the shape parameter was always given less value than colour in order to give more weight to spectrally homogenous pixels when segmenting. To identify the optimum image segments using the abovementioned parameters, studies have used trial and error method by varying their values (Ahmed et al. 2017; Hu et al. 2013; Mathieu et al. 2007; Vogels et al. 2017; Zhang et al. 2017). The image segmentation procedure is, therefore, pondered done when the objects produced visually matched the real-world features of interest when using the aforementioned optimisation method. Consequently, in order to identify the optimum segments in this study, the trial and error method assessed through visual inspection was used to regulate the scale, shape and colour parameters in segmentation. The scale parameter of 50 and the shape parameter of 0.2 were chosen as the optimum segmentation parameters in this study.

After image object segmentation, the variable selection was carried out for use in object-based classification. Variable feature selection procedure identifies a subset of optimum object features which will produce the best results in the classification process (Blaschke et al. 2014; Guan et al. 2013). The classification process can comprise a number of object feature properties ranging from context, size, spectral data, shape, and texture (Blaschke et al. 2014; Whiteside et al. 2011). The feature selection process can be carried out in two ways by either using software algorithms or manual process based on literature review and expert knowledge (Guan et al. 2013; Hu et al. 2013; Puissant et al. 2014; Witharana and Lynch 2016). In this study, a number of object characteristics were manually assessed based on literature review and expert knowledge in an attempt to identify the best subset of features for classification (Duro et al. 2012; Witharana and Lynch 2016). All the object features used as input variables in this study are listed in Table 6. 1. Image objects were spectrally differentiated using the mean spectral value of each band computed at the object level. To differentiate image objects with information extracted from their geometric features, the area extent of the image objects was used. Area extent of an object is measured by counting the number of pixels within it. This was done to differentiate objects of different sizes with similar spectral properties such as river sand and vitrified dung sites (Thabeng et al. 2019). Other various object characteristics and parameter settings such as shape, texture and class-related features were explored but did not produce suitable outcomes.

Table 6. 1 image object features used in this study

Type	Tested feature	Number of features	Description
Spectral	mean	8	Mean reflectance of each band for an object
Geometry extent	Area	1	Area of an object (Pixel)

6.2.4 Image Classification

6.2.4.1 Random forest

RF classifier was used to map the archaeological sites and other LULC cover types using the classes created on the segments. Since its inception by Breiman (2001), RF has been effectively used in a number of domains like pharmacology (Fernández-Blanco et al. 2013; West et al. 2010), medical imaging (Gray et al. 2013; Lebedev et al. 2014; Tustison et al. 2015) and genetics (Boulesteix et al. 2012; Díaz-Uriarte 2007; Strobl et al. 2007) because of its intrinsic ability to measure variable importance and its robust predictive power. Furthermore, and over the last decade, RF has increasingly been used in different remote sensing applications such as vegetation species mapping (Adam et al. 2012; Immitzer et al. 2012; Mureriwa et al. 2016), agriculture (Sirsat et al. 2017; Tatsumi et al. 2015) and archaeology (Thabeng et al. 2019).

RF is pronounced as an ensemble of classifiers which generates binary decision trees and allocates class basing on popular votes at each node (Chan and Paelinckx 2008). RF grows each tree using a different bootstrapped sample drawn from the training data, with about one-third of the training data not being included in building each tree (Breiman 2001; Breiman and Cutler 2007). The left-out sample is commonly known as the out-of-bag (OOB), is then used to assess the importance of each variable in classification and generalisation error (Breiman and Cutler 2007; Genuer et al. 2010). RF classification was done using the *randomForest* package within the R statistical environment (Belgiu and Drăguţ 2016). Training the RF classifier encompasses optimising two parameters: (1) number of variables used in a dataset to split trees at each node (*Mtry*) and (2) the number of trees in the forest (*ntree*) (Belgiu and Drăguţ 2016; Liu et al. 2015). Following the previous studies (Adam et al. 2014; Mureriwa et al. 2016; Rodriguez-Galiano et al. 2012b), this study used a grid search approach based on the OOB estimate of error to find the optimal combination of both *mtry* and *ntree* parameters. The

grid search value for *mtry* was varied from 1 to 9, while the range of the grid search value for the *ntree* parameter was varied from 500 to 9500 with an interval of 1000.

6.2.4.2 Support vector machines

SVM is a non-parametric supervised classifier which is gaining wide use in remote sensing because of its ability to achieve good generalisations even with inadequate training data (Dalponte et al. 2008; Melgani and Bruzzone 2004; Mountrakis et al. 2011). The SVM model was initially proposed by Vapnik and Chervonenkis (1971) before it was fully discussed by Vapnik (1999). In general SVMs are linear classifiers which are composed of hyperplanes that separate data classes by the largest margin within a high dimensional feature space (Huang et al. 2002; Kavzoglu and Colkesen 2009). The user chooses the SVM kernel function to be used for the training process that picks support vectors along the hyperplane surface (Huang and Wang 2006). Radial basis function (RBF) kernel was chosen for classification in this study. RBF has been applied to a number of land use and land cover (LULC) classifications where it achieved high classification accuracies than other SVM kernels and classification algorithms (Kavzoglu and Colkesen 2009). This is also supported by results from Pal and Mather (2005) who found out that RBF outperformed other classification algorithms in classifying land cover data. This might be largely because of its ability to handle non-linear relationships concerning class labels and attributes which is mostly the case with spatial data (Huang et al. 2002). In this study, the RBF classification process involved the identification optimal values of regularisation parameter *sigma* (C) and the width of the kernel *gamma* (γ) that are suitable for discriminating archaeological and non-archaeological classes (Hsu et al. 2003; Huang et al. 2002; Kavzoglu and Colkesen 2009). The optimization for the best combination of γ and C parameter values was performed using a 10-fold cross-validation and grid search. The grid search method tests different pairs of cost and gamma parameters and the one with the lowest cross-validation error is selected (Huang et al. 2008b; Lin et al. 2011). The optimisation of RBF parameters and classification were using e1071 and caret libraries of R statistical packages, respectively.

6.2.4.3 Reference data and accuracy assessment

Following a first visit to the confluence area in September 2015 with an archaeological expert who provided vital information on site locations and characteristics, fieldwork data collection was conducted in September 2016 with the purpose of acquiring ground reference points to classify the WorldView-2 image. Even though data collection was completed three years after

the image was captured, this will not have an effect on the classification results because the structure and chemical composition of the study material does not change within such a short period (Huffman et al., 2013). The period chosen for data collection also coincides with the spring season, which is the time when the image was acquired. The two visits revealed that the land is normally bare in the study area during the spring season, exposing surface archaeological remains. Moreover, most of the area chosen falls within a national park and world heritage site and a private game reserve. Changes in land use are minimal since the areas are protected against changes by legislation. The visits, therefore, confirmed that LULC changes did not occur and cannot have significant effects on the prediction model.

A purposive sampling method was used during the fieldwork data collection by visiting sites, which appear in the literature and have been dated to the period of interest. A global positioning system device (GPS) was used to navigate to these sites, whose coordinates were extracted from the site inventory constructed by Huffman (2009b, 2011). Although a variety of different remains characterise the farming communities' period in the Shashi-Limpopo confluence, the survey targeted only two archaeological classes: vitrified and non-vitrified dung deposits. Three additional LULC classes including bare land (natural soils), savannah woody vegetation, and irrigated agriculture (pivot agriculture) were extracted from the WorldView-2 data using collected ground reference points and were considered as variables during the image classification process. The natural vegetation in the study area was grouped into a single savannah woody vegetation class. The commercial farms were grouped into irrigated agriculture because of their pivot irrigation systems. This broad categorisation of the vegetation was deemed acceptable for the study that was aimed at distinguishing barren soil (archaeological and non-archaeological) from the surrounding vegetation classes and not at mapping different vegetation types in the area. For general LULC, we used our expert knowledge of the features in the study area to randomly select additional objects for each class through the visual inspection of a pan-sharpened version of the WV image. In total, 394 objects were chosen, of which 17 belonged to vitrified dung, 114 non-vitrified dung, 36 irrigated agriculture, 114 non-sites, and 114 Savannah woody vegetation.

The quality of thematic maps obtained from the RF and SVM classifiers was assessed using a holdout test dataset that was generated by randomly dividing the ground-referenced data for the study area into 70% and 30% for training and testing. The divisions mentioned above were done before classifying the data. This resulted in 117 polygons spread across the entire study area with different class sizes ranging between 5 and 34 polygons being chosen for validation.

This is because the polygons are the basic spatial units for the thematic maps created from the segments. This method was applied because it permits the assessment of the whole classification process, beginning with the segmentation. Some statistical analysis, which includes overall accuracy, user's accuracy and producer's accuracy, were then performed as a way of assessing the reliability of the maps generated for a site survey. The layout plans of archaeological sites drawn by Huffman (2004) and Calabrese (1997) were overlaid on the matching predicted sites in order to visually assess the accuracy of the above-mentioned classifiers in detecting site extent together with the distribution of archaeological and non-archaeological features within a site.

6.3 Results

6.3.1 Image segmentation

The optimum image segments were identified by varying the values for scale, colour and shape basing on trial and error approach. The results demonstrated that segmentation done using the scale, shape and colour parameters of 50, 0.2 and 0.8, respectively, produced accurate boundaries of geographic features (Figure 6. 2). The segmentation process produced 5189584 objects.

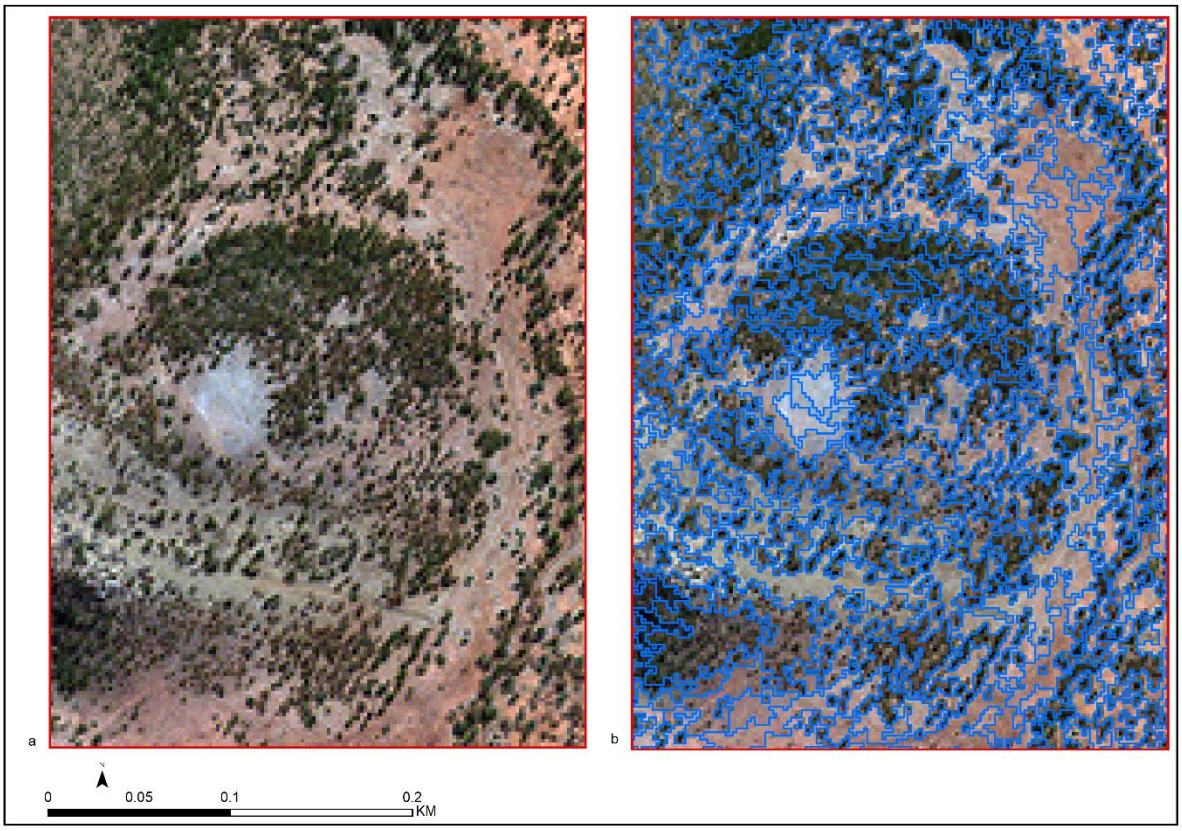

Figure 6. 2 Subsets of Worldview-2 image of the study area: (a) before segmentation, (b) after MRS segmentation at scale of 52. The greyish patch shown within the image is a non-vitrified dung site.

6.3.2 Tuning RF and SVM parameters

The RF algorithm parameters were optimized in predicting archaeological classes using a grid search procedure. The results have shown that a combination of the *mtry* value of 5 and *ntree* value of 500 produced the lowest OOB error rate of 0.059 (Figure 6. 3). The highest OOB error rates (0.072) were produced by combinations of *mtry* values of 9 and *ntree* values of 500 and 1500.

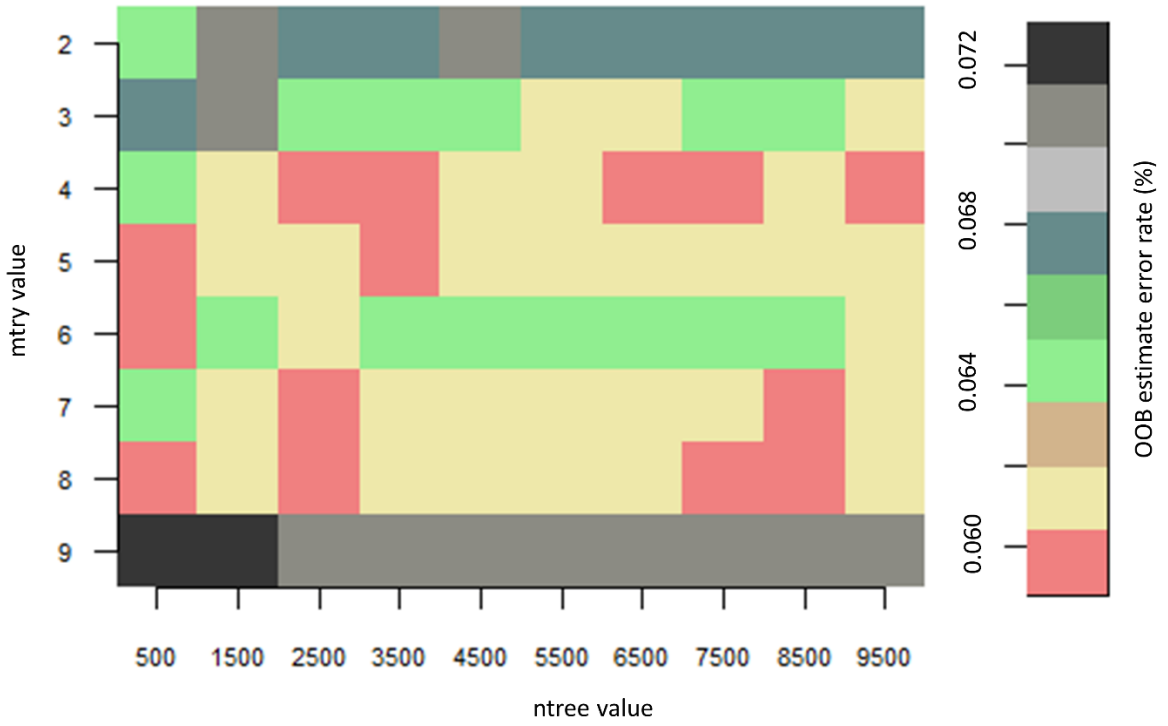

Figure 6. 3 OOB errors of RF parameters (*mtry* and *ntree*) optimised using grid search procedure.

The best-input parameters for classification using RBF in SVM were determined using 10-fold cross-validation and grid search. The optimisation results have demonstrated that the C $\left(\log_{10^{(100)}}\right)$ and γ ($\log_{10^{(0.01)}}$) are the best-input parameters for in predicting archaeological classes using RBF in SVM classifier (Figure 6. 4). The combination of the optimal C (100) and γ (0.01) produced the lowest cross validation error of 0.036. The highest cross validation error (0.8) was attained when C was set to $\log_{10^{(o.1)}}$ and γ was set to $\log_{10^{(1000)}}$ see Figure 6. 4.

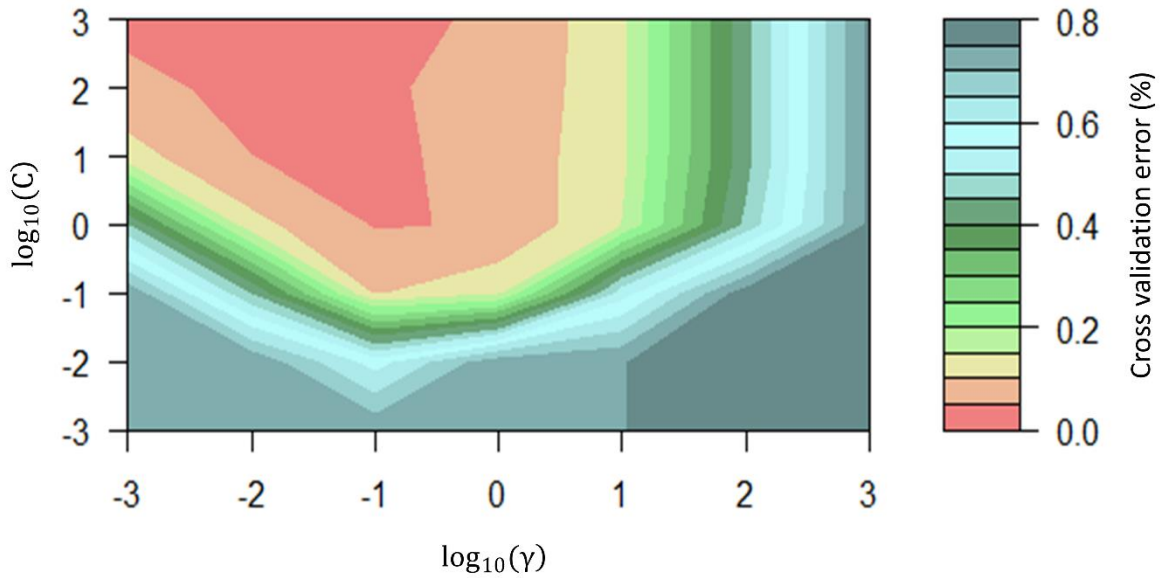

Figure 6. 4 Cross validation errors of SVM parameters (C and γ) optimised using grid search procedure. The cost and gamma values were varied between -1000 and 1000.

6.3.3 Image classification and site prediction

GEOBIA done using RF and SVM algorithms were able to classify non-sites, savannah woody vegetation, irrigated agriculture, vitrified dung and non-vitrified dung. Figure 6. 5 displays the image outputs of the aforementioned object-based classifications. Non-sites covers large parts of the study area followed by savannah woody vegetation, while other classes covers very small portions of the study area. A visual inspection of the predictive maps of RF and SVM shows that the two aforementioned classifiers have correctly predicted the locations of known archaeological sites (Figure 6. 5). However, there was a difference on how the two classifiers predicted the non-sites, savannah woody vegetation, irrigated agriculture, vitrified dung and non-vitrified dung sites across the study area (Figure 6. 5 and Table 6. 2). Non-sites on a map predicted by SVM (878 km^2) covered a large area when compared to the one predicted by RF (812.10 km^2). On the other hand, the map produced by RF (19.74 km^2) shows that non-vitrified dung covers large parts of the study area than the one on the map produced by SVM (13.28. km^2). The map predicted by RF shows that non-vitrified dung sites are widely spread in the northern parts of the study area when compared to the one produced by SVM.

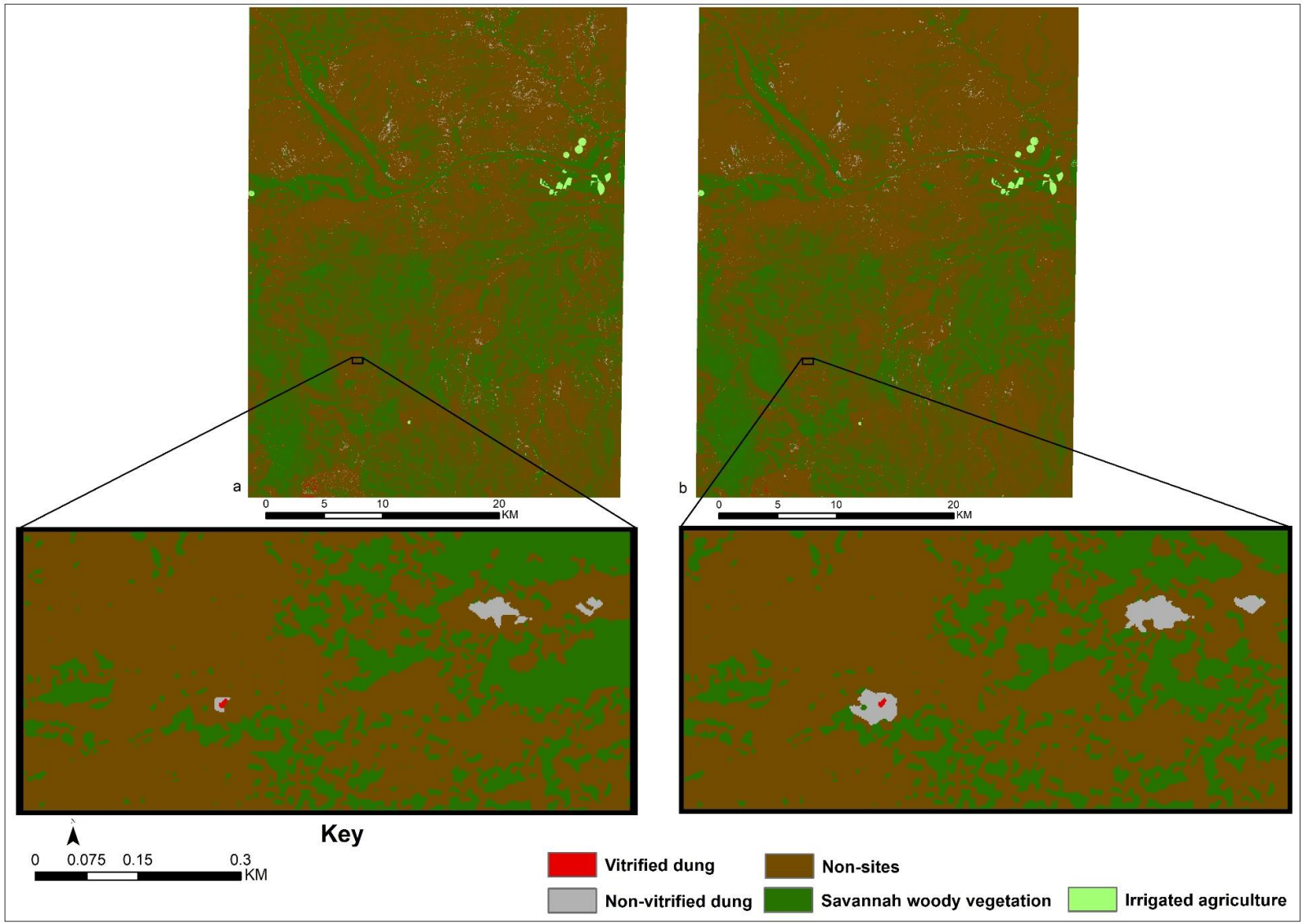

Figure 6. 5 Classification maps obtained using RF (a) and SVM (b) algorithm

Table 6. 2 Area (km^2) and the proportion of the study area covered by different LULC classes as predicted by RF and SVM classifier.

Class	RF		SVM	
	Area (km^2)	Area proportion (%)	Area (km^2)	Area proportion (%)
NS	812.10	59.20	878.88	64.07
NVD	19.74	1.44	13.28	0.97
IA	3.84	0.28	3.97	0.29
SWV	534.01	38.93	474.05	34.56
VD	2.14	0.16	1.64	0.12
Total	1371.83		1371.83	

6.3.4 Accuracy assessment

The accuracy assessment of the two classifiers was done using 195 holdout polygons created by partitioning reference data into training (70%) and validation (30%). In overall, SVM classifier achieved high classification accuracies than the RF (Table 6. 3 and Table 6. 4). SVM achieved an overall classification accuracy of 96.58% and a kappa coefficient of 0.9536 while the overall accuracy and kappa coefficient achieved by RF were 94.87% and 0.9305, respectively. With regard to the individual classes, a comparison between the two classifiers shows that the two classifiers, SVM and RF, achieved similar results for user's and producer's accuracies in most classes (Table 6. 3 and 6. 4). Table 6. 4 Vitrified dung achieved the lowest producer's and user's accuracies of 80% each in both RF and SVM classifiers. Irrigated agriculture and savannah woody vegetation achieved the highest user's and producer's accuracies of 100% each in both SVM and RF. Differences between the user's and producer's accuracies achieved by the two abovementioned classifiers were noted in the classification of non-vitrified dung and non-sites classes. Two non-vitrified dung sites were confused with other classes, one with vitrified dung and the other was confused with non-sites in RF. However, in SVM classification, the confusion occurred in only one non-vitrified dung site, which was confused with vitrified dung.

Table 6. 3 The confusion matrix showing overall accuracy and kappa coefficient for non-sites (NS), non-vitrified dung (NVD), irrigated agriculture (IA), savannah woody vegetation (SWV) and vitrified dung (VD) using SVM classifier

	NS	NVD	IA	SWV	VD	TOTAL	UA (%)
NS	32	0	0	0	0	32	100.00
NVD	2	33	0	0	1	36	91.67
IA	0	0	10	0	0	10	100.00
SWV	0	0	0	34	0	34	100.00
VD	0	1	0	0	4	5	80.00
TOTAL	34	34	10	34	5	117	
PA (%)	94.12	97.06	100.00	100.00	80.00		
OA	96.58%						
Kappa	0.9536						

Table 6. 4 The confusion matrix showing overall accuracy and kappa coefficient for non-sites (NS), non-vitrified dung (NVD), irrigated agriculture (IA), savannah woody vegetation (SWV) and vitrified dung (VD) using RF classifier

	NS	NVD	IA	SWV	VD	TOTAL	UA (%)
NS	31	1	0	0	0	32	96.88
NVD	3	32	0	0	1	36	88.89
IA	0	0	10	0	0	10	100.00
SWV	0	0	0	34	0	34	100.00
VD	0	1	0	0	4	5	80.00
TOTAL	34	34	10	34	5	117	
PA (%)	91.18	94.12	100.00	100.00	80.00		
OA	94.87%						
Kappa	0.9305						

The outlines of sites mapped were also used to assess the accuracy of the RF and SVM models in predicting the vitrified dung and non-vitrified dung deposits. The sites, which are in possible flat surfaces, are similar to those predicted by the abovementioned models in size Figure 6. 7. However, the sizes of sites predicted by the RF and SVM models in places which are potentially vulnerable to erosion are covering large area extent than the plans drawn by both Huffman (2004) and Calabrese (1997). Generally, the SVM model picked large extents of non-vitrified dung than RF model in most sites (Figure 6. 6 and Figure 6. 7). Additionally, some of the byres mapped by Calabrese (1997) were not detected by the SVM and RF models (Figure 6. 7). The

two abovementioned models also classified other archaeological features such as middens, grain bin and dagga as non-sites.

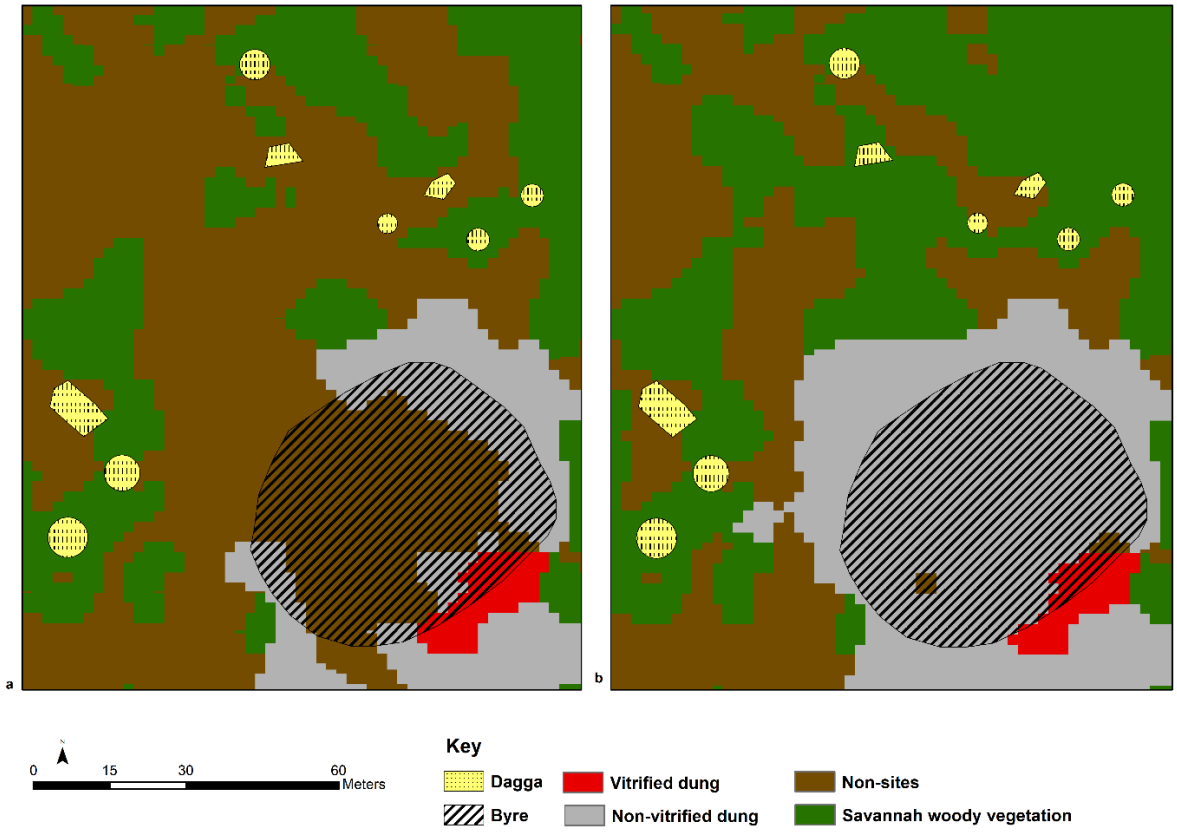

Figure 6. 6 Plan of site AA 14B overlaid on both RF (a) and SVM (b) classified images. Dagga and byre were digitised from a site plan drawn by Huffman (2004).

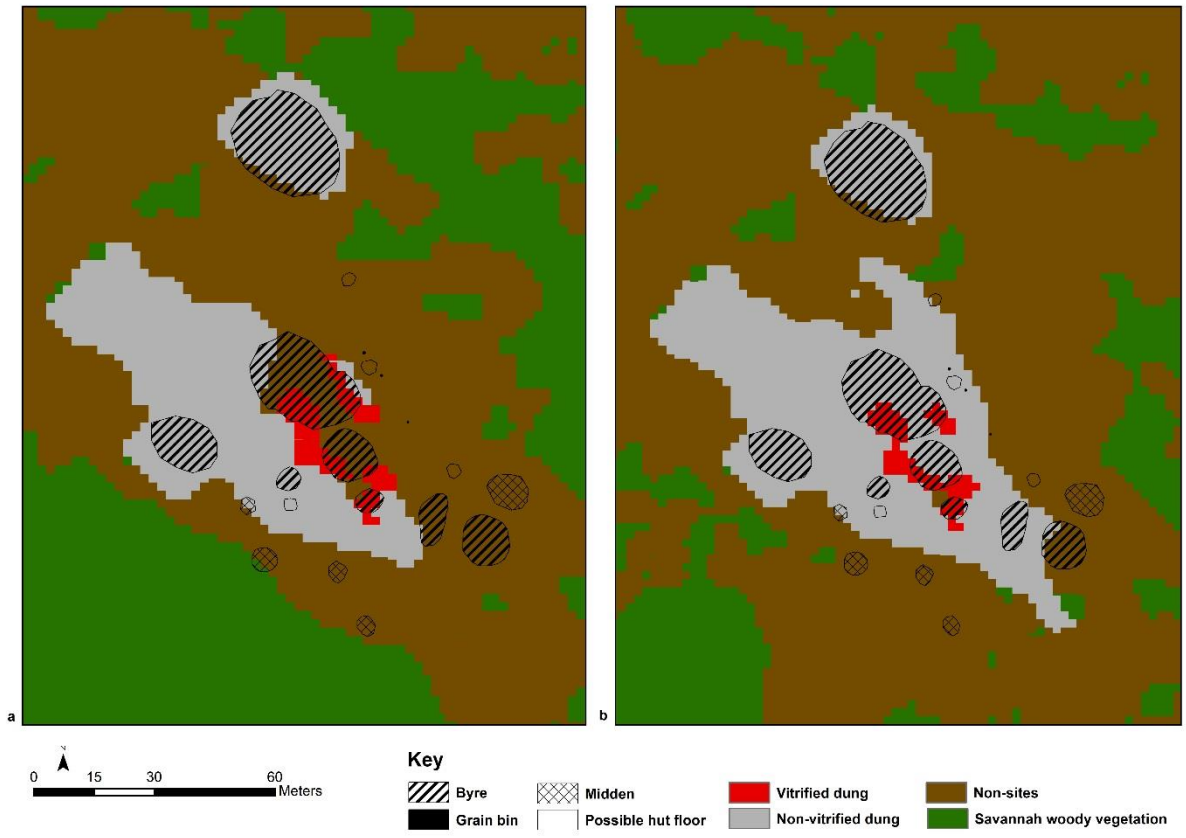

Figure 6. 7 A plan of site AD4 overlaid on both RF (a) and SVM (b) classified images. Byre, midden, grain bin and possible hut floor were digitised from a site plan drawn Calabrese (1997).

6.4 Discussion

The prospection and monitoring of archaeological sites using remote sensing techniques based on the differences in the spectral signatures of archaeological features and their surroundings is widely becoming a common practice (Biagetti et al. 2017; Lasaponara et al. 2014; Lasaponara and Masini 2006; Parcak 2007). Even though high classification accuracies have been achieved, some challenges in relation to subtle spectral differences between archaeological features and their surroundings have been reported (Corrie 2011; Thabeng et al. 2019). Areas characterised by archaeological features which were constructed using local materials or are covered with tracts of eroded archaeological material normally share spectral signatures with archaeological features in their locality (Corrie 2011; De Laet et al. 2007). The aforementioned challenge becomes a major limitation when using methods such as pixel-based techniques because they depend solely on spectral signatures to classify remote sensing data (Beck et al. 2007; De Laet et al. 2007). As a consequence, limiting the prospection and monitoring of archaeological sites using remote sensing techniques to areas with detectable spectral differences between archaeological features and non-archaeological features (Beck et

al. 2007; De Laet et al. 2007). The solution thus lies in using the classification methods which can integrate the spatial and spectral data in the classification process (Beck et al. 2007; Myint et al. 2011; Pu et al. 2011; Whiteside et al. 2011). Hence, the main intention of this study was to assess the possibility of discriminating non-vitrified dung, vitrified dung and non-sites using their spatial and spectral data as input variables in GEOBIA models based on advanced classification algorithms (RF and SVM). Furthermore, the classification outcomes of this study were assessed using confusion matrices and visual inspection.

Results of this study have shown that GEOBIA based on SVM and RF classifiers have the ability to differentiate archaeological and non-archaeological features even in the environments where there are different features with spectral homogeneity. The aforementioned success in the classification attained using GEOBIA can mainly be credited to its utilisation of spatial attributes to compensate for spectral homogeneity of various features (Whiteside et al. 2011). The high spatial resolution of the WorldView-2 images used in this study clearly defined the area covered by each site, thus facilitating the incorporation of the area extent of the individual image objects into classification models. The image objects depicting non-sites were generally larger than those depicting the vitrified dung sites. This enabled the classification models to discriminate vitrified dung from non-sites especially along the river where there was spectral confusion (Thabeng et al. 2019). Our findings concur with those of Hu et al. (2013) who successfully incorporated area as a spatial attribute to differentiate spectrally homogenous but spatially different features such as rivers and lakes. Despite the findings by the previous studies (Alexakis et al. 2009), the results of this study prove that GEOBIA based classifications can be successful in archaeological applications when site spatial characteristics other than shape are used as input variables in the model. This is because, the outlines of most sites are deformed by post-depositional processes (Alexakis et al. 2009; De Laet et al. 2007).

The accuracy assessment of the GEOBIA based RF and SVM classifiers have shown that they both achieved high overall classification accuracies and kappa coefficients. This is consistent with other studies (Li et al. 2016; Reyes et al. 2017; Vogels et al. 2017; Wahidin et al. 2015) which attained high classification accuracies when using GEOBIA based on SVM and RF classification algorithms to delineate features in complex landscapes. In this study, SVM outclassed RF in user's and producer's accuracies of non-vitrified dung, savannah woody vegetation, non-sites and irrigated agriculture (Table 6. 3 and Table 6. *4*). In general, this was a great improvement from the results of pixel-based SVM classification done by Thabeng et al. (2019) where RF was showing better overall performances than SVM. In contrast, the

performance of RF generally decreased in GEOBIA when compared to that of the pixel-based approach (Thabeng et al. 2019). Our results for this study support those of Kavzoglu et al. (2015) who found out that SVM outperforms RF in GEOBIA models.

Furthermore, when overlaid on the layouts of the sites, the results of the RF and SVM models showed differences in the prediction of the extent of individual archaeological sites (Figure 6. 6 and Figure 6. 7). SVM classifier detected areas possibly covered with thin layers of eroded materials from non-vitrified dung deposits while RF only picked thick deposits of the aforementioned material. As a result, the sizes of the sites predicted by the RF and SVM models are not a true representative of their original extent (Calabrese 1997; Huffman et al. 2004). However, the aforementioned differences in the accuracies of the RF and SVM models can complementarily be used to survey for archaeological sites as suggested by Thabeng et al. (2019). Generally, the visual inspection of the classifications produced by both RF and SVM models have shown that non-vitrified dung covers large areas and it always surrounds the deposits of vitrified dung. This supports the findings of Huffman (2013) who posits that not all dung vitrifies during the vitrification process. Moreover, some of the byres mapped by Calabrese (1997) were not detected by the models possibly because all of their materials have been eroded away. This is in line with the findings of Calabrese (1997) who posits that the majority of the sites are in danger of being extinct because of the erosion which is rampant in the area. Other archaeological features which the models could not detect include the middens, possibly because they had been eroded away.

A visual inspection of the classification results also shows that the two maps depict a moderately accurate representation of the land use land cover classes of interest within the study area. In general, both classifiers accurately predicted the archaeological sites characterised by non-vitrified dung and vitrified dung. However, there are differences in the classification accuracies of the RF and SVM classifiers especially on the prediction of non-vitrified dung deposits in the northern part of the study area. The non-vitrified dung class appears to be well represented by the SVM classifier in GEOBIA. For example, SVM depicts less confusion between non-vitrified dung and non-sites in the northern part of the study area (Figure 6. 5). The fact that GEOBIA reduces within class spectral heterogeneity by using means of spectral values of an object in classification might have contributed to the improvement of SVM classification accuracies in this study. The aforementioned assertion is in agreement with the findings from Maxwell (2015) that the classification accuracies of SVM improve when mean spectral values are used in the classification process. Overall, GEOBIA achieved better

classification accuracies than pixel-based classification when predicting vitrified dung, non-vitrified dung and non-sites in the SLCA (Thabeng et al. 2019). Our findings are similar to those of Myint et al. (2011) who found out that GEOBIA performs better than pixel-based classification. The success of the method presented in this study will help researchers and heritage managers to expand the use of remote sensing techniques into areas where there are subtle spectral differences between archaeological features and their surroundings. In addition, the use of remote sensing will also help the researchers and heritage managers to survey and monitor archaeological sites over large and inaccessible areas over a short period of time (Biagetti et al. 2017; Hadjimitsis et al. 2009; Lasaponara et al. 2014; Parcak 2007). We acknowledge that this study had some limitations which resulted in the confusion between classes, more especially non-vitrified dung and non-sites in the northern part of the study area. The aforementioned limitations can be attributed to the inability of the sensor to capture data in the near-infrared regions, which are sensitive to soil chromophores. A possible solution the above problem is the fusion of data from high spectral resolution and high spatial resolution sensors.

6.5 Conclusion

The outcomes of this study have shown that GEOBIA based on RF and SVM classifiers accurately discriminates between archaeological and non-archaeological deposits, in the SLCA area of South Africa. In fact GEOBIA managed the spectral confusion between archaeological and non-archaeological features such as vitrified dung deposits and non-sites, important for identifying archaeological sites previously occupied by farming communities, by combining their spatial and spectral attributes in the classification process. Even though SVM generally outperformed RF, both classifiers attained high prediction accuracies. This, therefore, means that both classifiers should be considered as reliable predictors of archaeological sites characterised by vitrified dung and non-vitrified dung deposits. In summary, this study has shown that GEOBIA method can be used to map surface archaeological features especially those with similar spectral characteristics to other objects in their surroundings, which is a common problem with the use of remote sensing in archaeology.

The mapping of archaeological features which have similar spectral properties with their surroundings using GEOBIA method will help researchers and heritage managers to expand archaeological remote sensing survey to areas where it was impossible before. Additionally, the use of remote sensing applications will help researchers and heritage resources managers to carry out fast, cheap and systematic regional archaeological site surveys and monitoring

more especially when taking into account the challenges and risks one has to face when carrying out foot surveys in certain areas of the world.

Acknowledgements

We thank the University of Botswana for the support in carrying out this research, SANParks for allowing access to Mapungubwe National Park and the DeBeers Group (through Duncan MacFadyen) for allowing access to the Venetia Nature Reserve and use the research facility. We are also thankful to the DigitalGlobe Foundation for making this research successful by providing WorldView-2 images for the study area. The foundation promotes the use of geospatial data by providing image grants, information and expertise to individuals at university-level academic institutions. The authors are also grateful to Prof. Thomas Huffman for making his data available and devoting his time by taking us through the study area, Lesego Madisha (former archaeologist at SANParks, Mapungubwe) for her kind assistance, South African National Parks Cultural Heritage Manager Crispen Chauke and the Venetia Nature Reserve staff for their help.

Funding Organisations

The University of Botswana training department and Digital Globe Foundation funded this research.

Conflict of interest

Authors declare no conflict of interest.

CHAPTER SEVEN

7 Synthesis, General conclusions and recommendations

7.1 Introduction

Surveying and documenting archaeological sites is one of the major challenges faced by heritage managers and archaeological researchers, especially in the African continent, where lack of funding and trained personnel often lead to inadequate survey and research at local and regional scales (Lavachery et al. 2005; Mabulla 2001; MacEachern 2001; Mcintosh 1993) (Connah 2008; Mcintosh 1993). However, remote sensing projects exist in the continent but they are mostly aimed at image enhancement, visualisation and direct digitisation of sites visible to the naked eye. As a result research in Africa is skewed towards more prominent archaeological sites, therefore, giving a partial account of the archaeological record in the continent (Breen 2007; Chirikure et al. 2016; Connah 2008; Huffman 1998, 2007a; Kankpeyeng and DeCorse 2004; Lavachery et al. 2005; Mitchell and Lane 2013; Mothulatshipi 2008). Moreover, there is high loss of archaeological information across the continent as more archaeological sites are being destroyed during conflicts, developments and by natural causes. As a consequence, there is an urgent need to expand survey and investigations to other sites in order to balance the research and knowledge of archaeological record in the continent, where the vast majority of the archaeological traces are not monumental nor always well preserved, as highlighted in chapter 2. This is because unbalanced research can lead to gaps and misinterpretations of archaeological record, which gives us an account of the past civilisations, cultures and their evolution to the contemporary. Hence, the need to develop a system which can enable cost-effective systematic regional survey and documentation of archaeological site characteristics including those which may be difficult to detect on the ground using field-based methods.

More recently, remote sensing has offered a relatively cheap, systematic and reproducible method of survey, which can be used to document, monitor and get a synoptic view of archaeological settlement patterns at regional scales. Furthermore, it also provides non-destructive and non-invasive ways of collecting archaeological data which helps to preserve archaeological heritage sites for future generations. Several studies have shown that different hyperspectral (finely defined spectral channels) and multispectral (broad spectral channels) sensors can be used in archaeological applications (Agapiou et al. 2012a; Lasaponara and Masini 2006; Parcak et al. 2016; Reid 2016). For example, Casana and Laigier (2017) used multispectral data to monitor the magnitude of damage of archaeological sites in Syria and northern Iraq during Syrian civil war. The main limitation of using remote sensing data in archaeological applications is that spectral signatures of archaeological features are local in

nature. Hence, in addition to optimum environmental conditions, there is a need to investigate the potential of applying remote sensing techniques in a particular archaeological context and identify a sensor with an optimum spectral resolution for discriminating against archaeological features of interest.

The objectives of this research were as follows:

- To give a comprehensive overview of historic and current trends on the applications of remote sensing in African archaeology from a perspective of three themes which are research publication details, data capturing and processing, and the footprint of remote sensing applications across the continent.
- To discriminate archaeological ash middens, vitrified dung, non-vitrified dung and natural soils (non-sites) associated with archaeological sited previously occupied by farming communities using field spectra measurements and chemical characteristics.
- To identify the optimum spectral resolution for the identification of archaeological ash middens, non-vitrified dung and vitrified dung sites using in situ hyperspectral data resampled to different spectral resolution remote sensing multispectral platforms
- To test the performance of pixel-based advanced machine learning classifiers (random forest and support vector machines) in archaeological applications and the feasibility of directly detecting archaeological sites characterised by vitrified dung and non-vitrified dung through the use of high spatial resolution satellite images.
- To further investigate the performance of other image classification techniques especially geographic object-based image analysis based on advance machine learning classifiers in mapping archaeological sites characterised by vitrified dung and non-vitrified dung through the use of high spatial resolution satellite images.

7.2 Summary of findings

A concise summary of the findings for each objective in this study is provided below.

7.2.1 Review the literature on the use of remote sensing in archaeology

Remote sensing offers a cost-effective, systematic and reproducible way of surveying, documenting and monitoring archaeological heritage sites over restricted areas (Biagetti et al. 2017; Corrie 2011; Parcak 2007). Additionally, remote sensing techniques are non-invasive and have the ability to gather a lot of data over large areas within a short period. As a result there has been a wide interest in the applications of remote sensing techniques in archaeology leading to publications of books (Lasaponara and Masini 2012; Parcak 2009), special issues in research journals (Lasaponara and Masini 2011; Tapete 2018) and some research articles (Clark et al. 1998; Corrie 2011; Mondino et al. 2012; Parcak 2007; Reid 2016). This study conducted a review of the published literature concerning the applications of remote sensing techniques in archaeological within the African context (Chapter 2). Its objectives were to establish: i) the remote sensing methods that have been used in archaeological applications across the continent ii), the distribution of remote sensing in archaeology across the African continent and, iii) the location of institutions that the lead authors are affiliated to and the locations of funding institutions.

The findings of this study have shown that archaeological researchers and heritage managers in the continent have used a wide variety of remote sensing data from groundborne, airborne and spaceborne sensors for archaeological applications in the continent. The majority of studies exploited data from the multispectral images from sensors aboard satellite platforms for archaeological applications, especially in mapping surface archaeological features. On the other hand, radar satellite images and geophysical survey techniques have been used to map sub-surface archaeological features. However, the use of remote sensing in the continent is sporadic and restricted to few archaeological contexts especially those characterised by open environments, such as deserts and grasslands, which allow easy detection of surface features with minimal vegetation interference. Hence, the need to expand the use of remote sensing to a wide variety of archaeological site contexts and regions in the African continent in order to enhance site survey, documentation and monitoring.

7.2.2 Spectral discrimination of archaeological ash middens, vitrified dung, non-vitrified dung and natural soils (non-sites)

Remote sensing is an evolving method of survey in archaeology, which is used to identify various features based on their spectral contrast with the surrounding environment. However, the spectral signatures of archaeological features varies depending on their context. Thus, there is a number of ongoing researches which are aimed at investigating the possibility of detecting different archaeological features under various contexts using remote sensing techniques. This study investigated whether field spectra measurement can discriminate amongst archaeological sites using soil properties as indicators and identify the important bands for doing so (Chapter 3). To achieve the above-mentioned goal, two approaches of data analysis were used to discriminate amongst non-sites, middens, vitrified dung and non-vitrified dung sites, in this study. In the first approach, the difference in the concertation of elements between different soil types was tested using analysis of variance while random forest and FVS were used to select important soil elements for the classification of the archaeological sites. In the second approach, the ability of field spectroscopy reflectance measurements to discriminate among non-sites, middens, vitrified dung and non-vitrified dung byres was evaluated. The guided regularised random forest was used to identify important wavelengths for discrimination. The selected soil elements and wavelengths were then used as input variables in random forest classifier to discriminate among the above-mentioned soils.

The findings indicate that there is a significant difference in the composition of elements across non-sites, middens, vitrified and non-vitrified dung. P, Ca, Sr, Mg, Fe, Zn and Co were selected by FVS based on RF algorithm as the important elements for discriminating the archaeological sites. The wavelengths with spectral difference deemed important for discriminating between the aforementioned classes were identified in the vis-near-infrared and short wave infrared regions of the electromagnetic spectrum. GRRF identified 549 nm, 624nm, 996 nm, 1026nm, 1665nm, 1774nm, 1934nm and 2290nm as important wavelengths for discriminating non-sites, middens, vitrified and non-vitrified dung. The selected wavelengths are in line with the spectral regions sensitive to the above-mentioned elements, which showed a significant difference in their concentration between the archaeological classes of interest in this study (Bogrekci and Lee 2005b; a; Thomasson et al. 2001). This, therefore, shows that the difference in the chemical composition of various archaeological materials has an influence in their spectral signatures. High classification accuracies of 84.62% and 87.62% were achieved when using the selected optimal chemical elements and spectral bands, respectively, as input variables in RF. The high

classification accuracies achieved when using field spectroscopy data proves the potential of remote sensing techniques in detecting and mapping archaeological features with distinct soil physical and chemical characteristics such as the ones used in this study is present.

7.2.3 The optimum spectral resolution for the identification of archaeological ash middens, non-vitrified dung and vitrified dung sites using in situ hyperspectral data resampled to different spectral resolution remote sensing multispectral platforms

The use of remote sensing in archaeology is now widespread and has allowed reaserchers and heritage managers to monitor the status of archaeological sites (Lasaponara et al. 2014; Parcak et al. 2016; Van Ess et al. 2006) and improve archaeological records by surveying inaccessible areas (Biagetti et al. 2017). However, the application of remote sensing in archaeological contexts depends largely on the spatial and spectral resolution of the sensor used to capture the dataset (Aqdus et al. 2008; Beck 2007; Lasaponara and Masini 2006). Hence the need to identify a sensor with abilities to detect archaeological features of interest. This study, therefore, evaluated the possibility of discriminating non-sites, middens, vitrified and non-vitrified dung using hyperspectral data resampled to the spectral resolutions of common satellite sensors (GeoEye, Landsat 8 OLI, RapidEye, Sentinel 2, SPOT 5 and WorldView-2) and advanced classification algorithms (SVM and RF) (Chapter 4). To identify satellite sensor with a spectral resolution that is suitable for discriminating middens, vitrified dung and non-vitrified dung, the importance of each satellite band in the classification process was also assessed using MDA in the RF model. The results of this study have shown that satellite sensors with a medium spatial resolution such as Landsat 8 OLI, Sentinel-2 and SPOT 5 possess spectral bands within the visible and SWIR, which are most suitable for discriminating the above-mentioned features. The advanced classification algorithms (RF and SVM) achieved varying classification accuracies for hyperspectral data resampled to the spectral resolutions of similar sensors. For example, classification accuracies of 92.38% and 81.90% were achieved when classifying hyperspectral data resampled to the spectral resolution of Sentinel-2 using SVM and RF classifiers, respectively. RF achieved lower prediction accuracies than SVM in all prediction models constructed using hyperspectral data resampled to different common multispectral sensors. Generally, high classification accuracies achieved using hyperspectral data resampled to the spectral resolutions of different multispectral satellite sensors show their potential in discriminating non-sites, middens, vitrified and non-vitrified dung. This is in line with other studies which have demonstrated the potential of multispectral sensors in archaeological applications (Lasaponara and Masini 2005; Parcak et al. 2016; Reid 2016).

7.2.4 Satellite remote sensing of archaeological non-vitrified dung and vitrified dung sites and the performance of pixel-based advanced machine learning classifiers (random forest and support vector machines) in archaeological applications

The use of remote sensing in archaeology conventionally relied on the use of aerial photographs because of their high spatial resolution when compared to that of early multispectral satellites (Lasaponara and Masini 2007). This restricted the application of remote sensing in archaeology because of the limited spectral abilities of the aerial photographs (Aqdus et al. 2008). However, the advent of new very high-resolution satellite sensors such as WorldView-2, QuickBird and Ikonos with the improved spatial and spectral capabilities, and the use of advanced classification algorithms offer the potential to broaden the use of remote sensing in archaeology and attain the high accuracies. This study investigated the possibility of detecting surface archaeological materials using WorldView-2, the importance of the new WorldView-2 bands in detecting archaeological features and the ability of pixel-based advanced classification algorithms in predicting the aforementioned sites (Chapter 5). The findings of this study have demonstrated that WorldView-2 images can be used to detect surface archaeological sites. However, the new spectral bands in the WorldView-2 were found to be of relatively less importance in discriminating non-sites, vitrified and non-vitrified dung, when compared to traditional bands. High classification accuracies achieved for SVM (88.82%) and RF (95.29%) using holdout test samples proved the ability of advanced classification algorithms to predict archaeological classes on very high-resolution satellite images. Additionally, validation carried out using independent dataset also achieved high classification accuracies for RF (97.71%) and SVM (95.88%). However, even though high classification accuracies were achieved using the above-mentioned pixel-based classification algorithms, there was spectral confusion between vitrified dung and river sand.

7.2.5 Improving classification accuracies of vitrified dung, non-vitrified dung and natural soils (non-sites) using geographic object-based image analysis based on random forest and support vector machines classifiers.

Feature prediction on the imagery can be done using pixel-based classification methods or GEOBIA approaches (Myint et al. 2011). Traditionally, the application of remote sensing in archaeology has been centred on the pixel-based analysis of the spectral contrast between archaeological materials and their surroundings (Corrie 2011; Wilkinson et al. 2006). Consequently, spectral confusion between two or more different features has been one of the major problems in the application of pixel-based remote sensing techniques in archaeology

(Corrie 2011; Thabeng et al. 2019). This is because the majority of commonly used pixel-based methods depend on spectral heterogeneity to separate data into different classes. On the other hand, studies have shown that GEOBIA manages spectral confusion by combining texture, spectral, contextual and spatial attributes in classification (Pu et al. 2011; Whiteside et al. 2011). In this study, the possibility of improving classification accuracies by combining spectral and spatial attributes of features is shown (Chapter six). To achieve its objective, this study used GEOBIA based on advanced classification algorithms (RF and SVM) to group objects into different classes using a combination of their area extent and spectral properties. The outcomes of this study have shown that the use of GEOBIA based on RF and SVM classifiers improved classification accuracies of both vitrified dung and non-vitrified dung sites. Overall classification accuracies of 94.87% and 96.58% were attained for RF and SVM, respectively. Even though there was a small decrease on the classification accuracy of RF on GEOBIA (94.87%) when compared to the one using pixel-based approach (95.29%), visual inspection of the image proved that both classifiers successfully differentiated vitrified dung from river sand. Our results support those of Myint (2011) who found out that GEOBIA performs better than pixel-based classification methods. This, therefore, means that GEOBIA approaches can be used to predict archaeological sites especially in complex landscapes where there is a lot of spectral confusion between archaeological features and their surroundings.

7.3 Conclusions

The aim of this project was to investigate the potential of remote sensing techniques in mapping archaeological features characteristic of farming community sites in the SLCA. The outcomes of this study have shown that remote sensing techniques can be used to discriminate middens, vitrified dung, non-vitrified dung and non-sites. The following conclusions can be made based on the main findings made in line with the objectives of this study:

1. Different studies have explored data from a wide variety of groundborne, airborne and spaceborne sensors under different archaeological contexts in the African continent and obtained positive results. The positive results achieved by studies using remote sensing techniques in African archaeology demonstrate that there is a potential for its application in African contexts. However, despite the potential for the application of remote sensing techniques in African archaeology, their use across the continent is sporadic. The majority of studies which used remote sensing techniques in the continent, mapped sites in open environments especially tell sites located in the Egyptian deserts.

2. There are differences in the chemical and physical properties of middens, vitrified, non-vitrified dung byres and natural soils, which makes it possible for field spectroscopy to discriminate among them. Wavelengths within visible-near infrared spectrum and elements such as P, Ca, Sr, Mg, Fe, Zn and Co can be used to discriminate among natural soils, middens, vitrified dung and non-vitrified dung byres when used as input variables in a classification model. This outcome triggered the desire to test the possibility of detecting different archaeological and non-archaeological sites using relatively cheap data acquired by lower spectral resolution spaceborne sensors.

3. The field spectrometry data resampled to the spectral resolutions of different multispectral satellite sensors have demonstrated that they spectral ability to discriminate non-sites, ash middens, non-vitrified dung and vitrified dung sites using bands in the visible portion of the electromagnetic spectrum. Additionally, Sentinel-2, Landsat 8 OLI and SPOT 5 possess spectral bands in SWIR, which are important for detecting the aforementioned features. As a result, the outcome points to the possibility of upscaling field measurements to satellite data for mapping and monitoring archaeological sites characterised by middens, vitrified dung and non-vitrified dung within their wider landscape.

4. Advanced pixel-based classification algorithms (RF and SVM) achieved high prediction accuracies when classifying sites characterised by non-sites, vitrified dung, and non-vitrified dung. The results of this study show that archaeological sites characterised abovementioned classes can be directly detected through the use of new high spatial resolution satellite images. Moreover, the study has shown that the new spectral bands in WorldView-2 are not important in discriminating non-sites, vitrified dung, and non-vitrified dung.

5. The integration of spectral data and spatial attributes of objects in GEOBIA based on SVM and RF advanced classification algorithms have the ability to accurately detect archaeological and non-archaeological materials. Furthermore, the findings of this study have shown that the spectral confusion between vitrified dung sites and non-sites observed on pixel-based classification can be removed by integrating area extent of features as part of input variables into the classification model. As a result, this will help the archaeologist to expand the use of remote sensing data into the areas where there is spectral confusion between archaeological sites and non-sites.

In summary, this study developed a relatively fast, cost-effective model for surveying, documentation, and monitoring of archaeological sites over large and inaccessible areas. The model will help researchers and heritage managers, especially those working with limited funding, to repetitively carry out fast systematic regional archaeological surveys, site monitoring and in-depth research based on spatial analysis. In fact the small scale view of archaeological landscapes provided by the model help in understanding regional settlement patterns. As a consequence, the approach used here, not only has been successful but has the potential to advance archaeological heritage management, improve the knowledge of archaeological record in the continent and give new perspectives of archaeological landscapes.

Some of the major limitations which were encountered while carrying out this study include:

1. The uncertainty in the detection of sites caused by post-depositional processes such as water and wind erosion which transport archaeological materials from their in-situ location to other areas thus causing confusion to site prediction models.
2. Very high spatial resolutions sensors aboard satellite platforms have limited spectral ability to differentiate archaeological features with subtle spectral differences from their environment such as non-sites and non-vitrified dung sites as established in this study.

The of the abovementioned limitations is clearly indicates that even though there are improvements in the development of remote sensing techniques their application in archaeological contexts is still limited.

7.4 Recommendations

This study recommends the following approaches for future research:

1. The present study has shown that very high spatial resolution satellite sensors have the ability to detect surface archaeological deposits. However, images from very high spatial resolution satellites sensors are expensive to be acquired by heritage management institutions especially those in developing countries. As a result, there is a need to evaluate the performance of open source and medium spatial resolution satellites such as Sentinel-2 for use in detecting archaeological material, in order to curb the cost hindrance associated with data very high spatial resolution satellites sensors as discussed above.
2. Furthermore, research should also investigate the possibility of fusing data from high spatial resolution satellite sensors such as WorldView-2 and GeoEye with that

from high spectral sensors such as Sentinel-2 and Landsat 8 OLI in order to deal with spectral confusion between soils and the vitrified dung and non-vitrified dung deposits. This will enable the researchers to compensate for low spatial resolutions in the above-mentioned high spectral resolution satellite sensors, which have been found to possess the spectral resolution suitable for separating the archaeological deposits of interest in this study. This will improve the classification accuracies of the models because it will reduce the spectral confusion between materials including soil and archaeological deposits of vitrified dung and non-vitrified dung, which is common in low spectral resolution satellite data.

3. There is limited used of advanced classification algorithms including RF and SVM in remote sensing applications in archaeology. Hence, it is recommended that the classification models used in this study should be tested in other areas characterised by surface archaeological features such as middens, vitrified dung and non-vitrified dung deposits in order to affirm their reliability in site prediction. Successful results will help with fast and cost-effective documentation and monitoring of archaeological sites over large and inaccessible areas by researchers and heritage managers.
4. The major limitation of this study is the inability to differentiate recent and contemporary byres from the archaeological ones. As a result, a study that will collect the spectra of historical byres and analyses it in relation to that of archaeological ones is recommended.

References

Abdel-Rahman, E. M., Ahmed, F. B., and Ismail, R. (2013), "Random forest regression and spectral band selection for estimating sugarcane leaf nitrogen concentration using EO-1 Hyperion hyperspectral data," *International Journal of Remote Sensing*, 34, 712–728.

Abdel-Rahman, E. M., Makori, D. M., Landmann, T., Piiroinen, R., Gasim, S., Pellikka, P., and Raina, S. K. (2015), "The utility of AISA eagle hyperspectral data and random forest classifier for flower mapping," *Remote Sensing*, 7, 13298–13318.

Abdel-Rahman, E. M., Mutanga, O., Adam, E., and Ismail, R. (2014), "Detecting Sirex noctilio grey-attacked and lightning-struck pine trees using airborne hyperspectral data, random forest and support vector machines classifiers," *ISPRS Journal of Photogrammetry and Remote Sensing*, 88, 48–59.

Adam, E., Deng, H., Odindi, J., Abdel-Rahman, E. M., and Mutanga, O. (2017), "Detecting the Early Stage of Phaeosphaeria Leaf Spot Infestations in Maize Crop Using In Situ Hyperspectral Data and Guided Regularized Random Forest Algorithm," *Journal of Spectroscopy*, 2017.

Adam, E., Mutanga, O., and Ismail, R. (2013), "Determining the susceptibility of Eucalyptus nitens forests to Coryphodema tristis (cossid moth) occurrence in Mpumalanga, South Africa," *International Journal of Geographical Information Science*, 27, 1924–1938.

Adam, E., Mutanga, O., Odindi, J., and Abdel-Rahman, E. M. (2014), "Land-use/cover classification in a heterogeneous coastal landscape using RapidEye imagery: evaluating the performance of random forest and support vector machines classifiers," *International Journal of Remote Sensing*, 35, 3440–3458.

Adam, E., Mutanga, O., Rugege, D., and Ismail, R. (2009), "Field spectrometry of papyrus vegetation (Cyperus papyrus L.) in swamp wetlands of St Lucia, South Africa," IEEE, pp. IV-260-IV–263.

Adam, E., Mutanga, O., Rugege, D., and Ismail, R. (2012), "Discriminating the papyrus vegetation (Cyperus papyrus L.) and its co-existent species using random forest and hyperspectral data resampled to HYMAP," *International Journal of Remote Sensing*, 33, 552–569.

Agapiou, A., Alexakis, D. D., and Hadjimitsis, D. G. (2014a), "Spectral sensitivity of ALOS, ASTER, IKONOS, LANDSAT and SPOT satellite imagery intended for the detection of archaeological crop marks," *International Journal of Digital Earth*, 7, 351–372.

Agapiou, A., Alexakis, D. D., Lysandrou, V., Sarris, A., Cuca, B., Themistocleous, K., and Hadjimitsis, D. G. (2015), "Impact of urban sprawl to cultural heritage monuments: The case study of Paphos area in Cyprus," *Journal of Cultural Heritage*, 16, 671–680.

Agapiou, A., Alexakis, D. D., Sarris, A., and Hadjimitsis, D. G. (2014b), "Evaluating the potentials of Sentinel-2 for archaeological perspective," *Remote Sensing*, 6, 2176–2194.

Agapiou, A., Alexakis, D. D., Stavrou, M., Sarris, A., Themistocleous, K., and Hadjimitsis, D. G. (2013), "Prospects and limitations of vegetation indices in archaeological research: the Neolithic Thessaly case study," in *SPIE 8893*, eds. U. Michel, D. L. Civco, K. Schulz, M. Ehlers, and K. G. Nikolakopoulos, Dresden, Germany, p. 88930D. https://doi.org/10.1117/12.2028661.

Agapiou, A., and Hadjimitsis, D. G. (2011), "Vegetation indices and field spectroradiometric measurements for validation of buried architectural remains: verification under area surveyed with geophysical campaigns," *Journal of Applied Remote Sensing*, 5, 1–15. https://doi.org/10.1117/1.3645590.

Agapiou, A., Hadjimitsis, D. G., and Alexakis, D. D. (2012a), "Evaluation of broadband and narrowband vegetation indices for the identification of archaeological crop marks," *Remote Sensing*, 4, 3892–3919.

Agapiou, A., Hadjimitsis, D. G., Alexakis, D., and Sarris, A. (2012b), "Observatory validation of Neolithic tells ('Magoules') in the Thessalian plain, central Greece, using hyperspectral spectroradiometric data," *Journal of Archaeological Science*, 39, 1499–1512.

Agapiou, A., Hadjimitsis, D., Sarris, A., Themistocleous, K., and Papadavid, G. (2010), "Hyperspectral ground truth data for the detection of buried architectural remains," in *Euro-Mediterranean Conference*, Springer, pp. 318–331.

Agapiou, A., and Lysandrou, V. (2015), "Remote sensing archaeology: Tracking and mapping evolution in European scientific literature from 1999 to 2015," *Journal of Archaeological Science: Reports*, 4, 192–200. https://doi.org/10.1016/j.jasrep.2015.09.010.

Aguilar, M. A., Novelli, A., Nemamoui, A., Aguilar, F. J., Lorca, A. G., and González-Yebra, Ó. (2017), "Optimizing multiresolution segmentation for extracting plastic greenhouses from WorldView-3 imagery," in *International Conference on Intelligent Interactive Multimedia Systems and Services*, Springer, pp. 31–40.

Ahmad, S., Kalra, A., and Stephen, H. (2010), "Estimating soil moisture using remote sensing data: A machine learning approach," *Advances in Water Resources*, 33, 69–80. https://doi.org/10.1016/j.advwatres.2009.10.008.

Ahmed, A. A., Kalantar, B., Pradhan, B., Mansor, S., and Sameen, M. I. (2017), "Land Use and Land Cover Mapping Using Rule-Based Classification in Karbala City, Iraq," in *GCEC 2017*, Lecture Notes in Civil Engineering, ed. B. Pradhan, Springer Singapore, pp. 1019–1027.

Ajbilou, R., Marañón, T., and Arroyo, J. (2006), "Ecological and biogeographical analyses of Mediterranean forests of northern Morocco," *Acta Oecologica*, 29, 104–113.

Akar, Ö., and Güngör, O. (2013), "Classification of multispectral images using Random Forest algorithm," *Journal of Geodesy and Geoinformation*, 1.

Alexakis, D. D., Daliakopoulos, I. N., Panagea, I. S., and Tsanis, I. K. (2016), "Assessing soil salinity using WorldView-2 multispectral images in Timpaki, Crete, Greece," *Geocarto International*, 1–18.

Alexakis, D., Sarris, A., Astaras, T., and Albanakis, K. (2009), "Detection of Neolithic settlements in Thessaly (Greece) through multispectral and hyperspectral satellite imagery," *Sensors*, 9, 1167–1187.

Al-Houdalieh, S. H., and Sauders, R. R. (2009), "Building destruction: The consequences of rising urbanization on cultural heritage in the Ramallah province," *International Journal of Cultural Property*, 16, 1–23.

ALS, - (2018), *ME-ICP61 Trace Level Methods Using Conventional ICP-AES Analysis*, Johannesburg: ALSGLOBAL.

Altaweel, M. (2005), "The use of ASTER satellite imagery in archaeological contexts," *Archaeological Prospection*, 12, 151–166.

Ambrose, S. H. (1998), "Chronology of the Later Stone Age and food production in East Africa," *Journal of archaeological science*, 25, 377–392.

Aminzadeh, B., and Samani, F. (2006), "Identifying the boundaries of the historical site of Persepolis using remote sensing," *Remote Sensing of Environment*, 102, 52–62. https://doi.org/10.1016/j.rse.2006.01.018.

Analytical Spectral Devices, Inc. (2018), "FieldSpec 4 Standard-Res Spectroradiometer," Available athttps://www.asdi.com/products-and-services/fieldspec-spectroradiometers/fieldspec-4-standard-res.

Andreu-Lanoe, G. (1997), *Egypt in the Age of the Pyramids*, Ithaca: Cornell University Press.
Antonites, A., and Ashley, C. Z. (2016), "The mobilities turn and archaeology: new perspectives on socio-political complexity in thirteenth-century northern South Africa," *Azania: Archaeological Research in Africa*, 51, 469–488. https://doi.org/10.1080/0067270X.2016.1249586.
Antonites, A. R. (2016), "Zhizo and Leokwe period human remains and burial practices at Schroda," *The South African Archaeological Bulletin*, 71, 14–26.
Aqdus, S. A., Drummond, J., and Hanson, W. S. (2008), "Discovering archaeological cropmarks: a hyperspectral approach," *Int. Arch. Photogramm. Remote Sens. Spat. Inf. Sci*, 361–366.
Aqdus, S. A., Hanson, W. S., and Drummond, J. (2012), "The potential of hyperspectral and multi-spectral imagery to enhance archaeological cropmark detection: A comparative study," *Journal of Archaeological Science*, 39, 1915–1924.
Archer, K. J., and Kimes, R. V. (2008), "Empirical characterization of random forest variable importance measures," *Computational Statistics & Data Analysis*, 52, 2249–2260.
Arthur, C. (2008), "The archaeology of indigenous herders in the Western Cape of South Africa," *Southern African Humanities*, 20, 205–220.
Badenhorst, S. (2010), "Descent of Iron Age Farmers in Southern Africa During the Last 2000 Years," *The South African Archaeological Review*, 27, 87–106.
Badenhorst, S., Plug, I., and Boshoff, W. S. (2011), "Faunal remains from test excavations at Middle and Late Iron Age sites in the Limpopo Valley, South Africa," *Annals of the Ditsong National Museum of Natural History*, 1, 23–31.
Bailey, R. C., Head, G., Jenike, M., Owen, B., Rechtman, R., and Zechenter, E. (1989), "Hunting and Gathering in Tropical Rain Forest: Is It Possible?," *American Anthropologist*, 91, 59–82. https://doi.org/10.1525/aa.1989.91.1.02a00040.
Bajcsy, P., and Groves, P. (2004), "Methodology for hyperspectral band selection," *Photogrammetric Engineering & Remote Sensing*, 70, 793–802.
Bandama, F., Manyanga, M., and Chirikure, S. (2018), "Copper wire objects from Jahunda and Little Mapela: technology, value systems and networks in Iron Age southern Africa," *Azania: Archaeological Research in Africa*, 53, 528–545. https://doi.org/10.1080/0067270X.2018.1540213.
Bangira, C., and Manyevere, A. (2009), *Baseline report on the soils of the Limpopo River Basin, a contribution to the Challenge Program on Water and Food Project 17 "Integrated Water Resource Management for Improved Rural Livelihoods: Managing risk, mitigating drought and improving water productivity in the water scarce Limpopo Basin,"* WaterNet, Harare: WaterNet Working Paper 8.
Banning, E. B., Hawkins, A. L., and Stewart, S. T. (2006), "Detection functions for archaeological survey," *American Antiquity*, 71, 723–742.
Bard, K. A. (1994), "The Egyptian Predynastic: A review of the evidence," *Journal of Field Archaeology*, 21, 265–288.
Barham, L., and Mitchell, P. (2008), *The first Africans: African archaeology from the earliest tool makers to most recent foragers*, Cambridge: Cambridge University Press.
Barich, B. E. (2014), "Northwest Libya from the Early to Late Holocene: new data on environment and subsistence from the Jebel Gharbi," *Quaternary International*, 320, 15–27.
Barich, B. E. (2016), "The introduction of Neolithic resources to North Africa: A discussion in light of the Holocene research between Egypt and Libya," *Quaternary International*, 410, 198–216.

Bartholomeus, H. M., Schaepman, M. E., Kooistra, L., Stevens, A., Hoogmoed, W. B., and Spaargaren, O. S. P. (2008), "Spectral reflectance based indices for soil organic carbon quantification," *Geoderma*, 145, 28–36.

Basell, L. S. (2008), "Middle Stone Age (MSA) site distributions in eastern Africa and their relationship to Quaternary environmental change, refugia and the evolution of Homo sapiens," *Quaternary Science Reviews*, 27, 2484–2498.

Baumanova, M. (2018), "Pillar Tombs and the City: Creating a Sense of Shared Identity in Swahili Urban Space," *Archaeologies*, 14, 377–411. https://doi.org/10.1007/s11759-018-9338-x.

Bazi, Y., and Melgani, F. (2006), "Toward an optimal SVM classification system for hyperspectral remote sensing images," *IEEE Transactions on Geoscience and Remote Sensing*, 44, 3374–3385.

Beck, A., Philip, G., Abdulkarim, M., and Donoghue, D. (2007), "Evaluation of Corona and Ikonos high resolution satellite imagery for archaeological prospection in western Syria," *Antiquity*, 81, 161–175.

Beck, A. R. (2007), "Archaeological site detection: the importance of contrast," The Remote Sensing and Photogrammetry Society, pp. 307–312.

Bedeian, A. G., and Mossholder, K. W. (2000), "On the use of the coefficient of variation as a measure of diversity," *Organizational Research Methods*, 3, 285–297.

Belgiu, M., and Csillik, O. (2018), "Sentinel-2 cropland mapping using pixel-based and object-based time-weighted dynamic time warping analysis," *Remote sensing of environment*, 204, 509–523.

Belgiu, M., and Drăguţ, L. (2014), "Comparing supervised and unsupervised multiresolution segmentation approaches for extracting buildings from very high resolution imagery," *ISPRS Journal of Photogrammetry and Remote Sensing*, 96, 67–75.

Belgiu, M., and Drăguţ, L. (2016), "Random forest in remote sensing: A review of applications and future directions," *ISPRS Journal of Photogrammetry and Remote Sensing*, 114, 24–31.

Belmonte, J. A., Esteban, C., Betancort, M. A. P., and Marrero, R. (2002), "Archaeoastronomy in the Sahara: The Tombs of the Garamantes at Wadi El Agial, Fezzan, Libya," *Journal for the History of Astronomy*, 33, S1–S19. https://doi.org/10.1177/002182860203302701.

Ben-Dor, E., Granot, A., and Notesco, G. (2017), "A simple apparatus to measure soil spectral information in the field under stable conditions," *Geoderma*, 306, 73–80. https://doi.org/10.1016/j.geoderma.2017.06.025.

Ben-Dor, E., Inbar, Y., and Chen, Y. (1997), "The reflectance spectra of organic matter in the visible near-infrared and short wave infrared region (400–2500 nm) during a controlled decomposition process," *Remote Sensing of Environment*, 61, 1–15.

Ben-Dor, E., Ong, C., and Lau, I. C. (2015), "Reflectance measurements of soils in the laboratory: Standards and protocols," *Geoderma*, 245, 112–124.

Ben-Hur, A., and Weston, J. (2010), "A user's guide to support vector machines," *Data mining techniques for the life sciences*, 223–239.

Bennett, R., Welham, K., Hill, R. A., and Ford, A. (2013), "Airborne spectral imagery for archaeological prospection in grassland environments—an evaluation of performance," *Antiquity*, 87, 220–236. https://doi.org/10.1017/S0003598X00048730.

Bennett, R., Welham, K., Hill, R. A., and Ford, A. L. J. (2012), "The application of vegetation indices for the prospection of archaeological features in grass-dominated environments," *Archaeological Prospection*, 19, 209–218.

Bewick, V., Cheek, L., and Ball, J. (2004), "Statistics review 9: one-way analysis of variance," *Critical care*, 8, 130.

Bewley, R. H. (2003), "Aerial survey for archaeology," *The Photogrammetric Record*, 18, 273–292.

Biagetti, S., Merlo, S., Adam, E., Lobo, A., Conesa, F. C., Knight, J., Bekrani, H., Crema, E. R., Alcaina-Mateos, J., and Madella, M. (2017), "High and medium resolution satellite imagery to evaluate late holocene human–environment interactions in arid lands: a case study from the central Sahara," *Remote Sensing*, 9, 351.

Bintliff, J. L. (2000), "The concepts of'site'and'offsite'archaeology in surface artefact survey," in *Non-destructive techniques applied to landscape archaeology*, The archaeology of mediterranean landscapes, eds. M. Pasquinucci and F. Trément, Oxbow Books: Oxford.

Blaschke, T. (2010), "Object based image analysis for remote sensing," *ISPRS Journal of Photogrammetry and Remote Sensing*, 65, 2–16. https://doi.org/10.1016/j.isprsjprs.2009.06.004.

Blaschke, T., Hay, G. J., Kelly, M., Lang, S., Hofmann, P., Addink, E., Feitosa, R. Q., Van der Meer, F., Van der Werff, H., and Van Coillie, F. (2014), "Geographic object-based image analysis–towards a new paradigm," *ISPRS journal of photogrammetry and remote sensing*, 87, 180–191.

Blaschke, T., and Strobl, J. (2001), "What's wrong with pixels? Some recent developments interfacing remote sensing and GIS," *Geo-Informations-Systeme*, 14, 12–17.

Blasco, J. M. D., Verstraeten, G., and Hanssen, R. F. (2017), "Detecting modern desert to urban transitions from space in the surroundings of the Giza World Heritage site and Greater Cairo," *Journal of Cultural Heritage*, Beyond the modern landscape: Earth Observation to see the unseen, 23, 71–78. https://doi.org/10.1016/j.culher.2016.10.014.

Blom, R. G., Farr, T. G., Feynmann, J., Ruzmaikin, A., and Paillou, P. (2009), "The green Sahara: Climate change, hydrologic history and human occupation," in *2009 IEEE Radar Conference*, pp. 1–4. https://doi.org/10.1109/RADAR.2009.4977129.

Bogrekci, I., and Lee, W. S. (2005a), "Improving phosphorus sensing by eliminating soil particle size effect in spectral measurement," *Transactions of the ASAE*, 48, 1971–1978.

Bogrekci, I., and Lee, W. S. (2005b), "Spectral measurement of common soil phosphates," *Transactions of the ASAE*, 48, 2371–2378.

Bordy, E. M., and Catuneanu, O. (2002), "Sedimentology of the Beaufort-Molteno Karoo fluvial strata in the Tuli Basin, South Africa," *South African Journal of Geology*, 105, 51–66.

Boulesteix, A.-L., Janitza, S., Kruppa, J., and König, I. R. (2012), "Overview of random forest methodology and practical guidance with emphasis on computational biology and bioinformatics," *Wiley Interdisciplinary Reviews: Data Mining and Knowledge Discovery*, 2, 493–507.

Bouzouggar, A., Barton, R. N. E., Blockley, S., Bronk-Ramsey, C., Collcutt, S. N., Gale, R., Higham, T. F. G., Humphrey, L. T., Parfitt, S., and Turner, E. (2008), "Reevaluating the age of the Iberomaurusian in Morocco," *African Archaeological Review*, 25, 3–19.

Bradbury, G., Mitchell, K., and Weyrich, T. (2013), "Multi-spectral Material Classification in Landscape Scenes Using Commodity Hardware," in *International Conference on Computer Analysis of Images and Patterns*, Springer, pp. 209–216.

Breen, C. (2007), "Advocacy, international development and World Heritage Sites in sub-Saharan Africa," *World Archaeology*, 39, 355–370. https://doi.org/10.1080/00438240701464772.

Breiman, L. (1996), "Bagging predictors," *Machine learning*, 24, 123–140.

Breiman, L. (2001), "Random forests," *Machine learning*, 45, 5–32.

Breiman, L., and Cutler, A. (2007), "Random forests-classification description," *Department of Statistics, Berkeley*, Available athttps://www.stat.berkeley.edu/~breiman/RandomForests/cc_home.htm.

Breunig, P., Neumann, K., and Van Neer, W. (1996), "New research on the Holocene settlement and environment of the Chad Basin in Nigeria," *African Archaeological Review*, 13, 111–145.

Brieuc, M. S. O., Ono, K., Drinan, D. P., and Naish, K. A. (2015), "Integration of Random Forest with population-based outlier analyses provides insight on the genomic basis and evolution of run timing in Chinook salmon (Oncorhynchus tshawytscha)," *Molecular Ecology*, 24, 2729–2746.

Brooks, N. (2005), "Cultural heritage and conflict: The threatened archaeology of Western Sahara," *The Journal of North African Studies*, 10, 413–439.

Brooks, N. (2006), "Cultural responses to aridity in the Middle Holocene and increased social complexity," *Quaternary International*, 151, 29–49.

Brown, K. S., Marean, C. W., Herries, A. I. R., Jacobs, Z., Tribolo, C., Braun, D., Roberts, D. L., Meyer, M. C., and Bernatchez, J. (2009), "Fire as an engineering tool of early modern humans," *Science*, 325, 859–862.

Bubenzer, O., and Riemer, H. (2007), "Holocene climatic change and human settlement between the central Sahara and the nile valley: Archaeological and geomorphological results," *Geoarchaeology-an International Journal*, 22, 607–620. https://doi.org/10.1002/gea.20176.

Buck, P. E., Sabol, D. E., and Gillespie, A. R. (2003), "Sub-pixel artifact detection using remote sensing," *Journal of Archaeological Science*, 8, 973–989.

Burai, P., Deák, B., Valkó, O., and Tomor, T. (2015), "Classification of herbaceous vegetation using airborne hyperspectral imagery," *Remote Sensing*, 7, 2046–2066.

Burger, J., and Gowen, A. (2011), "Data handling in hyperspectral image analysis," *Chemometrics and Intelligent Laboratory Systems*, 108, 13–22.

Burgess, N., Hales, J. D., Underwood, E., Dinerstein, E., Olson, D., Itoua, I., Schipper, J., Ricketts, T., and Newman, K. (2004), *Terrestrial Ecoregions of Africa and Madagascar A Conservation Assessment*, Washington: Island Press.

Cai, X., Wen, G., Wei, J., Li, J., and Yu, Z. (2014), "Perceptual relativity-based semi-supervised dimensionality reduction algorithm," *Applied Soft Computing*, 16, 112–123.

Calabrese, J. A. (1997), *Report on the 1996 field season Shashi-Limpopo archaeological project*, (U. of the W. Department of Archaeology, tran.), Unpublished report: DeBeers consolidated mines and the national monuments council.

Calabrese, J. A. (2000), "Interregional interaction in southern Africa: Zhizo and Leopard's Kopje relations in northern South Africa, southwestern Zimbabwe, and eastern Botswana, AD 1000 to 1200," *African Archaeological Review*, 17, 183–210.

Carter, P. L., and Flight, C. (1972), "A report on the fauna from the sites of Ntereso and Kintampo Rock Shelter Six in Ghana: with evidence for the practice of animal husbandry during the second millennium BC," *Man*, 7, 277–282.

Casa, R., Castaldi, F., Pascucci, S., Palombo, A., and Pignatti, S. (2013), "A comparison of sensor resolution and calibration strategies for soil texture estimation from hyperspectral remote sensing," *Geoderma*, 197, 17–26.

Casana, J., and Laugier, E. J. (2017), "Satellite imagery-based monitoring of archaeological site damage in the Syrian civil war," *PLOS ONE*, 12, e0188589. https://doi.org/10.1371/journal.pone.0188589.

Caspari, G., Balz, T., Gang, L., Wang, X., and Liao, M. (2014), "Application of Hough Forests for the detection of grave mounds in high-resolution satellite imagery," in *2014 IEEE Geoscience and Remote Sensing Symposium*, pp. 906–909. https://doi.org/10.1109/IGARSS.2014.6946572.

Castaldi, F., Palombo, A., Santini, F., Pascucci, S., Pignatti, S., and Casa, R. (2016), "Evaluation of the potential of the current and forthcoming multispectral and

hyperspectral imagers to estimate soil texture and organic carbon," *Remote Sensing of Environment*, 179, 54–65.
Causey, M. J. (2010), "New archaeological discoveries from the Laikipia Plateau, Kenya," *Azania: Archaeological Research in Africa*, 45, 112–136.
Cavalli, R. M., Colosi, F., Palombo, A., Pignatti, S., and Poscolieri, M. (2007), "Remote hyperspectral imagery as a support to archaeological prospection," *Journal of Cultural Heritage*, 8, 272–283.
Cavalli, R. M., Licciardi, G. A., and Chanussot, J. (2013), "Detection of anomalies produced by buried archaeological structures using nonlinear principal component analysis applied to airborne hyperspectral image," *IEEE Journal of Selected Topics in Applied Earth Observations and Remote Sensing*, 6, 659–669. https://doi.org/10.1109/JSTARS.2012.2227301.
Cerra, D., Agapiou, A., Cavalli, R. M., and Sarris, A. (2018), "An Objective Assessment of Hyperspectral Indicators for the Detection of Buried Archaeological Relics," *Remote Sensing*, 10, 500.
Chagas, C. da S., de Carvalho Junior, W., Bhering, S. B., and Calderano Filho, B. (2016), "Spatial prediction of soil surface texture in a semiarid region using random forest and multiple linear regressions," *CATENA*, 139, 232–240. https://doi.org/10.1016/j.catena.2016.01.001.
Challis, K., and Howard, A. J. (2006), "A review of trends within archaeological remote sensing in alluvial environments," *Archaeological Prospection*, 13, 231–240.
Chan, J. C.-W., and Paelinckx, D. (2008), "Evaluation of Random Forest and Adaboost tree-based ensemble classification and spectral band selection for ecotope mapping using airborne hyperspectral imagery," *Remote Sensing of Environment*, 112, 2999–3011.
Chase, A. F., Chase, D. Z., Weishampel, J. F., Drake, J. B., Shrestha, R. L., Slatton, K. C., Awe, J. J., and Carter, W. E. (2011), "Airborne LiDAR, archaeology, and the ancient Maya landscape at Caracol, Belize," *Journal of Archaeological Science*, 38, 387–398. https://doi.org/10.1016/j.jas.2010.09.018.
Chen, F., Masini, N., Yang, R., Milillo, P., Feng, D., and Lasaponara, R. (2015), "A Space View of Radar Archaeological Marks: First Applications of COSMO-SkyMed X-Band Data," *Remote Sensing*, 7, 24–50. https://doi.org/10.3390/rs70100024.
Chen, L., Comer, D. C., Priebe, C. E., Sussman, D., and Tilton, J. C. (2013a), "Refinement of a method for identifying probable archaeological sites from remotely sensed data," in *Mapping archaeological landscapes from space*, eds. D. C. Comer and M. J. Harrower, New York: Springer Science & Business Media.
Chen, L., Priebe, C. E., Sussman, D. L., Comer, D. C., Megarry, W. P., and Tilton, J. C. (2013b), "Enhanced archaeological predictive modelling in space archaeology," Available athttps://arxiv.org/abs/1301.2738.
Chen, Y.-W., and Lin, C.-J. (2006), "Combining SVMs with various feature selection strategies," *Springer*, 315–324.
Chinoda, G., Moyce, W., Matura, N., and Owen, R. (2009a), *The Geology of The Limpopo Basin Area*, Harare, Zimbabwe: Mineral Resources Centre, University of Zimbabwe, pp. 1–44.
Chinoda, G., Moyce, W., Matura, N., and Owen, R. (2009b), "Baseline Report on the Geology of the Limpopo Basin Area.," *WaterNet Working Paper 7*.
Chirikure, S. (2013), "Heritage conservation in Africa: The good, the bad, and the challenges," *South African Journal of Science*, 109, 1–3. https://doi.org/10.1590/sajs.2013/a003.
Chirikure, S., Bandama, F., House, M., Moffett, A., Mukwende, T., and Pollard, M. (2016), "Decisive Evidence for Multidirectional Evolution of Sociopolitical Complexity in

Southern Africa," *African Archaeological Review*, 33, 75–95. https://doi.org/10.1007/s10437-016-9215-1.

Chirikure, S., Manyanga, M., Pollard, A. M., Bandama, F., Mahachi, G., and Pikirayi, I. (2014), "Zimbabwe culture before Mapungubwe: new evidence from Mapela Hill, south-western Zimbabwe," *PloS one*, 9, e111224.

Chirwa, P. W., Syampungani, S., and Geldenhuys, C. J. (2008), "The ecology and management of the Miombo woodlands for sustainable livelihoods in southern Africa: the case for non-timber forest products," *Southern Forests: a Journal of Forest Science*, 70, 237–245.

Churcher, C. S., Kleindienst, M. R., and Schwarcz, H. P. (1999), "Faunal remains from a Middle Pleistocene lacustrine marl in Dakhleh Oasis, Egypt: palaeoenvironmental reconstructions," *Palaeogeography, Palaeoclimatology, Palaeoecology*, 154, 301–312. https://doi.org/10.1016/S0031-0182(99)00104-2.

Chyla, J. M. (2017), "How Can Remote Sensing Help in Detecting the Threats to Archaeological Sites in Upper Egypt?," *Geosciences*, 7, 97. https://doi.org/10.3390/geosciences7040097.

Cihlar, J., Laurent, L., and Dyer, J. A. (1991), "Relation between the normalized difference vegetation index and ecological variables," *Remote sensing of Environment*, 35, 279–298.

Cilliers, S. S., Müller, N., and Drewes, E. (2004), "Overview on urban nature conservation: situation in the western-grassland biome of South Africa," *Urban Forestry & Urban Greening*, 3, 49–62.

Ciminale, M., Gallo, D., Lasaponara, R., and Masini, N. (2009), "A multiscale approach for reconstructing archaeological landscapes: applications in Northern Apulia (Italy)," *Archaeological Prospection*, 16, 143–153.

Clark, C. D., Garrod, S. M., and Pearson, M. P. (1998), "Landscape archaeology and remote sensing in southern Madagascar," *International Journal of Remote Sensing*, 19, 1461–1477.

Cleere, H. (1989), "Introduction: the rationale of archaeological heritage management," in *Archaeological heritage management in the modern world*, ed. H. Cleere, New York: Routledge, pp. 1–22.

Clist, B., Cranshof, E., de Schryver, G., Herremans, D., Karklins, K., Matonda, I., Polet, C., Sengeløv, A., Steyaert, F., Verhaeghe, C., and Bostoen, K. (2015), "The Elusive Archaeology of Kongo Urbanism: the Case of Kindoki, Mbanza Nsundi (Lower Congo, DRC)," *African Archaeological Review*, 32, 369–412. https://doi.org/10.1007/s10437-015-9199-2.

Clist, B.-O. (1987), "A critical reappraisal of the chronological framework of the Early Iron Age Urewe Industry," *MUNTU*, 6, 35–62.

Cochrane, M. A. (2000), "Using vegetation reflectance variability for species level classification of hyperspectral data," *International Journal of Remote Sensing*, 21, 2075–2087. https://doi.org/10.1080/01431160050021303.

Congalton, R. G. (1991), "A review of assessing the accuracy of classifications of remotely sensed data," *Remote sensing of environment*, 37, 35–46.

Connah, G. (2004), *Forgotten Africa: An introduction to its archaeology*, Abingdon: Routledge.

Connah, G. (2008), "Urbanism and the archaeological visibility of African complex societies," *Journal of African Archaeology*, 6, 233–241.

Contreras, D. A., and Brodie, N. (2010), "The utility of publicly-available satellite imagery for investigating looting of archaeological sites in Jordan," *Journal of Field Archaeology*, 35, 101–114.

Cooke, C. K. (1960), "Report on archaeological sites Bubye / Limpopo valleys of Southern Rhodesia," *South African Archaeological Bulletin*, 15, 95–109.
Cornelissen, E. (2013), "Hunting and Gathering in Africa's Tropical Forests at the End of The Pleistocene and in the Early Holocene," in *The Oxford handbook of African archaeology*, eds. P. Mitchell and P. Lane, Oxford: Oxford University Press.
Corrie, R. K. (2011), "Detection of ancient Egyptian archaeological sites using satellite remote sensing and digital image processing," International Society for Optics and Photonics, pp. 81811B-81811B–19.
Costa, H., Foody, G. M., and Boyd, D. S. (2017), "Using mixed objects in the training of object-based image classifications," *Remote sensing of environment*, 190, 188–197.
Coulson, S., Staurset, S., and Walker, N. (2011), "Ritualized behavior in the middle stone age: evidence from Rhino Cave, Tsodilo Hills, Botswana," *PaleoAnthropology*, 2011, 18–61.
Cowen, D. J., Jensen, J. R., Bresnahan, P. J., Ehler, G. B., Graves, D., Huang, X., Wiesner, C., and Mackey, H. E. (1995), "The design and implementation of an integrated geographic information system for environmental applications," *Photogrammetric Engineering and Remote Sensing*, 61, 1393–1404.
Cozzolino, D., and Moron, A. (2003), "The potential of near-infrared reflectance spectroscopy to analyse soil chemical and physical characteristics," *The Journal of Agricultural Science*, 140, 65–71.
Cracknell, A. P., and Hayes, L. (2007), *Introduction to Remote Sensing*, Boca Raton, FL, USA: CRC Press.
Crawford, O. G. S. (1923), "Air survey and archaeology," *Geographical Journal*, 342–360.
Creasman, P. P., Sassen, D., Koepnick, S., and Doyle, N. (2010), "Ground-penetrating radar survey at the pyramid complex of Senwosret III at Dahshur, Egypt, 2008: search for the lost boat of a Pharaoh," *Journal of Archaeological Science*, 37, 516–524.
Cremaschi, M., and Di Lernia, S. (1999), "Holocene Climatic Changes and Cultural Dynamics in the Libyan Sahara," *African Archaeological Review*, 16.
Cremaschi, M., and Di Lernia, S. (2001), "Environment and settlements in the Mid-Holocene palaeo-oasis of Wadi Tanezzuft (Libyan Sahara)," *Antiquity*, 75, 815–825.
Cremaschi, M., and di Lernia, S. (1998), "The geoarchaeological survey in the central Tadrart Acacus and surroundings (Libyan Sahara). Environment and cultures," in *Wadi Teshuinat. Palaeoenvironment and Prehistory in South-Western Fezzan (Libyan Sahara) Survey and excavations in the Tadrart Acacus, Erg Uan Kasa, Messak Settafet and Edeyen of Murzuq, 1990-1995*, eds. M. Cremaschi and S. di Lernia, Florence: All'Insegna del Giglio, pp. 245–298.
Crow, P., Benham, S., Devereux, B. J., and Amable, G. S. (2007), "Woodland vegetation and its implications for archaeological survey using LiDAR," *Forestry: An International Journal of Forest Research*, 80, 241–252. https://doi.org/10.1093/forestry/cpm018.
Cumming, D. H. M., Fenton, M. B., Rautenbach, I. L., Taylor, R. D., Cumming, G. S., Cumming, M. S., Dunlop, J. M., Ford, A. G., Hovorka, M. D., and Johnston, D. S. (1997), "Elephants, woodlands and biodiversity in southern Africa," *South African Journal of Science*, 93, 231–236.
Custer, J. F., Eveleigh, T., Klemas, V., and Wells, I. (1986), "Application of LANDSAT Data and Synoptic Remote Sensing to Predictive Models for Prehistoric Archaeological Sites: An Example from the Delaware Coastal Plain," *Society for American Antiquity*, 51, 572–588. https://doi.org/10.2307/281753.
Dalponte, M., Bruzzone, L., and Gianelle, D. (2008), "Fusion of Hyperspectral and LIDAR Remote Sensing Data for Classification of Complex Forest Areas," *IEEE Transactions*

on Geoscience and Remote Sensing, 46, 1416–1427. https://doi.org/10.1109/TGRS.2008.916480.

D'Andrea, A. C. (2008), "T'ef (Eragrostis tef) in ancient agricultural systems of highland Ethiopia," *Economic Botany*, 62, 547–566.

D'Andrea, A. C., and Casey, J. (2002), "Pearl Millet and Kintampo Subsistence," *African Archaeological Review*, 3, 147–173.

D'Andrea, A. C., Klee, M., and Casey, J. (2001), "Archaeobotanical evidence for pearl millet (Pennisetum glaucum) in sub-Saharan West Africa," *Antiquity*, 75, 341.

Danner, M., Locherer, M., Hank, T., and Richter, K. (2015), *Spectral Sampling with the ASD FieldSpec 4 – Theory, Measurement, Problems, Interpretation*, EnMAP Field Guides Technical Report, GFZ Data Services. https://doi.org/10.2312/enmap.2015.008.

Davis, D. S., and Douglass, K. (2020), "Aerial and Spaceborne Remote Sensing in African Archaeology: A Review of Current Research and Potential Future Avenues," *African Archaeological Review*, 37, 9–24. https://doi.org/10.1007/s10437-020-09373-y.

De Laet, V., van Loon, G., Van der Perre, A., Deliever, I., and Willems, H. (2015), "Integrated remote sensing investigations of ancient quarries and road systems in the Greater Dayr al-Barshā Region, Middle Egypt: a study of logistics," *Journal of Archaeological Science*, 55, 286–300. https://doi.org/10.1016/j.jas.2014.10.009.

De Laet, V., Paulissen, E., and Waelkens, M. (2007), "Methods for the extraction of archaeological features from very high-resolution Ikonos-2 remote sensing imagery, Hisar (southwest Turkey)," *Journal of Archaeological Science*, 34, 830–841.

deMenocal, P. B. (1995), "Plio-Pleistocene African Climate," *Science*, 270, 53–59.

Denbow, J. (2012), "Pride, prejudice, plunder and preservation: archaeology and the re-envisioning of ethnogenesis on the Loango coast of the Republic of Congo," *Antiquity*, 86, 383–408. https://doi.org/10.1017/S0003598X00062839.

Denbow, J. R. (1979), "Cenchrus ciliaris: an ecological indicator of Iron Age middens using aerial photography in eastern Botswana," *South African Journal of Science*, 75, 405–408.

Denbow, J. R. (1981), "Broadhurst: A 14th Century A.D. Expression of the Early Iron Age in South-Eastern Botswana," *The South African Archaeological Bulletin*, 36, 66–74. https://doi.org/10.2307/3888495.

Denbow, J. R. (1986), "A new look at the later prehistory of the Kalahari," *The Journal of African History*, 27, 3–28.

Denbow, J. R. (1990), "Congo to Kalahari: data and hypotheses about the political economy of the western stream of the Early Iron Age," *African Archaeological Review*, 8, 139–175.

Denbow, J. R., and Wilmsen, E. N. (1986), "Advent and course of pastoralism in the Kalahari," *Science*, 234, 1509–1515.

Deng, H., and Runger, G. (2012), "Feature selection via regularized trees," IEEE, pp. 1–8.

Deng, H., and Runger, G. (2013), "Gene selection with guided regularized random forest," *Pattern Recognition*, 46, 3483–3489.

Deroin, J.-P., Te´reygeol, F., and Ju¨rgen, H. (2012), "Remote Sensing Study of the Ancient Jabali Silver Mines(Yemen)," in *Satellite Remote Sensing: A new Tool for Archaeology*, eds. R. Lasaponara and N. Masini, Dordrecht: Springer, pp. 231–246. https://doi.org/10.1017/CBO9781107415324.004.

Devereux, B. J., Amable, G. S., Crow, P., and Cliff, A. D. (2005), "The potential of airborne lidar for detection of archaeological features under woodland canopies," *Antiquity*, 79, 648–660.

Dhau, I., Adam, E., Mutanga, O., Ayisi, K., Abdel-Rahman, E. M., Odindi, J., and Masocha, M. (2018a), "Testing the capability of spectral resolution of the new multispectral

sensors on detecting the severity of grey leaf spot disease in maize crop," *Geocarto International*, 33, 1223–1236. https://doi.org/10.1080/10106049.2017.1343391.

Dhau, I., Adam, E., Mutanga, O., and Ayisi, K. K. (2018b), "Detecting the severity of maize streak virus infestations in maize crop using in situ hyperspectral data," *Transactions of the Royal Society of South Africa*, 73, 8–15. https://doi.org/10.1080/0035919X.2017.1370034.

Diarra, L. (1988), "Changes in Vetiveria nigritiana and Eragrostis barteri grasslands in the Niger floodplain, central Mali."

Díaz-Uriarte, R. (2007), "GeneSrF and varSelRF: a web-based tool and R package for gene selection and classification using random forest," *BMC bioinformatics*, 8, 328.

Díaz-Uriarte, R., and De Andres, S. A. (2006), "Gene selection and classification of microarray data using random forest," *BMC bioinformatics*, 7, 3.

DigitalGlobe, . (2010), *White paper: the benefits of the 8 spectral bands of WorldView-2*, Longmont: DigitalGlobe.

di Lernia, S., and Gallinaro, M. (2010), "The date and context of Neolithic rock art in the Sahara: engravings and ceremonial monuments from Messak Settafet (south-west Libya)," *Antiquity*, 84, 954–975. https://doi.org/10.1017/S0003598X00067016.

Djoudi, H., Brockhaus, M., and Locatelli, B. (2013), "Once there was a lake: vulnerability to environmental changes in northern Mali," *Regional Environmental Change*, 13, 493–508.

Doneus, M., Briese, C., Fera, M., and Janner, M. (2008), "Archaeological prospection of forested areas using full-waveform airborne laser scanning," *Journal of Archaeological Science*, 35, 882–893.

Doneus, M., Verhoeven, G., Atzberger, C., Wess, M., and Ruš, M. (2014), "New ways to extract archaeological information from hyperspectral pixels," *Journal of Archaeological Science*, 52, 84–96.

van Doornum, B. (2014), "Balerno Shelter 3 : a Later Stone Age site in the Shashe-Limpopo confluence area , South Africa," *Southern African Humanities*, 26, 129–155.

Du Piesanie, J. (2009), "Understanding the socio-political status of Leokwe society during the Middle Iron Age in the Shashe-Limpopo Basin through a landscape approach," Thesis, Johannesburg: University of the Witwatersrand.

Dueppen, S. A. (2016), "The Archaeology of West Africa, ca. 800 BCE to 1500 CE," *History Compass*, 14, 247–263.

Dumitru, I. A., and Harrower, M. J. (2018), "From rural collectables to global commodities: Copper from Oman and Obsidian from Ethiopia," in *Globalization in Prehistory: Understanding Contact and Exchange between Peoples without History*, eds. N. Boivin and M. D. Frachetti, Cambridge: Cambridge University Press, pp. 232–261.

Durand, J. F., Meeuvis, J., and Fourie, M. (2010), "The threat of mine effluent to the UNESCO status of the Cradle of Humankind World Heritage Site," *TD : The Journal for Transdisciplinary Research in Southern Africa*, 6, 73–92.

Duro, D. C., Franklin, S. E., and Dubé, M. G. (2012), "A comparison of pixel-based and object-based image analysis with selected machine learning algorithms for the classification of agricultural landscapes using SPOT-5 HRG imagery," *Remote Sensing of Environment*, 118, 259–272.

Eastwood, E. B., and Blundell, G. (1999), "Re-discovering the rock art of the Limpopo-Shashi confluence area, southern Africa," *Southern African Field Archaeology*, 8, 17–27.

Ebert, J. I. (1984), "Remote Sensing Applications in Archaeology," *Advances in Archaeological Method and Theory*, 7, 293–362.

El-Amier, Y. A., El-Halawany, E.-S. F., Haroun, S. A., and Mohamud, S. G. (2015), "Vegetation analysis and soil characteristics on two species of genus Achillea growing in Egyptian Desert," *Open Journal of Ecology*, 5, 420–433.

El-Baz, F., Robinson, C. A., and Al-Saud, T. S. M. (2007), "Radar Images and Geoarchaeology of the Eastern Sahara," in *Remote Sensing in Archaeology*, eds. J. Wiseman and F. El-Baz, New York, NY: Springer New York, pp. 47–69. https://doi.org/10.1007/0-387-44455-6_2.

El-Behaedi, R., and Ghoneim, E. (2018), "Flood risk assessment of the Abu Simbel temple complex (Egypt) based on high-resolution spaceborne stereo imagery," *Journal of Archaeological Science: Reports*, 20, 458–467. https://doi.org/10.1016/j.jasrep.2018.05.019.

Elfadaly, A., Attia, W., and Lasaponara, R. (2018), "Monitoring the Environmental Risks Around Medinet Habu and Ramesseum Temple at West Luxor, Egypt, Using Remote Sensing and GIS Techniques," *Journal of Archaeological Method and Theory*, 25, 587–610. https://doi.org/10.1007/s10816-017-9347-x.

Eloff, J. F., and Meyer, A. (1981), "The Greefswald sites," in *Guide to archaeological sites in the northern and eastern Transvaal*, ed. E. A. Voigt, Pretoria: Transvaal museum, pp. 7–22.

Eloundou, L., and Avango, D. (2012), *Mission Report: Reactive Monitoring Mission to Mapungubwe Cultural Landscape*, Saint Petersburg, Russia: World Heritage.

Entwistle, J. A., Abrahams, P. W., and Dodgshon, R. A. (2000), "The geoarchaeological significance and spatial variability of a range of physical and chemical soil properties from a former habitation site, Isle of Skye," *Journal of archaeological science*, 27, 287–303.

Esch, T., Thiel, M., Bock, M., Roth, A., and Dech, S. (2008), "Improvement of image segmentation accuracy based on multiscale optimization procedure," *IEEE Geoscience and Remote Sensing Letters*, 5, 463–467.

Evans, D., and Fletcher, R. (2015), "The landscape of Angkor Wat redefined," *Antiquity*, 89, 1402–1419. https://doi.org/10.15184/aqy.2015.157.

Evans, D. H., Fletcher, R. J., Pottier, C., Chevance, J.-B., Soutif, D., Tan, B. S., Im, S., Ea, D., Tin, T., Kim, S., Cromarty, C., De Greef, S., Hanus, K., Baty, P., Kuszinger, R., Shimoda, I., and Boornazian, G. (2013), "Uncovering archaeological landscapes at Angkor using lidar," *Proceedings of the National Academy of Sciences*, 110, 12595–12600. https://doi.org/10.1073/pnas.1306539110.

Evans, R., and Jones, R. J. A. (1977), "Crop marks and soils at two archaeological sites in Britain," *Journal of Archaeological Science*, 4, 63–76.

Fagan, B. (1964), "The Greefswald Sequence: Bambandyanalo and Mapungubwe," *The Journal of African History*, 5, 337–361. https://doi.org/10.1017/S0021853700005053.

Fagan, B. (2012), *Archaeology: A brief introduction*, New York: Routledge.

Farhat, M. R., Sultana, R., Iartchouk, O., Bozeman, S., Galagan, J., Sisk, P., Stolte, C., Nebenzahl-Guimaraes, H., Jacobson, K., and Sloutsky, A. (2016), "Genetic determinants of drug resistance in Mycobacterium tuberculosis and their diagnostic value," *American journal of respiratory and critical care medicine*, 194, 621–630.

Farr, T. G., and Paillou, P. (2012), "Radar remote sensing of the Sahara landscape," in *EUSAR 2012; 9th European Conference on Synthetic Aperture Radar*, pp. 717–718.

Farrell, M. D., and Mersereau, R. M. (2005), "On the impact of PCA dimension reduction for hyperspectral detection of difficult targets," *IEEE Geoscience and Remote Sensing Letters*, 2, 192–195.

Fattovich, R. (2010), "The development of ancient states in the northern Horn of Africa, c. 3000 BC–AD 1000: an archaeological outline," *Journal of World Prehistory*, 23, 145–175.

Fayolle, A., Swaine, M. D., Bastin, J., Bourland, N., Comiskey, J. A., Dauby, G., Doucet, J., Gillet, J., Gourlet-Fleury, S., and Hardy, O. J. (2014), "Patterns of tree species composition across tropical African forests," *Journal of biogeography*, 41, 2320–2331.

Featherstone, R., Horne, P., Macleod, D., and Bewley, R. (1999), "Aerial reconnaissance over England in summer 1996," *Archaeological Prospection*, 6, 47–62. https://doi.org/10.1002/(SICI)1099-0763(199906)6:2<47::AID-ARP113>3.0.CO;2-Y.

Feng, J., Jiao, L., Liu, F., Sun, T., and Zhang, X. (2016), "Unsupervised feature selection based on maximum information and minimum redundancy for hyperspectral images," *Pattern Recognition*, 51, 295–309.

Fernández-Blanco, E., Aguiar-Pulido, V., Munteanu, C. R., and Dorado, J. (2013), "Random Forest classification based on star graph topological indices for antioxidant proteins," *Journal of theoretical biology*, 317, 331–337.

Fernandez-Diaz, J. C., Carter, W. E., Shrestha, R. L., Leisz, S. J., Fisher, C. T., González, A. M., Thompson, D., and Elkins, S. (2014), "Archaeological prospection of north Eastern Honduras with airborne mapping LiDAR," in *2014 IEEE Geoscience and Remote Sensing Symposium*, pp. 902–905. https://doi.org/10.1109/IGARSS.2014.6946571.

Fernández-Manso, A., Fernández-Manso, O., and Quintano, C. (2016), "SENTINEL-2A red-edge spectral indices suitability for discriminating burn severity," *International journal of applied earth observation and geoinformation*, 50, 170–175.

Fleisher, J., and LaViolette, A. (1999), "Elusive wattle-and-daub: Finding the hidden majority in the archaeology of the Swahili," *Azania: Archaeological Research in Africa*, 34, 87–108. https://doi.org/10.1080/00672709909511473.

Fleisher, J., and Sulas, F. (2015), "Deciphering public spaces in urban contexts: geophysical survey, multi-element soil analysis, and artifact distributions at the 15th–16th-century AD Swahili settlement of Songo Mnara, Tanzania," *Journal of archaeological science*, 55, 55–70.

Fleisher, J., Wynne-Jones, S., Steele, C., and Welham, K. (2012), "Geophysical Survey at Kilwa Kisiwani, Tanzania," *Journal of African Archaeology*, 10, 207–220.

Fletcher, M., and Lock, G. R. (2005), *Digging numbers: elementary statistics for archaeologists*, Oxford Univ School of Archaeology.

Foard, G. (1977), "Systematic fieldwalking and the investigation of Saxon settlement in Northamptonshire," *World Archaeology*, 9, 357–374.

Foissner, W., Agatha, S., and Berger, H. (2002), *Soil ciliates (Protozoa, Ciliophora) from Namibia (Southwest Africa), with emphasis on two contrasting environments, the Etosha region and the Namib Desert. art I: Text and line drawings. Part II: Photographs*, Denisia: Biologiezentrum der Oberösterreichischen Landesmuseums.

Forssman, T. (2013), "A PRELIMINARY REPORT ON FIELDWORK IN THE NORTHERN TULI GAME RESERVE, NORTHEASTERN BOTSWANA," *South African Archaeological Bulletin*, 68, 63–71.

Forssman, T. (2014), "The Spaces Between Places: A Landscape Study of Foragers on the Greater Mapungubwe Landscape, Southern Africa," *Azania: Archaeological Research in Africa*, 49, 282–282. https://doi.org/10.1080/0067270X.2014.891874.

Forssman, T., and Pargeter, J. (2014), "Assessing surface movement at Stone Age open-air sites: first impressions from a pilot experiment in northeastern Botswana," *SOUTHERN AFRICAN HUMANITIES*, 20.

Fowler, M. J. F. (1996), "High-resolution satellite imagery in archaeological application: a Russian satellite photograph of the Stonehenge region," *Antiquity*, 70, 667–671. https://doi.org/10.1017/S0003598X00083812.

Fowler, M. J. F. (2002), "Satellite remote sensing and archaeology: a comparative study of satellite imagery of the environs of Figsbury Ring, Wiltshire," *Archaeological Prospection*, 9, 55–69.

Fukunaga, K., and Hayes, R. R. (1989), "Effects of sample size in classifier design," *IEEE Transactions on Pattern Analysis and Machine Intelligence*, 11, 873–885.

Fuller, D., and Hildebrand, E. (2013), "Domesticating plants in Africa," in *The Oxford Handbook of African Archaeology*, eds. P. Mitchell and P. Lane, Oxford: Oxford University Press, pp. 507–526.

Gaber, A., Koch, M., Griesh, M. H., Sato, M., and El-Baz, F. (2013), "Near-surface imaging of a buried foundation in the Western Desert, Egypt, using space-borne and ground penetrating radar," *Journal of Archaeological Science*, 40, 1946–1955. https://doi.org/10.1016/j.jas.2012.12.019.

Gandariasbeitia, M., Besga, G., Albizu, I., Larregla, S., and Mendarte, S. (2017), "Prediction of chemical and biological variables of soil in grazing areas with visible-and near-infrared spectroscopy," *Geoderma*, 305, 228–235.

Garcea, E. A. A. (2004), "An alternative way towards food production: the perspective from the Libyan Sahara," *Journal of World Prehistory*, 18, 107–154.

Garfield, E. (1999), "Journal impact factor: a brief review," *CMAJ*, 161, 979–980.

Garlake, P. S. (1968), "Test excavations at Mapela Hill, near the Shashi River, Rhodesia," *Arnoldia Rhodesia*, 3, 1–29.

Garrison, T. G., Houston, S. D., Golden, C., Inomata, T., Nelson, Z., and Munson, J. (2008), "Evaluating the use of IKONOS satellite imagery in lowland Maya settlement archaeology," *Journal of Archaeological Science*, 35, 2770–2777.

Geldenhuys, C. J., and Golding, J. S. (2008), "Resource use activities, conservation and management of natural resources of African savannas," *Savannas: desafios e estrategias para o equilibrio entre sociedade, agrenegocio e recursos naturais. Embrapa Cerrados, Planaltina, DF*, 225–260.

Genuer, R., Poggi, J.-M., and Tuleau-Malot, C. (2010), "Variable selection using random forests," *Pattern Recognition Letters*, 31, 2225–2236.

Ghosh, A., Fassnacht, F. E., Joshi, P. K., and Koch, B. (2014), "A framework for mapping tree species combining hyperspectral and LiDAR data: Role of selected classifiers and sensor across three spatial scales," *International Journal of Applied Earth Observation and Geoinformation*, 26, 49–63.

Gifford-Gonzalez, D. (2005), "Pastoralism and its consequences," in *African archaeology: a critical introduction*, Blackwell studies in global archaeology, ed. A. B. Stahl, Malden, MA: Blackwell Publishing, pp. 187–224.

Ginau, A., Schiestl, R., Kern, F., and Wunderlich, J. (2017), "Identification of historic landscape features and settlement mounds in the Western Nile Delta by means of remote sensing time series analysis and the evaluation of vegetation characteristics," *Journal of Archaeological Science: Reports*, 16, 170–184. https://doi.org/10.1016/j.jasrep.2017.09.034.

Gislason, P. O., Benediktsson, J. A., and Sveinsson, J. R. (2006), "Random forests for land cover classification," *Pattern Recognition Letters*, 27, 294–300.

Glenn, E. P., Huete, A. R., Nagler, P. L., and Nelson, S. G. (2008), "Relationship between remotely-sensed vegetation indices, canopy attributes and plant physiological processes: What vegetation indices can and cannot tell us about the landscape," *Sensors*, 8, 2136–2160.

Gliganic, L. A., Jacobs, Z., Roberts, R. G., Domínguez-Rodrigo, M., and Mabulla, A. Z. P. (2012), "New ages for Middle and Later Stone Age deposits at Mumba rockshelter, Tanzania: Optically stimulated luminescence dating of quartz and feldspar grains," *Journal of Human Evolution*, 62, 533–547.

Gojda, M., and Hejcman, M. (2012), "Cropmarks in main field crops enable the identification of a wide spectrum of buried features on archaeological sites in Central Europe," *Journal of Archaeological Science*, 39, 1655–1664.

Gole, T. W., Borsch, T., Denich, M., and Teketay, D. (2008), "Floristic composition and environmental factors characterizing coffee forests in southwest Ethiopia," *Forest Ecology and Management*, 255, 2138–2150.

Gomez, C., Rossel, R. A. V., and McBratney, A. B. (2008), "Soil organic carbon prediction by hyperspectral remote sensing and field vis-NIR spectroscopy: An Australian case study," *Geoderma*, 146, 403–411.

Götze, A. R., Cilliers, S. S., and Bezuidenhout, H. (2008), "Analysis of the vegetation of the sandstone ridges (Ib land type) of the north-eastern parts of the Mapungubwe National Park, Limpopo Province, South Africa," *Koedoe: African Protected Area Conservation and Science*, 50, 72–81.

Götze, A. R., Cilliers, S. S., Bezuidenhout, H., and Kellner, K. (2003), "Analysis of the riparian vegetation (Ia land type) of the proposed Vhembe-Dongola National Park, Limpopo Province, South Africa," *Koedoe*, 46, 45–64.

Govaerts, B., and Verhulst, N. (2010), "The normalized difference vegetation index (NDVI) Greenseeker (TM) handheld sensor: toward the integrated evaluation of crop management. Part A-Concepts and case studies," Available athttp://www.nue.okstate.edu/GreenSeeker/NDVI-PartA-mayo.pdf.

Gray, K. R., Aljabar, P., Heckemann, R. A., Hammers, A., Rueckert, D., and Initiative, A. D. N. (2013), "Random forest-based similarity measures for multi-modal classification of Alzheimer's disease," *NeuroImage*, 65, 167–175.

Griffith, M. A. (1980), "A pedological investigation of an archaeological site in Ontario, Canada, I. An examination of the soils in and adjacent to a former village," *Geoderma*, 24, 327–336.

Grimm, R., Behrens, T., Märker, M., and Elsenbeer, H. (2008), "Soil organic carbon concentrations and stocks on Barro Colorado Island — Digital soil mapping using Random Forests analysis," *Geoderma*, 146, 102–113. https://doi.org/10.1016/j.geoderma.2008.05.008.

Guan, H., Li, J., Chapman, M., Deng, F., Ji, Z., and Yang, X. (2013), "Integration of orthoimagery and lidar data for object-based urban thematic mapping using random forests," *International Journal of Remote Sensing*, 34, 5166–5186. https://doi.org/10.1080/01431161.2013.788261.

Haaland, R. (1995), "Sedentism, Cultivation, and Plant Domestication in the Holocene Middle Nile Region," *Journal of Field Archaeology*, 157–174.

Haaland, R. (1997), "Emergence of sedentism: new ways of living, new ways of symbolizing," *Antiquity*, 71, 374–385.

Haaland, R., and Haaland, G. (2013), "Early farming societies along the Nile," in *The Oxford Handbook of African Archaeology*, eds. P. Mitchell and P. Lane, Oxford: Oxford University Press, pp. 541–554.

Hadjimitsis, D. G., Themistocleous, K., Agapiou, A., and Clayton, C. R. I. (2009), "Monitoring archaeological site landscapes in Cyprus using multi-temporal atmospheric corrected image data," *International Journal of Architectural Computing*, 7, 121–138.

Hall, S., and Smith, B. (2000), "Empowering Places: Rock Shelters and Ritual Control in Farmer-Forager Interactions in the Northern Province," *Goodwin Series*, 8, 30–46. https://doi.org/10.2307/3858044.

Ham, J., Chen, Y., Crawford, M. M., and Ghosh, J. (2005), "Investigation of the random forest framework for classification of hyperspectral data," *IEEE Transactions on Geoscience and Remote Sensing*, 43, 492–501.

Hanisch, E. O. M. (1980), "An archaeological interpretation of certain Iron Age sites in the Limpopo/Shashi Valley," Unpublished: University of Pretoria.

Hanisch, E. O. M. (1981a), "Schroda: a Zhizo site in the northern Transvaal," in *Guide to archaeological sites in the northern and eastern Transvaal*, ed. E. A. Voigt, Pretoria: South African Association of Archaeologists, pp. 37– 53.

Hanisch, E. O. M. (1981b), "The northern Transvaal: environment and archaeology," in *Guide to archaeological sites in the northern and eastern Transvaal. Pretoria: Transvaal Museum*, ed. E. A. Voigt, Pretoria: Transvaal Museum, pp. 1–6.

Hanisch, E. O. M. (2002), "Schroda: the archaeological evidence," in *Sculptured in clay: Iron Age figurines from Schroda, Limpopo Province, South Africa.*, Pretoria: National Cultural History Museum, pp. 20–39.

Hanisch, E. O. M., and Maumela, V. (2002), "Classification of the Schroda clay figurines," in *Sculptured in Clay: Iron Age Figurines from Schroda, Limpopo Province, South Africa*, Pretoria, South Africa: National Cultural History Museum, p. : 47–67.

Harrower, M. J., and D'Andrea, A. C. (2014), "Landscapes of state formation: Geospatial analysis of Aksumite settlement patterns (Ethiopia)," *African Archaeological Review*, 31, 513–541.

Hart, T. B. (1995), "Seed, seedling and sub-canopy survival in monodominant and mixed forests of the Ituri Forest, Africa," *Journal of Tropical Ecology*, 11, 443–459.

Hart, T. B., and Hart, J. A. (1986), "The ecological basis of hunter-gatherer subsistence in African Rain Forests: The Mbuti of Eastern Zaire," *Human Ecology*, 14, 29–55.

Hassan, F. A. (1988), "The predynastic of Egypt," *Journal of World Prehistory*, 2, 135–185.

Hassan, F. A. (1997), "The dynamics of a riverine civilization: a geoarchaeological perspective on the Nile Valley, Egypt," *World Archaeology*, 29, 51–74.

Hassan, F. A. (2002), "Palaeoclimate, Food and Culture Change in Africa: An Overview," in *Droughts, Food and Culture*, ed. F. A. Hassan, Boston: Kluwer Academic Publishers, pp. 11–26. https://doi.org/10.1007/0-306-47547-2_2.

Hassan, S. N. (2011), "Influence of early dry season fires on primary production in western Serengeti grasslands, Tanzania," *Open Journal of Ecology*, 1, 24.

Hassani, F. (2015), "Documentation of cultural heritage techniques, potentials and constraints.," *International Archives of the Photogrammetry, Remote Sensing & Spatial Information Sciences*, 40.

Hawkins, A. L., Stewart, S. T., and Banning, E. B. (2003), "Interobserver bias in enumerated data from archaeological survey," *Journal of Archaeological Science*, 30, 1503–1512.

He, T., Wang, J., Lin, Z., and Cheng, Y. (2009), "Spectral features of soil organic matter," *Geo-spatial Information Science*, 12, 33–40.

Hejcman, M., Ondráček, J., and Smrž, Z. (2011), "Ancient waste pits with wood ash irreversibly increase crop production in Central Europe," *Plant and soil*, 339, 341–350.

Hejcman, M., and Smrž, Z. (2010), "Cropmarks in stands of cereals, legumes and winter rape indicate sub-soil archaeological features in the agricultural landscape of Central Europe," *Agriculture, Ecosystems & Environment*, 138, 348–354. https://doi.org/10.1016/j.agee.2010.06.004.

Henn, B. M., Gignoux, C. R., Jobin, M., Granka, J. M., Macpherson, J. M., Kidd, J. M., Rodríguez-Botigué, L., Ramachandran, S., Hon, L., and Brisbin, A. (2011), "Hunter-

gatherer genomic diversity suggests a southern African origin for modern humans," *Proceedings of the National Academy of Sciences*, 108, 5154–5162.

Henshilwood, C. (1996), "A revised chronology for pastoralism in southernmost Africa: new evidence of sheep at c. 2000 bp from Blombos Cave, South Africa," *Antiquity*, 70, 945–949.

Henshilwood, C. S., D'errico, F., Marean, C. W., Milo, R. G., and Yates, R. (2001), "An early bone tool industry from the Middle Stone Age at Blombos Cave, South Africa: implications for the origins of modern human behaviour, symbolism and language," *Journal of Human Evolution*, 41, 631–678.

Henshilwood, C. S., d'Errico, F., and Watts, I. (2009), "Engraved ochres from the Middle Stone Age levels at Blombos Cave, South Africa," *Journal of Human Evolution*, 57, 27–47. https://doi.org/10.1016/j.jhevol.2009.01.005.

Hesse, R. (2015), "Combining structure-from-motion with high and intermediate resolution satellite images to document threats to archaeological heritage in arid environments," *Journal of Cultural Heritage*, 16, 192–201.

Hildebrand, E. A., and Grillo, K. M. (2012), "Early herders and monumental sites in eastern Africa: dating and interpretation," *Antiquity*, 86, 338–352.

Hildebrand, E. A., Grillo, K. M., Sawchuk, E. A., Pfeiffer, S. K., Conyers, L. B., Goldstein, S. T., Hill, A. C., Janzen, A., Klehm, C. E., Helper, M., Kiura, P., Ndiema, E., Ngugi, C., Shea, J. J., and Wang, H. (2018), "A monumental cemetery built by eastern Africa's first herders near Lake Turkana, Kenya," *Proceedings of the National Academy of Sciences*, 115, 8942–8947. https://doi.org/10.1073/pnas.1721975115.

Hildebrand, E. A., Shea, J. J., and Grillo, K. M. (2011), "Four middle Holocene pillar sites in West Turkana, Kenya," *Journal of Field Archaeology*, 36, 181–200.

Hitchings, P. M. N., Abu Jayyab, K., Bikoulis, P., and Banning, E. B. (2013), "A Bayesian approach to archaeological survey in North-West Jordan," *Antiquity*, 87, 336.

Hitchner, R. B. (1995), "Historical text and archaeological context in Roman North Africa: the Albertini Tablets and the Kasserine Survey," in *Methods in the Mediterranean: historical and archaeological views on texts and archaeology*, ed. D. B. Small, Leiden: E. J. Brill, pp. 124–142.

Holdaway, S., Phillipps, R., Emmitt, J., and Wendrich, W. (2016), "The Fayum revisited: Reconsidering the role of the Neolithic package, Fayum north shore, Egypt," *Quaternary International*, 410, 173–180.

Holliday, V. T., and Gartner, W. G. (2007), "Methods of soil P analysis in archaeology," *Journal of archaeological science*, 34, 301–333.

Holtorf, C. J. (2001), "Is the past a non-renewable resource?," in *Destruction and Conservation of Cultural Property*, eds. R. Layton, P. Stone, and J. Thomas, London: Routledge, pp. 286–297.

Horton, R. (1979), "Ancient Ife: a reassessment," *Journal of the Historical Society of Nigeria*, 9, 69–149.

Hritz, C. (2010), "Tracing settlement patterns and channel systems in southern Mesopotamia using remote sensing," *Journal of Field Archaeology*, 35, 184–203.

Hsu, C.-W., Chang, C.-C., and Lin, C.-J. (2003), "A practical guide to support vector classification," Taiwan: Department of Computer Science and Information Engineering.

Hu, Q., Wu, W., Xia, T., Yu, Q., Yang, P., Li, Z., and Song, Q. (2013), "Exploring the Use of Google Earth Imagery and Object-Based Methods in Land Use/Cover Mapping," *Remote Sensing*, 5, 6026–6042. https://doi.org/10.3390/rs5116026.

Huang, C., Davis, L. S., and Townshend, J. R. G. (2002), "An assessment of support vector machines for land cover classification," *International Journal of Remote Sensing*, 23, 725–749.
Huang, C., Song, K., Kim, S., Townshend, J. R. G., Davis, P., Masek, J. G., and Goward, S. N. (2008a), "Use of a dark object concept and support vector machines to automate forest cover change analysis," *Remote Sensing of Environment*, 112, 970–985.
Huang, C.-L., Liao, H.-C., and Chen, M.-C. (2008b), "Prediction model building and feature selection with support vector machines in breast cancer diagnosis," *Expert Systems with Applications*, 34, 578–587. https://doi.org/10.1016/j.eswa.2006.09.041.
Huang, C.-L., and Wang, C.-J. (2006), "A GA-based feature selection and parameters optimizationfor support vector machines," *Expert Systems with Applications*, 31, 231–240. https://doi.org/10.1016/j.eswa.2005.09.024.
Huffman, T. N. (1982), "Archaeology and ethnohistory of the African Iron Age," *Annual review of Anthropology*, 11, 133–150.
Huffman, T. N. (1989a), "Ceramics, settlements and late Iron Age migrations," *African archaeological review*, 7, 155–182.
Huffman, T. N. (1989b), *Iron Age Migrations: The Ceramic Sequence in Southern Zambia; Excavations at Gundu and Ndonde*, Johannesburg: Witwatersrand University Press.
Huffman, T. N. (1998), "Presidential Address: The Antiquity of Lobola," *The South African Archaeological Bulletin*, 53, 57–62. https://doi.org/10.2307/3889180.
Huffman, T. N. (2000), "Mapungubwe and the origins of the Zimbabwe culture," *Goodwin Series*, 14–29.
Huffman, T. N. (2001), "The Central Cattle Pattern and interpreting the past," *Southern African Humanities*, 13, 19–35.
Huffman, T. N. (2002), "Archaeological background," in *Sculptured in clay: Iron Age figurines from Schroda, Limpopo Province, South Africa.*, eds. J. A. van Schalkwyk and E. O. M. Hanisch, Pretoria: National Cultural History Museum, pp. 9–20.
Huffman, T. N. (2007a), "Leokwe and K2: Ethnic Stratification during the Middle Iron Age in Southern Africa," *Journal of African Archaeology*, 5, 163–188.
Huffman, T. N. (2007b), *Handbook to the Iron Age: The Archaeology of Pre-colonial Farming Societies in Southern Africa.*, Pietermaritzburg: University of KwaZulu-Natal Press.
Huffman, T. N. (2008), "Climate change during the iron age in the Shashe-limpopo basin, southern Africa," *Journal of Archaeological Science*, 35, 2032–2047.
Huffman, T. N. (2009a), "Mapungubwe and Great Zimbabwe: The origin and spread of social complexity in southern Africa," *Journal of Anthropological Archaeology*, 28, 37–54.
Huffman, T. N. (2009b), *Origins of Mapungubwe project, progress report 2008 prepared for De Beers, the NRF, SAHRA and SANParks*, (A. R. Management, tran.), Unpublished, pp. 1–65.
Huffman, T. N. (2011), *Origins of Mapungubwe project, progress report 2011 prepared for De Beers, the NRF, SAHRA and SANParks*, (A. R. Management, tran.), Unpublished, pp. 1–35.
Huffman, T. N. (2012), "Historical archaeology of the Mapungubwe area: Boer, Birwa, Sotho-Tswana and Machete," *Southern African Humanities*, 24, 33–59.
Huffman, T. N., and Du Piesanie, J. (2011), "Khami and the Venda in the Mapungubwe landscape," *Journal of African Archaeology*, 9, 189–206.
Huffman, T. N., Elburg, M., and Watkeys, M. (2013), "Vitrified cattle dung in the Iron Age of southern Africa," *Journal of Archaeological Science*, 40, 3553–3560.
Huffman, T. N., and Kinahan, J. (2003), "Archaeological Mitigation of Letsibogo Dam: Agropastoralism in southeastern Botswana," *Southern Africa Field Archaeology*, 11 & 12, 4–63.

Huffman, T. N., Murimbika, M., and Schoeman, M. H. (2004), *Origins of Mapungubwe project, progress report 2004 prepared for De Beers, the NRF, SAHRA and SANParks*, (A. R. Management, tran.), Unpublished, pp. 1–21.

Hutson, S. R., Magnoni, A., Beach, T., Terry, R. E., Dahlin, B. H., and Schabel, M. J. (2009), "Phosphate fractionation and spatial patterning in ancient ruins: A case study from Yucatan," *Catena*, 78, 260–269.

Immitzer, M., Atzberger, C., and Koukal, T. (2012), "Tree species classification with random forest using very high spatial resolution 8-band WorldView-2 satellite data," *Remote Sensing*, 4, 2661–2693.

Ismail, R., and Mutanga, O. (2011), "Discriminating the early stages of Sirex noctilio infestation using classification tree ensembles and shortwave infrared bands," *International journal of remote sensing*, 32, 4249–4266.

Jacobson, L., Loock, J. C., Van der Westhuizen, W. A., Huffman, T. N., and Dreyer, J. J. B. (2003), "The occurrence of vitrified dung from the Kamdeboo district, southern Karoo, and Den Staat, Limpopo Valley, South Africa: research in action," *South African journal of science*, 99, 26–28.

Jahns, S. (1996), "Vegetation history and climate changes in West Equatorial Africa during the Late Pleistocene and Holocene, based on a marine pollen diagram from the Congo fan," *Vegetation History and Archaeobotany*, 5, 207–213. https://doi.org/10.1007/BF00217498.

Jain, A. K., and Waller, W. G. (1978), "On the optimal number of features in the classification of multivariate Gaussian data," *Pattern recognition*, 10, 365–374.

Japp, S., Gerlach, I., Hitgen, H., and Schnelle, M. (2011), "Yeha and Hawelti: cultural contacts between Sabaʾ and DʿMT—New research by the German Archaeological Institute in Ethiopia," JSTOR, pp. 145–160.

Jensen, J. R. (2015), *Introductory digital image processing: a remote sensing perspective*, Glenview, IL: Pearson.

Jia, X., and Richards, J. A. (1999), "Segmented principal components transformation for efficient hyperspectral remote-sensing image display and classification," *IEEE Transactions on Geoscience and Remote Sensing*, 37, 538–542.

Jones, B. G. (1986), "Experiencing Loss," in *Protecting Historic Architecture and Museum Collections from Natural Disasters*, ed. B. G. Jones, Butterworth-Heinemann, pp. 3–14. https://doi.org/10.1016/B978-0-409-90035-4.50005-4.

Jouan-Rimbaud, D., Massart, D. L., and De Noord, O. E. (1996), "Random correlation in variable selection for multivariate calibration with a genetic algorithm," *Chemometrics and Intelligent Laboratory Systems*, 35, 213–220.

Jürgens, N. (1991), "A new approach to the Namib Region," *Plant Ecology*, 97, 21–38.

Kankpeyeng, B. W., and DeCorse, C. R. (2004), "Ghana's Vanishing Past: Development, Antiquities, and the Destruction of the Archaeological Record," *African Archaeological Review*, 21, 89–128. https://doi.org/10.1023/B:AARR.0000030786.24067.19.

Kavzoglu, T., and Colkesen, I. (2009), "A kernel functions analysis for support vector machines for land cover classification," *International Journal of Applied Earth Observation and Geoinformation*, 11, 352–359.

Kavzoglu, T., Colkesen, I., and Yomralioglu, T. (2015), "Object-based classification with rotation forest ensemble learning algorithm using very-high-resolution WorldView-2 image," *Remote Sensing Letters*, 6, 834–843. https://doi.org/10.1080/2150704X.2015.1084550.

Keay, S. J., Parcak, S. H., and Strutt, K. D. (2014), "High resolution space and ground-based remote sensing and implications for landscape archaeology: the case from Portus, Italy," *Journal of Archaeological Science*, 52, 277–292.

Keeney, J., and Hickey, R. (2015), "Using satellite image analysis for locating prehistoric archaeological sites in Alaska's Central Brooks Range," *Journal of Archaeological Science: Reports*, 3, 80–89.

Keitumetse, S. O. (2011), "Sustainable development and cultural heritage management in Botswana: Towards sustainable communities," *Sustainable Development*, 19, 49–59.

Khandlhela, M., and May, J. (2006), "Poverty, vulnerability and the impact of flooding in the Limpopo Province, South Africa," *Natural Hazards*, 39, 275–287.

Kim, N. C., and Kusimba, C. M. (2008), "Pathways to Social Complexity and State Formation in the Southern Zambezian Region," *African Archaeological Review*, 25, 131–152. https://doi.org/10.1007/s10437-008-9031-3.

Klapwijk, M. (1974), "A preliminary report on pottery from the north-eastern Transvaal, South Africa," *The South African Archaeological Bulletin*, 19–23.

Klapwijk, M., and Huffman, T. N. (1996), "Excavations at Silver Leaves: a final report," *The South African Archaeological Bulletin*, 84–93.

Klehm, C., Barnes, A., Follett, F., Simon, K., Kiahtipes, C., and Mothulatshipi, S. (2019), "Toward archaeological predictive modeling in the Bosutswe region of Botswana: Utilizing multispectral satellite imagery to conceptualize ancient landscapes," *Journal of Anthropological Archaeology*, 54, 68–83. https://doi.org/10.1016/j.jaa.2019.02.002.

Klehm, C. E. (2017), "Local Dynamics and the Emergence of Social Inequality in Iron Age Botswana," *Current Anthropology*, 58, 604–633. https://doi.org/10.1086/693960.

Klehm, C. E., and Ernenwein, E. G. (2016), "Iron Age Transformations at Mmadipudi Hill, Botswana: Identifying Spatial Organization Through Electromagnetic Induction Survey," *African Archaeological Review*, 33, 45–59.

Klehm, C., and Gokee, C. (2020), "Geospatial Analysis in African Archaeology: Current Theories, Topics, and Methods," *African Archaeological Review*, 37, 1–7. https://doi.org/10.1007/s10437-020-09376-9.

Klein, R. G. (1986), "The prehistory of stone age herders in the Cape Province of South Africa," *Goodwin Series*, 5–12.

Klein, R. G. (2000), "The Earlier Stone Age of Southern Africa," *The South African Archaeological Bulletin*, 55, 107. https://doi.org/10.2307/3888960.

Knorn, J., Rabe, A., Radeloff, V. C., Kuemmerle, T., Kozak, J., and Hostert, P. (2009), "Land cover mapping of large areas using chain classification of neighboring Landsat satellite images," *Remote Sensing of Environment*, 113, 957–964.

Kokaly, R. F. (2001), "Investigating a physical basis for spectroscopic estimates of leaf nitrogen concentration," *Remote Sensing of Environment*, 75, 153–161.

Kokaly, R. F. (2016), "Evaluating impacts of imaging spectrometer calibration on mineral identification and mapping using airborne data collections in Alaska, USA, and Khandahar, Afghanistan," in *2016 IEEE International Geoscience and Remote Sensing Symposium (IGARSS)*, pp. 1931–1934. https://doi.org/10.1109/IGARSS.2016.7729497.

Kopačková, V., and Koucká, L. (2017), "Integration of Absorption Feature Information from Visible to Longwave Infrared Spectral Ranges for Mineral Mapping," *Remote Sensing*, 9, 1006.

Kröpelin, S., Versch0uren, D., Lézine, A.-M., Eggermont, H., Cocquyt, C., Francus, P., Cazet, J.-P., Fagot, M., Rumes, B., and Russell, J. M. (2008), "Climate-Driven Ecosystem Succession in the Sahara: The Past 6000 Years," *science*, 320, 765–768.

Kruse, F. A., Boardman, J. W., and Huntington, J. F. (2003), "Comparison of airborne hyperspectral data and EO-1 Hyperion for mineral mapping," *IEEE Transactions on Geoscience and Remote Sensing*, 41, 1388–1400. https://doi.org/10.1109/TGRS.2003.812908.

Kuman, K., Le Baron, J. C., and Gibbon, R. J. (2005), "Earlier stone age archaeology of the Vhembe-Dongola National Park (South Africa) and vicinity," *Quaternary International*, 129, 23–32.

Kuper, R., and Kröpelin, S. (2006), "Climate-controlled Holocene occupation in the Sahara: motor of Africa's evolution," *Science*, 313, 803–807.

Kusimba, S. B. (1999), "Hunter–gatherer land use patterns in Later Stone Age East Africa," *Journal of Anthropological Archaeology*, 18, 165–200.

Kusimba, S. B. (2005), "What is a hunter-gatherer? Variation in the archaeological record of eastern and southern Africa," *Journal of Archaeological Research*, 13, 337–366.

Lagacherie, P., Baret, F., Feret, J.-B., Netto, J. M., and Robbez-Masson, J. M. (2008), "Estimation of soil clay and calcium carbonate using laboratory, field and airborne hyperspectral measurements," *Remote Sensing of Environment*, 112, 825–835.

Lakhdari, W., and Dehliz, A. (2016), "Ethnobotanical study of some plants used in traditional medicine in the region of Oued Righ (Algerian Sahara)," *Journal of Medicinal Plants*, 4, 204–211.

Lane, P. (2013), "The archaeology of pastoralism and stock-keeping in East Africa," in *The Oxford Handbook of African Archaeology*, eds. P. Mitchell and P. Lane, Oxford: Oxford University Press, pp. 585–602.

Lane, P. J. (2011), "Future urban growth and archaeological heritage management: Some implications for research activity in Africa," *Conservation and Management of Archaeological Sites*, 13, 134–159.

Lange, D. (2007), "The emergence of Social complexity in the Southern Chad Basin towards 500 BC: Archaeological and other evidence," *Borno Museum Society Newsletter*, 1, 68–71.

Lanza, S. G. (2003), "Flood hazard threat on cultural heritage in the town of Genoa (Italy)," *Journal of Cultural Heritage*, 4, 159–167. https://doi.org/10.1016/S1296-2074(03)00042-6.

Lasaponara, R., Elfadaly, A., and Attia, W. (2016a), "Low Cost Space Technologies for Operational Change Detection Monitoring Around the Archaeological Area of Esna-Egypt," in *Computational Science and Its Applications – ICCSA 2016*, Lecture Notes in Computer Science, eds. O. Gervasi, B. Murgante, S. Misra, A. M. A. C. Rocha, C. M. Torre, D. Taniar, B. O. Apduhan, E. Stankova, and S. Wang, Springer International Publishing, pp. 611–621.

Lasaponara, R., Lanorte, A., Coluzzi, R., and Masini, N. (2007), "Quickbird imagery processing for archaeological applications: performance evaluation from data fusion algorithms," *XXI. International Symposium CIPA 2007*.

Lasaponara, R., Leucci, G., Masini, N., and Persico, R. (2014), "Investigating archaeological looting using satellite images and GEORADAR: the experience in Lambayeque in North Peru," *Journal of Archaeological Science*, 42, 216–230.

Lasaponara, R., Leucci, G., Masini, N., Persico, R., and Scardozzi, G. (2016b), "Towards an operative use of remote sensing for exploring the past using satellite data: The case study of Hierapolis (Turkey)," *Remote Sensing of Environment*, 174, 148–164.

Lasaponara, R., and Masini, N. (2005), "QuickBird-based analysis for the spatial characterization of archaeological sites: Case study of the Monte Serico medieval village," *Geophysical Research Letters*, 32. https://doi.org/10.1029/2005GL022445.

Lasaponara, R., and Masini, N. (2006), "Identification of archaeological buried remains based on the normalized difference vegetation index (NDVI) from quickbird satellite data," *IEEE Geoscience and Remote Sensing Letters*, 3, 325–328.

Lasaponara, R., and Masini, N. (2007), "Detection of archaeological crop marks by using satellite QuickBird multispectral imagery," *Journal of Archaeological Science*, 34, 214–221.

Lasaponara, R., and Masini, N. (2011), "Satellite remote sensing in archaeology: Past, present and future perspectives," *Journal of Archaeological Science*, 38, 1995–2496. https://doi.org/10.1016/j.jas.2011.02.002.

Lasaponara, R., and Masini, N. (eds.) (2012), *Satellite Remote Sensing: A New Tool for Archaeology*, Dordrecht: Springer Science & Business Media.

Lasaponara, R., and Masini, N. (2013), "Remote Sensing in Archaeology: an overview," *Journal of Aeronautics and Space Technologies*, 6, 7–17.

Lasaponara, R., Masini, N., Rizzo, E., and Orefici, G. (2011), "New discoveries in the Piramide Naranjada in Cahuachi (Peru) using satellite, Ground Probing Radar and magnetic investigations," *Journal of Archaeological Science*, Satellite remote sensing in archaeology: past, present and future perspectives, 38, 2031–2039. https://doi.org/10.1016/j.jas.2010.12.010.

Lavachery, P., MacEachern, S., Bouimon, T., Gouem, B. G., Kinyock, P., Mbairo, J., and Nkonkonda, O. (2005), "KOMÉ TO EBOMÉ: ARCHAEOLOGICAL RESEARCH FOR THE CHAD EXPORT PROJECT, 1999-2003," *Journal of African Archaeology*, 3, 20.

LaViolette, A. (2008), "Swahili cosmopolitanism in Africa and the Indian Ocean world, AD 600–1500," *Archaeologies*, 4, 24–49.

LaViolette, A., and Fleisher, J. (2005), "The archaeology of sub-Saharan urbanism: cities and their countrysides," in *African archaeology: A critical introduction*, ed. A. B. Stahl, Oxford, UK: Blackwell Publishing, pp. 327–352.

Lawrence, R. L., Wood, S. D., and Sheley, R. L. (2006), "Mapping invasive plants using hyperspectral imagery and Breiman Cutler classifications (RandomForest)," *Remote Sensing of Environment*, 100, 356–362.

Le Baron, J. C., Kuman, K., and Grab, S. W. (2010), "The landscape distribution of Stone Age artefacts on the Hacthorne Plateau, Limpopo River Valley, South Africa," *South African Archaeological Bulletin*, 65, 123–131.

Le Houérou, H. N. (2001), "Biogeography of the arid steppeland north of the Sahara," *Journal of Arid Environments*, 48, 103–128.

Lebedev, A. V., Westman, E., Van Westen, G. J. P., Kramberger, M. G., Lundervold, A., Aarsland, D., Soininen, H., Kłoszewska, I., Mecocci, P., and Tsolaki, M. (2014), "Random Forest ensembles for detection and prediction of Alzheimer's disease with a good between-cohort robustness," *NeuroImage: Clinical*, 6, 115–125.

de Leeuw, J., Jia, H., Yang, L., Liu, X., Schmidt, K., and Skidmore, A. K. (2006), "Comparing accuracy assessments to infer superiority of image classification methods," *International Journal of Remote Sensing*, 27, 223–232.

Leisz, S. J. (2013), "An overview of the application of remote sensing to archaeology during the twentieth century," in *Mapping archaeological landscapes from space*, Springer, pp. 11–19.

di Lernia, S. (2006), "Building monuments, creating identity: Cattle cult as a social response to rapid environmental changes in the Holocene Sahara," *Quaternary International*, 151, 50–62.

di Lernia, S. (2013), "The emergence and spread of herding in Northern Africa: a critical reappraisal," in *Oxford handbook of African archaeology.*, eds. P. Mitchell and P. Lane, Oxford: Oxford University Press, pp. 527–540.

Leucci, G., Negri, S., and Ricchetti, E. (2002), "Integration of high resolution optical satellite imagery and geophysical survey for archaeological prospection in Hierapolis (Turkey)," IEEE, pp. 1991–1993. https://doi.org/10.1109/IGARSS.2002.1026423.

Li, M., Ma, L., Blaschke, T., Cheng, L., and Tiede, D. (2016), "A systematic comparison of different object-based classification techniques using high spatial resolution imagery in agricultural environments," *International Journal of Applied Earth Observation and Geoinformation*, 49, 87–98.

Li, Q., Wang, C., Zhang, B., and Lu, L. (2015a), "Object-based crop classification with Landsat-MODIS enhanced time-series data," *Remote Sensing*, 7, 16091–16107.

Li, S., Wu, H., Wan, D., and Zhu, J. (2011), "An effective feature selection method for hyperspectral image classification based on genetic algorithm and support vector machine," *Knowledge-Based Systems*, 24, 40–48.

Li, W., Chen, C., Su, H., and Du, Q. (2015b), "Local Binary Patterns and Extreme Learning Machine for Hyperspectral Imagery Classification," *IEEE Trans. Geoscience and Remote Sensing*, 53, 3681–3693.

Lightfoot, D. R., and Miller, J. A. (1996), "Sijilmassa: The rise and fall of a walled oasis in medieval Morocco," *Annals of the association of American geographers*, 86, 78–101.

Lillesand, T., Kiefer, R. W., and Chipman, J. (2008), *Remote sensing and image interpretation*, New York: John Wiley & Sons.

Lin, F., Yeh, C.-C., and Lee, M.-Y. (2011), "The use of hybrid manifold learning and support vector machines in the prediction of business failure," *Knowledge-Based Systems*, 24, 95–101. https://doi.org/10.1016/j.knosys.2010.07.009.

Lin, H.-T., and Lin, C.-J. (2003), "A study on sigmoid kernels for SVM and the training of non-PSD kernels by SMO-type methods," *Neural Computation*, 1–32.

Liu, M., Liu, X., Liu, D., Ding, C., and Jiang, J. (2015), "Multivariable integration method for estimating sea surface salinity in coastal waters from in situ data and remotely sensed data using random forest algorithm," *Computers & Geosciences*, 75, 44–56. https://doi.org/10.1016/j.cageo.2014.10.016.

Liverani, M. (2000), "The Garamantes: A Fresh Approach," *Libyan Studies*, 31, 17–28. https://doi.org/10.1017/S0263718900005306.

Lombard, M. (2013), "Hunter-Gatherers in Southern Africa Before 20,000 Years Ago," in *The Oxford Handbook of African Archaeology*, eds. P. Mitchell and P. Lane, Oxford: Oxford University Press.

Lovegrove, B. (1993), *The living deserts of southern Africa*, Cape Town: Fernwood Press.

Lu, D., and Weng, Q. (2007), "A survey of image classification methods and techniques for improving classification performance," *International Journal of Remote Sensing*, 28, 823–870.

Luo, H., Wang, L., Shao, Z., and Li, D. (2015), "Development of a multi-scale object-based shadow detection method for high spatial resolution image," *Remote Sensing Letters*, 6, 59–68.

Luo, L., Wang, X., Liu, C., Guo, H., and Du, X. (2014), "Integrated RS, GIS and GPS approaches to archaeological prospecting in the Hexi Corridor, NW China: a case study of the royal road to ancient Dunhuang," *Journal of Archaeological Science*, 50, 178–190. https://doi.org/10.1016/j.jas.2014.07.009.

Luzzadder-Beach, S., Beach, T., Terry, R. E., and Doctor, K. Z. (2011), "Elemental prospecting and geoarchaeology in Turkey and Mexico," *Catena*, 85, 119–129.

Ma, J.-P., Zheng, Z.-B., Tong, Q.-X., and Zheng, L.-F. (2003), "An application of genetic algorithms on band selection for hyperspectral image classification," in *Machine Learning and Cybernetics, 2003 International Conference on*, IEEE, pp. 2810–2813.

Mabulla, A. Z. P. (2001), "Strategy for Cultural Heritage Management (CHM) in Africa: A Case Study," *African Archaeological Review*, 23.

MacDonald, K. (2013), "Complex societies, urbanism, and trade in the Western Sahel," in *The Oxford Handbook of African Archaeology*, eds. P. Mitchell and P. Lane, Oxford: University of Oxford Press, pp. 829–844.

MacDonald, K. C., Vernet, R., Fuller, D., and Woodhouse, J. (2003), "New Light on the Tichitt Tradition: A preliminary report on survey and excavation at Dhar Nema," in *Researching Africa's past: New contributions from British Archaeologists*, eds. P. Mitchell, A. Haour, and J. Hobart, Oxford: Oxford University School of Archaeology, pp. 73–80.

MacEachern, S. (2001), "Cultural resource management and Africanist archaeology," *Antiquity*, 75, 866–871. https://doi.org/10.1017/S0003598X00089444.

Maggs, T. M. O. (1984), "The Iron Age south of the Zambezi," in *Southern African prehistory and palaeoenvironments*, ed. R. G. Klein, Rotterdam: A. A. Balkema Publishers, pp. 329–360.

Malika, B., Mostafa, D. B., Hacina, S., and Mohamed, O. E. H. (2015), "Distribution study of some species of spontaneous Flora in two Saharan Regions of the North-East of Algeria (Ouargla and Ghardaa)," *International Journal of Biodiversity and Conservation*, 7, 41–47.

Malville, J. M., Schild, R., Wendorf, F., and Brenmer, R. (2008), "Astronomy of Nabta Playa," in *African Cultural Astronomy*, Astrophysics and Space Science Proceedings, eds. J. C. Holbrook, J. O. Urama, and R. T. Medupe, Dordrecht: Springer Netherlands, pp. 131–143. https://doi.org/10.1007/978-1-4020-6639-9_11.

Manning, K., Pelling, R., Higham, T., Schwenniger, J.-L., and Fuller, D. Q. (2011), "4500-year old domesticated pearl millet (Pennisetum glaucum) from the Tilemsi Valley, Mali: new insights into an alternative cereal domestication pathway," *Journal of Archaeological Science*, 38, 312–322.

Mansour, K., Mutanga, O., Everson, T., and Adam, E. (2012), "Discriminating indicator grass species for rangeland degradation assessment using hyperspectral data resampled to AISA Eagle resolution," *ISPRS Journal of Photogrammetry and Remote Sensing*, 70, 56–65.

Manyanga, M. (2007), "Resilient landscapes socio-environmental dynamics in the Shashi-Limpopo basin, Southern Zimbabwe C. AD 800 to the present," Uppsala: Societa Archaeologica Uppsaliensis.

Manyanga, M., Pikirayi, I., and Ndoro, W. (2000), "Coping with Dryland Environments : Preliminary Results from Mapungubwe and Zimbabwe Phase Sites in the Mateke Hills , South-Eastern Zimbabwe," *Goodwin Series*, 8, 69–77.

Marshall, F., and Hildebrand, E. (2002), "Cattle before crops: the beginnings of food production in Africa," *Journal of World Prehistory*, 16, 99–143.

Marshall, F., Reid, R. E. B., Goldstein, S., Storozum, M., Wreschnig, A., Hu, L., Kiura, P., Shahack-Gross, R., and Ambrose, S. H. (2018), "Ancient herders enriched and restructured African grasslands," *Nature*, 561, 387–390. https://doi.org/10.1038/s41586-018-0456-9.

Marshall, F., Stewart, K., and Barthelme, J. (1984), "Early domestic stock at Dongodien in northern Kenya," *AZANIA: Journal of the British Institute in Eastern Africa*, 19, 120–127.

Mas, J. F., and Flores, J. J. (2008), "The application of artificial neural networks to the analysis of remotely sensed data," *International Journal of Remote Sensing*, 29, 617–663.
Mashimbye, P. M. (2013), "Spherulites: evidence of herding strategies at Mapungubwe," Johannesburg: University of the Witwatersrand.
Masini, N., and Lasaponara, R. (2007), "Investigating the spectral capability of QuickBird data to detect archaeological remains buried under vegetated and not vegetated areas," *Journal of Cultural Heritage*, 8, 53–60.
Masini, N., Lasaponara, R., and Orefici, G. (2009), "Addressing the challenge of detecting archaeological adobe structures in Southern Peru using QuickBird imagery," *Journal of Cultural Heritage*, ICT and Remote sensing for Cultural Resource Management and Documentation, 10, e3–e9. https://doi.org/10.1016/j.culher.2009.10.005.
Mason, R. J. (1968), "Transvaal and Natal Iron Age settlement revealed by aerial photography and excavation," *African studies*, 27, 167–180.
Mathieu, R., Aryal, J., and Chong, A. (2007), "Object-based classification of Ikonos imagery for mapping large-scale vegetation communities in urban areas," *Sensors*, 7, 2860–2880.
Matthew, M. W., Adler-Golden, S. M., Berk, A., Felde, G., Anderson, G. P., Gorodetzky, D., Paswaters, S., and Shippert, M. (2002), "Atmospheric correction of spectral imagery: evaluation of the FLAASH algorithm with AVIRIS data," IEEE, pp. 157–163.
Mattingly, D. J. (2011), "The Garamantes of Fazzan. An early Libyan state with trans-Saharan connections," in *Money, trade and trade routes in pre-Islamic North Africa*, eds. A. Dowler and E. R. Galvin, London: The British Museum Press, pp. 49–60.
Mattingly, D. J., Lahr, M., Armitage, S., Barton, H., Dore, J., Drake, N., Foley, R., Merlo, S., Salem, M., and Stock, J. (2007), "Desert Migrations: people, environment and culture in the Libyan Sahara," *Libyan Studies*, 38, 115–156.
Mattingly, D. J., Reynolds, T., and Dore, J. (2003), "Synthesis of human activities in Fazzan," in *The archaeology of Fazzan*, eds. D. J. Mattingly, C. M. Daniels, J. N. Dore, D. Edwards, and J. Hawthorne, London: Society for Libyan Studies, pp. 327–373.
Mattingly, D. J., and Sterry, M. (2013), "The first towns in the central Sahara," *Antiquity*, 87, 503–518.
Maxwell, A. E., Warner, T. A., Strager, M. P., Conley, J. F., and Sharp, A. L. (2015), "Assessing machine-learning algorithms and image- and lidar-derived variables for GEOBIA classification of mining and mine reclamation," *International Journal of Remote Sensing*, 36, 954–978. https://doi.org/10.1080/01431161.2014.1001086.
McBrearty, S., and Brooks, A. S. (2000), "The revolution that wasn't: a new interpretation of the origin of modern human behavior," *Journal of Human Evolution*, 39, 453–563. https://doi.org/10.1006/jhev.2000.0435.
McCauley, J. F., Breed, C. S., Schaber, G. G., McHugh, W. P., Issawi, B., Haynes, C. V., Grolier, M. J., and El Kilani, A. (1986), "Paleodrainages of the Eastern Sahara-The Radar Rivers Revisited (SIR-A/B Implications for a Mid-Tertiary Trans-Afnrcan Drainage System)," *IEEE Transactions on Geoscience and Remote Sensing*, 624–648.
McCauley, J. F., Schaber, G. G., Breed, C. S., Grolier, M. J., Haynes, C. V., Issawi, B., Elachi, C., and Blom, R. (1982), "Subsurface valleys and geoarcheology of the eastern Sahara revealed by shuttle radar," *Science*, 218, 1004–1020.
McDonald, J. H. (2009a), *Handbook of biological statistics*, Sparky House Publishing Baltimore, MD.
McDonald, M. M. A. (2009b), "Increased sedentism in the central oases of the Egyptian Western Desert in the early to mid-Holocene: Evidence from the peripheries," *African Archaeological Review*, 26, 3–43.

McHenry, H. M., and Coffing, K. (2000), "Australopithecus to Homo: transformations in body and mind," *Annual review of Anthropology*, 125–146.
McHugh, M. L. (2012), "Interrater reliability: the kappa statistic," *Biochemia medica: Biochemia medica*, 22, 276–282.
Mcintosh, S. K. (1993), "Archaeological heritage management and site inventory systems in Africa," *Journal of Field Archaeology*, 20, 500–504.
McIntosh, S. K., and McIntosh, R. J. (1988), "From stone to metal: New perspectives on the later prehistory of West Africa," *Journal of World Prehistory*, 2, 89–133.
McIntosh, S. K., and McIntosh, R. J. (1993), "Field survey in the tumulus zone of Senegal," *African Archaeological Review*, 11, 73–107.
Megarry, W. P., Cooney, G., Comer, D. C., and Priebe, C. E. (2016), "Posterior probability modeling and image classification for archaeological site prospection: Building a survey efficacy model for identifying neolithic felsite workshops in the Shetland Islands," *Remote Sensing*, 8, 529.
Meister, C. (2008), "Recent archaeological investigations in the tropical rainforest of South-West Cameroon," in *Dynamics of Forest Ecosystems in Central Africa During the Holocene: Past – Present – Future: Palaeoecology of Africa, An International Yearbook of Landscape Evolution and Palaeoenvironments*, ed. J. Runge, Leiden: CRC Press, pp. 43–58.
Melgani, F., and Bruzzone, L. (2004), "Classification of Hyperspectral Remote Sensing Images With Support Vector Machines," *IEEE TRANSACTIONS ON GEOSCIENCE AND REMOTE SENSING*, 42.
Melillos, M., Themistocleous, K., Agapiou, A., Michaelides, S., and Hadjimitsis, D. G. (2018), "Detecting underground structures in Cyprus using field spectroscopy," in *Sixth International Conference on Remote Sensing and Geoinformation of the Environment (RSCy2018)*, Paphos, Cyprus: Proc. SPIE 10773.
Mercader, J. (2002), "Forest people: The role of African rainforests in human evolution and dispersal," *Evolutionary Anthropology: Issues, News, and Reviews*, 11, 117–124. https://doi.org/10.1002/evan.10022.
Mercuri, A. M. (2008), "Plant exploitation and ethnopalynological evidence from the Wadi Teshuinat area (Tadrart Acacus, Libyan Sahara)," *Journal of Archaeological science*, 35, 1619–1642.
Metternicht, G., Zinck, J. A., Blanco, P. D., and Del Valle, H. F. (2010), "Remote sensing of land degradation: Experiences from Latin America and the Caribbean," *Journal of environmental quality*, 39, 42–61.
Meyer, A. (2000), "K2 and Mapungubwe," *Goodwin Series*, 4–13.
Meyer, D., Dimitriadou, E., Hornik, K., Weingessel, A., Leisch, F., Chang, C.-C., Lin, C.-C., and Meyer, M. D. (2017), "Package 'e1071.'"
Middleton, W. D. (2004), "Identifying chemical activity residues on prehistoric house floors: a methodology and rationale for multi-elemental characterization of a mild acid extract of anthropogenic sediments," *Archaeometry*, 46, 47–65.
Middleton, W. D., and Price, D. T. (1996), "Identification of Activity Areas by Multi-element Characterization of Sediments from Modern and Archaeological House Floors Using Inductively Coupled Plasma-atomic Emission Spectroscopy," *Journal of Archaeological Science*, 23, 673–687. https://doi.org/DOI: 10.1006/jasc.1996.0064.
Milton, S. J., and Dean, W. R. J. (2000), "Disturbance, drought and dynamics of desert dune grassland, South Africa," *Plant Ecology*, 150, 37–51.
Mitchell, P. (2002), *The archaeology of southern Africa*, Cambridge: Cambridge University Press.

Mitchell, P. (2013), “Early Farming Communities of Southern and South-Central Africa,” in *The Oxford Handbook of African Archaeology*, eds. P. Mitchell and P. J. Lane, Oxford: Oxford University Press, pp. 657–670.

Mitchell, P. J. (1997), “Holocene Later Stone Age Hunter-Gatherers South of the Limpopo River, Ca. 10,000–2000 B.P.,” *Journal of World Prehistory*, 11, 359–424.

Mitchell, P., and Lane, P. J. (2013), “Introducing African Archaeology,” in *The Oxford Handbook of African Archaeology*, eds. P. Mitchell and P. J. Lane, Oxford: Oxford University Press. https://doi.org/10.1093/oxfordhb/9780199569885.013.0001.

Mondino, E. B., Perotti, L., and Piras, M. (2012), “High resolution satellite images for archeological applications: the Karima case study (Nubia region, Sudan),” *European Journal of Remote Sensing*, 45, 243–259. https://doi.org/10.5721/EuJRS20124522.

Morales, J., Jordà, G. P., Pena-Chocarro, L., Bokbot, Y., Vera, J. C., Sánchez, R. M. M., and Linstädter, J. (2016), “The introduction of South-Western Asian domesticated plants in North-Western Africa: an archaeobotanical contribution from Neolithic Morocco,” *Quaternary International*, 412, 96–109.

Morton, F. (2013), “Settlements, landscapes and identities among the Tswana of the western Transvaal and eastern Kalahari before 1820,” *The South African Archaeological Bulletin*, 68(197), 15–26.

Mosothwane, M. N. (2011), “The Tuli mummy: A preliminary report from northeastern botswana,” *South African Archaeological Bulletin*, 66, 157.

Mothulatshipi, S. M. (2008), “Landscape Archaeology of the Later Farming Communities of the Shashe Limpopo Basin, Eastern Botswana: Land use Diversity and Human Behaviour,” Unpublished PhD thesis: University of Edinburgh.

Mountrakis, G., Im, J., and Ogole, C. (2011), “Support vector machines in remote sensing: A review,” *ISPRS Journal of Photogrammetry and Remote Sensing*, 66, 247–259.

Mulder, V. L., De Bruin, S., Schaepman, M. E., and Mayr, T. R. (2011), “The use of remote sensing in soil and terrain mapping—A review,” *Geoderma*, 162, 1–19.

Mumford, G., and Parcak, S. H. (2002), “Satellite image analysis and archaeological fieldwork in El-Markha Plain (South Sinai),” *Antiquity*, 76, 953–954.

Munson, P. J. (1980), “Archaeology and the prehistoric origins of the Ghana empire,” *The Journal of African History*, 21, 457–466.

Mureriwa, N., Adam, E., Sahu, A., and Tesfamichael, S. (2016), “Examining the spectral separability of Prosopis glandulosa from co-existent species using field spectral measurement and guided regularized random forest,” *Remote Sensing*, 8, 144.

Musyoki, A., Thifhulufhelwi, R., and Murungweni, F. M. (2016), “The impact of and responses to flooding in Thulamela Municipality, Limpopo Province, South Africa,” *Jàmbá : Journal of Disaster Risk Studies*, 8. https://doi.org/10.4102/jamba.v8i2.166.

Mutanga, O., Adam, E., Adjorlolo, C., and Abdel-Rahman, E. M. (2015), “Evaluating the robustness of models developed from field spectral data in predicting African grass foliar nitrogen concentration using WorldView-2 image as an independent test dataset,” *International Journal of Applied Earth Observation and Geoinformation*, 34, 178–187.

Mutanga, O., Adam, E., and Cho, M. A. (2012), “High density biomass estimation for wetland vegetation using WorldView-2 imagery and random forest regression algorithm,” *International Journal of Applied Earth Observation and Geoinformation*, 18, 399–406.

Myers, A. (2010), “Field work in the age of digital reproduction: a review of the potentials and limitations of Google Earth for archaeologists,” *SAA Archaeological Record*, 10.

Myers, N. (1988), “Threatened biotas:" hot spots" in tropical forests,” *Environmentalist*, 8, 187–208.

Myint, S. W., Gober, P., Brazel, A., Grossman-Clarke, S., and Weng, Q. (2011), "Per-pixel vs. object-based classification of urban land cover extraction using high spatial resolution imagery," *Remote sensing of environment*, 115, 1145–1161.

Na, X., Zhang, S., Li, X., Yu, H., and Liu, C. (2010), "Improved land cover mapping using random forests combined with landsat thematic mapper imagery and ancillary geographic data," *Photogrammetric Engineering & Remote Sensing*, 76, 833–840.

Nawar, S., Buddenbaum, H., Hill, J., and Kozak, J. (2014), "Modeling and mapping of soil salinity with reflectance spectroscopy and landsat data using two quantitative methods (PLSR and MARS)," *Remote Sensing*, 6, 10813–10834.

Nawar, S., Buddenbaum, H., Hill, J., Kozak, J., and Mouazen, A. M. (2016), "Estimating the soil clay content and organic matter by means of different calibration methods of vis-NIR diffuse reflectance spectroscopy," *Soil and Tillage Research*, 155, 510–522.

Nguyen, T.-T., Zhao, H., Huang, J. Z., Nguyen, T. T., and Li, M. J. (2015), "A New Feature Sampling Method in Random Forests for Predicting High-Dimensional Data," Springer, pp. 459–470.

Nicodemus, K. K., Malley, J. D., Strobl, C., and Ziegler, A. (2010), "The behaviour of random forest permutation-based variable importance measures under predictor correlation," *BMC bioinformatics*, 11, 110.

Nienaber, W. C., Keough, N., Steyn, M., and Meiring, J. H. (2008), "Reburial of the Mapungubwe Human Remains: An Overview of Process and Procedure," *The South African Archaeological Bulletin*, 63, 164–169. https://doi.org/10.2307/20475012.

Nikita, E., Ysi Siew, Y., Stock, J., Mattingly, D., and Mirazón Lahr, M. (2011), "Activity patterns in the Sahara Desert: An interpretation based on cross-sectional geometric properties," *American journal of physical anthropology*, 146, 423–434.

Nocita, M., Stevens, A., Toth, G., Panagos, P., van Wesemael, B., and Montanarella, L. (2014), "Prediction of soil organic carbon content by diffuse reflectance spectroscopy using a local partial least square regression approach," *Soil Biology and Biochemistry*, 68, 337–347.

Noi, P. T., and Kappas, M. (2018), "Comparison of Random Forest, k-Nearest Neighbor, and Support Vector Machine Classifiers for Land Cover Classification Using Sentinel-2 Imagery," *Sensors*, 18, 18. https://doi.org/10.3390/s18010018.

Nolet, C., Poortinga, A., Roosjen, P., Bartholomeus, H., and Ruessink, G. (2014), "Measuring and modeling the effect of surface moisture on the spectral reflectance of coastal beach sand," *PloS one*, 9, e112151.

Nsanziyera, A. F., Rhinane, H., Oujaa, A., and Mubea, K. (2018), "GIS and Remote-Sensing Application in Archaeological Site Mapping in the Awsard Area (Morocco)," *Geosciences*, 8, 207. https://doi.org/10.3390/geosciences8060207.

Nyamushosho, R. T. (2017), "Living on the margin?: The Iron Age communities of Mananzve Hill, Shashi region, South-western Zimbabwe," Cape Town: University of Cape Town.

Ogen, Y., Goldshleger, N., and Ben-Dor, E. (2017), "3D spectral analysis in the VNIR–SWIR spectral region as a tool for soil classification," *Geoderma*, 302, 100–110.

Ogen, Y., Neumann, C., Chabrillat, S., Goldshleger, N., and Ben-Dor, E. (2018), "Evaluating the detection limit of organic matter using point and imaging spectroscopy," *Geoderma*, 321, 100–109.

Ogundiran, A. (2013), "Towns and states of the West African forest belt," in *The Oxford handbook of African Archaeology*, eds. P. Mitchell and P. Lane, Oxford: Oxford University Press, pp. 859–874.

Oonk, S., Slomp, C. P., Huisman, D. J., and Vriend, S. P. (2009), "Geochemical and mineralogical investigation of domestic archaeological soil features at the Tiel-Passewaaij site, The Netherlands," *Journal of Geochemical Exploration*, 101, 155–165.

Oonk, S., and Spijker, J. (2015), "A supervised machine-learning approach towards geochemical predictive modelling in archaeology," *Journal of Archaeological Science*, 59, 80–88.

Opitz, R., and Herrmann, J. (2018), "Recent Trends and Long-standing Problems in Archaeological Remote Sensing," *Journal of Computer Applications in Archaeology*, 1, 19–41. https://doi.org/10.5334/jcaa.11.

Osicki, A., and Sjogren, D. (2000), "A review of remote sensing application in archaeological research," *Geography*, 795, 1–21.

Oslisly, R., White, L., Bentaleb, I., Favier, C., Fontugne, M., Gillet, J., and Sebag, D. (2013), "Climatic and cultural changes in the west Congo Basin forests over the past 5000 years," *Philosophical Transactions of the Royal Society B: Biological Sciences*, 368, 20120304. https://doi.org/10.1098/rstb.2012.0304.

Otto, F. E. L., Jones, R. G., Halladay, K., and Allen, M. R. (2013), "Attribution of changes in precipitation patterns in African rainforests," *Philosophical Transactions of the Royal Society of London B: Biological Sciences*, 368, 20120299.

Oumar, Z., and Mutanga, O. (2010), "Predicting plant water content in Eucalyptus grandis forest stands in KwaZulu-Natal, South Africa using field spectra resampled to the Sumbandila Satellite Sensor," *International Journal of Applied Earth Observation and Geoinformation*, 12, 158–164. https://doi.org/10.1016/j.jag.2010.02.002.

Ouyang, Z., Zhang, M., Xie, X., Shen, Q., Guo, H., and Zhao, B. (2011), "A comparison of pixel-based and object-oriented approaches to VHR imagery for mapping saltmarsh plants," *Ecological Informatics*, 6, 136–146. https://doi.org/10.1016/j.ecoinf.2011.01.002.

Pal, M., and Mather, P. M. (2005), "Support vector machines for classification in remote sensing," *International Journal of Remote Sensing*, 26, 1007–1011.

Pan, Y., Nie, Y., Watene, C., Zhu, J., and Liu, F. (2017), "Phenological Observations on Classical Prehistoric Sites in the Middle and Lower Reaches of the Yellow River Based on Landsat NDVI Time Series," *Remote Sensing*, 9, 374.

Parcak, S. H. (2007), "Satellite remote sensing methods for monitoring archaeological tells in the Middle East," *Journal of Field Archaeology*, 32, 65–81.

Parcak, S. H. (2009), *Satellite Remote Sensing for Archaeology*, Routledge.

Parcak, S. H. (2015), "Archaeological looting in Egypt: A geospatial view (Case Studies from Saqqara, Lisht, and el Hibeh)," *Near Eastern Archaeology*, 78, 196–203.

Parcak, S. H., Gathings, D., Childs, C., Mumford, G., and Cline, E. (2016), "Satellite evidence of archaeological site looting in Egypt: 2002–2013," *Antiquity*, 90, 188–205.

Parcak, S. H., Mumford, G., and Childs, C. (2017), "Using Open Access Satellite Data Alongside Ground Based Remote Sensing: An Assessment, with Case Studies from Egypt's Delta," *Geosciences*, 7, 94. https://doi.org/10.3390/geosciences7040094.

Parnell, J. J., Terry, R. E., and Nelson, Z. (2002), "Soil chemical analysis applied as an interpretive tool for ancient human activities in Piedras Negras, Guatemala," *Journal of Archaeological Science*, 29, 379–404.

Patruno, J., Fitrzyk, M., and Blasco, J. M. D. (2020), "Monitoring and Detecting Archaeological Features with Multi-Frequency Polarimetric Analysis," *Remote Sensing*, Multidisciplinary Digital Publishing Institute, 12, 1. https://doi.org/10.3390/rs12010001.

Pelletier, C., Valero, S., Inglada, J., Champion, N., and Dedieu, G. (2016), "Assessing the robustness of random forests to map land cover with high resolution satellite image time series over large areas," *Remote Sensing of Environment*, 187, 156–168.

Peter, B. (2001), "Vitrified dung in archaeological contexts: an experimental study on the process of its formation in the Mosu and Bobirwa areas," *Pula: Botswana Journal of African Studies*, 15, 125–143.
Phillipson, D. W. (2005), *African archaeology*, Cambridge: Cambridge University Press.
Phillipson, D. W. (2013), "Complex societies of the Eritrean/Ethiopian highlands and their neighbours," in *The Oxford handbook of African archaeology*, eds. P. Mitchell and P. Lane, Oxford: Oxford University Press, pp. 799–816.
Pikirayi, I. (2007), "Ceramics and group identities: Towards a social archaeology in southern African Iron Age ceramic studies," *Journal of Social Archaeology*, 7, 286–301. https://doi.org/10.1177/1469605307081389.
Pikirayi, I. (2015), "The future of archaeology in Africa," *Antiquity*, 89, 531–541.
Platt, R. V., and Rapoza, L. (2008), "An evaluation of an object-oriented paradigm for land use/land cover classification," *The Professional Geographer*, 60, 87–100.
Plug, I. (1998), "Some Evidence for Seasonality amongst Later Stone Age Hunter-gatherers in Southern Africa," *Environmental Archaeology*, 3, 103–107. https://doi.org/10.1179/env.1998.3.1.103.
Plug, I. (2000), "Overview of Iron Age Fauna from the Limpopo Valley," *Goodwin Series*, 8, 117–126. https://doi.org/10.2307/3858053.
Pollarolo, L., and Kuman, K. (2009), "Excavation at Kudu Koppie site, Limpopo Province, South Africa," *South African Archaeological Bulletin*, 64, 69.
Pollarolo, L., Wilkins, J., Kuman, K., and Galletti, L. (2010), "Site formation at Kudu Koppie: a late earlier and middle stone age site in northern Limpopo Province, South Africa," *Quaternary International*, 216, 151–161.
Pontius Jr, R. G., and Millones, M. (2011), "Death to Kappa: birth of quantity disagreement and allocation disagreement for accuracy assessment," *International Journal of Remote Sensing*, 32, 4407–4429. https://doi.org/10.1080/01431161.2011.552923.
Pryce, T. O., and Abrams, M. J. (2010), "Direct detection of Southeast Asian smelting sites by ASTER remote sensing imagery: technical issues and future perspectives," *Journal of Archaeological Science*, 37, 3091–3098.
Pu, R., Landry, S., and Yu, Q. (2011), "Object-based urban detailed land cover classification with high spatial resolution IKONOS imagery," *International Journal of Remote Sensing*, 32, 3285–3308. https://doi.org/10.1080/01431161003745657.
Puissant, A., Rougier, S., and Stumpf, A. (2014), "Object-oriented mapping of urban trees using Random Forest classifiers," *International Journal of Applied Earth Observation and Geoinformation*, 26, 235–245. https://doi.org/10.1016/j.jag.2013.07.002.
Pwiti, G. (1996), "Settlement and subsistence of prehistoric farming communities in the mid-Zambezi Valley, northern Zimbabwe," *The South African Archaeological Bulletin*, 3–6.
Raath, A. (2014), "An Archaeological Investigation of Zhizo/Leokwe Foodways at Schroda and Pont Drift, Limpopo Valley, South Africa," Ph.D., United States -- Connecticut: Yale University.
Raczko, E., and Zagajewski, B. (2017), "Comparison of support vector machine, random forest and neural network classifiers for tree species classification on airborne hyperspectral APEX images," *European Journal of Remote Sensing*, 50, 144–154.
Rani, N., Mandla, V. R., and Singh, T. (2017), "Evaluation of atmospheric corrections on hyperspectral data with special reference to mineral mapping," *Geoscience Frontiers*, Special Issue: Deep Seated Magmas and Their Mantle Roots, 8, 797–808. https://doi.org/10.1016/j.gsf.2016.06.004.
Rayne, L., Bradbury, J., Mattingly, D., Philip, G., Bewley, R., and Wilson, A. (2017), "From Above and on the Ground: Geospatial Methods for Recording Endangered Archaeology

in the Middle East and North Africa," *Geosciences*, 7, 100. https://doi.org/10.3390/geosciences7040100.
Reeves, D. M. (1936), "Aerial Photography and Archaeology," *American Antiquity*, 2, 102. https://doi.org/10.2307/275881.
Reid, A. (2013), "The emergence of states in Great Lakes Africa," in *The Oxford Handbook of African Archaeology*, eds. P. Mitchell and P. Lane, Oxford: Oxford University Press, pp. 887–900.
Reid, A., and Segobye, A. (2000), "Politics, society and trade on the eastern margins of the Kalahari," *Goodwin Series*, 58–68.
Reid, S. H. (2016), "Satellite remote sensing of archaeological vegetation signatures in coastal west Africa," *African Archaeological Review*, 33, 163–182.
Renfrew, C., and Bahn, P. (2012), *Archaeology: theories, methods, and practice*, London: Thames and Hudson.
Reyes, A., Solla, M., and Lorenzo, H. (2017), "Comparison of different object-based classifications in LandsatTM images for the analysis of heterogeneous landscapes," *Measurement*, 97, 29–37. https://doi.org/10.1016/j.measurement.2016.11.012.
Riley, D. N. (1987), *Air photography and archaeology*, London: Gerald Duckworth& Co. Ltd.
Robbins, L. H., Murphy, M. L., Brook, G. A., Ivester, A. H., Campbell, A. C., Klein, R. G., Milo, R. G., Stewart, K. M., Downey, W. S., and Stevens, N. J. (2000), "Archaeology, palaeoenvironment, and chronology of the Tsodilo Hills White Paintings rock shelter, northwest Kalahari Desert, Botswana," *Journal of Archaeological Science*, 27, 1085–1113.
Rodriguez-Galiano, V. F., Chica-Olmo, M., Abarca-Hernandez, F., Atkinson, P. M., and Jeganathan, C. (2012a), "Random forest classification of mediterranean land cover using multi-seasonal imagery and multi-seasonal texture," *Remote Sensing of Environment*, 121, 93–107.
Rodriguez-Galiano, V. F., and Chica-Rivas, M. (2014), "Evaluation of different machine learning methods for land cover mapping of a Mediterranean area using multi-seasonal Landsat images and Digital Terrain Models," *International Journal of Digital Earth*, 7, 492–509. https://doi.org/10.1080/17538947.2012.748848.
Rodriguez-Galiano, V. F., Ghimire, B., Rogan, J., Chica-Olmo, M., and Rigol-Sanchez, J. P. (2012b), "An assessment of the effectiveness of a random forest classifier for land-cover classification," *ISPRS Journal of Photogrammetry and Remote Sensing*, 67, 93–104.
Roosevelt, C. H., and Luke, C. (2006), "Mysterious shepherds and hidden treasures: the culture of looting in Lydia, western Turkey," *Journal of Field Archaeology*, 185–198.
Rosenfield, G. H., and Fitzpatrick-Lins, K. (1986), "A coefficient of agreement as a measure of thematic classification accuracy," *Photogrammetric engineering and remote sensing*, 52, 223–227.
Rossel, R. A. V., and Behrens, T. (2010), "Using data mining to model and interpret soil diffuse reflectance spectra," *Geoderma*, 158, 46–54.
Rossel, R. A. V., Minasny, B., Roudier, P., and McBratney, A. B. (2006), "Colour space models for soil science," *Geoderma*, 133, 320–337.
Rowlands, A., and Sarris, A. (2007), "Detection of exposed and subsurface archaeological remains using multi-sensor remote sensing," *Journal of Archaeological Science*, 34, 795–803.
Sadr, K. (2003), "The Neolithic of Southern Africa," *Journal of African History*, 44, 195–209.
Sadr, K. (2008), "Invisible herders? The archaeology of Khoekhoe pastoralists," *Southern African Humanities*, 20, 179–203.

Sadr, K. (2015), "A Comparison of Accuracy and Precision in Remote Sensing Stone-walled Structures with Google Earth, High Resolution Aerial Photography and LiDAR; a Case Study from the South African Iron Age," *Archaeological Prospection*.

Sadr, K. (2016a), "Reducing inter-analyst variability in the classification of Iron Age stone-walled structures from satellite imagery of the southern Gauteng Province, South Africa," *South African Archaeological Bulletin*, 7.

Sadr, K. (2016b), "The impact of coder reliability on reconstructing archaeological settlement patterns from satellite imagery: A case study from South Africa," *Archaeological Prospection*, 23, 45–54.

Sadr, K. (2019), "KWENENG: HOW TO LOSE A PRECOLONIAL CITY," *South African Archaeological Bulletin*, 7.

Sadr, K., and Rodier, X. (2012), "Google Earth, GIS and stone-walled structures in southern Gauteng, South Africa," *Journal of Archaeological Science*, 39, 1034–1042.

Salman, A. B., Howari, F. M., El-Sankary, M. M., Wali, A. M., and Saleh, M. M. (2010), "Environmental impact and natural hazards on Kharga Oasis monumental sites, Western Desert of Egypt," *Journal of African Earth Sciences*, 58, 341–353. https://doi.org/10.1016/j.jafrearsci.2010.03.011.

Salvi, M. C., Salvini, R., Cartocci, A., Kozciak, S., Gallotti, R., and Piperno, M. (2011), "Multitemporal analysis for preservation of obsidian sources from Melka Kunture (Ethiopia): integration of fieldwork activities, digital aerial photogrammetry and multispectral stereo-IKONOS II analysis," *Journal of Archaeological Science*, 38, 2017–2023.

Salzmann, U., and Hoelzmann, P. (2005), "The Dahomey Gap: an abrupt climatically induced rain forest fragmentation in West Africa during the late Holocene," *The Holocene*, 15, 190–199. https://doi.org/10.1191/0959683605hl799rp.

Samadzadeh, G. R., Rigi, T., and Ganjali, A. R. (2013), "Comparison of four search engines and their efficacy with emphasis on literature research in addiction (prevention and treatment)," *International journal of high risk behaviors & addiction*, 1, 166.

Sarris, A., Papadopoulos, N., Agapiou, A., Salvi, M. C., Hadjimitsis, D. G., Parkinson, W. A., Yerkes, R. W., Gyucha, A., and Duffy, P. R. (2013), "Integration of geophysical surveys, ground hyperspectral measurements, aerial and satellite imagery for archaeological prospection of prehistoric sites: the case study of Vésztő-Mágor Tell, Hungary," *Journal of Archaeological Science*, 40, 1454–1470.

Saturno, W., Sever, T. L., Irwin, D. E., Howell, B. F., and Garrison, T. G. (2007), "Putting Us on the Map: Remote Sensing Investigation of the Ancient Maya Landscape," in *Remote Sensing in Archaeology*, Interdisciplinary Contributions To Archaeology, eds. J. Wiseman and F. El-Baz, New York, NY: Springer New York, pp. 137–160. https://doi.org/10.1007/0-387-44455-6_6.

Schmid, T., Koch, M., DiBlasi, M., and Hagos, M. (2008), "Spatial and spectral analysis of soil surface properties for an archaeological area in Aksum, Ethiopia, applying high and medium resolution data," *Catena*, 75, 93–101. https://doi.org/10.1016/j.catena.2008.04.008.

Schmidt, K. S., and Skidmore, A. K. (2003), "Spectral discrimination of vegetation types in a coastal wetland," *Remote sensing of Environment*, 85, 92–108.

Schmidt, M. J., Py-Daniel, A. R., de Paula Moraes, C., Valle, R. B. M., Caromano, C. F., Texeira, W. G., Barbosa, C. A., Fonseca, J. A., Magalhães, M. P., and do Carmo Santos, D. S. (2014), "Dark earths and the human built landscape in Amazonia: a widespread pattern of anthrosol formation," *Journal of archaeological science*, 42, 152–165.

Schmidt, P. R. (2006), *Historical Archaeology in Africa: Representation, Social Memory, and Oral Traditions*, Lanham: Rowman Altamira.

Schoeman, A. (2013), "Southern African Late Farming Communities," in *The Oxford Handbook of African Archaeology*, eds. P. Mitchell and P. J. Lane, Oxford: Oxford University Press, pp. 929–941.

Schoeman, M. H. (2006), "Imagining rain-places: rain-control and changing ritual landscapes in the Shashe-Limpopo Confluence Area, South Africa," *The South African Archaeological Bulletin*, 152–165.

Schoenbrun, D. L. (1993), "We are what we eat: ancient agriculture between the Great Lakes," *The Journal of African History*, 34, 1–31.

Schuetter, J., Goel, P., McCorriston, J., Park, J., Senn, M., and Harrower, M. (2013), "Autodetection of ancient Arabian tombs in high-resolution satellite imagery," *International Journal of Remote Sensing*, 34, 6611–6635. https://doi.org/10.1080/01431161.2013.802054.

Schulz, E., Abichou, A., Adamou, A., Ballaouche, A., and Ousseïni, I. (2009), "The desert in the Sahara. Transitions and boundaries," in *Palaeoecology of Africa and the Surrounding Islands*, eds. R. Braumhauer and J. Runge, London: Taylor & Francis Group, pp. 63–89.

Seddon, J. D. (1968a), "An aerial survey of settlement and living patterns in the Transvaal Iron Age: preliminary report," *African Studies*, 27, 189–194.

Seddon, J. D. (1968b), "An aerial survey of settlement and living patterns in the Transvaal Iron Age: preliminary report," *African Studies*, 27, 189–194. https://doi.org/10.1080/00020186808707296.

Segokgo, L. B. (2012), "The study of spatial organisation of stone wall enclosures at Motsenekatse using geographic information systems and remote sensing approach.," BA Thesis, University of Botswana.

Selier, S.-A. J. (2007), "The social structure, distribution and demographic status of the African elephant population in the Central Limpopo River Valley of Botswana, Zimbabwe and South Africa," Pretoria: University of Pretoria.

Serpico, S. B., and Moser, G. (2007), "Extraction of spectral channels from hyperspectral images for classification purposes," *IEEE transactions on geoscience and remote sensing*, 45, 484–495.

Sesnie, S. E., Finegan, B., Gessler, P. E., Thessler, S., Bendana, Z. R., and Smith, A. M. S. (2010), "The multispectral separability of Costa Rican rainforest types with support vector machines and Random Forest decision trees," *International Journal of Remote Sensing*, 31, 2885–2909. https://doi.org/10.1080/01431160903140803.

Sever, T. L., and Irwin, D. E. (2003), "Landscape archaeology: Remote-sensing investigation of the ancient Maya in the Peten rainforest of northern Guatemala," *Ancient Mesoamerica*, 14, 113–122.

Shao, Y., and Lunetta, R. S. (2012), "Comparison of support vector machine, neural network, and CART algorithms for the land-cover classification using limited training data points," *ISPRS Journal of Photogrammetry and Remote Sensing*, 70, 78–87.

Shaw, T., Andah, B., Okpoko, A., and Sinclair, P. (eds.) (1993), *The Archaeology of Africa: Food, Metals and Towns*, Routledge.

Shea, J. J., and Hildebrand, E. A. (2010), "The Middle Stone Age of West Turkana, Kenya," *Journal of Field Archaeology*, 35, 355–364.

Shennan, S. (1997), *Quantifying archaeology*, University of Iowa Press.

Shepherd, K. D., and Walsh, M. G. (2002), "Development of reflectance spectral libraries for characterization of soil properties," *Soil science society of America*, 66, 988–998.

Siart, C., Eitel, B., and Panagiotopoulos, D. (2008), "Investigation of past archaeological landscapes using remote sensing and GIS: a multi-method case study from Mount Ida, Crete," *Journal of Archaeological Science*, 35, 2918–2926.

Sibanda, M., Mutanga, O., and Rouget, M. (2016), "Discriminating rangeland management practices using simulated hyspIRI, landsat 8 OLI, sentinel 2 MSI, and VENμs spectral data," *IEEE Journal of Selected Topics in Applied Earth Observations and Remote Sensing*, 9, 3957–3969.

Silveira, E. M. O., Silva, S. H. G., Acerbi-Junior, F. W., Carvalho, M. C., Carvalho, L. M. T., Scolforo, J. R. S., and Wulder, M. A. (2019), "Object-based random forest modelling of aboveground forest biomass outperforms a pixel-based approach in a heterogeneous and mountain tropical environment," *International Journal of Applied Earth Observation and Geoinformation*, 78, 175–188. https://doi.org/10.1016/j.jag.2019.02.004.

Sirsat, M. S., Cernadas, E., Fernández-Delgado, M., and Khan, R. (2017), "Classification of agricultural soil parameters in India," *Computers and electronics in agriculture*, 135, 269–279.

Sittler, B. (2004), "Revealing Historical Landscapes by Using Airborne Laser Scanning. A 3-D Modell of Ridge and Furrow in Forests near Rastatt (Germany)," *Proceedings of Natscan, Laser-Scanners for Forest and Landscape Assessment - Instruments, Processing Methods and Applications. International Archives of Photogrammetry and Remote Sensing*, 36, 258–261.

Sivitskis, A. J., Harrower, M. J., David-Cuny, H., Dumitru, I. A., Nathan, S., Wiig, F., Viete, D. R., Lewis, K. W., Taylor, A. K., Dollarhide, E. N., Zaitchik, B., Al-Jabri, S., Livi, K. J. T., and Braun, A. (2018), "Hyperspectral satellite imagery detection of ancient raw material sources: Soft-stone vessel production at Aqir al-Shamoos (Oman)," *Archaeological Prospection*, 25, 363–374. https://doi.org/10.1002/arp.1719.

Smith, A. B. (1992), "Origins and spread of pastoralism in Africa," *Annual Review of Anthropology*, 21, 125–141.

Smith, B. (2012), "Helping to defend Africa's heritage: the African Archaeological Conservation Advisory Committee of the PanAfrican Archaeological Association," *Azania: Archaeological Research in Africa*, 47, 379–380. https://doi.org/10.1080/0067270X.2012.711574.

Smith, J., Lee-Thorp, J., and Hall, S. (2007), "Climate change and agropastoralist settlement in the Shashe-Limpopo River Basin, southern Africa: AD 880 to 1700," *The South African Archaeological Bulletin*, 62, 115–125.

Smith, J. M. (2005), "CLIMATE CHANGE AND AGROPASTORAL SUSTAINABILITY IN THE SHASHE/LIMPOPO RIVER BASIN FROM AD 900," PhD Thesis, University of the Witwatersrand. https://doi.org/10.1017/CBO9781107415324.004.

Snyman, H. A., Ingram, L. J., and Kirkman, K. P. (2013), "Themeda triandra: a keystone grass species," *African Journal of Range & Forage Science*, 30, 99–125.

Sørensen, L. K., and Dalsgaard, S. (2005), "Determination of clay and other soil properties by near infrared spectroscopy," *Soil Science Society of America Journal*, 69, 159–167.

Spear, T. (2000), "Early Swahili history reconsidered," *The International Journal of African Historical Studies*, 33, 257–290.

Stahl, A. B. (1986), "Early food production in West Africa: rethinking the role of the Kintampo Culture," *Current Anthropology*, 27, 532–536.

Stahl, A. B. (1994), "Innovation, diffusion, and culture contact: the Holocene archaeology of Ghana," *Journal of World Prehistory*, 8, 51–112.

Stehman, S. V., and Foody, G. M. (2019), "Key issues in rigorous accuracy assessment of land cover products," *Remote Sensing of Environment*, 231, 111199. https://doi.org/10.1016/j.rse.2019.05.018.

Sterry, M., Mattingly, D., Ahmed, M., Savage, T., White, K., and Wilson, A. (2011), "DMP XIII: Reconnaissance Survey of Archaeological Sites in the Murzuq Area," *Libyan Studies*, 42, 103–116.

Stevens, A., Udelhoven, T., Denis, A., Tychon, B., Lioy, R., Hoffmann, L., and Van Wesemael, B. (2010), "Measuring soil organic carbon in croplands at regional scale using airborne imaging spectroscopy," *Geoderma*, 158, 32–45.

Stewart, C., Lasaponara, R., and Schiavon, G. (2013), "ALOS PALSAR Analysis of the Archaeological Site of Pelusium," *Archaeological Prospection*, 20, 109–116. https://doi.org/10.1002/arp.1447.

Stewart, C., Lasaponara, R., and Schiavon, G. (2014), "Multi-frequency, polarimetric SAR analysis for archaeological prospection," *International Journal of Applied Earth Observation and Geoinformation*, 28, 211–219. https://doi.org/10.1016/j.jag.2013.11.007.

Steyn, M. (1997), "A Reassessment of the Human Skeletons from K2 and Mapungubwe (South Africa)," *The South African Archaeological Bulletin*, 52, 14. https://doi.org/10.2307/3888972.

Stone, E. C. (2015), "An update on the looting of archaeological sites in Iraq," *Near Eastern Archaeology*, 78, 178–186.

Strobl, C., Boulesteix, A.-L., Zeileis, A., and Hothorn, T. (2007), "Bias in random forest variable importance measures: Illustrations, sources and a solution," *BMC bioinformatics*, 8, 25.

Subias, E., Fiz, I., and Cuesta, R. (2013a), "The Middle Nile Valley: Elements in an approach to the structuring of the landscape from the Greco-Roman era to the nineteenth century," *Quaternary International*, 312, 27–44. https://doi.org/10.1016/j.quaint.2013.08.027.

Subias, E., Fiz, I., and Cuesta, R. (2013b), "The Middle Nile Valley: Elements in an approach to the structuring of the landscape from the Greco-Roman era to the nineteenth century," *Quaternary International*, LAC 2012: 2nd International Landscape and Archaeology Conference, Berlin, 312, 27–44. https://doi.org/10.1016/j.quaint.2013.08.027.

Svetnik, V., Liaw, A., Tong, C., Culberson, J. C., Sheridan, R. P., and Feuston, B. P. (2003), "Random forest: a classification and regression tool for compound classification and QSAR modeling," *Journal of Chemical Information and Computer Sciences*, 43, 1947–1958.

Tahmtan, I., Afshar, A. S., and Ahamdzadeh, K. (2016), "Factors affecting number of citations: a comprehensive review of the literature | SpringerLink," *Scientometrics*, 107, 1195–1225.

Tang, L., and Shao, G. (2015), "Drone remote sensing for forestry research and practices," *Journal of Forestry Research*, 26, 791–797. https://doi.org/10.1007/s11676-015-0088-y.

Tapete, D. (2018), "Remote Sensing and Geosciences for Archaeology," *Geosciences*, 8, 41. https://doi.org/10.3390/geosciences8020041.

Tapete, D., and Cigna, F. (2018), "Appraisal of Opportunities and Perspectives for the Systematic Condition Assessment of Heritage Sites with Copernicus Sentinel-2 High-Resolution Multispectral Imagery," *Remote Sensing*, 10.

Taşkın, G., Kaya, H., and Bruzzone, L. (2017), "Feature selection based on high dimensional model representation for hyperspectral images," *IEEE Transactions on Image Processing*, 26, 2918–2928.

Tatsumi, K., Yamashiki, Y., Torres, M. A. C., and Taipe, C. L. R. (2015), "Crop classification of upland fields using Random forest of time-series Landsat 7 ETM+ data," *Computers and Electronics in Agriculture*, 115, 171–179.

Thabeng, O. L., Merlo, S., and Adam, E. (2019), "High-resolution remote sensing and advanced classification techniques for the prospection of archaeological sites' markers: The case of dung deposits in the Shashi-Limpopo Confluence area (southern Africa)," *Journal of Archaeological Science*, 102, 48–60. https://doi.org/10.1016/j.jas.2018.12.003.

Thackeray, A. I. (1992), "The Middle Stone Age South of the Limpopo River," *Journal of World Prehistory*, 6, 385–440.

Thomas, D. C., Kidd, F. J., Nikolovski, S., and Zipfel, C. (2008), "The archaeological sites of Afghanistan in Google Earth," *AARGnews*, 37, 22–30.

Thomasson, J. A., Sui, R., Cox, M. S., and Al–Rajehy, A. (2001), "Soil reflectance sensing for determining soil properties in precision agriculture," *Transactions of the ASAE*, 44, 1445.

Thy, P., Segobye, A. K., and Ming, D. W. (1995), "Implications of prehistoric glassy biomass slag from east-central Botswana," *Journal of archaeological science*, 22, 629–637.

Tian, F., Yang, L., Lv, F., and Zhou, P. (2009), "Predicting liquid chromatographic retention times of peptides from the Drosophila melanogaster proteome by machine learning approaches," *Analytica chimica acta*, 644, 10–16.

Tierney, J. E., Pausata, F. S. R., and deMenocal, P. B. (2017), "Rainfall regimes of the Green Sahara," *Science Advances*, 3, e1601503. https://doi.org/10.1126/sciadv.1601503.

Todd, S. W., Hoffer, R. M., and Milchunas, D. G. (1998), "Biomass estimation on grazed and ungrazed rangelands using spectral indices," *International Journal of Remote Sensing*, 19, 427–438.

Toure, S. I., Stow, D. A., Shih, H.-C., Weeks, J., and Lopez-Carr, D. (2018), "Land cover and land use change analysis using multi-spatial resolution data and object-based image analysis," *Remote Sensing of Environment*, 210, 259–268. https://doi.org/10.1016/j.rse.2018.03.023.

Touw, W. G., Bayjanov, J. R., Overmars, L., Backus, L., Boekhorst, J., Wels, M., and van Hijum, S. A. F. T. (2012), "Data mining in the Life Sciences with Random Forest: a walk in the park or lost in the jungle?," *Briefings in bioinformatics*, 14, 315–326.

Traviglia, A., and Cottica, D. (2011), "Remote sensing applications and archaeological research in the Northern Lagoon of Venice: the case of the lost settlement of Constanciacus," *Journal of Archaeological science*, 38, 2040–2050.

Treichel, S., Brinckmann, E., Scheitler, B., and von Willert, D. J. (1984), "Occurrence and changes of proline content in plants in the southern Namib Desert in relations to increasing and decreasing drought," *Planta*, 162, 236–242.

Tucker, C. J. (1979), "Red and photographic infrared linear combinations for monitoring vegetation," *Remote sensing of Environment*, 8, 127–150.

Tustison, N. J., Shrinidhi, K. L., Wintermark, M., Durst, C. R., Kandel, B. M., Gee, J. C., Grossman, M. C., and Avants, B. B. (2015), "Optimal symmetric multimodal templates and concatenated random forests for supervised brain tumor segmentation (simplified) with ANTsR," *Neuroinformatics*, 13, 209–225.

Ucko, P. J. (1993), "Foreword," in *The Archaeology of Africa: Food, Metals and Towns*, eds. B. Andah, A. Okpoko, T. Shaw, and P. Sinclair, New York: Routledge.

Uddin, T., and Uddiny, A. (2015), "A guided random forest based feature selection approach for activity recognition," IEEE, pp. 1–6.

Ustuner, M., Sanli, F. B., and Dixon, B. (2015), "Application of support vector machines for landuse classification using high-resolution RapidEye images: a sensitivity analysis," *European Journal of Remote Sensing*, 48, 403–422.

Van Coillie, F. M. B., Verbeke, L. P. C., and De Wulf, R. R. (2007), "Feature selection by genetic algorithms in object-based classification of IKONOS imagery for forest mapping in Flanders, Belgium," *Remote Sensing of Environment*, 110, 476–487.

Van Doornum, L. B. (2006), "Changing places, spaces and identity in the Shashe Limpopo region of Limpopo Province, South Africa," Thesis, Johannesburg: University of the Witwatersrand.

Van Ess, M., Becker, H., Fassbinder, J., Kiefl, R., Lingenfelder, I., Schreier, G., and Zevenbergen, A. (2006), "Detection of looting activities at archaeological sites in Iraq using Ikonos imagery," in *Agenwandte Geo-Informatik*, Breitrage zum 18. AGIT Symposium Salzburg, eds. J. Stroble, T. Blaschke, and G. Griesebner, Heidelberg: Wichman Verlag, pp. 669–678.

Van Zinderen Bakker, E. M. (1975), "The origin and palaeoenvironment of the Namib Desert biome," *Journal of Biogeography*, 65–73.

Vapnik, V. N. (1999), "An overview of statistical learning theory," *IEEE Transactions on Neural Networks*, 10, 988–999. https://doi.org/10.1109/72.788640.

Vapnik, V. N., and Chervonenkis, A. Y. (1971), "On the Uniform Convergence of Relative Frequencies of Events to Their Probabilities," *Theory of Probability and its Applications; Philadelphia*, 16, 17. http://dx.doi.org/10.1137/1116025.

Verhagen, P., and Drăguţ, L. (2012), "Object-based landform delineation and classification from DEMs for archaeological predictive mapping," *Journal of Archaeological Science*, 39, 698–703.

Verhoeven, G., and Vermeulen, F. (2016), "Engaging with the canopy—Multi-dimensional vegetation mark visualisation using archived aerial images," *Remote Sensing*, 8, 752.

Verrelst, J., Rivera, J. P., Moreno, J., and Camps-Valls, G. (2013), "Gaussian processes uncertainty estimates in experimental Sentinel-2 LAI and leaf chlorophyll content retrieval," *ISPRS Journal of Photogrammetry and Remote Sensing*, 86, 157–167. https://doi.org/10.1016/j.isprsjprs.2013.09.012.

Villa, P., Soriano, S., Tsanova, T., Degano, I., Higham, T. F. G., d'Errico, F., Backwell, L., Lucejko, J. J., Colombini, M. P., and Beaumont, P. B. (2012), "Border cave and the beginning of the later stone age in South Africa," *Proceedings of the National Academy of Sciences*, 109, 13208–13213.

Vogel, J. C., and Calabrese, J. A. (2000), "Dating of the Leokwe Hill site and implications for the regional chronology," *Goodwin Series*, 47–50.

Vogels, M. F. A., De Jong, S. M., Sterk, G., and Addink, E. A. (2017), "Agricultural cropland mapping using black-and-white aerial photography, object-based image analysis and random forests," *International Journal of Applied Earth Observation and Geoinformation*, 54, 114–123.

Vohland, M., Ludwig, M., Thiele-Bruhn, S., and Ludwig, B. (2014), "Determination of soil properties with visible to near-and mid-infrared spectroscopy: Effects of spectral variable selection," *Geoderma*, 223, 88–96.

Voigt, E. A. (1983), *Mapungubwe: an archaeological interpretation of an iron age community*, Transvaal Museum Monographs, Pretoria: Transvaal Museum.

Voigt, E. A. (1986), "Iron Age Herding: Archaeological and Ethnoarchaeological Approaches to Pastoral Problems," *Goodwin Series*, 5, 13–21. https://doi.org/10.2307/3858141.

Von Den Driesch, A., and Deacon, H. J. (1985), "Sheep remains from Boomplaas Cave, South Africa," *The South African Archaeological Bulletin*, 39–44.

van Waarden, C. (1979), "Archaeological Investigation of Leeukop: a functional Approach," *Botswana Notes and Records*, 11, 1–13.
Wadley, L. (1993), "The Pleistocene Later Stone Age south of the Limpopo River," *Journal of World Prehistory*, 7, 243–296. https://doi.org/10.1007/BF00974721.
Wahidin, N., Siregar, V. P., Nababan, B., Jaya, I., and Wouthuyzen, S. (2015), "Object-based Image Analysis for Coral Reef Benthic Habitat Mapping with Several Classification Algorithms," *Procedia Environmental Sciences*, The 1st International Symposium on LAPAN-IPB Satellite (LISAT) for Food Security and Environmental Monitoring, 24, 222–227. https://doi.org/10.1016/j.proenv.2015.03.029.
Walker, N. J. (1983), "The significance of an early date for pottery and sheep in Zimbabwe," *The South African Archaeological Bulletin*, 88–92.
Walker, N. J. (1994), "The late stone age of Botswana: Some recent excavations," *Botswana Notes and Records*, 26, 1–35.
Wang, L., Zhou, X., Zhu, X., Dong, Z., and Guo, W. (2016), "Estimation of biomass in wheat using random forest regression algorithm and remote sensing data," *The Crop Journal*, 4, 212–219.
Ward, D. (2009), *The biology of deserts*, Oxford: Oxford University Press.
Warfe, A. R. (2003), "Cultural origins of the Egyptian Neolithic and Predynastic: an evaluation of the evidence from the Dakhleh oasis (South Central Egypt)," *African Archaeological Review*, 20, 175–202.
Watson, D. J. (2010), "Within savanna and forest: a review of the late Stone Age Kintampo tradition, Ghana," *Azania: Archaeological Research in Africa*, 45, 141–174.
Wei, C.-L., Rowe, G. T., Escobar-Briones, E., Boetius, A., Soltwedel, T., Caley, M. J., Soliman, Y., Huettmann, F., Qu, F., and Yu, Z. (2010), "Global patterns and predictions of seafloor biomass using random forests," *PLoS One*, 5, e15323.
Wei, J., Meng, M., Wang, J., Ma, Q., and Wang, X. (2016), "Adaptive semi-supervised dimensionality reduction with sparse representation using pairwise constraints," *Neurocomputing*, 177, 564–571.
Weidong, L., Baret, F., Xingfa, G., Qingxi, T., Lanfen, Z., and Bing, Z. (2002), "Relating soil surface moisture to reflectance," *Remote sensing of environment*, 81, 238–246.
Weih, R. C., and Riggan, N. D. (2010), "Object-based classification vs . pixel-based classification : comparitive importance of multi-resolution imagery," in *GEOBIA 2010*, Part 4/C7, Ghent, Belgium: The International Archives of the Photogrammetry, Remote Sensing and Spatial Information Sciences, p. 6.
Wendorf, F., and Schild, R. (1994), "Are the early Holocene cattle in the Eastern Sahara domestic or wild?," *Evolutionary Anthropology: Issues, News, and Reviews*, 3, 118–128.
Wengrow, D., Dee, M., Foster, S., Stevenson, A., and Ramsey, C. B. (2014), "Cultural convergence in the Neolithic of the Nile Valley: a prehistoric perspective on Egypt's place in Africa," *Antiquity*, 88, 95–111.
Wenke, R. J., Long, J. E., and Buck, P. E. (1988), "Epipaleolithic and Neolithic subsistence and settlement in the Fayyum Oasis of Egypt," *Journal of Field Archaeology*, 15, 29–51.
West, P. R., Weir, A. M., Smith, A. M., Donley, E. L. R., and Cezar, G. G. (2010), "Predicting human developmental toxicity of pharmaceuticals using human embryonic stem cells and metabolomics," *Toxicology and applied pharmacology*, 247, 18–27.
White, F. (1983), *The vegetation of Africa, a descriptive memoir to accompany the UNESCO/AETFAT/UNSO vegetation map of Africa (3 Plates, Northwestern Africa, Northeastern Africa, and Southern Africa, 1: 5,000,000)*, Paris: United Nations Educational, Scientific and Cultural Organization.

White, L. J. T., and Oates, J. F. (1999), "New data on the history of the plateau forest of Okomu, southern Nigeria: an insight into how human disturbance has shaped the African rain forest," *Global Ecology and Biogeography,* 8, 355–361. https://doi.org/10.1046/j.1365-2699.1999.00149.x.

Whiteside, T. G., Boggs, G. S., and Maier, S. W. (2011), "Comparing object-based and pixel-based classifications for mapping savannas," *International Journal of Applied Earth Observation and Geoinformation,* 13, 884–893.

Wilkins, J., Pollarolo, L., and Kuman, K. (2010), "Prepared core reduction at the site of Kudu Koppie in northern South Africa: Temporal patterns across the Earlier and Middle Stone Age boundary," *Journal of Archaeological Science,* 37, 1279–1292. https://doi.org/10.1016/j.jas.2009.12.031.

Wilkinson, K. N., Beck, A. R., and Philip, G. (2006), "Satellite imagery as a resource in the prospection for archaeological sites in central Syria," *Geoarchaeology,* 21, 735–750.

Wilson, C. A., Davidson, D. A., and Cresser, M. S. (2008), "Multi-element soil analysis: an assessment of its potential as an aid to archaeological interpretation," *Journal of Archaeological Science,* 35, 412–424.

Wilson, C. A., Davidson, D. A., and Cresser, M. S. (2009), "An evaluation of the site specificity of soil elemental signatures for identifying and interpreting former functional areas," *Journal of Archaeological Science,* 36, 2327–2334.

Wilson, D. R. (1975), "Aerial reconnaissance for archaeology," in *Aerial reconnaissance for archaeology, CBA Research Report.*, ed. D. R. Wilson, London: The Council for British archaeology.

Witharana, C., and Civco, D. L. (2014), "Optimizing multi-resolution segmentation scale using empirical methods: Exploring the sensitivity of the supervised discrepancy measure Euclidean distance 2 (ED2)," *ISPRS Journal of Photogrammetry and Remote Sensing,* 87, 108–121.

Witharana, C., and Lynch, H. J. (2016), "An Object-Based Image Analysis Approach for Detecting Penguin Guano in very High Spatial Resolution Satellite Images," *Remote Sensing,* 8, 375. https://doi.org/10.3390/rs8050375.

Wolf, A. F. (2012), "Using WorldView-2 Vis-NIR multispectral imagery to support land mapping and feature extraction using normalized difference index ratios," International Society for Optics and Photonics, p. 83900N.

Wood, M. (2000), "Making Connections: Relationships between International Trade and Glass Beads from the Shashe-Limpopo Area," *Goodwin Series,* 8, 78. https://doi.org/10.2307/3858049.

Wu, C. (2009), "Quantifying high-resolution impervious surfaces using spectral mixture analysis," *International Journal of Remote Sensing,* 30, 2915–2932. https://doi.org/10.1080/01431160802558634.

Wu, J., Liu, H., Duan, X., Ding, Y., Wu, H., Bai, Y., and Sun, X. (2008), "Prediction of DNA-binding residues in proteins from amino acid sequences using a random forest model with a hybrid feature," *Bioinformatics,* 25, 30–35.

Wynne-Jones, S. (2007), "Creating urban communities at Kilwa Kisiwani, Tanzania, AD 800-1300," *Antiquity,* 81, 368–380.

Wynne-Jones, S., and Fleisher, J. (2016), "The multiple territories of Swahili urban landscapes," *World Archaeology,* 48, 349–362. https://doi.org/10.1080/00438243.2016.1179128.

Xu, C., Zeng, W., Huang, J., Wu, J., and Van Leeuwen, W. J. D. (2016), "Prediction of soil moisture content and soil salt concentration from hyperspectral laboratory and field data," *Remote Sensing,* 8, 42.

Yang, M.-D., and Yang, Y.-F. (2004), "Genetic algorithm for unsupervised classification of remote sensing imagery," in *Image Processing: Algorithms and Systems III*, International Society for Optics and Photonics, pp. 395–403.

Zhang, T., Fu, X., Goh, R. S. M., Kwoh, C. K., and Lee, G. K. K. (2009), "A GA-SVM feature selection model based on high performance computing techniques," IEEE, pp. 2653–2658.

Zhang, X., Chen, G., Wang, W., Wang, Q., and Dai, F. (2017), "Object-Based Land-Cover Supervised Classification for Very-High-Resolution UAV Images Using Stacked Denoising Autoencoders," *IEEE Journal of Selected Topics in Applied Earth Observations and Remote Sensing*, 10, 3373–3385. https://doi.org/10.1109/JSTARS.2017.2672736.

Zhu, G., and Blumberg, D. G. (2002), "Classification using ASTER data and SVM algorithms; The case study of Beer Sheva, Israel," *Remote Sensing of Environment*, 80, 233–240.

Zhuo, L., Zheng, J., Li, X., Wang, F., Ai, B., and Qian, J. (2008), "A genetic algorithm based wrapper feature selection method for classification of hyperspectral images using support vector machine," in *Geoinformatics 2008 and Joint Conference on GIS and Built Environment: Classification of Remote Sensing Images*, International Society for Optics and Photonics, p. 71471J.